

Table of Contents

| | |
|--|-------|
| Schedule At A Glance | 5 |
| Special Events and University Center Floor Plans | 6 |
| Session Schedule At A Glance | 7 |
| Presenting Author List | 8-10 |
| Final Program | |
| Monday | 11-13 |
| Tuesday | 13-16 |
| Wednesday | 16-18 |
| Thursday | 18-22 |
| Friday | 23-24 |
| Posters | 25-27 |

MEETING REGULATIONS

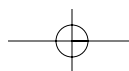
The American Ceramic Society is a nonprofit scientific organization that facilitates the exchange of knowledge along with the expression, interchange and fertilization of ideas. The Society accomplishes its purposes through meetings, which it conducts for the presentation and discussion of papers, and by the publication of those papers for future reference. The Society, as the producer, owns and retains full right to control its publications and its meetings. The Society administration and management have an obligation to protect its members and its meetings from intrusion by others who may wish to use the meetings for their own private promotion purpose. Literature found not to be in agreement with the Society's goals, in competition with Society services or of an offensive nature will not be displayed anywhere in the vicinity of the meeting. Promotional literature of any kind may not be displayed if the Society is holding an exhibit in conjunction with the meeting unless the Society provides tables for this purpose. Literature not conforming to this policy or displayed in other than designated areas will be disposed. The Society will not permit unauthorized scheduling of promotional activities during its meeting by any person or group when those activities are conducted at its meeting place in interference with its programs and scheduled activities. The Society will not permit requisitioning of space in meetings, registration areas or in the hallways of its meeting hotels for any display material considered to be contrary to the best interests of the meeting and the Society. The Society will not permit the publication of its programs by others without its knowledge and consent. The Society does not object to appropriate activities by others during its meetings if it is consulted with regard to time, place, and suitability. Any person or group wishing to conduct any activity at the time and location of the Society meeting must obtain permission from the Executive Director, giving full details regarding desired time, place and nature of activity.

Registration Requirements: Attendance at any meeting of the Society shall be limited to duly registered persons.

Disclaimer: Statements of fact and opinion are the responsibility of the authors alone and do not imply an opinion on the part of the officers, staff or members of The American Ceramic Society. The American Ceramic Society assumes no responsibility for the statements and opinions advanced by the contributors to its publications or by the speakers at its programs; nor does The American Ceramic Society assume any liability for losses or injuries suffered by attendees at its meetings. Registered names and trademarks, etc. used in its publications, even without specific indications thereof, are not to be considered unprotected by the law. Mention of trade names of commercial products does not constitute endorsement or recommendations for use by the publishers, editors or authors.

Final determination of the suitability of any information, procedure or products for use contemplated by any user, and the manner of that use, is the sole responsibility of the user. Expert advice should be obtained at all times when implementation is being considered, particularly where hazardous materials or processes are encountered.

Copyright © 2008. The American Ceramic Society (www.ceramics.org). All rights reserved.



Welcome

Greetings and welcome to the 15th International Conference on Textures of Materials (ICOTOM 15). This conference will bring together the substantial international community of scientists and engineers who share an interest in the development of our understanding of texture in materials, its experimental characterization, influence on materials properties, and description by models.

This conference series looks back on a history of over 30 years. As has transpired in many scientific disciplines, a small group of scientists working independently and more or less on isolated issues related to texture and anisotropy of materials in the 1960's felt the need to exchange information and ideas on how to tackle the mutually interesting, scientifically challenging experimental and theoretical approaches of texture measurement and evaluation, and a first meeting was held in Clausthal, Germany in 1969. The success of this first meeting prompted successive conferences with attendance reaching more than 300 in 2005.

ICOTOM is dedicated to the goal of promoting all aspects of texture research and applications in all kinds of crystalline materials, from metals to rocks to polymers. As examples, the development of experimental and theoretical tools for texture research, the improvement of prediction of texture and anisotropy, the utilization of texture to advance materials science, and the optimization of anisotropic materials properties are all objectives of the texture community and of ICOTOM.

The established texture characterization methods, which developed largely from investigation of the processing and properties of traditional materials (especially metals), have found increasing application in other areas such as biomaterials research. This means that one of the essential functions of the ICOTOM conference is to bring together the various scientific communities that share a common interest in crystallographic textures. Thus the conference aims to enable newcomers to the field to acquaint themselves with state of the art theoretical concepts and sophisticated experimental techniques developed over many years of texture research.

In summary, the conference series on textures, ICOTOM, serves a steadily broadening community and aims to extend our understanding and the application of texture studies to the entire range of materials. I believe you will enjoy the conference camaraderie and hope that you and your work will benefit greatly.

A number of extra events will be available to ICOTOM participants. An electron back scatter diffraction system demonstration and a tour of the CMU Materials Science & Engineering Department will be held on Wednesday. On Thursday evening there will be a lecture-recital at the Heinz Memorial Chapel in which the operation of the organ will be illustrated with musical examples, along with various materials science aspects.

Enjoy!

A.D. (Tony) Rollett
ICOTOM 15 Organizing Committee Chair

Professor of Materials Science and Engineering,
 Carnegie Mellon University

ICOTOM 15 International Committee

Chair: Bevis Hutchinson, KIMAB, Sweden
Brent Adams, Brigham Young University, USA
Pete Bate, University of Manchester, UK
Brian Duggan, The University of Hong Kong, Hong Kong
Olaf Engler, Hydro Aluminium Deutschland GmbH
 and R&D Center Bonn, Germany
Paul van Houtte, Katholieke Universiteit Leuven, Belgium
Hirosuke Inagaki, INATEX, Japan
Dorte Juul Jensen, Riso National Laboratory, Sweden
Dong Nyung Lee, Seoul National University, Korea
Richard Penelle, Universite de Paris-Sud, France
Ranjit Ray, Tata Steel, India
Jerzy Szpunar, McGill University, Canada

ICOTOM 15 Organizing Committee Chair

A.D. (Tony) Rollett
 Professor of Materials Science and Engineering
 Carnegie Mellon University

ICOTOM 15 Organizing Committee

Brent Adams, Brigham Young University
Katy Barmak, Carnegie Mellon University
Armand Beaudoin, University of Illinois
Tom Bieler, Michigan State University
John Bingert, Los Alamos Nat'l Lab
Keith Bowman, Purdue University
Paul Dawson, Cornell University
Anthony DeArdo, University of Pittsburgh
Roger Doherty, Drexel University
David Field, Washington State University
Hamid Garmestani, Georgia Institute of Technology
Amit Goyal, Oak Ridge Nat'l Lab
Erik Hilinski, US Steel
Surya Kalidindi, Drexel University
Peter Kalu, FAMU/FSU
Michael Kassner, University of Southern California
Mukul Kumar, Lawrence Livermore Nat'l Lab
Tom Mason, Los Alamos Nat'l Lab
KL Murty, North Carolina State University
Carl Necker, Los Alamos Nat'l Lab
Warren Poole, UBC
Greg Rohrer, Carnegie Mellon University
Lee Semiatin, Air Force Research Lab
Jerzy Szpunar, McGill University
Carlos Tomé, Los Alamos Nat'l Lab
Sven Vogel, Los Alamos Nat'l Lab
Hasso Weiland, Alcoa
Rudy Wenk, UC Berkeley
Jörg Wiezorek, University of Pittsburgh
Stuart Wright, EDAX/TSL

Schedule At A Glance

Sunday, June 1, 2008

| | | |
|-------------------|-------------------|-------------------------------------|
| Registration | 7:30 AM – 6:30 PM | McKenna |
| Welcome Reception | 5:00 PM – 7:00 PM | CMU – College of Fine Arts Building |

Monday, June 2, 2008

| | | |
|--------------------------------|---------------------|---|
| Registration | 7:30 AM – 6:00 PM | McKenna |
| Plenary Session | 8:30 AM – 9:30 AM | McConomy Auditorium |
| Coffee Break | 9:30 AM – 10:15 AM | Hochs Commons |
| Technical Sessions | 10:15 AM – 12:30 PM | Rangos 1, McConomy Auditorium, & Connan |
| Posters and Table Top Exhibits | 12:30 PM – 6:00 PM | Rangos 2–3 |
| Lunch On Own | 12:30 PM – 1:45 PM | |
| Technical Sessions | 1:45 PM – 6:00 PM | Rangos 1, McConomy Auditorium, & Connan |
| Coffee Break | 3:30 PM – 4:15 PM | Hochs Commons |

Tuesday, June 3, 2008

| | | |
|--------------------------------|---------------------|---|
| Registration | 8:00 AM – 6:00 PM | McKenna |
| Technical Sessions | 8:30 AM – 12:30 PM | Rangos 1, McConomy Auditorium, & Connan |
| Coffee Break | 10:00 AM – 10:45 AM | Hochs Commons |
| Posters and Table Top Exhibits | 8:30 AM – 6:00 PM | Rangos 2–3 |
| Lunch On Own | 12:30 PM – 1:45 PM | |
| Technical Sessions | 1:45 PM – 6:00 PM | Rangos 1, McConomy Auditorium, & Connan |
| Coffee Break | 3:30 PM – 4:15 PM | Hochs Commons |

Wednesday, June 4, 2008

| | Time | Room |
|--------------------------|---------------------|--|
| Registration | 8:00 AM – 1:00 PM | McKenna |
| Technical Sessions | 8:30 AM – 12:30 PM | Rangos 1, Rangos 2, Rangos 3, & Connan |
| Coffee Break | 10:00 AM – 10:30 AM | Hochs Commons |
| Lunch On Own & Free Time | 12:30 PM – 4:00 PM | |
| Dinner River Cruise | 4:00 PM – 9:00 PM | Depart University Center at 4:00 PM for Gateway Clipper Fleet Docks |

Thursday, June 5, 2007

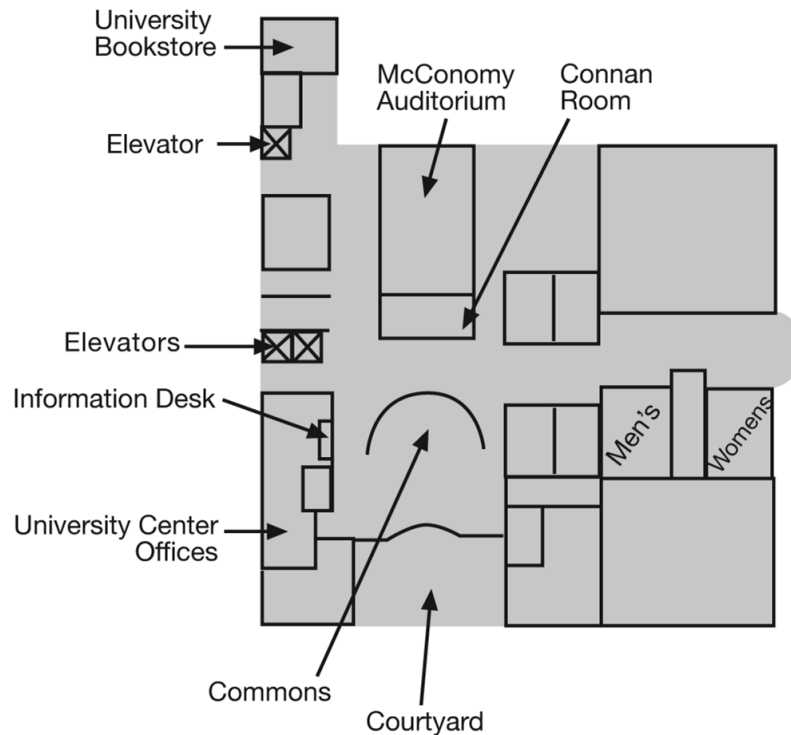
| | | |
|--------------------|---------------------|--|
| Registration | 8:00 AM – 6:00 PM | McKenna |
| Technical Sessions | 8:30 AM – 12:30 PM | Rangos 1, Rangos 2, Rangos 3, & Connan |
| Coffee Break | 10:00 AM – 10:30 AM | Hochs Commons |
| Lunch On Own | 12:30 PM – 1:45 PM | |
| Technical Sessions | 1:45 PM – 6:00 PM | Rangos 1, Rangos 2, Rangos 3, & Connan |
| Coffee Break | 3:30 PM – 4:00 PM | Hochs Commons |

Friday, June 6, 2007

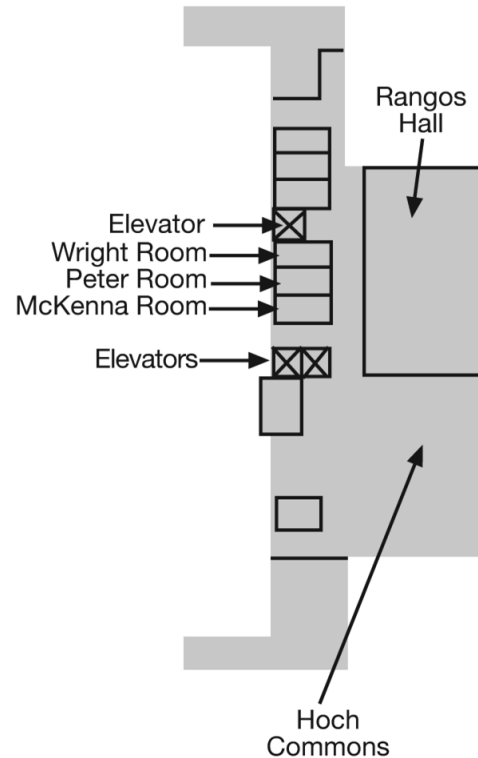
| | | |
|--------------------|---------------------|--|
| Registration | 8:00 AM – 12:30 PM | McKenna |
| Technical Sessions | 8:30 AM – 12:30 PM | Rangos 1, Rangos 2, Rangos 3, & Connan |
| Coffee Break | 10:00 AM – 10:30 AM | Hochs Commons |

University Center Floor Plans

First Floor



Second Floor



Special Events

Welcome Reception – Please join us on Sunday, June 1st, from 5 PM – 7 PM at The College of Fine Arts Building Great Hall.

River Dinner Cruise – Experience Pittsburgh from the Monongahela, Allegheny, and Ohio Rivers while enjoying dinner and fellow attendee's companionship on Wednesday, June 4th. Buses will transport attendees from The University Center at Carnegie Mellon University to the docks of the Gateway Clipper Fleet. Buses will be departing The University Center at 4 PM. Boarding of the Party Liner vessel will be from 5 PM to 5:30 PM. Dinner and the river tour will take approximately two and a half hours. Buses will depart the Gateway Clipper Fleet docks at 8 PM and return to The University Center at approximately 9 PM. Space is limited on the vessel and available on a first come, first serve basis. Please stop by registration in the McKenna room at University Center to see if space is available.

Session Schedule-At-A-Glance

| Time | McConomy Auditorium | Connan | Rangos 1 | Rangos 2 | Rangos 3 |
|--------------------------|--|----------------------------------|------------------------------------|----------------------------|--------------------------------------|
| Monday, June 2 | | | | | |
| 8:30 - 9:30 am | Plenary Session | | | | |
| 10:15 - 12:15 pm | Deformation Mechanisms | | | | |
| 10:15 - 12:15 pm | | Effects of Magnetic Fields | | | |
| 10:15 - 12:30 pm | | | Novel Methods Including 3D - I | | |
| 1:45 - 5:45 pm | Texture Evolution During TMP | | | Posters | Posters |
| 1:45 - 6 pm | | | Novel Methods Including 3D - II | ↓ | ↓ |
| 1:40 - 6 pm | | Biomaterials | | ↓ | ↓ |
| Tuesday, June 3 | | | | | |
| 8:30 - 12 Noon | Texture Modeling | | | Posters | Posters |
| 8:30 - 12:15 pm | | Complex Oxides & Other Compounds | | ↓ | ↓ |
| 8:30 - 12 Noon | | | Novel Methods Including 3D - III | ↓ | ↓ |
| 1:45 - 5:15 pm | Texture Evolution & Severe Plastic Deformation | | | ↓ | ↓ |
| 1:45 - 6 pm | | Texture Materials Design I | | ↓ | ↓ |
| 1:45 - 6 pm | | | Interface Textures I | ↓ | ↓ |
| Wednesday, June 4 | | | | | |
| 8:30 - 11:45 am | | | | Texture-Property Relations | |
| 8:30 - 12 Noon | | | | | Low Carbon and IF Steels |
| 8:30 - 12:30 pm | | | Interface Textures II | | |
| 8:30 - 12:30 pm | | Texture Materials Design II | | | |
| Thursday, June 5 | | | | | |
| 8:30 - 12:30 pm | | Texture in Materials Design III | | | |
| 8:30 - 12:30 pm | | | Digital Microstructures | | |
| 8:30 - 12:30 pm | | | | Thin Films | |
| 8:30 - 12:30 pm | | | | | Stainless Steels & Electrical Steels |
| 1:45 - 6 pm | | Damage Accumulation I | | | |
| 1:45 - 6 pm | | | Texture at Non-Ambient Conditions | | |
| 1:45 - 6 pm | | | | Recrystallization I | |
| 1:45 - 6 pm | | | | | High Strength Steels |
| Friday, June 6 | | | | | |
| 8:30 - 11:15 am | | Damage Accumulation II | | | |
| 8:30 - 12:45 pm | | | Friction Stir Welding & Processing | | |
| 8:30 - 12:15 pm | | | | Recrystallization II | |
| 8:30 - 12:30 pm | | | | | Texture Analysis & Simulations |

Posters and Tabletop Exhibits will be on display after Noon on Monday and all day Tuesday in Rangos 2&3

Presenting Author List

| Name | Date | Time | Room | Abstract Number | Name | Date | Time | Room | Abstract Number |
|-------------------|-------|---------|---------------------|---------------------|---------------------|-------|---------|---------------------|---------------------|
| A | | | | | | | | | |
| Adams, B.L. | 4-Jun | 9:15AM | Connan | ICOTOM-S12-016-2008 | Decroos, K. | 2-Jun | 9:30AM | Rangos 2 & 3 | ICOTOM-P-022-2008 |
| Ahmadi, S. | 4-Jun | 11:00AM | Connan | ICOTOM-S12-021-2008 | Delannay, L. | 5-Jun | 10:30AM | Rangos 1 | ICOTOM-S14-005-2008 |
| Akbarzadeh, A. | 2-Jun | 9:30AM | Rangos 2 & 3 | ICOTOM-P-013-2008 | Detavernier, C. | 4-Jun | 9:30AM | Rangos 1 | ICOTOM-S7-016-2008 |
| Akbarzadeh, A. | 2-Jun | 9:30AM | Rangos 2 & 3 | ICOTOM-P-063-2008 | Dey, S.R. | 3-Jun | 9:30AM | Rangos 1 | ICOTOM-S5-022-2008 |
| Akimune, Y. | 3-Jun | 10:45AM | Connan | ICOTOM-S6-007-2008 | Dey, S.R. | 2-Jun | 9:30AM | Rangos 2 & 3 | ICOTOM-P-057-2008 |
| Al-Buhamad, O. | 5-Jun | 5:00PM | Connan | ICOTOM-S13-011-2008 | Dhawan, N. | 2-Jun | 9:30AM | Rangos 2 & 3 | ICOTOM-P-074-2008 |
| Al-Fadhlah, K.J. | 4-Jun | 11:45AM | Connan | ICOTOM-S12-024-2008 | DiAntonio, C. | 3-Jun | 11:30AM | Connan | ICOTOM-S6-009-2008 |
| Al-Sawalimih, A. | 2-Jun | 3:15PM | Connan | ICOTOM-S11-004-2008 | Dillamore, I. | 2-Jun | 8:30AM | McConomy Auditorium | ICOTOM-PL-001-2008 |
| Alankar, A. | 6-Jun | 9:00AM | Connan | ICOTOM-S13-014-2008 | Dillon, S.J. | 2-Jun | 3:15PM | Rangos 1 | ICOTOM-S5-013-2008 |
| Azzi, M. | 4-Jun | 10:30AM | Rangos 2 | ICOTOM-S9-041-2008 | Dmitrieva, O. | 2-Jun | 3:00PM | Rangos 1 | ICOTOM-S5-012-2008 |
| Azzi, M. | 5-Jun | 9:15AM | Rangos 3 | ICOTOM-S3-013-2008 | Duchêne, L. | 5-Jun | 10:30AM | Connan | ICOTOM-S12-032-2008 |
| B | | | | | | | | | |
| Baars, D.C. | 6-Jun | 11:30AM | Rangos 2 | ICOTOM-S10-023-2008 | Eisenlohr, P. | 5-Jun | 9:00AM | Rangos 1 | ICOTOM-S14-002-2008 |
| Bacroix, B. | 4-Jun | 11:45AM | Rangos 3 | ICOTOM-S3-010-2008 | El-Dasher, B. | 5-Jun | 5:30PM | Rangos 1 | ICOTOM-S4-012-2008 |
| Balachandran, S. | 5-Jun | 11:15AM | Connan | ICOTOM-S13-016-2008 | Elia, J. | 2-Jun | 9:30AM | Rangos 2 & 3 | ICOTOM-PL-001-2008 |
| Barabash, O.M. | 2-Jun | 9:30AM | Rangos 2 & 3 | ICOTOM-P-002-2008 | Engler, O. | 3-Jun | 11:30AM | Rangos 1 | ICOTOM-S5-026-2008 |
| Barabash, R.I. | 2-Jun | 12:00PM | Rangos 1 | ICOTOM-S5-006-2008 | Esling, C. | 2-Jun | 11:00AM | Connan | ICOTOM-S8-003-2008 |
| Barbe, L. | 2-Jun | 9:30AM | Rangos 2 & 3 | ICOTOM-P-024-2008 | | | | | |
| Barbier, D. | 5-Jun | 4:30PM | Rangos 3 | ICOTOM-S3-032-2008 | | | | | |
| Barbier, D. | 2-Jun | 9:30AM | Rangos 2 & 3 | ICOTOM-P-016-2008 | | | | | |
| Barbé, L. | 5-Jun | 2:45PM | Rangos 3 | ICOTOM-S3-027-2008 | Fanta, A.B. | 5-Jun | 5:15PM | Rangos 3 | ICOTOM-S3-035-2008 |
| Barlat, F. | 6-Jun | 9:30AM | Connan | ICOTOM-S13-016-2008 | Fanta, A.B. | 2-Jun | 9:30AM | Rangos 2 & 3 | ICOTOM-P-028-2008 |
| Barmak, K. | 5-Jun | 11:30AM | Rangos 2 | ICOTOM-S2-008-2008 | Fast, T. | 2-Jun | 9:30AM | Rangos 2 & 3 | ICOTOM-P-072-2008 |
| Barnett, M.R. | 2-Jun | 10:15AM | McConomy Auditorium | ICOTOM-S9-001-2008 | Field, D. | 2-Jun | 9:30AM | Rangos 2 & 3 | ICOTOM-P-008-2008 |
| Beausir, B. | 3-Jun | 1:45PM | McConomy Auditorium | ICOTOM-S9-029-2008 | Field, D.P. | 6-Jun | 9:30AM | Rangos 1 | ICOTOM-S1-003-2008 |
| Ben Achma, R. | 2-Jun | 9:30AM | Rangos 2 & 3 | ICOTOM-P-033-2008 | Fonda, R.W. | 6-Jun | 8:30AM | Rangos 1 | ICOTOM-S1-001-2008 |
| Bennett, T. | 5-Jun | 3:15PM | Rangos 2 | ICOTOM-S10-007-2008 | Fromm, B.S. | 3-Jun | 9:00AM | McConomy Auditorium | ICOTOM-S9-021-2008 |
| Bhattacharyya, A. | 2-Jun | 9:30AM | Rangos 2 & 3 | ICOTOM-P-025-2008 | Frommert, M. | 5-Jun | 10:45AM | Rangos 3 | ICOTOM-S3-017-2008 |
| Bieler, T.R. | 6-Jun | 9:15AM | Connan | ICOTOM-S13-015-2008 | Fukutomi, H. | 5-Jun | 9:45AM | Connan | ICOTOM-S12-031-2008 |
| Bingert, J. | 4-Jun | 9:45AM | Rangos 2 | ICOTOM-S9-040-2008 | Fullwood, D. | 4-Jun | 8:30AM | Connan | ICOTOM-S12-014-2008 |
| Bocher, P. | 5-Jun | 5:15PM | Connan | ICOTOM-S13-012-2008 | | | | | |
| Boehlert, C.J. | 4-Jun | 10:45AM | Rangos 2 | ICOTOM-S9-042-2008 | | | | | |
| Bollmann, C. | 2-Jun | 9:30AM | Rangos 2 & 3 | ICOTOM-P-052-2008 | Gao, M. | 2-Jun | 9:30AM | Rangos 2 & 3 | ICOTOM-P-038-2008 |
| Bolmaro, R.E. | 6-Jun | 12:00PM | Rangos 3 | ICOTOM-S3-051-2008 | Garbe, U. | 3-Jun | 9:45AM | Rangos 1 | ICOTOM-S5-023-2008 |
| Bolmaro, R.E. | 6-Jun | 8:30AM | Rangos 2 | ICOTOM-S10-014-2008 | Garcia, R. | 3-Jun | 11:00AM | Connan | ICOTOM-S6-008-2008 |
| Bolmaro, R.E. | 2-Jun | 9:30AM | Rangos 2 & 3 | ICOTOM-P-027-2008 | Garcia, R. | 5-Jun | 11:45AM | Connan | ICOTOM-S12-037-2008 |
| Bolmaro, R.E. | 2-Jun | 9:30AM | Rangos 2 & 3 | ICOTOM-P-039-2008 | Garmestani, H. | 2-Jun | 5:45PM | Connan | ICOTOM-S11-010-2008 |
| Bolmaro, R.E. | 2-Jun | 9:30AM | Rangos 2 & 3 | ICOTOM-P-080-2008 | Garmestani, H. | 2-Jun | 9:30AM | Rangos 2 & 3 | ICOTOM-P-043-2008 |
| Bouzy, E. | 2-Jun | 3:00PM | McConomy Auditorium | ICOTOM-S9-012-2008 | Gerspach, F. | 6-Jun | 11:00AM | Rangos 2 | ICOTOM-S10-021-2008 |
| Bowman, K.J. | 3-Jun | 12:00PM | Connan | ICOTOM-S6-011-2008 | Gervasyeva, I. | 5-Jun | 12:15PM | Rangos 2 | ICOTOM-S2-010-2008 |
| Bozzolo, N. | 2-Jun | 1:45PM | McConomy Auditorium | ICOTOM-S9-008-2008 | Gervasyeva, I. | 2-Jun | 9:30AM | Rangos 2 & 3 | ICOTOM-P-006-2008 |
| Brahme, A. | 5-Jun | 5:00PM | Rangos 3 | ICOTOM-S3-034-2008 | Gholinia, A. | 3-Jun | 11:15AM | Rangos 1 | ICOTOM-S5-025-2008 |
| Brown, D.W. | 2-Jun | 11:15AM | McConomy Auditorium | ICOTOM-S9-004-2008 | Gibala, R. | 6-Jun | 9:00AM | Rangos 3 | ICOTOM-S3-040-2008 |
| Budai, J.D. | 2-Jun | 11:30AM | Rangos 1 | ICOTOM-S5-005-2008 | Godet, S. | 5-Jun | 3:15PM | Rangos 3 | ICOTOM-S3-029-2008 |
| Buffiere, J. | 5-Jun | 1:45PM | Connan | ICOTOM-S13-001-2008 | Goyal, A. | 5-Jun | 11:45AM | Rangos 2 | ICOTOM-S2-009-2008 |
| | | | | | | | | | |
| C | | | | | | | | | |
| Calcagnotto, M. | 5-Jun | 1:45PM | Rangos 3 | ICOTOM-S3-023-2008 | Grekhov, M. | 2-Jun | 9:30AM | Rangos 2 & 3 | ICOTOM-P-050-2008 |
| Camata, R.P. | 2-Jun | 4:15PM | Connan | ICOTOM-S11-005-2008 | Griera, A. | 2-Jun | 9:30AM | Rangos 2 & 3 | ICOTOM-P-076-2008 |
| Cernik, M. | 5-Jun | 5:30PM | Rangos 3 | ICOTOM-S3-036-2008 | Griesshaber, E. | 2-Jun | 2:45PM | Connan | ICOTOM-S11-003-2008 |
| Chakraborty, A. | 6-Jun | 9:15AM | Rangos 3 | ICOTOM-S3-041-2008 | Griesshaber, E. | 2-Jun | 9:30AM | Rangos 2 & 3 | ICOTOM-P-060-2008 |
| Chan, L.H. | 3-Jun | 5:00PM | Rangos 1 | ICOTOM-S7-009-2008 | Griesshaber, E. | 2-Jun | 9:30AM | Rangos 2 & 3 | ICOTOM-P-061-2008 |
| Chang, S.K. | 5-Jun | 9:45AM | Rangos 3 | ICOTOM-S3-015-2008 | Gueguen, O. | 4-Jun | 12:15PM | Connan | ICOTOM-S12-026-2008 |
| Chen, L. | 6-Jun | 11:45AM | Rangos 3 | ICOTOM-S3-050-2008 | Gupta, V.K. | 5-Jun | 3:00PM | Connan | ICOTOM-S13-005-2008 |
| Chen, L. | 2-Jun | 9:30AM | Rangos 2 & 3 | ICOTOM-P-079-2008 | Gurao, N. | 2-Jun | 9:30AM | Rangos 2 & 3 | ICOTOM-P-070-2008 |
| Cho, J. | 3-Jun | 3:15PM | McConomy Auditorium | ICOTOM-S9-033-2008 | Gurao, N.P. | 5-Jun | 5:15PM | Rangos 1 | ICOTOM-S4-011-2008 |
| Cho, J. | 6-Jun | 10:45AM | Rangos 1 | ICOTOM-S1-005-2008 | | | | | |
| Cho, J. | 2-Jun | 9:30AM | Rangos 2 & 3 | ICOTOM-P-054-2008 | | | | | |
| Choi, J. | 2-Jun | 9:30AM | Rangos 2 & 3 | ICOTOM-P-047-2008 | | | | | |
| Choi, S. | 3-Jun | 10:45AM | McConomy Auditorium | ICOTOM-S9-025-2008 | | | | | |
| Chun-Chih, L. | 5-Jun | 11:15AM | Rangos 3 | ICOTOM-S3-019-2008 | | | | | |
| Clausen, B. | 5-Jun | 4:00PM | Rangos 1 | ICOTOM-S4-006-2008 | | | | | |
| Coghe, F. | 4-Jun | 9:00AM | Rangos 2 | ICOTOM-S9-037-2008 | | | | | |
| Comer, M.L. | 5-Jun | 12:15PM | Rangos 1 | ICOTOM-S14-011-2008 | | | | | |
| Cottam, R. | 2-Jun | 4:30PM | McConomy Auditorium | ICOTOM-S9-015-2008 | | | | | |
| Cottam, R. | 2-Jun | 9:30AM | Rangos 2 & 3 | ICOTOM-P-056-2008 | | | | | |
| | | | | | | | | | |
| D | | | | | | | | | |
| da Fonseca, J.Q. | 2-Jun | 12:00PM | McConomy Auditorium | ICOTOM-S9-007-2008 | Haldar, A. | 4-Jun | 9:45AM | Rangos 3 | ICOTOM-S3-004-2008 |
| Dawson, P. | 5-Jun | 9:30AM | Rangos 1 | ICOTOM-S14-004-2008 | Haldar, A. | 4-Jun | 11:15AM | Rangos 3 | ICOTOM-S3-008-2008 |
| Daymond, M.R. | 2-Jun | 5:00PM | McConomy Auditorium | ICOTOM-S9-017-2008 | Haldar, A. | 5-Jun | 2:30PM | Rangos 1 | ICOTOM-S4-003-2008 |
| De Keyser, K. | 5-Jun | 11:00AM | Rangos 2 | ICOTOM-S2-006-2008 | Hantcherli, L.A. | 5-Jun | 2:30PM | Rangos 3 | ICOTOM-S3-026-2008 |
| | | | | | Hartley, C.S. | 4-Jun | 10:45AM | Connan | ICOTOM-S12-020-2008 |
| | | | | | He, Y. | 3-Jun | 4:45PM | Rangos 1 | ICOTOM-S7-008-2008 |
| | | | | | Hernandez-Silva, O. | 5-Jun | 4:45PM | Rangos 2 | ICOTOM-S10-011-2008 |
| | | | | | Herrera, C. | 5-Jun | 8:30AM | Rangos 3 | ICOTOM-S3-010-2008 |
| | | | | | Hiwarkar, V.D. | 2-Jun | 5:15PM | McConomy Auditorium | ICOTOM-S9-018-2008 |
| | | | | | Hochrainer, T. | 3-Jun | 11:15AM | McConomy Auditorium | ICOTOM-S9-027-2008 |
| | | | | | Hoseini, M. | 5-Jun | 10:45AM | Connan | ICOTOM-S12-033-2008 |
| | | | | | Hou, C. | 6-Jun | 11:30AM | Rangos 3 | ICOTOM-S3-049-2008 |
| | | | | | Hou, C. | 2-Jun | 9:30AM | Rangos 2 & 3 | ICOTOM-P-015-2008 |
| | | | | | House, J.W. | 5-Jun | 11:00AM | Connan | ICOTOM-S12-034-2008 |
| | | | | | Hrabcakova, L. | 6-Jun | 10:45AM | Rangos 3 | ICOTOM-S3-046-2008 |
| | | | | | Hu, X. | 6-Jun | 10:30AM | Connan | ICOTOM-S13-017-2008 |
| | | | | | | | | | |
| | | | | | E | | | | |
| | | | | | | | | | |
| | | | | | F | | | | |
| | | | | | | | | | |
| | | | | | G | | | | |
| | | | | | | | | | |
| | | | | | H | | | | |
| | | | | | | | | | |

Presenting Author List

| Name | Date | Time | Room | Abstract Number | Name | Date | Time | Room | Abstract Number |
|------------------|-------|---------|---------------------|---------------------|----------------|-------|---------|---------------------|---------------------|
| Huh, M. | 3-Jun | 5:30PM | Connan | ICOTOM-S12-012-2008 | Lim, C. | 6-Jun | 9:15AM | Rangos 2 | ICOTOM-S10-016-2008 |
| Humbert, M. | 2-Jun | 9:30AM | Rangos 2 & 3 | ICOTOM-P-048-2008 | Lischewski, I. | 5-Jun | 4:45PM | Rangos 1 | ICOTOM-S4-009-2008 |
| Hutchinson, B. | 6-Jun | 8:45AM | Rangos 3 | ICOTOM-S3-039-2008 | Liu, D. | 5-Jun | 9:30AM | Connan | ICOTOM-S12-030-2008 |
| I | | | | | Liu, T. | 2-Jun | 2:45PM | Rangos 1 | ICOTOM-S5-011-2008 |
| Inagaki, H. | 4-Jun | 9:00AM | Rangos 3 | ICOTOM-S3-002-2008 | Liu, T. | 5-Jun | 9:30AM | Rangos 2 | ICOTOM-S2-004-2008 |
| Inal, K. | 3-Jun | 5:15PM | Connan | ICOTOM-S12-011-2008 | Liu, T. | 2-Jun | 9:30AM | Rangos 2 & 3 | ICOTOM-P-011-2008 |
| Inoue, H. | 5-Jun | 5:15PM | Rangos 2 | ICOTOM-S10-013-2008 | Liu, Y. | 6-Jun | 11:00AM | Connan | ICOTOM-S13-019-2008 |
| Ioana, A. | 6-Jun | 9:30AM | Rangos 3 | ICOTOM-S3-042-2008 | Logé, R.E. | 5-Jun | 11:00AM | Rangos 1 | ICOTOM-S14-006-2008 |
| Isaenkova, M. | 4-Jun | 9:30AM | Rangos 2 | ICOTOM-S9-039-2008 | Lu, Y. | 2-Jun | 9:30AM | Rangos 2 & 3 | ICOTOM-P-035-2008 |
| Ito, K. | 5-Jun | 2:45PM | Rangos 2 | ICOTOM-S10-005-2008 | Lubin, S. | 4-Jun | 9:30AM | Rangos 3 | ICOTOM-S3-003-2008 |
| J | | | | | M | | | | |
| Jepson, P. | 2-Jun | 5:30PM | Rangos 1 | ICOTOM-S5-018-2008 | Ma, D. | 3-Jun | 4:45PM | Connan | ICOTOM-S12-009-2008 |
| Jiang, L. | 2-Jun | 11:00AM | McConomy Auditorium | ICOTOM-S9-003-2008 | MacSleyne, J. | 5-Jun | 12:00PM | Rangos 1 | ICOTOM-S14-010-2008 |
| Jiang, L. | 3-Jun | 4:30PM | McConomy Auditorium | ICOTOM-S9-035-2008 | Majumdar, B.S. | 5-Jun | 3:15PM | Rangos 1 | ICOTOM-S4-005-2008 |
| Jones, J.L. | 3-Jun | 11:45AM | Connan | ICOTOM-S6-010-2008 | Majumdar, B.S. | 5-Jun | 9:00AM | Connan | ICOTOM-S12-028-2008 |
| Joo, H. | 2-Jun | 9:30AM | Rangos 2 & 3 | ICOTOM-P-018-2008 | Mallapur, D.G. | 2-Jun | 9:30AM | Rangos 2 & 3 | ICOTOM-P-065-2008 |
| K | | | | | Man, C. | 5-Jun | 8:30AM | Connan | ICOTOM-S12-027-2008 |
| Kacher, J.P. | 3-Jun | 9:00AM | Rangos 1 | ICOTOM-S5-020-2008 | Maniatty, A. | 6-Jun | 8:30AM | Connan | ICOTOM-S13-013-2008 |
| Kalidindi, S. | 3-Jun | 1:45PM | Connan | ICOTOM-S12-001-2008 | Mao, W. | 2-Jun | 5:00PM | Rangos 1 | ICOTOM-S5-016-2008 |
| Kamikawa, N. | 5-Jun | 3:15PM | Connan | ICOTOM-S13-006-2008 | Mao, W. | 5-Jun | 12:00PM | Rangos 3 | ICOTOM-S3-022-2008 |
| Kanjarla, A.K. | 3-Jun | 4:30PM | Connan | ICOTOM-S12-008-2008 | Mao, W. | 2-Jun | 9:30AM | Rangos 2 & 3 | ICOTOM-P-064-2008 |
| Karthikeyan, T. | 2-Jun | 9:30AM | Rangos 2 & 3 | ICOTOM-P-085-2008 | Martin, A. | 2-Jun | 4:15PM | McConomy Auditorium | ICOTOM-S9-014-2008 |
| Kashihara, K. | 5-Jun | 2:15PM | Rangos 2 | ICOTOM-S10-003-2008 | Mason, J. | 4-Jun | 10:30AM | Connan | ICOTOM-S12-019-2008 |
| Kashyap, K. | 2-Jun | 9:30AM | Rangos 2 & 3 | ICOTOM-P-084-2008 | Masui, H. | 3-Jun | 8:30AM | Connan | ICOTOM-S6-001-2008 |
| Kestens, L.A. | 4-Jun | 8:30AM | Rangos 3 | ICOTOM-S3-001-2008 | Masui, H. | 5-Jun | 1:45PM | Rangos 2 | ICOTOM-S10-001-2008 |
| Khatirkar, R. | 4-Jun | 11:30AM | Rangos 3 | ICOTOM-S3-009-2008 | Merkel, S. | 5-Jun | 1:45PM | Rangos 1 | ICOTOM-S4-001-2008 |
| Kim, D. | 2-Jun | 9:30AM | Rangos 2 & 3 | ICOTOM-P-053-2008 | Merriman, C.C. | 5-Jun | 5:00PM | Rangos 1 | ICOTOM-S4-010-2008 |
| Kim, I. | 3-Jun | 9:30AM | Connan | ICOTOM-S6-005-2008 | Mguil, S. | 3-Jun | 9:45AM | McConomy Auditorium | ICOTOM-S9-024-2008 |
| Kim, I. | 5-Jun | 12:00PM | Connan | ICOTOM-S12-038-2008 | Mguil, S. | 4-Jun | 11:15AM | Connan | ICOTOM-S12-022-2008 |
| Kim, I. | 2-Jun | 9:30AM | Rangos 2 & 3 | ICOTOM-P-019-2008 | Miller, H.M. | 3-Jun | 5:45PM | Rangos 1 | ICOTOM-S7-012-2008 |
| Kimura, K. | 5-Jun | 9:00AM | Rangos 3 | ICOTOM-S3-012-2008 | Miller, M.P. | 2-Jun | 4:15PM | Rangos 1 | ICOTOM-S5-014-2008 |
| Kimura, T. | 3-Jun | 3:15PM | Rangos 1 | ICOTOM-S7-006-2008 | Mishra, S.K. | 6-Jun | 10:30AM | Rangos 3 | ICOTOM-S3-045-2008 |
| Kinderlehrer, D. | 3-Jun | 5:30PM | Rangos 1 | ICOTOM-S7-011-2008 | Mohamed, W.M. | 4-Jun | 9:15AM | Rangos 2 | ICOTOM-S9-038-2008 |
| King, A. | 5-Jun | 9:00AM | Rangos 2 | ICOTOM-S2-002-2008 | Mohamed, W.M. | 4-Jun | 11:00AM | Rangos 2 | ICOTOM-S9-043-2008 |
| Knezevic, M. | 4-Jun | 12:00PM | Connan | ICOTOM-S12-025-2008 | Molodov, D.A. | 2-Jun | 11:15AM | Connan | ICOTOM-S8-004-2008 |
| Knipling, K. | 6-Jun | 11:30AM | Rangos 1 | ICOTOM-S1-008-2008 | Morawiec, A. | 3-Jun | 9:15AM | Rangos 1 | ICOTOM-S5-021-2008 |
| Ko, K. | 2-Jun | 9:30AM | Rangos 2 & 3 | ICOTOM-P-023-2008 | Morris, P.R. | 4-Jun | 9:00AM | Connan | ICOTOM-S12-015-2008 |
| Kobayashi, S. | 5-Jun | 4:30PM | Connan | ICOTOM-S13-009-2008 | Mu, S. | 3-Jun | 11:00AM | McConomy Auditorium | ICOTOM-S9-026-2008 |
| Kozaczek, K. | 5-Jun | 10:30AM | Rangos 2 | ICOTOM-S2-005-2008 | N | | | | |
| Kulovits, A. | 5-Jun | 9:15AM | Rangos 2 | ICOTOM-S2-003-2008 | Nakamichi, H. | 2-Jun | 9:30AM | Rangos 2 & 3 | ICOTOM-P-017-2008 |
| Kulovits, A. | 5-Jun | 4:00PM | Connan | ICOTOM-S13-007-2008 | Namba, E. | 5-Jun | 11:00AM | Rangos 3 | ICOTOM-S3-018-2008 |
| Kumar, V. | 4-Jun | 9:15AM | Rangos 1 | ICOTOM-S7-015-2008 | Necker, C.T. | 6-Jun | 10:30AM | Rangos 2 | ICOTOM-S10-019-2008 |
| Kusters, S. | 4-Jun | 9:30AM | Connan | ICOTOM-S12-017-2008 | Neil, C. | 3-Jun | 9:15AM | McConomy Auditorium | ICOTOM-S9-022-2008 |
| L | | | | | Niezgoda, S.R. | 5-Jun | 11:45AM | Rangos 1 | ICOTOM-S14-009-2008 |
| Lagoeiro, L. | 3-Jun | 2:15PM | Rangos 1 | ICOTOM-S7-002-2008 | Nnamchi, P. | 2-Jun | 9:30AM | Rangos 2 & 3 | ICOTOM-P-012-2008 |
| Lagoeiro, L. | 6-Jun | 11:45AM | Rangos 2 | ICOTOM-S10-024-2008 | Noureddine, M. | 5-Jun | 4:15PM | Rangos 3 | ICOTOM-S3-031-2008 |
| Landheer, H. | 4-Jun | 12:00PM | Rangos 1 | ICOTOM-S7-024-2008 | Nowell, M. | 6-Jun | 11:15AM | Rangos 3 | ICOTOM-S3-048-2008 |
| Landi, G. | 3-Jun | 3:00PM | Connan | ICOTOM-S12-005-2008 | O | | | | |
| Landon, C.D. | 2-Jun | 4:45PM | Rangos 1 | ICOTOM-S5-015-2008 | Oertel, C. | 5-Jun | 9:15AM | Connan | ICOTOM-S12-029-2008 |
| Laughlin, D.E. | 5-Jun | 11:15AM | Rangos 2 | ICOTOM-S2-007-2008 | Oh, K. | 2-Jun | 1:45PM | Rangos 1 | ICOTOM-S5-008-2008 |
| Lebensohn, R. | 3-Jun | 2:45PM | Connan | ICOTOM-S12-004-2008 | Okayasu, K. | 2-Jun | 9:30AM | Rangos 2 & 3 | ICOTOM-P-055-2008 |
| Lebensohn, R. | 5-Jun | 8:30AM | Rangos 1 | ICOTOM-S14-001-2008 | Ozer, I.O. | 2-Jun | 9:30AM | Rangos 2 & 3 | ICOTOM-P-068-2008 |
| LeDonne, J. | 3-Jun | 5:15PM | Rangos 1 | ICOTOM-S7-010-2008 | P | | | | |
| Lee, D. | 6-Jun | 9:45AM | Rangos 2 | ICOTOM-S10-018-2008 | Papillon, F. | 3-Jun | 2:45PM | Rangos 1 | ICOTOM-S7-004-2008 |
| Lee, H. | 2-Jun | 9:30AM | Rangos 2 & 3 | ICOTOM-P-037-2008 | Park, J. | 2-Jun | 9:30AM | Rangos 2 & 3 | ICOTOM-P-021-2008 |
| Lee, M. | 2-Jun | 2:15PM | Connan | ICOTOM-S11-002-2008 | Park, N. | 4-Jun | 11:15AM | Rangos 2 | ICOTOM-S9-044-2008 |
| Lee, M. | 2-Jun | 5:15PM | Connan | ICOTOM-S11-008-2008 | Park, S. | 5-Jun | 3:00PM | Rangos 3 | ICOTOM-S3-028-2008 |
| Lee, S. | 2-Jun | 9:30AM | Rangos 2 & 3 | ICOTOM-P-031-2008 | Park, Y. | 4-Jun | 11:45AM | Rangos 1 | ICOTOM-S7-023-2008 |
| Lee, S. | 2-Jun | 9:30AM | Rangos 2 & 3 | ICOTOM-P-041-2008 | Paul, H. | 2-Jun | 9:30AM | Rangos 2 & 3 | ICOTOM-P-029-2008 |
| Leffers, T. | 3-Jun | 5:45PM | Connan | ICOTOM-S12-013-2008 | Paul, H. | 2-Jun | 9:30AM | Rangos 2 & 3 | ICOTOM-P-067-2008 |
| Leffers, T. | 4-Jun | 9:45AM | Connan | ICOTOM-S12-018-2008 | Penelle, R. | 5-Jun | 10:30AM | Rangos 3 | ICOTOM-S3-016-2008 |
| Lewis, A.C. | 3-Jun | 4:15PM | Connan | ICOTOM-S12-007-2008 | Penelle, R. | 5-Jun | 11:45AM | Rangos 3 | ICOTOM-S3-021-2008 |
| León García, O. | 5-Jun | 2:45PM | Connan | ICOTOM-S13-004-2008 | Penelle, R. | 2-Jun | 9:30AM | Rangos 2 & 3 | ICOTOM-P-001-2008 |
| Li, B. | 2-Jun | 4:45PM | Connan | ICOTOM-S11-006-2008 | Penelle, R. | 2-Jun | 9:30AM | Rangos 2 & 3 | ICOTOM-P-058-2008 |
| Li, B. | 2-Jun | 9:30AM | Rangos 2 & 3 | ICOTOM-P-046-2008 | Perlovich, Y. | 2-Jun | 11:00AM | Rangos 1 | ICOTOM-S5-003-2008 |
| Li, H. | 3-Jun | 11:30AM | McConomy Auditorium | ICOTOM-S9-028-2008 | Petrov, R.H. | 2-Jun | 12:15PM | Rangos 1 | ICOTOM-S5-007-2008 |
| Li, J. | 6-Jun | 10:45AM | Connan | ICOTOM-S13-018-2008 | Petrova, R. | 2-Jun | 9:30AM | Rangos 2 & 3 | ICOTOM-P-034-2008 |
| Li, S. | 3-Jun | 2:45PM | McConomy Auditorium | ICOTOM-S9-031-2008 | Pinto, A.L. | 4-Jun | 10:30AM | Rangos 3 | ICOTOM-S3-005-2008 |
| Lienert, U. | 3-Jun | 8:30AM | Rangos 1 | ICOTOM-S5-019-2008 | Pinto, A.L. | 2-Jun | 9:30AM | Rangos 2 & 3 | ICOTOM-P-014-2008 |

Presenting Author List

| Name | Date | Time | Room | Abstract Number | Name | Date | Time | Room | Abstract Number |
|-----------------------|-------|---------|---------------------|---------------------|------|------|------|------|-----------------|
| Piot, D.J. | 3-Jun | 5:00PM | Connan | ICOTOM-S12-010-2008 | | | | | |
| Poulon, A. | 6-Jun | 10:45AM | Rangos 2 | ICOTOM-S10-020-2008 | | | | | |
| Prakash, A. | 4-Jun | 11:30AM | Connan | ICOTOM-S12-023-2008 | | | | | |
| | | | Q | | | | | | |
| Quadir, M.Z. | 5-Jun | 12:15PM | Connan | ICOTOM-S12-039-2008 | | | | | |
| Quadir, M.Z. | 2-Jun | 9:30AM | Rangos 2 & 3 | ICOTOM-P-069-2008 | | | | | |
| Quey, R. | 2-Jun | 10:45AM | Rangos 1 | ICOTOM-S5-002-2008 | | | | | |
| | | | R | | | | | | |
| Raabe, D. | 2-Jun | 11:15AM | Rangos 1 | ICOTOM-S5-004-2008 | | | | | |
| Raabe, D. | 2-Jun | 2:30PM | McConomy Auditorium | ICOTOM-S9-010-2008 | | | | | |
| Raabe, D. | 2-Jun | 1:45PM | Connan | ICOTOM-S11-001-2008 | | | | | |
| Raabe, D. | 2-Jun | 5:00PM | Connan | ICOTOM-S11-007-2008 | | | | | |
| Raabe, D. | 3-Jun | 2:15PM | Connan | ICOTOM-S12-002-2008 | | | | | |
| Raabe, D. | 5-Jun | 2:00PM | Rangos 3 | ICOTOM-S3-024-2008 | | | | | |
| Radhakrishnan, B. | 2-Jun | 9:30AM | Rangos 2 & 3 | ICOTOM-P-082-2008 | | | | | |
| Raghunathan, S.L. | 5-Jun | 4:15PM | Rangos 1 | ICOTOM-S4-007-2008 | | | | | |
| Ramesh, M. | 5-Jun | 2:15PM | Connan | ICOTOM-S13-002-2008 | | | | | |
| Randle, V. | 3-Jun | 4:15PM | Rangos 1 | ICOTOM-S7-007-2008 | | | | | |
| Rao, K.S. | 3-Jun | 3:00PM | Rangos 1 | ICOTOM-S7-005-2008 | | | | | |
| Raveendra, S. | 5-Jun | 4:15PM | Rangos 2 | ICOTOM-S10-009-2008 | | | | | |
| Ray, R.K. | 4-Jun | 11:00AM | Rangos 3 | ICOTOM-S3-007-2008 | | | | | |
| Ray, R.K. | 6-Jun | 9:30AM | Rangos 2 | ICOTOM-S10-017-2008 | | | | | |
| Resk, H. | 5-Jun | 9:15AM | Rangos 1 | ICOTOM-S14-003-2008 | | | | | |
| Reynolds, A.P. | 6-Jun | 9:45AM | Rangos 1 | ICOTOM-S1-004-2008 | | | | | |
| Riesterer, J.L. | 3-Jun | 2:30PM | Rangos 1 | ICOTOM-S7-003-2008 | | | | | |
| Roberts, C. | 2-Jun | 9:30AM | Rangos 2 & 3 | ICOTOM-P-078-2008 | | | | | |
| Rohrer, G.S. | 3-Jun | 1:45PM | Rangos 1 | ICOTOM-S7-001-2008 | | | | | |
| Romano, P. | 4-Jun | 11:15AM | Rangos 1 | ICOTOM-S7-020-2008 | | | | | |
| Romero, J. | 5-Jun | 4:30PM | Rangos 1 | ICOTOM-S4-008-2008 | | | | | |
| Rowenhorst, D. | 4-Jun | 8:30AM | Rangos 1 | ICOTOM-S7-013-2008 | | | | | |
| Roy, S. | 2-Jun | 3:15PM | McConomy Auditorium | ICOTOM-S9-013-2008 | | | | | |
| Roy, S. | 2-Jun | 9:30AM | Rangos 2 & 3 | ICOTOM-P-049-2008 | | | | | |
| Rugg, D. | 3-Jun | 8:30AM | McConomy Auditorium | ICOTOM-S9-019-2008 | | | | | |
| Ryttberg, K. | 5-Jun | 5:45PM | Rangos 3 | ICOTOM-S3-037-2008 | | | | | |
| Ryu, H. | 2-Jun | 9:30AM | Rangos 2 & 3 | ICOTOM-P-062-2008 | | | | | |
| | | | S | | | | | | |
| Saha, R. | 4-Jun | 10:45AM | Rangos 3 | ICOTOM-S3-006-2008 | | | | | |
| Sahoo, S.K. | 2-Jun | 11:45AM | McConomy Auditorium | ICOTOM-S9-006-2008 | | | | | |
| Saimoto, S. | 5-Jun | 4:45PM | Connan | ICOTOM-S13-010-2008 | | | | | |
| Sakai, T. | 3-Jun | 2:15PM | McConomy Auditorium | ICOTOM-S9-030-2008 | | | | | |
| Salem, A.A. | 2-Jun | 2:15PM | McConomy Auditorium | ICOTOM-S9-009-2008 | | | | | |
| Samajdar, I. | 6-Jun | 11:45AM | Rangos 1 | ICOTOM-S1-009-2008 | | | | | |
| Samajdar, I. | 2-Jun | 9:30AM | Rangos 2 & 3 | ICOTOM-P-003-2008 | | | | | |
| Sandim, H.R. | 5-Jun | 9:30AM | Rangos 3 | ICOTOM-S3-014-2008 | | | | | |
| Sato, Y.S. | 6-Jun | 9:00AM | Rangos 1 | ICOTOM-S1-002-2008 | | | | | |
| Saukkonen, T. | 6-Jun | 11:15AM | Rangos 1 | ICOTOM-S1-007-2008 | | | | | |
| Schaarschuch, R. | 2-Jun | 9:30AM | Rangos 2 & 3 | ICOTOM-P-010-2008 | | | | | |
| Schmahl, W. | 2-Jun | 5:30PM | Connan | ICOTOM-S11-009-2008 | | | | | |
| Schäfer, C. | 5-Jun | 2:30PM | Rangos 2 | ICOTOM-S10-004-2008 | | | | | |
| Seefeldt, M. | 5-Jun | 4:45PM | Rangos 3 | ICOTOM-S3-033-2008 | | | | | |
| Serebryany, V. | 2-Jun | 11:30AM | McConomy Auditorium | ICOTOM-S9-005-2008 | | | | | |
| Serebryany, V. | 4-Jun | 11:30AM | Rangos 2 | ICOTOM-S9-045-2008 | | | | | |
| Sha, Y. | 5-Jun | 11:30AM | Rangos 3 | ICOTOM-S3-020-2008 | | | | | |
| Sha, Y. | 2-Jun | 9:30AM | Rangos 2 & 3 | ICOTOM-P-044-2008 | | | | | |
| Shahbazian Yassar, R. | 6-Jun | 12:00PM | Rangos 2 | ICOTOM-S10-025-2008 | | | | | |
| Sheikh-Ali, A.D. | 2-Jun | 10:45AM | Connan | ICOTOM-S8-002-2008 | | | | | |
| Shi, M. | 3-Jun | 4:15PM | McConomy Auditorium | ICOTOM-S9-034-2008 | | | | | |
| Sidor, J. | 5-Jun | 4:00PM | Rangos 2 | ICOTOM-S10-008-2008 | | | | | |
| Signorelli, J.W. | 2-Jun | 9:30AM | Rangos 2 & 3 | ICOTOM-P-073-2008 | | | | | |
| Sintay, S.D. | 5-Jun | 2:30PM | Connan | ICOTOM-S13-003-2008 | | | | | |
| Skrotzki, W. | 3-Jun | 8:45AM | Connan | ICOTOM-S6-002-2008 | | | | | |
| Snel, M. | 2-Jun | 9:30AM | Rangos 2 & 3 | ICOTOM-P-032-2008 | | | | | |
| Sotoudeh, K. | 5-Jun | 11:30AM | Connan | ICOTOM-S12-036-2008 | | | | | |
| Specht, E. | 2-Jun | 9:30AM | Rangos 2 & 3 | ICOTOM-P-005-2008 | | | | | |
| Suter, R.M. | 3-Jun | 10:45AM | Rangos 1 | ICOTOM-S5-024-2008 | | | | | |
| Suwes, S. | 2-Jun | 2:45PM | McConomy Auditorium | ICOTOM-S9-011-2008 | | | | | |
| Suzuki, T.S. | 2-Jun | 11:45AM | Connan | ICOTOM-S8-005-2008 | | | | | |
| | | | T | | | | | | |
| te Nijenhuis, J. | 2-Jun | 9:30AM | Rangos 2 & 3 | ICOTOM-P-026-2008 | | | | | |
| Takashima, M. | 2-Jun | 9:30AM | Rangos 2 & 3 | ICOTOM-P-030-2008 | | | | | |
| Takayama, Y. | 6-Jun | 11:15AM | Rangos 2 | ICOTOM-S10-022-2008 | | | | | |
| Tanimoto, Y. | 2-Jun | 12:00PM | Connan | ICOTOM-S8-006-2008 | | | | | |
| Tayon, W. | 2-Jun | 9:30AM | Rangos 2 & 3 | ICOTOM-P-040-2008 | | | | | |
| Thomspon, C.V. | 5-Jun | 8:30AM | Rangos 2 | ICOTOM-S2-001-2008 | | | | | |
| Tomida, T. | 6-Jun | 8:30AM | Rangos 3 | ICOTOM-S3-038-2008 | | | | | |
| Tommaseo, C.E. | 5-Jun | 4:30PM | Rangos 2 | ICOTOM-S10-010-2008 | | | | | |
| Tong, W. | 2-Jun | 9:30AM | Rangos 2 & 3 | ICOTOM-P-059-2008 | | | | | |
| Toth, L.S. | 3-Jun | 11:45AM | McConomy Auditorium | ICOTOM-S9-046-2008 | | | | | |
| | | | U | | | | | | |
| Ushioda, K. | 4-Jun | 11:30AM | Rangos 1 | ICOTOM-S7-022-2008 | | | | | |
| Uta, E. | 4-Jun | 8:30AM | Rangos 2 | ICOTOM-S9-036-2008 | | | | | |
| | | | V | | | | | | |
| Vadlamani, S.S. | 4-Jun | 11:00AM | Rangos 1 | ICOTOM-S7-019-2008 | | | | | |
| Vadlamani, S.S. | 6-Jun | 9:00AM | Rangos 2 | ICOTOM-S10-015-2008 | | | | | |
| Van Bael, A. | 3-Jun | 3:15PM | Connan | ICOTOM-S12-006-2008 | | | | | |
| Van Boxel, S. | 5-Jun | 11:15AM | Rangos 1 | ICOTOM-S14-007-2008 | | | | | |
| Van Houtte, P. | 3-Jun | 2:30PM | Connan | ICOTOM-S12-003-2008 | | | | | |
| Verbeken, K. | 5-Jun | 2:15PM | Rangos 3 | ICOTOM-S3-025-2008 | | | | | |
| Vogel, S.C. | 5-Jun | 2:15PM | Rangos 1 | ICOTOM-S4-002-2008 | | | | | |
| Voorhees, P. | 4-Jun | 10:30AM | Rangos 1 | ICOTOM-S7-018-2008 | | | | | |
| | | | W | | | | | | |
| Wang, S. | 5-Jun | 3:00PM | Rangos 2 | ICOTOM-S10-006-2008 | | | | | |
| Wang, Y. | 3-Jun | 3:00PM | McConomy Auditorium | ICOTOM-S9-032-2008 | | | | | |
| Waryoba, D.R. | 4-Jun | 9:00AM | Rangos 1 | ICOTOM-S7-014-2008 | | | | | |
| Waryoba, D.R. | 2-Jun | 9:30AM | Rangos 2 & 3 | ICOTOM-P-004-2008 | | | | | |
| Watanabe, T. | 2-Jun | 10:15AM | Connan | ICOTOM-S8-001-2008 | | | | | |
| Wauthier, A. | 5-Jun | 4:00PM | Rangos 3 | ICOTOM-S3-030-2008 | | | | | |
| Wauthier, A. | 2-Jun | 9:30AM | Rangos 2 & 3 | ICOTOM-P-036-2008 | | | | | |
| Wenk, H. | 5-Jun | 2:45PM | Rangos 1 | ICOTOM-S4-004-2008 | | | | | |
| Whitacre, J. | 2-Jun | 9:30AM | Rangos 2 & 3 | ICOTOM-P-007-2008 | | | | | |
| Wilson, S. | 4-Jun | 9:45AM | Rangos 1 | ICOTOM-S7-017-2008 | | | | | |
| Winning, M. | 5-Jun | 2:00PM | Rangos 2 | ICOTOM-S10-002-2008 | | | | | |
| Winter, M. | 3-Jun | 9:45AM | Connan | ICOTOM-S6-006-2008 | | | | | |
| Winther, G. | 2-Jun | 10:15AM | Rangos 1 | ICOTOM-S5-001-2008 | | | | | |
| Wollmershauser, J.A. | 3-Jun | 9:00AM | Connan | ICOTOM-S6-003-2008 | | | | | |
| Wright, S.I. | 6-Jun | 11:00AM | Rangos 3 | ICOTOM-S3-047-2008 | | | | | |
| Wu, G. | 2-Jun | 5:15PM | Rangos 1 | ICOTOM-S5-017-2008 | | | | | |
| Wu, Q. | 6-Jun | 9:45AM | Rangos 3 | ICOTOM-S3-044-2008 | | | | | |
| | | | X | | | | | | |
| Xie, Q. | 3-Jun | 9:30AM | McConomy Auditorium | ICOTOM-S9-023-2008 | | | | | |
| Xu, W. | 2-Jun | 2:30PM | Rangos 1 | ICOTOM-S5-010-2008 | | | | | |
| Xue-bin, W. | 2-Jun | 9:30AM | Rangos 2 & 3 | ICOTOM-P-081-2008 | | | | | |
| Xusheng, Y. | 5-Jun | 4:15PM | Connan | ICOTOM-S13-008-2008 | | | | | |
| | | | Y | | | | | | |
| Yandong, L. | 5-Jun | 8:45AM | Rangos 3 | ICOTOM-S3-011-2008 | | | | | |
| Yang, N. | 2-Jun | 9:30AM | Rangos 2 & 3 | ICOTOM-P-083-2008 | | | | | |
| Yang, P. | 2-Jun | 10:45AM | McConomy Auditorium | ICOTOM-S9-002-2008 | | | | | |
| Yang, P. | 2-Jun | 9:30AM | Rangos 2 & 3 | ICOTOM-P-009-2008 | | | | | |
| | | | Z | | | | | | |
| Zaefferer, S. | 2-Jun | 2:15PM | Rangos 1 | ICOTOM-S5-009-2008 | | | | | |
| Zaefferer, S. | 2-Jun | 4:45PM | McConomy Auditorium | ICOTOM-S9-016-2008 | | | | | |
| Zakaria, B. | 2-Jun | 9:30AM | Rangos 2 & 3 | ICOTOM-P-051-2008 | | | | | |
| Zambaldi, C. | 3-Jun | 9:15AM | Connan | ICOTOM-S6-004-2008 | | | | | |
| Zeng, Q. | 5-Jun | 5:00PM | Rangos 2 | ICOTOM-S10-012-2008 | | | | | |
| Zhang, Y. | 2-Jun | 9:30AM | Rangos 2 & 3 | ICOTOM-P-042-2008 | | | | | |
| Zhang, Y. | 2-Jun | 9:30AM | Rangos 2 & 3 | ICOTOM-P-075-2008 | | | | | |
| Zhao, X. | 2-Jun | 9:30AM | Rangos 2 & 3 | ICOTOM-P-045-2008 | | | | | |
| Zisman, A. | 5-Jun | 11:30AM | Rangos 1 | ICOTOM-S14-008-2008 | | | | | |
| Zisman, A. | 2-Jun | 9:30AM | Rangos 2 & 3 | ICOTOM-P-077-2008 | | | | | |

Monday, June 2, 2008

Monday, June 2, 2008**Plenary Session**

Room: McConomy Auditorium

Session Chair: Anthony Rollett, Carnegie Mellon University

8:30 AM**(ICOTOM-PL-001-2008) Annealing Texture Evolution (Invited)**

I. Dillamore*, Birmingham University, United Kingdom

Novel Texture Measurement Techniques Including 3D**Novel Methods Including 3D - I**

Room: Rangos 1

Session Chair: Ulrich Lienert, Argonne National Laboratory

10:15 AM**(ICOTOM-S5-001-2008) Deformation Texture Evolution Observed at the Grain Scale (Invited)**

G. Winther*, Technical University of Denmark, Denmark

10:45 AM**(ICOTOM-S5-002-2008) Local Crystal Rotations of Bulk Grains during Hot PSC in Al – 0.1 % Mn Polycrystals by High-Resolution EBSD**

R. Quey*, D. Plet, J. Driver, Ecole des Mines de Saint-Etienne, France

11:00 AM**(ICOTOM-S5-003-2008) Three Laws of Substructure Anisotropy of Textured Metal Materials, Revealed by X-ray Method of Generalized Pole Figures**

Y. Perlovich*, M. Isaenkova, V. Fesenko, Moscow Engineering Physics Institute, Russian Federation

11:15 AM**(ICOTOM-S5-004-2008) Tomographic 3D EBSD Analysis of Deformation and Rotation Patterns around Nanoindentations**

D. Raabe*, N. Zaafarani, F. Roters, S. Zaeferrer, Max-Planck-Institut für Eisenforschung, Germany

11:30 AM**(ICOTOM-S5-005-2008) Submicron-Resolution Mapping of Domains, Texture and Strain Using X-Ray Microdiffraction (Invited)**

J. D. Budai*, B. Larson, G. Ice, Oak Ridge National Laboratory, USA; W. Liu, Argonne National Lab, USA; J. Tischler, Oak Ridge National Laboratory, USA; A. Rollett, Carnegie Mellon University, USA; K. Janssens, Swiss Federal Inst. of Tech., Switzerland; D. Norton, Univ. of Florida, USA; Z. Pan, Univ. of Georgia, USA; D. Sarma, Indian Inst. of Sci., India; G. Shenoy, Argonne National Lab, USA

12:00 PM**(ICOTOM-S5-006-2008) 3D Measurements of Lattice Reorientation in the Near Surface Microstructures and Thin Layers Via Polychromatic Microdiffraction**

R. I. Barabash*, G. E. Ice, Oak Ridge National Laboratory, USA

12:15 PM**(ICOTOM-S5-007-2008) Comparative Study of 3D Techniques for Microstructural and Texture Characterization**

R. H. Petrov*, Ghent University, Belgium; O. León-García, Netherlands Institute for Metals Research, Netherlands; P. Gobernado Hernandez, Ghent University, Belgium; L. Kestens, Delft University of Technology, Netherlands

Effects of Magnetic Fields**Effects of Magnetic Fields**

Room: Connan

Session Chair: Claude Esling, CNRS UMR 7078

10:15 AM**(ICOTOM-S8-001-2008) New Approach to Texturing and Grain Boundary Engineering by Magnetic Field Application (Invited)**

T. Watanabe*, X. Zhao, L. Zuo, Northeastern University, China; S. Tsurekawa, Kumamoto University, Japan; C. Esling, Y. Zhang, University of Metz, France

10:45 AM**(ICOTOM-S8-002-2008) Effect of Ultra-high Magnetic Fields on Grain Growth and Recrystallization in Metals**

A. D. Sheikh-Ali*, H. Garmestani, Kazakh-British Technical University, Kazakhstan

11:00 AM**(ICOTOM-S8-003-2008) Eutectoid Point Shift and Orientation Relationships between Ferrite and Cementite in Pearlite in a High Magnetic Field**

C. Esling*, Y. Zhang, University of Metz, France; X. Zhao, L. Zuo, Northeastern University, China

11:15 AM**(ICOTOM-S8-004-2008) Impact of a Magnetic Field on Recrystallization Texture Evolution in Non-Ferromagnetic Metals (Invited)**

D. A. Molodov*, RWTH Aachen University, Germany

11:45 AM**(ICOTOM-S8-005-2008) Texture Development in Diamagnetic Ceramics Prepared by Slip Casting in a Strong Magnetic Field**

T. S. Suzuki*, T. Uchikoshi, Y. Sakka, National Institute for Materials Science, Japan

12:00 PM**(ICOTOM-S8-006-2008) Applications of Strong Magnetic Field to Materials Science**

Y. Tanimoto*, Hiroshima University, Japan

Hexagonal Metals**Deformation Mechanisms**

Room: McConomy Auditorium

Session Chair: Thomas Bieler, Michigan State University

10:15 AM**(ICOTOM-S9-001-2008) Non-Schmid Behaviour of Twinning in a Magnesium Alloy (Invited)**

M. R. Barnett*, Z. Keshavarz, A. G. Beer, Deakin University, Australia; X. Ma, SINTEF, Sweden

10:45 AM**(ICOTOM-S9-002-2008) Microstructure and Microtexture Evolution of Compression Twins in Magnesium**

P. Yang*, University of Science & Technology Beijing, China

11:00 AM**(ICOTOM-S9-003-2008) Effect of Twinning on the Strain Hardening Behaviors of Two Mg Alloys Subjected to Different Strain Paths**

L. Jiang*, J. J. Jonas, McGill University, Canada

11:15 AM**(ICOTOM-S9-004-2008) Development of Internal Strains and Texture during Cyclic Deformation of Extruded Mg AZ31B**

D. W. Brown*, S. C. Vogel, Los Alamos National Lab, USA; S. R. Agnew, University of Virginia, USA

11:30 AM**(ICOTOM-S9-005-2008) Dislocations in Textured Mg-4,5%Al-1%Zn Alloy: TEM and Statistical Studies**

V. Serebryany*, V. Timofeev, Y. Zaliznyak, A.A. Baikov Institute of Metallurgy and Material Science, RAS, Russian Federation

FINAL PROGRAM

Monday, June 2, 2008

11:45 AM**(ICOTOM-S9-006-2008) Heterogeneous Deformation in Single-Phase Zircaloy 2**

S. K. Sahoo*, V. D. Hiwarkar, I. Samajdar, P. Pant, IIT Bombay, India; G. K. Dey, D. Srivastav, R. Tewari, S. Banerjee, Bhabha Atomic Research Centre, India

12:00 PM**(ICOTOM-S9-007-2008) Twinning and the Texture Changes in a Zr Alloy after Small Plastic Strains**

J. Q. da Fonseca*, V. Allen, M. Preuss, The University of Manchester, United Kingdom

Novel Texture Measurement Techniques Including 3D**Novel Methods including 3D - II**

Room: Rangos 1

Session Chair: Robert Suter, Carnegie Mellon University

1:45 PM**(ICOTOM-S5-008-2008) Statistically Reliable EBSD Analysis Method of Grain Boundary Characterization (Invited)**

K. Oh*, J. Kang, E. Her, D. Kim, S. Kim, H. Han, SNU, South Korea; D. Kim, Korea Institute of Science and Technology, South Korea; H. Lee, SNU, South Korea

2:15 PM**(ICOTOM-S5-009-2008) Study on the Recrystallisation Nucleation Mechanisms of Heavily Deformed Fe36% Ni by High Resolution 3-Dimensional Orientation Microscopy**

S. Zaefferer*, Max-Planck-Institute for Iron Research, Germany

2:30 PM**(ICOTOM-S5-010-2008) Study on the Behaviours of Nucleation and Grain Growth in Deformed Ni and IF Steel by 3-D FIB-EBSD Tomography**

W. Xu*, M. Ferry, University of New South Wales, Australia

2:45 PM**(ICOTOM-S5-011-2008) 3D EBSD Texture Study on CVD Diamond Films**

T. Liu*, S. Zaefferer, D. Raabe, Max-Planck-Institut fuer Eisenforschung, Germany

3:00 PM**(ICOTOM-S5-012-2008) 3D EBSD Investigation of Orientation Patterning Phenomena in Weakly Deformed Cu Single Crystals**

O. Dmitrieva*, D. Raabe, Max-Planck-Institut fuer Eisenforschung, Germany

3:15 PM**(ICOTOM-S5-013-2008) 3D FIB-OIM of Ceramic Materials**

S. J. Dillon*, G. S. Rohrer, Carnegie Mellon University, USA

3:30 PM**Break****4:15 PM****(ICOTOM-S5-014-2008) Measuring Strain Pole Figures and Distributions of Crystal Stresses in Deforming Polycrystals Using Synchrotron X-rays (Invited)**

M. P. Miller*, J. Park, J. C. Schuren, Cornell University, USA

4:45 PM**(ICOTOM-S5-015-2008) Description of Plastic Deformation Substructure by Pair Correlations of the Dislocation Tensor**

C. D. Landon*, J. Kacher, B. L. Adams, D. Fullwood, Brigham Young University, USA

5:00 PM**(ICOTOM-S5-016-2008) Rapid Texture Determination Based on Two Dimensional X-Ray Detector**

W. Mao*, University of Science and Technology Beijing, China

5:15 PM**(ICOTOM-S5-017-2008) Development of a TEM-based Orientation Microscopy System and its Application to Study of Microstructure and Texture of Nanocrystalline NiCo Samples**

G. Wu*, S. Zaefferer, Max-Planck-Institute for Iron Research, Germany

5:30 PM**(ICOTOM-S5-018-2008) New Method for Quantification of Texture Uniformity of Plate**

P. Jepsen*, H.C. Starck Inc., USA; R. S. Bailey, Tosoh SMD, Inc., USA

Hexagonal Metals**Texture Evolution During TMP**

Room: McConomy Auditorium

Session Chair: S. Lee Semiatin, Air Force Research Laboratory

1:45 PM**(ICOTOM-S9-008-2008) Textures in hcp Titanium and Zirconium (Invited)**

N. Bozzolo*, F. Wagner, Université Paul Verlaine - Metz, France

2:15 PM**(ICOTOM-S9-009-2008) Effect of Cooling Rate on Microtexture Heterogeneity during Hot Working of Titanium Alloys with a Duplex Microstructure**

A. A. Salem*, M. G. Glavicic, S. L. Semiatin, Air Force Research Laboratory, USA

2:30 PM**(ICOTOM-S9-010-2008) Texture Evolution during Casting, Rolling and Heat Treatment of Ti-Nb and Ti-Mo-based beta-Titanium Alloys**

B. Sander, D. Ma, D. Raabe*, Max-Planck-Institut fur Eisenforschung, Germany

2:45 PM**(ICOTOM-S9-011-2008) Evolution of Transformation Texture in a Metastable β -Titanium Alloy**

S. Suwas*, N. P. Gurao, A. Ali, Indian Institute of Science, India

3:00 PM**(ICOTOM-S9-012-2008) Evolution of the Texture and Microstructure in TiAl Alloys During Heat Treatments via Massive Transformation**

A. Sankaran, E. Bouzy*, J. J. Fundenberger, A. Hazotte, Paul verline Université, France

3:15 PM**(ICOTOM-S9-013-2008) Texture Evolution in Electron Beam Melted Boron Modified Ti-6Al-4V Alloy**

S. Roy*, N. P. Gurao, S. Suwas, Indian Institute of Science, India; S. Tamirisakandala, Ohio University, USA; D. B. Miracle, Wright-Patterson AFB, USA; R. Srinivasan, Wright State University, USA

3:30 PM**Break****4:15 PM****(ICOTOM-S9-014-2008) EBSD Study of Orientation Relationships During the Dynamic Recrystallisation of Mg AM30 Deformed in the High Temperature Regime**

<. Martin*, McGill University, Canada; S. Godet, Université Libre de Bruxelles, Belgium; L. Jiang, A. Elwazri, McGill University, Canada; P. Jacques, Université Catholique de Louva, Belgium; J. Jonas, McGill University, Canada

4:30 PM**(ICOTOM-S9-015-2008) Texture Evolution During the Static Recrystallization of Three Binary Mg-Y Alloys**

R. Cottam*, J. Robson, G. Lorimer, University of Manchester, United Kingdom; B. Davis, Magnesium Elektron, United Kingdom

Monday - Tuesday, June 2-3, 2008

4:45 PM**(ICOTOM-S9-016-2008) On the Role of Twin-Intersections for the Formation of the Recrystallisation Texture in Pure Magnesium**

I. Schestakow, Max-Planck-Institute for Iron Research, Germany; S. Yi, TU Clausthal, Germany; S. Zaefferer*, Max-Planck-Institute for Iron Research, Germany

5:00 PM**(ICOTOM-S9-017-2008) Texture Inheritance and Variant Selection through the α - β Phase Transformation in Zr-2.5Nb**

M. R. Daymond*, R. A. Holt, Queen's University, Canada; S. Vogel, Los Alamos National Lab, USA

5:15 PM**(ICOTOM-S9-018-2008) Annealing Related Microstructural Developments in a Two-Phase Zr-2.5 Nb Alloy**

V. D. Hiwarkar*, S. Sahoo, I. Samajdar, K. Narasimhan, IIT, Bombay, India; K. V. Mani Krishna, G. K. Dey, D. Srivastav, R. Tiwari, S. Banarjee, Bhabha Atomic Research Centre, India

Biomaterials**Biomaterials**

Room: Connan

Session Chair: Stuart Wright, EDAX-TSL

1:45 PM**(ICOTOM-S11-001-2008) Crystallographic and Topological Textures of Biological Materials and the Resulting Anisotropy of the Mechanical Properties (Invited)**

D. Raabe*, C. Sachs, H. Fabritius, Max-Planck-Institut fuer Eisenforschung, Germany; A. Al-Sawalmih, Max-Planck-Institute of Colloids and Interfaces, Germany; L. Raue, Max-Planck-Institut fuer Eisenforschung, Germany; H. Klein, Georg-August-Universität, Germany

2:15 PM**(ICOTOM-S11-002-2008) Peering into the Eyes of Trilobites Using EBSD (Invited)**

M. Lee*, C. Torney, A. W. Owen, University of Glasgow, United Kingdom

2:45 PM**(ICOTOM-S11-003-2008) Textures and Multi-Structure of Single to Multi-Layered Modern Brachiopod Shells (Invited)**

E. Griesshaber*, A. Götz, W. Schmahl, LMU München, Germany; L. Carsten, Humboldt Universität, Germany; R. Neuser, Ruhr Universität, Germany

3:15 PM**(ICOTOM-S11-004-2008) Investigation of the Orientation Relationship Between α -Chitin and Calcite in Crustacean Cuticle Using Microbeam Synchrotron X-ray Diffraction**

A. Al-Sawalmih*, Max-Planck-Institute for Colloids and Interfaces, Germany; H. Fabritius, S. Yi, Max-Planck Institute for Iron Research, Germany; C. Li, S. Siegel, Max-Planck-Institute for Colloids and Interfaces, Germany; D. Raabe, Max-Planck Institute for Iron Research, Germany; O. Paris, Max-Planck-Institute for Colloids and Interfaces, Germany

3:30 PM**Break****4:15 PM****(ICOTOM-S11-005-2008) Crystallographic Texture in Calcium Phosphate Bioceramics (Invited)**

R. P. Camata*, University of Alabama at Birmingham, USA

4:45 PM**(ICOTOM-S11-006-2008) Texture and Anisotropy of MP35N Wire for Conductor Leads**

B. Li*, T. Steigauf, Medtronic, USA

5:00 PM**(ICOTOM-S11-007-2008) Crystallographic Textures from the Exoskeleton of the Lobster *Homarus Americanus* and Calculation of the Mechanical Properties of the Calcite Phase**

L. Raue, Max-Planck-Institute for Iron Research, Germany; H. Klein, University of Goettingen, Germany; D. Raabe*, Max-Planck-Institute for Iron Research, Germany

5:15 PM**(ICOTOM-S11-008-2008) Common Control of Texture in Calcite Biominerals of Bivalved Shells**

M. Cusack, A. Pérez-Huerta, P. Dalbeck, M. Lee*, University of Glasgow, United Kingdom

5:30 PM**(ICOTOM-S11-009-2008) Texture and Ultrastructure of Brachiopod Shells: A Mechanically Optimized Material with Hierarchical Architecture**

W. Schmahl*, LMU München, Germany; K. Kelm, Universität Bonn, Germany; E. Griesshaber, LMU München, Germany; S. Enders, Stuttgart, Germany

5:45 PM**(ICOTOM-S11-010-2008) Wear Resistance and Microstructure in Annealed Ultra High Molecular Weight Polyethylenes**

D. S. Li, H. Garmestani*, Georgia Institute of Technology, USA; A. O. Chu, H. Ahzi, G. Alapati, M. Khatonabadi, O. S. Es-Said, M. T. Siniawski, Loyola Marymount University, USA; L. Matriciano, MEDITECH Medical Polymers, USA; S. Ahzi, University Louis Pasteur, France

Tuesday, June 3, 2008**Novel Texture Measurement Techniques Including 3D****Novel Methods including 3D - III**

Room: Rangos 1

Session Chair: Matthew Miller, Cornell University

8:30 AM**(ICOTOM-S5-019-2008) Far Field Diffraction Studies of Individual Embedded Grains in Polycrystals (Invited)**

U. Lienert*, J. Almer, D. Haefner, ANL, USA

9:00 AM**(ICOTOM-S5-020-2008) Separating Coincident Electron Backscatter Diffraction Patterns near Interfaces**

J. P. Kacher*, B. L. Adams, D. T. Fullwood, C. D. Landon, Brigham Young University, USA

9:15 AM**(ICOTOM-S5-021-2008) Semiautomatic Determination of Orientations and Elastic Strain from Kossel Microdiffraction**

A. Morawiec*, Polish Academy of Sciences, Poland; R. Pesci, Ecole Nationale Supérieure d'Arts et Métiers, France; J. Lecomte, Université de Metz, France

9:30 AM**(ICOTOM-S5-022-2008) Three Dimensional Characterization of Timetal 21S Alloy by Combination of X-ray Microtomography with EBSD**

S. R. Dey*, Technische Universität, Germany; E. M. Lauridsen, Risø National Laboratory, Denmark; W. Ludwig, European Synchrotron Radiation Facility, France; D. Rowenhorst, R. W. Fonda, U.S. Naval Research Laboratory, USA

9:45 AM**(ICOTOM-S5-023-2008) Continuous Pole Figure Measurements at the Materials Science Diffractometer STRESS-SPEC at FRM-II**

U. Garbe*, GKSS, Germany; S. Flemming, C. Randau, HMI, Germany; M. Hofmann, TU-Munich, Germany; H. Brokmeier, TU-Clausthal, Germany

10:00 AM**Break****10:45 AM****(ICOTOM-S5-024-2008) Watching Grains Anneal in Three Dimensions (Invited)**

C. M. Hefferan, Carnegie Mellon University, USA; U. Lienert, Argonne National Laboratory, USA; R. M. Suter*, Carnegie Mellon University, USA

11:15 AM**(ICOTOM-S5-025-2008) Texture and Microstructure Analysis Using 3D-EBSD**

A. Gholinia*, P. Konijnenberg, Oxford Instruments HKL A/S, Denmark

FINAL PROGRAM

Tuesday, June 3, 2008

11:30 AM**(ICOTOM-S5-026-2008) Comparison of X-ray and EBSD Textures for Back-Annealed Al-Mg Alloys**

O. Engler*, Hydro Aluminium Deutschland GmbH, Germany

11:45 AM**(ICOTOM-S5-027-2008) Integration of Focused Ion Beam Serial Sectioning and Orientation Imaging Microscopy for 3-D Microstructure Reconstruction in a Ni-base Superalloy**

S. Lee*, E. B. Gulsoy, Carnegie Mellon University, USA; M. Groeber, Ohio State University, USA; G. S. Rohrer, A. D. Rollett, Carnegie Mellon University, USA; M. Uchic, J. P. Simmons, Wright Patterson Air Force Base, USA; M. De Graef, Carnegie Mellon University, USA

Complex Oxides and Other Compounds**Complex Oxides and Other Compounds**

Room: Connan

Session Chair: Keith Bowman, Purdue University

8:30 AM**(ICOTOM-S6-001-2008) Tentative Simulation of Crystal Rotation for NaCl Structural Type**

H. Masui*, Teikyo University, Japan

8:45 AM**(ICOTOM-S6-002-2008) Cast and Rolling Textures of NiMnGa Alloys**

W. Skrotzki*, R. Chulist, Technische Universität Dresden, Germany; M. Pötschke, Leibniz-Institut für Festkörper- und Werkstofforschung, Germany; A. Böhm, Fraunhofer-Institut Für Werkzeugmaschinen und Umformtechnik, Germany; H. Brokmeier, GKSS Forschungszentrum, Germany; U. Garbe, ZWE FRM II, Germany; C. Oertel, Technische Universität Dresden, Germany

9:00 AM**(ICOTOM-S6-003-2008) Texture of Hot-Rolled Rare Earth Metal-Containing Intermetallic Alloys**

J. A. Wollmershauser*, M. C. Heisel, S. R. Agnew, University of Virginia, USA

9:15 AM**(ICOTOM-S6-004-2008) Determination of Texture and Microstructure of Ordering Domains in gamma-TiAl**

C. Zambaldi*, Max-Planck-Institute for Iron Research, Germany; S. I. Wright, EDAX/TSL, USA; S. Zaefferer, Max-Planck-Institute for Iron Research, Germany

9:30 AM**(ICOTOM-S6-005-2008) Effect of Texture on the Pore Exact Arrangement and Precision of AAO Nano-Template**

I. Kim*, B. Park, Kum Oh National Institute of Technology, South Korea

9:45 AM**(ICOTOM-S6-006-2008) Lead-Free Textured Materials with Improved Dielectric and Piezoelectric Properties Fabricated Using Scalable Processing and Forming Techniques**

M. Winter*, C. DiAntonio, N. Bell, M. Rodriguez, P. Yang, Sandia National Laboratories, USA

10:00 AM

Break

10:45 AM**(ICOTOM-S6-007-2008) Domain Control Effect on Voltage-Strain Relation in BaTiO3 Single Crystal**

Y. Akimune*, K. Matsuo, R. Ooishi, AIST, Japan; A. Okada, Nissan Motor Co., Ltd., Japan

11:00 AM**(ICOTOM-S6-008-2008) Effect of Crystallographic Texture on Ferroelectric Ceramics (Invited)**

R. Garcia*, Purdue University, USA

11:30 AM**(ICOTOM-S6-009-2008) Enhanced Ferroelectric and Dielectric Property Relationships Induced by Textured Processing for Several Ceramic Compositions**

C. DiAntonio*, N. Bell, M. Rodriguez, P. Yang, M. Winter, Sandia National Laboratories, USA

11:45 AM**(ICOTOM-S6-010-2008) Time-Dependent Changes to Preferred Orientation in Ferroelectric Materials and Implications to Macroscopic Properties**

J. L. Jones*, University of Florida, USA

12:00 PM**(ICOTOM-S6-011-2008) Directionality and Anisotropy in Piezoelectric Materials with and without Crystallographic Textures**

K. J. Bowman*, Purdue University, USA

Hexagonal Metals**Texture Modeling**

Room: McConomy Auditorium

Session Chair: Carlos Tome, Los Alamos National Lab

8:30 AM**(ICOTOM-S9-019-2008) Textures in Titanium Alloys: An Industrial Perspective on Deformation, Transformation and Properties (Invited)**

D. Furrer, Rolls-Royce Corporation, USA; D. Rugg*, Rolls-Royce plc, United Kingdom

9:00 AM**(ICOTOM-S9-021-2008) Grain Size and Orientation Distribution Function of High Purity Alpha-Titanium**

B. S. Fromm*, B. L. Adams, S. Ahmadi, Brigham Young University, USA

9:15 AM**(ICOTOM-S9-022-2008) Elastoplastic Self-Consistent Modeling of Polycrystal Plasticity at Finite Strains**

C. Neel*, University of Virginia, USA; B. Clausen, C. Tome, Los Alamos National Laboratory, USA; S. R. Agnew, University of Virginia, USA

9:30 AM**(ICOTOM-S9-023-2008) Dependence of Deformation Mechanism in Polycrystalline Magnesium Alloys AZ31 and Textures Calculated by Sachs Model**

Q. Xie*, P. Yang, University of Science and Technology Beijing, China

9:45 AM**(ICOTOM-S9-024-2008) Comparison Between Non-Linear Intermediate and Self-Consistent Modeling for the Simulation of Large Deformation Behavior and Texture Evolution in HCP Metals**

S. Mgüil*, S. Ahzi, H. Youssef, University Louis Pasteur – IMFS, France; R. Lebensohn, Los Alamos National Laboratory, USA

10:00 AM

Break

10:45 AM**(ICOTOM-S9-025-2008) Prediction of Anisotropic Properties in Mg Alloy Sheets by Using Crystal Plasticity Finite Element Method**

S. Choi*, D. Kim, Suncheon National University, South Korea; H. Kim, Korea Institute of Industrial Technology, South Korea

11:00 AM**(ICOTOM-S9-026-2008) Introduction of Twinning into Cluster Type Deformation Texture Models**

S. Mu*, V. Mohles, G. Gottstein, Institut für Metallkunde und Metallphysik RWTH, Germany

11:15 AM**(ICOTOM-S9-027-2008) Grain Interaction Model Applied to Texture Predictions of Magnesium**

T. Hochrainer*, H. Riedel, A. Prakash, D. Helm, Fraunhofer IWM, Germany

11:30 AM**(ICOTOM-S9-028-2008) Mechanism of Determining the Formability of AZ31 Near Room Temperature**

H. Li*, E. Hsu, J. Szpunar, McGill University, Canada

Tuesday, June 3, 2008

11:45 AM

(ICOTOM-S9-046-2008) Texture Modeling in Equal Channel Angular Extrusion Using a General Flow Line Function
L. S. Toth*, A. Hasani, Université Paul Verlaine de Metz, France

Interface Textures

Interface Textures I

Room: Rangos 1

Session Chairs: Greg Rohrer, Carnegie Mellon University; Valerie Randle, University of Wales Swansea

1:45 PM

(ICOTOM-S7-001-2008) Origin of Characteristic Grain Boundary Distributions in Polycrystalline Materials (Invited)
G. S. Rohrer*, Carnegie Mellon University, USA

2:15 PM

(ICOTOM-S7-002-2008) Grain Boundary Patterns in Dynamically Recrystallized Quartz Aggregates
L. Lagoeiro*, C. Castro, Federal University of Ouro Preto, Brazil

2:30 PM

(ICOTOM-S7-003-2008) Orientation Effects in Liquid Phase Sintered Ceramics
J. L. Riesterer*, University of Minnesota, USA; J. K. Farrer, Brigham Young University, USA; C. Carter, University of Connecticut, USA

2:45 PM

(ICOTOM-S7-004-2008) Effects of Bi Segregation on the Grain Boundary Properties of Ni
F. Papillon*, P. Wynblatt, G. Rohrer, Carnegie Mellon University, USA

3:00 PM

(ICOTOM-S7-005-2008) Possible Role of Complexions in Secondary Recrystallization of Silicon Iron
K. S. Rao*, Lehigh University, USA; A. D. Rollett, S. J. Dillon, Carnegie Mellon University, USA; C. J. Kiely, M. P. Harmer, Lehigh University, USA

3:15 PM

(ICOTOM-S7-006-2008) Role of Interface in Textured Development in Piezoelectric Ceramics made by Templated Grain Growth Process
T. Kimura*, K. Tsuzuki, T. Motohashi, T. Shoji, Keio University, Japan

3:30 PM**Break****4:15 PM**

(ICOTOM-S7-007-2008) Effect of Strain Path and Annealing on Development of Resistance to Intergranular Degradation in Austenitic Stainless Steels (Invited)
V. Randle*, R. Jones, University of Wales Swansea, United Kingdom; J. Marrow, D. Engleberg, University of Manchester, United Kingdom

4:45 PM

(ICOTOM-S7-008-2008) Rodrigues-Frank Space for Orientations, Misorientations and Orientation Relationships of Any Crystallographic Point Groups
Y. He*, Cornell University, USA; J. J. Jonas, McGill University, Canada

5:00 PM

(ICOTOM-S7-009-2008) Correlation Between Grain Boundary Character and Intergranular Corrosion Susceptibility of 2124 Aluminum Alloy
L. H. Chan*, A. Rollett, G. Rohrer, Carnegie Mellon University, USA; H. Weiland, S. Cheong, Alcoa Inc., USA

5:15 PM

(ICOTOM-S7-010-2008) Fatigue Crack Dependence on Boundary Texture
J. LeDonne*, S. Sintay, R. K. Ray, A. D. Rollett, Carnegie Mellon University, USA

5:30 PM

(ICOTOM-S7-011-2008) New Perspectives on Texture Evolution
K. Barmak, M. Emelianenko, D. Golovaty, D. Kinderlehrer*, S. Ta'asan, Carnegie Mellon University, USA

5:45 PM

(ICOTOM-S7-012-2008) Evolution of the Grain Boundary Plane Distribution in SrTiO₃ during Grain Growth
G. S. Rohrer, H. M. Miller*, Carnegie Mellon University, USA

Hexagonal Metals

Texture Evolution and Severe Plastic Deformation

Room: McConomy Auditorium

Session Chair: Ayman Salem, Air Force Research Laboratory

1:45 PM

(ICOTOM-S9-029-2008) Evolution of Deformation Textures Under Dynamic Recrystallization in Hexagonal Metals During Large Strain Simple Shear (Invited)
B. Beausir*, University of Metz, France; S. Suwas, Indian Institute of Science, India; L. S. Toth, University of Metz, France; K. W. Neale, University of Sherbrooke, Canada; J. Fundenberger, University of Metz, France

2:15 PM

(ICOTOM-S9-030-2008) Texture of Magnesium Alloy Sheets Heavily Rolled by High Speed Warm Rolling (Invited)
T. Sakai*, H. Koh, S. Minamiguchi, H. Utsunomiya, Osaka University, Japan

2:45 PM

(ICOTOM-S9-031-2008) Texture Evolution during Multi-Pass Equal Channel Angular Extrusion of Beryllium
S. Li*, X. Liu, South China University of Technology, China

3:00 PM

(ICOTOM-S9-032-2008) Texture Characteristics and Mechanical Properties in an AZ31 Magnesium Alloy Sheet Fabricated by Asymmetric Hot Extrusion
Y. Wang*, L. Chang, Dalian University of Technology, China; X. Zhao, Northeastern University, China

3:15 PM

(ICOTOM-S9-033-2008) Investigation of Texture and Microstructure Evolution During Asymmetric Rolling of Mg Alloys
J. Cho*, S. Kang, H. Kim, Korea Institute of Materials Science, South Korea

3:30 PM**Break****4:15 PM**

(ICOTOM-S9-034-2008) Microstructure and Texture Gradient in Titanium Severely Strained by Friction Roll Processing and Subsequent Annealing
M. Shi*, T. Umetsu, Y. Takayama, H. Kato, H. Watanabe, Department of Mechanical Systems Engineering, Utsunomiya University, Japan

4:30 PM

(ICOTOM-S9-035-2008) Texture and Mechanical Properties of Equiaxed Ultrafine Grained Zirconium Fabricated by Accumulative Roll Bonding
L. Jiang*, University of Southern California, USA; M. Pérez-Prado, O. Ruano, National Center for Metallurgical Research (CENIM), CSIC, Spain; M. Kassner, University of Southern California, USA

FINAL PROGRAM

Tuesday - Wednesday, June 3–4, 2008

Texture in Materials Design

Texture in Materials Design I

Room: Connan

Session Chair: Brent Adams, Brigham Young University

1:45 PM

(ICOTOM-S12-001-2008) Microstructure Characterization and Localization Tensors Using 2-point Correlations (Invited)

S. Kalidindi*, S. Niezgodna, G. Landi, D. Fullwood, Drexel University, USA

2:15 PM

(ICOTOM-S12-002-2008) Using ab initio Simulations in Texture Research

D. Raabe*, D. Ma, F. Roters, A. Counts, M. Friák, M. Petrov, J. Neugebauer, Max-Planck-Institut fuer Eisenforschung, Germany

2:30 PM

(ICOTOM-S12-003-2008) Hierarchical Multi-Level Modelling of Plastic Anisotropy Using Convex Plastic Potentials

P. Van Houtte*, S. K. Yerra, A. Van Bael, Katholieke Universiteit Leuven, Belgium

2:45 PM

(ICOTOM-S12-004-2008) Constitutive Modelling of the Dilatational Plasticity of Textured Aggregates

R. Lebensohn*, C. N. Tome, Los Alamos National Laboratory, USA; P. Ponte Castaneda, University of Pennsylvania, USA

3:00 PM

(ICOTOM-S12-005-2008) Spectral Representation of Higher-Order Localization Relationships for Elastic Behavior of Polycrystalline Cubic Materials

G. Landi*, D. T. Fullwood, S. R. Kalidindi, Drexel University, USA

3:15 PM

(ICOTOM-S12-006-2008) Texture-Based Plastic Potentials in Stress Space for Finite Element Simulations

A. Van Bael*, S. Yerra, P. Van Houtte, Katholieke Universiteit Leuven, Belgium

3:30 PM

Break

4:15 PM

(ICOTOM-S12-007-2008) Using 3D Image-Based Finite Element Modeling to Investigate Interactions among Microstructure, Crystallography and Mechanical Response

A. C. Lewis*, Naval Research Laboratory, USA; M. A. Qidwai, SAIC, USA; A. B. Geltmacher, Naval Research Laboratory, USA

4:30 PM

(ICOTOM-S12-008-2008) Plastic Heterogeneity Due to Grain Boundaries and Its Influence on Global Deformation Textures

A. K. Kanjarla*, P. Van Houtte, Katholieke Universiteit Leuven, Belgium; L. Delannay, Université Catholique de Louvain (UCL), Belgium

4:45 PM

(ICOTOM-S12-009-2008) Modeling Rolling Textures of Beta Ti Alloys Using Constitutive Data From Ab-initio Simulations

D. Ma*, D. Raabe, F. Roters, M. Friák, J. Neugebauer, Max-Planck-Institut fuer Eisenforschung, Germany

5:00 PM

(ICOTOM-S12-010-2008) Texture Gradients in Hot-Rolled Al-Alloy Plates for Aeronautical Applications

D. J. Plet*, W. Robert, R. Quey, J. H. Driver, Ecole des mines de Saint-Étienne, France; F. Eberl, Alcan centre de recherches de Voreppe, France

5:15 PM

(ICOTOM-S12-011-2008) Numerical Modeling of Postnecking Deformation in AA5754 Aluminum Sheets

M. Gesing, A. Izadbakhsh, K. Inal*, University of Waterloo, Canada; R. K. Mishra, General Motors, USA

5:30 PM

(ICOTOM-S12-012-2008) Rolling Parameters Governing the Evolution of Strain States and Textures during Asymmetrical Cold Rolling in AA 5052

H. Kang, M. Huh*, Korea University, South Korea; O. Engler, Hydro Aluminium Deutschland GmbH, R&D Center Bonn, Germany

5:45 PM

(ICOTOM-S12-013-2008) The Variation Range of the Results of FCC Texture Simulations Based on {111}<110> SLIP

T. Leffers*, Risø National Laboratory, Technical University of Denmark, Denmark

Wednesday, June 4, 2008

Texture and Anisotropy in Steels

Low Carbon and IF Steels

Room: Rangos 3

Session Chairs: Leo Kestens, Delft University of Technology; Arunansu Haldar, Tata Steel Ltd.

8:30 AM

(ICOTOM-S3-001-2008) Texture Control in Manufacturing Current and Future Grades of Low-Carbon Steel Sheet (Invited)

L. A. Kestens*, Delft University of Technology, Netherlands; R. Petrov, Ghent University, Belgium

9:00 AM

(ICOTOM-S3-002-2008) Importance of Dislocation Substructures in Texture Control of Low Carbon Steels (Invited)

H. Inagaki*, INATEX, Japan

9:30 AM

(ICOTOM-S3-003-2008) EBSD Investigation of Phase Transformations in Low Carbon Steels

S. Lubin*, Ecole des Mines de Paris, France; H. Réglé, Arcelor-Mittal Research, France; A. Gourgues, Ecole des Mines de Paris, France

9:45 AM

(ICOTOM-S3-004-2008) Texture Memory Effects in Low and Ultra Low Carbon Steels

A. Haldar*, Tata Steel Ltd., India

10:00 AM

Break

10:30 AM

(ICOTOM-S3-005-2008) Influence of the Al to N Ratio on the Texture of Batch Annealed Low Carbon Tin Plate for DWI Can Production

A. L. Pinto*, Instituto Militar de Engenharia, Brazil; C. S. da Costa Viana, Universidade Federal Fluminense, Brazil; P. R. Campissi, Companhia Siderúrgica Nacional, Brazil

10:45 AM

(ICOTOM-S3-006-2008) Development of Texture, Microstructure and Grain Boundary Character Distribution after Heavy Cold Rolling and Annealing in a Boron Added Interstitial Free (IF) Steel

R. Saha*, R. K. Ray, TATA STEEL, India

11:00 AM

(ICOTOM-S3-007-2008) Effects of Composition and Coiling Temperature on Texture Formation in a Few Interstitial Free High Strength Steels

P. Ghosh, R. K. Ray*, TATA Steel, India

11:15 AM

(ICOTOM-S3-008-2008) Texture Development in Warm Rolled High Strength IF Steels Containing Cu, P and B

A. Haldar*, C. Ghosh, Tata Steel Ltd, India

Wednesday, June 4, 2008

11:30 AM**(ICOTOM-S3-009-2008) Relative Preference for Strain Localizations in Ultra Low Carbon Steel**

R. Khatirkar*, Visvesvaraya National Institute of Technology, India; L. Kestens, Delft University of Technology, Netherlands; R. Petrov, Ghent University, Belgium; I. Samajdar, Indian Institute of Technology Bombay, India

Interface Textures**Interface Textures II**

Room: Rangos 1

Session Chairs: Peter Voorhees, Northwestern University; David Rowenhorst, U.S. Naval Research Lab

8:30 AM**(ICOTOM-S7-013-2008) Investigations of Interface Textures Using Advanced 3D Reconstructions (Invited)**

D. Rowenhorst*, A. Lewis, G. Spanos, U.S. Naval Research Lab, USA

9:00 AM**(ICOTOM-S7-014-2008) Microtexture of the PED Nano-twin Copper Films**

D. R. Waryoba*, FAMU-FSU College of Engineering, USA; B. Cui, National High Magnetic Field laboratory, USA; P. N. Kalu, FAMU-FSU College of Engineering, USA

9:15 AM**(ICOTOM-S7-015-2008) Interface Texture in Cemented Tungsten Carbides and its Role in Microstructural Evolution during Sintering**

V. Kumar*, Z. Z. Fang, University of Utah, USA; S. I. Wright, M. M. Nowell, EDAX Inc., USA

9:30 AM**(ICOTOM-S7-016-2008) Thin Films on Single Crystal Substrates as Model Systems for the Study of Interphase Boundaries**

C. Detavernier*, K. De Keyser, Ghent University, Belgium; S. Gaudet, École Polytechnique de Montréal, Canada; J. Jordan-Sweet, C. Lavoie, IBM T. J. Watson Research Center, USA

9:45 AM**(ICOTOM-S7-017-2008) Grain Boundary Character Evolution in Different Grain Growth Models**

S. Wilson*, F. Uyar, J. Gruber, A. D. Rollett, Carnegie Mellon University, USA

10:00 AM

Break

10:30 AM**(ICOTOM-S7-018-2008) Simulation of Anisotropic Grain Growth in Three Dimensions (Invited)**

M. Gururajan, I. McKenna, P. Voorhees*, Northwestern University, USA

11:00 AM**(ICOTOM-S7-019-2008) Microstructural Modification in a 15Cr-15Ni-2.2 Mo-Ti modified Austenitic Stainless Steel through Twin induced Grain Boundary Engineering**

S. Mandal, S. Palle, Indira Gandhi Centre for Atomic Research, India; S. S. Vadlamani*, Indian Institute of Technology Madras, India

11:15 AM**(ICOTOM-S7-020-2008) Use of Orientation Gradients for the Identification of Different Microconstituents in Multiphase Steels**

P. Romano*, S. Zaeferrer, D. Raabe, Max Planck Institute for Iron Research, Germany; F. Friedel, ThyssenKrupp AG, Germany

11:30 AM**(ICOTOM-S7-022-2008) Nucleation of Primary Al phase on TiAl3 during Solidification in Zn-11%Al-3%Mg-0.2%Si Coated Steel Sheet**

K. Honda, K. Ushioda*, W. Yamada, Nippon Steel Corp., Japan

11:45 AM**(ICOTOM-S7-023-2008) Texture Development and Grain Growth during Annealing in Electrodeposited Ni/Fe-Ni Bimetals**

J. Seo, J. Kang, J. Kim, Y. Park*, Suncheon National University, South Korea

12:00 PM**(ICOTOM-S7-024-2008) 3D-EBSD Study of Solid-state Nucleation in a Co-Fe Alloy**

H. Landheer*, E. Offerman, Delft University of Technology, Netherlands; T. Takeuchi, M. Enomoto, Ibaraki University, Japan; Y. Adachi, National Institute for Materials Science, Japan; L. Kestens, Delft University of Technology, Netherlands

Hexagonal Metals**Texture-Property Relations**

Room: Rangos 2

Session Chair: Matthew Barnett, Deakin University

8:30 AM**(ICOTOM-S9-036-2008) Characterization and Study of Texture Heterogeneities in Titanium Alloy IMI 834 in the Framework of Creep and Fatigue Investigations (Invited)**

E. Uta*, UPVM, France; P. Bocher, ETS, Canada; N. Gey, M. Humbert, UPVM, France

9:00 AM**(ICOTOM-S9-037-2008) Strain Hardening Behaviour of an Initially Textured Ti6Al4V Titanium Alloy as a Function of Strain Rate and Compression Direction**

F. Coghe*, L. Rabet, Royal Military Academy, Belgium; P. Van Houtte, KU Leuven, Belgium

9:30 AM**(ICOTOM-S9-039-2008) Texture Aspects of Delayed Hydride Cracking in Products from Zr-based Alloys**

M. Isaenkova*, Y. Perlovich, Moscow Engineering Physics Institute, Russian Federation

9:45 AM**(ICOTOM-S9-040-2008) Anisotropy, Twinning, and Texture Development in Rhenium**

J. Bingert*, P. J. Maudlin, M. F. Lopez, Los Alamos National Laboratory, USA

10:00 AM

Break

10:30 AM**(ICOTOM-S9-041-2008) Electrochemical Behavior of {001}, {100} and {110} Ti Single Crystals under Simulated Body Fluid Condition**

M. Azzi*, S. Faghihi, M. Tabrizian, J. Szpunar, McGill University, Canada

10:45 AM**(ICOTOM-S9-042-2008) Effect of Processing, Microstructure, and Texture on the Elevated-Temperature Creep Behavior of Ti-6Al-4V-XB Alloys**

C. J. Boehlert*, W. Chen, Michigan State University, USA; M. Glavicic, UES, Inc., USA; S. Tamirisakandala, FMW Composite Systems, Inc., USA; D. Miracle, Air Force Research Laboratory, USA

11:00 AM**(ICOTOM-S9-045-2008) Role of Initial Texture in Low Temperature Plasticity of Mg-4.5%Al-1%Zn Alloy**

V. Serebryany*, K. E. Mel'nikov, A.A. Baikov Institute of Metallurgy and Material Science, RAS, Russian Federation

Texture in Materials Design**Texture in Materials Design II**

Room: Connan

Session Chair: Surya Kalidindi, Drexel University

8:30 AM**(ICOTOM-S12-014-2008) Spectral Methods in the Statistical Description and Design of Microstructure (Invited)**

D. Fullwood*, Brigham Young University, USA; S. Niezgodza, S. Kalidindi, Drexel University, USA; B. Adams, Brigham Young University, USA

FINAL PROGRAM

Wednesday - Thursday, June 4–5, 2008

9:00 AM

(ICOTOM-S12-015-2008) Two-point Orientation Coherence Functions: An Orthonormal Series Solution (Invited)
P. R. Morris*, retired, USA

9:15 AM

(ICOTOM-S12-016-2008) Accessing the Texture Hull and Properties Closure by Rotation and Lamination
B. L. Adams*, B. Aydelotte, S. Ahmadi, C. Nylander, Brigham Young University, USA

9:30 AM

(ICOTOM-S12-017-2008) On the Correlation of Surface Texture and Strain Induced Surface Roughness in AA6xxx Aluminium Sheet
S. Kusters*, M. Seefeldt, P. Van Houtte, KULeuven, Belgium

9:45 AM

(ICOTOM-S12-018-2008) Microstructure-based Models to Predict the Formation of the Brass-type Texture
T. Leffers*, RISO National Laboratory, Technical University of Denmark, Denmark; R. Lebensohn, Los Alamos National Laboratory, USA

10:00 AM

Break

10:30 AM

(ICOTOM-S12-019-2008) Representation of Textures Using Quaternions Distributions
J. Mason*, C. A. Schuh, Massachusetts Institute of Technology, USA

10:45 AM

(ICOTOM-S12-020-2008) Deformation Textures and Mechanical Properties of FCC and HCP Metals Predicted by Crystal Plasticity Codes
C. S. Hartley*, El Arroyo Enterprises LLC, USA; P. R. Dawson, D. Boyce, Cornell University, USA; S. R. Kalidindi, M. Knezevic, Drexel University, USA; C. Tomé, R. Lebensohn, Los Alamos National Laboratory, USA; L. Semiati, T. J. Turner, Air Force Research Laboratory, USA; A. A. Salem, Universal Energy Systems, USA

11:00 AM

(ICOTOM-S12-021-2008) Variance of the Orientation Distribution Function and the Yield Surface
S. Ahmadi*, B. L. Adams, B. S. Fromm, Brigham Young University, USA

11:15 AM

(ICOTOM-S12-022-2008) Prediction of the Evolution of Polycrystalline Yield Surfaces in Deformed Metals Using a New Non-linear Intermediate Viscoplastic Model
S. Mguil*, S. Ahzi, F. Barlat, University Louis Pasteur – IMFS, France

11:30 AM

(ICOTOM-S12-023-2008) Comparison of Twinning Modeling Approaches with Application to TWIP Steels
A. Prakash*, T. Hochrainer, H. Riedel, Fraunhofer Institute for Mechanics of Materials, Germany

11:45 AM

(ICOTOM-S12-024-2008) Modeling Rolling Texture of Twinned Copper Single Crystals
K. J. Al-Fadhalah*, Kuwait University, Kuwait; A. J. Beaudoin, University of Illinois at Urbana-Champaign, USA; M. Niewczas, McMaster University, Canada

12:00 PM

(ICOTOM-S12-025-2008) Novel Spectral Approach for the Design of Deformation Processing Operations to Achieve Desired Textures in Polycrystalline FCC Metals
M. Knezevic*, D. Illson, Drexel University, USA; D. Fullwood, Brigham Young University, USA; S. R. Kalidindi, Drexel University, USA

12:15 PM

(ICOTOM-S12-026-2008) Micromechanical Modeling of Plastic Deformation and Texture Evolution in Semi-Crystalline Polymers: Self-Consistent vs. an Upper Bound Approach
O. Gueguen*, S. Ahzi, A. Makradi, IMFS, France; S. Belouettar, Research Center Henry Tudor, Luxembourg; S. Nikolov, Max-Planck Institut für Eisenforschung, Germany; R. A. Lebensohn, Los Alamos National Laboratory, USA

Thursday, June 5, 2008**Thin Films (Microelectronics, HTSC)****Thin Films**

Room: Rangos 2

Session Chair: Jay Whitacre, Carnegie Mellon University

8:30 AM

(ICOTOM-S2-001-2008) Texture Development and Abnormal Grain Growth in Thin Films (Invited)
C. V. Thompson*, MIT, USA; H. J. Frost, Dartmouth College, USA

9:00 AM

(ICOTOM-S2-002-2008) Grain Growth and Texture Development in Lithium Fluoride Thin Films
A. King*, H. Kim, Purdue University, USA

9:15 AM

(ICOTOM-S2-003-2008) EBSD Analysis of the Texture Evolution of Rapidly Solidified Cu Thin Films
A. Kulovits*, R. Zong, J. P. Leonard, J. M. Wiezorek, University of Pittsburgh, USA

9:30 AM

(ICOTOM-S2-004-2008) Microtexture Evolution in Free-standing CVD Diamond Films: Growth and Twinning Mechanisms
T. Liu*, D. Raabe, Max-Planck-Institut fuer Eisenforschung, Germany; W. Mao, University of Science and Technology, China; S. Zaeferrer, Max-Planck-Institut fuer Eisenforschung, Germany

9:45 AM

Break

10:30 AM

(ICOTOM-S2-005-2008) Microstructure Control in Formation of NiSi Thin Films (Invited)
K. Kozaczek*, NOVA Measuring Instruments, Inc., USA

11:00 AM

(ICOTOM-S2-006-2008) Texture of Thin NiSi Films and its Effect on Agglomeration
K. De Keyser*, C. Detavernier, R. Van Meirhaeghe, Ghent University, Belgium; J. Jordan-Sweet, C. Lavoie, IBM T. J. Watson Research Center, USA

11:15 AM

(ICOTOM-S2-007-2008) Control of Texture in Polycrystalline Thin Films used as Data Storage Media (Invited)
D. E. Laughlin*, H. Yuan, E. Yang, C. Wang, Carnegie Mellon University, USA

11:30 AM

(ICOTOM-S2-008-2008) Determination of the Long Range Order Parameter in Fiber-Textured Films of L₁₀ FePt
K. Barmak*, D. C. Berry, B. Wang, Carnegie Mellon University, USA

11:45 AM

(ICOTOM-S2-009-2008) Epitaxial, Electrical/Electronic Devices via Reel-to-Reel Web-Coating in Kilometer Lengths on Flexible, Substrates with Strict Control of Crystallographic Texture and Grain Boundary Networks (Invited)
A. Goyal*, Oak Ridge National Laboratory, USA

12:15 PM

(ICOTOM-S2-010-2008) Cube Texture Formation in Ni-Pd and Ni-Pd-W Alloys for HTS Coated Tapes
I. Gervasyeva*, D. Rodionov, J. Khlebnikova, Russian Academy of Sciences, Russian Federation; G. Dosovitskii, A. Kaul, Lomonosov Moscow State University, Russian Federation

Thursday, June 5, 2008

Texture and Anisotropy in Steels

Stainless Steels and Electrical Steels

Room: Rangos 3

Session Chairs: Jerzy Szpunar, McGill University; Hugo Sandim, EEL-USP

8:30 AM**(ICOTOM-S3-010-2008) Microtexture Characterization of Duplex Stainless Steel after Hot Working**

C. Herrera*, D. Ponge, D. Raabe, Max-Planck-Institut für Eisenforschung, Germany

8:45 AM**(ICOTOM-S3-011-2008) Textures and Microstructures Evolution in Hot-Cold Rolling Microalloyed Ferrite Stainless Steel**

L. Yandong*, Key Laboratory for Anisotropy and Texture of Materials (Ministry of Education), China; B. Hongyun, L. Weidong, Baosteel Research Institute, China; C. Liqing, J. Yongming, Z. Liang, Key Laboratory for Anisotropy and Texture of Materials (Ministry of Education), China

9:00 AM**(ICOTOM-S3-012-2008) Influence of Texture on Surface-Roughening during Press Forming in Ti Added High Purity Ferritic Stainless Steel Sheets**

K. Kimura*, Nippon Steel Corporation, Japan; M. Hatano, A. Takahashi, Nippon Steel & Sumikin Stainless Steel Corporation, Japan

9:15 AM**(ICOTOM-S3-013-2008) Effects of Texture and Microstructure on the Corrosion Resistance of SS304 Stainless Steel**

M. Azzi*, J. Szpunar, McGill University, Canada

9:30 AM**(ICOTOM-S3-014-2008) Texture of Nb-Containing Ferritic Stainless Steels after Secondary Recrystallization**

H. R. Sandim*, S. P. Rodrigo, EEL-USP, Brazil; T. R. Oliveira, ACESITA S.A., Brazil

9:45 AM**(ICOTOM-S3-015-2008) Control of Rotated Cube Texture of {001}$\langle 110 \rangle$ in 2.7Si-Electrical Steels**

S. K. Chang*, S. I. Lee, D. N. Lee, POSTECH, South Korea

10:00 AM

Break

10:30 AM**(ICOTOM-S3-016-2008) Texture and Microstructure Evolution in a Fe-Si Sheet during the Processing Route before Secondary Recrystallization**

F. Cruz-Gandarilla, National Polytechnical Institute, Mexico; R. Penelle*, T. Baudin, University of Paris-Sud Orsay, France; H. Mendoza-Leon, National Polytechnical Institute, Mexico

10:45 AM**(ICOTOM-S3-017-2008) Measurement of the Texture Sharpness in Grain-oriented Electrical Steels**

M. Frommert*, C. Zobrist, Max-Planck-Institute for Iron Research, Germany; L. Lahn, A. Böttcher, ThyssenKrupp Electrical Steel, Germany; D. Raabe, S. Zaefferer, Max-Planck-Institute for Iron Research, Germany

11:00 AM**(ICOTOM-S3-018-2008) Stability of Secondary Recrystallization in Grain Oriented Silicon Steel**

E. Namba*, S. Arai, H. Homma, Nippon Steel Corporation, Japan

11:15 AM**(ICOTOM-S3-019-2008) Effect of Tin on the Recrystallization Behavior and Texture of Grain Oriented Electrical Steels**

L. Chun-Chih*, H. Chun-Kan, National Yunlin University of Science and Technology, Taiwan

11:30 AM**(ICOTOM-S3-020-2008) Evolution of Recrystallization Texture in Asymmetrically Rolled Non-Oriented Silicon Steel**

W. Pei, Y. Sha*, C. Sun, L. Zuo, Key Laboratory for Anisotropy and Texture of Materials, China

11:45 AM**(ICOTOM-S3-021-2008) Influence of Precipitate Distribution on Grain Growth Simulation: Case of the MnS and AlN Precipitates in a Fe-3%Si Electrical Steel HiB**

C. Sekkak, N. Rouag, Université Mentouri Constantine, Algeria; R. Penelle*, Université Paris-Sud, France

12:00 PM**(ICOTOM-S3-022-2008) Influence of Grain Orientation and Additional Cementite Precipitation on the Magnetic Aging of a Non-Oriented Silicon Steel**

L. Xu, W. Mao*, P. Yang, H. Feng, University of Science and Technology Beijing, China

Texture in Materials Design

Texture in Materials Design III

Room: Connan

Session Chair: David Fullwood, Brigham Young University

8:30 AM**(ICOTOM-S12-027-2008) Earing, Texture and Drawing Ratio in Deep Drawing of Orthorhombic Sheets of Cubic Metals (Invited)**

M. Huang, Nanchang University, China; C. Man*, University of Kentucky, USA; T. Zheng, Nanchang University, China

9:00 AM**(ICOTOM-S12-028-2008) Texture Development in a Nanocrystalline Al-alloy**

B. Ye, B. S. Majumdar*, New Mexico Tech, USA; S. Vogel, Los Alamos National Laboratories, USA; V. Seetharaman, T. Watson, Pratt & Whitney, USA

9:15 AM**(ICOTOM-S12-029-2008) Texture Development of Molybdenum Sheets during Last Steps of Heat Treatment**

W. Skrotzki, C. Oertel*, I. Hünsche, W. Knabl, A. Lorch, Technische Universität Dresden, Germany

9:30 AM**(ICOTOM-S12-030-2008) Development of High Strength, Low Magnetism and Strongly Cube-textured Composite Ni-7%W/Ni-10%W Substrate for Coated Superconductor**

D. Liu*, Beijing University of Technology, China

9:45 AM**(ICOTOM-S12-031-2008) Effect of Deformation Constraints on the Texture Formation in Al-5mass%Mg Solid Solution at High Temperatures**

K. Okayasu, M. Sakakibara, H. Fukutomi*, Yokohama National University, Japan

10:00 AM

Break

10:30 AM**(ICOTOM-S12-032-2008) Multiscale Modeling of Equal Channel Angular Extruded Aluminium with Strain Gradient Crystal Plasticity and Phenomenological Models**

L. Duchêne*, University of Liège, Belgium; M. Geers, M. Brekelmans, Eindhoven University of Technology, Netherlands; A. Habraken, University of Liège, Belgium

10:45 AM**(ICOTOM-S12-033-2008) Simulation of Texture Development in Pure Aluminum Deformed by Equal Channel Angular Pressing**

M. Hoseini*, L. Hualong, J. Szpunar, McGill University, Canada; M. Meratian, Isfahan University of Technology, Iran

11:00 AM**(ICOTOM-S12-034-2008) Texture Evolution in Tantalum Processed by Equal Channel Angular Pressing**

J. W. House*, P. J. Flater, Air Force Research Laboratory, USA; J. M. O'Brien, O'Brien and Associates, USA; W. F. Hosford, University of Michigan, USA

FINAL PROGRAM

Thursday, June 5, 2008

11:15 AM**(ICOTOM-S12-035-2008) Textures in Nb Processed by Equal Channel Angular Extrusion**

S. Balachandran*, K. T. Hartwig, R. B. Griffin, Texas A&M University, USA; T. Bieler, D. Baars, Michigan State University, USA; R. E. Barber, Shear Form Inc., USA

11:30 AM**(ICOTOM-S12-036-2008) Solute, Superplasticity and Texture change in Aluminium Alloys**

K. Sotoudeh*, P. Bate, J. Humphreys, The University of Manchester, United Kingdom

11:45 AM**(ICOTOM-S12-037-2008) Effect of Microstructure in Thermoelectric Nanodots, Nanowire Composites, and Polycrystalline Materials**

R. Garcia*, Purdue University, USA

12:00 PM**(ICOTOM-S12-038-2008) Drawability and Texture Change of Asymmetry Rolled Al Alloy Sheets**

I. Kim*, S. Akramov, H. Jeoung, Kum Oh National Institute of Technology, South Korea

12:15 PM**(ICOTOM-S12-039-2008) Processing of Straight and Sheared Layers in Alternating Al and Al(0.3%Sc) ARB Sheets**

M. Z. Quadir*, O. Al-Buhamad, L. Bassman, M. Ferry, The University of New South Wales, Australia

Digital Microstructures**Digital Microstructures**

Room: Rangos 1

Session Chair: Marc DeGraef, Carnegie Mellon University

8:30 AM**(ICOTOM-S14-001-2008) Predictions and Experimental Validation of the Development of Intragranular Misorientations in Copper under Tension Using Direct Input from OIM Images (Invited)**

R. Lebensohn*, Los Alamos National Laboratory, USA; R. Brenner, O. Castelnaud, Université Paris XIII, France; A. D. Rollett, Carnegie-Mellon University, USA

9:00 AM**(ICOTOM-S14-002-2008) Accurate Texture Reconstruction with a Set of Orientations Based on Integral Approximation of the Scaled Orientation Distribution Function**

P. Eisenlohr*, F. Roters, Max-Planck-Institut für Eisenforschung, Germany

9:15 AM**(ICOTOM-S14-003-2008) Adaptive Mesh Refinement in Crystal Plasticity Finite Element Simulations of Large Deformations in Polycrystalline Aggregates**

H. Resk*, M. Bernacki, T. Coupez, ENSMP, France; L. Delannay, Université catholique de Louvain UCL, Belgium; R. Logé, ENSMP, France

9:30 AM**(ICOTOM-S14-004-2008) Interfacing Finite Element Simulations with Three Dimensional Characterizations of Polycrystalline Microstructures via the 3D Materials Atlas (Invited)**

P. Dawson*, D. E. Boyce, M. P. Miller, Cornell University, USA

10:00 AM**Break****10:30 AM****(ICOTOM-S14-005-2008) CPFEM Investigation of the Effect of Grain Shape on the Planar Anisotropy and the Shear Banding of Textured Metal Sheets (Invited)**

L. Delannay*, M. A. Melchior, Université catholique de Louvain (UCL), Belgium; A. K. Kanjarla, P. Van Houtte, K.U.Leuven, Belgium; J. W. Signorelli, Fac. de Ciencias Exactas, Ingeniería y Agrimensura, CONICET-UNR, Argentina

11:00 AM**(ICOTOM-S14-006-2008) Linking Plastic Deformation to Recrystallization in Metals, Using Digital Microstructures**

R. E. Logé*, M. Bernacki, H. Resk, H. Dignonet, Y. Chastel, T. Coupez, Ecole des Mines de Paris, France

11:15 AM**(ICOTOM-S14-007-2008) Multiscale Model for Anisotropic Work Hardening of Aluminium Including Transient Effects during Strain Path Changes**

S. Van Boxel*, M. Seefeldt, B. Verlinden, P. Van Houtte, Katholieke Universiteit Leuven, Belgium

11:30 AM**(ICOTOM-S14-008-2008) Gradient Matrix Method to Image Crystal Curvature with Discrete Orientation Data: Case Study of Triple Junction in Deformed IF Steel**

A. Zisman*, CRISM "Prometey", Russian Federation; M. Seefeldt, S. Van Boxel, P. Van Houtte, Catholic University of Leuven, Belgium

11:45 AM**(ICOTOM-S14-009-2008) Representative Volume Elements for the input into Structure-Property-Processing Relationships**

S. R. Niezgodna*, D. Fullwood, S. Kalidindi, Drexel University, USA

12:00 PM**(ICOTOM-S14-010-2008) Moment Invariant Shape Descriptors for 2-D and 3-D Microstructure Representation**

J. MacSleyme*, Carnegie Mellon University, USA; J. P. Simmons, Wright Patterson Air Force Base, USA; M. De Graef, Carnegie Mellon University, USA

12:15 PM**(ICOTOM-S14-011-2008) Minimally Supervised Segmentation Algorithms for Serial Section Image Data**

P. Chuang, M. L. Comer*, Purdue University, USA; J. P. Simmons, AFRL/MLLMD, USA; M. De Graef, Carnegie Mellon University, USA

Texture and Anisotropy in Steels**High Strength Steels**

Room: Rangos 3

Session Chairs: Dierk Raabe, Max-Planck-Institut für Eisenforschung; Martin Cernik, U.S. Steel Kosice

1:45 PM**(ICOTOM-S3-023-2008) Microstructure and -Texture Evolution during Intercritical Annealing with and without Deformation in the Production of Ultrafine Grained Ferrite/Martensite Dual Phase Steels**

M. Calcagno*, D. Ponge, D. Raabe, Max-Planck-Institut für Eisenforschung, Germany

2:00 PM**(ICOTOM-S3-024-2008) Inhomogeneity of the Crystallographic Texture in Hot Rolled High-manganese TWIP Steels**

D. Raabe*, Max-Planck-Institut für Eisenforschung, Germany; H. Hofmann, ThyssenKrupp Steel AG, Germany; G. Frommeyer, K. Verbeken, Max-Planck-Institut für Eisenforschung, Germany

2:15 PM**(ICOTOM-S3-025-2008) Microstructural and Textural Evolutions in a Cold Rolled High Mn TWIP Steel**

K. Verbeken*, Max-Planck-Institut für Eisenforschung, Germany; L. Bracke, Corus Research, Development and Technology, Netherlands; L. Kestens, Delft University of Technology, Netherlands; J. Penning, Ghent University, Belgium

2:30 PM**(ICOTOM-S3-026-2008) On the Role of Mechanical Twinning in Microstructure Evolution of High Manganese Steels: Experiments and Modelling**

L. A. Hantcherli*, P. Eisenlohr, F. Roters, D. Raabe, Max-Planck-Institut für Eisenforschung, Germany

Thursday, June 5, 2008

2:45 PM**(ICOTOM-S3-027-2008) Crystallographic Characterization of a Phosphorus Added TRIP Steel**

K. Verbeken, L. Barbé*, Ghent University, Belgium; D. Raabe, Max-Planck-Institut für Eisenforschung, Germany

3:15 PM**(ICOTOM-S3-029-2008) Quantitative Analysis of Variant Selection and Orientation Relationships during the γ -to- α Phase Transformation in Hot-Rolled TRIP Steels**

M. Loic, Université Libre de Bruxelles, ULB, Belgium; P. J. Jacques, Université catholique de Louvain, UCL, Belgium; S. Godet*, Université Libre de Bruxelles, ULB, Belgium

3:30 PM**Break****4:00 PM****(ICOTOM-S3-030-2008) Stored Energy Evolution in a Cold-Rolled IF Steel**

A. Wauthier*, Arcelor Mittal R&D, France; B. Bacroix, T. Chauveau, O. Castelnaud, CNRS, France; H. Regle, Arcelor Mittal R&D, France

4:15 PM**(ICOTOM-S3-031-2008) Monte Carlo Algorithm for Ziner Drag Effect in the Fe-3%Si Magnetic Alloys**

M. Noureddine*, Université du 20 août 55-Skikda, Algeria; P. Richard, B. Thierry, E. Anne-laure, Université de Paris Sud, France

4:30 PM**(ICOTOM-S3-032-2008) Evolution and Relation between Texture-Microstructure-Mechanical Behaviour of a FeMnC TWIP Steel during Tensile Test**

D. Barbier*, N. Gey, B. Bolle, M. Humbert, LETAM, France; S. Allain, Arcelor Research, France

4:45 PM**(ICOTOM-S3-033-2008) Grain Subdivision in Niobium during ECAP: EBSD Characterization and Multiscale Modeling**

M. Seefeldt*, B. Verlinden, P. Van Houtte, K.U. Leuven, Belgium

5:00 PM**(ICOTOM-S3-034-2008) Texture Component Model for Predicting Recrystallization Textures**

A. Brahme*, M. Winning, D. Raabe, Max-Planck Institut für Eisenforschung, Germany

5:15 PM**(ICOTOM-S3-035-2008) Relationship Between Microstructure and Texture Evolution during Cold Deformation of TWIP-Steels**

A. B. Fanta*, S. Zaefferer, Max Planck Institute for Iron Research, Germany; I. Thomas, ThyssenKrupp Steel, Germany; D. Raabe, Max Planck Institute for Iron Research, Germany

5:30 PM**(ICOTOM-S3-036-2008) Texture of Non-oriented Rolled Steels by X-ray and Electron Diffraction**

M. Cernik*, M. Predmersky, A. Lesko, U.S. Steel Kosice, Slovakia

5:45 PM**(ICOTOM-S3-037-2008) Texture Development during Cold Ring Rolling of 100Cr6**

K. Rytberg*, M. Knutson Wedel, Chalmers University of Technology, Sweden; P. Dahlman, SKF Sverige AB, Sweden; L. Nyborg, Chalmers University of Technology, Sweden

Texture at Non-Ambient Conditions**Texture at Non-Ambient Conditions**

Room: Rangos 1

Session Chairs: Sven Vogel, Los Alamos National Laboratory; Bjorn Clausen, Los Alamos National Laboratory

1:45 PM**(ICOTOM-S4-001-2008) High Pressure Deformation Mechanisms from In Situ Texture Measurements (Invited)**

S. Merkel*, CNRS - University Lille 1, France

2:15 PM**(ICOTOM-S4-002-2008) High Pressure Deformation Study of Zirconium ad Beryllium**

S. C. Vogel*, D. W. Brown, Los Alamos National Laboratory, USA; N. Nishiyama, APS, USA; H. Reiche, T. A. Sisneros, H. M. Volz, Los Alamos National Laboratory, USA; Y. Wang, APS, USA; J. Zhang, Y. Zhao, Los Alamos National Laboratory, USA

2:30 PM**(ICOTOM-S4-003-2008) Texture Development in Copper after Cryogenic Rolling and Heat Treatment**

A. Haldar*, Tata Steel Ltd., India; D. Das, P. P. Chattopadhyay, Bengal Engineering and Science University, India

2:45 PM**(ICOTOM-S4-004-2008) Texture Changes during Phase Transformations Studied In-Situ with Neutron Diffraction (Invited)**

H. Wenk*, University of California, USA

3:15 PM**(ICOTOM-S4-005-2008) Texture Memory and Modeling In A NiTi Shape Memory Alloy**

B. Ye, B. S. Majumdar*, New Mexico Tech, USA

3:30 PM**Break****4:00 PM****(ICOTOM-S4-006-2008) Texture Development during Compressive Loading of Extruded Magnesium**

B. Clausen*, C. N. Tome, D. W. Brown, Los Alamos National Laboratory, USA; S. R. Agnew, University of Virginia, USA

4:15 PM**(ICOTOM-S4-007-2008) In Situ Observation of Texture Evolution in Ti-10-2-3**

S. L. Raghunathan*, R. J. Dashwood, M. Jackson, D. Dye, Imperial College, United Kingdom

4:30 PM**(ICOTOM-S4-008-2008) Texture Evolution of Zirconium Alloys During Processing on the High Temperature Beta Phase**

J. Romero*, J. Q. da Fonseca, M. Preuss, The University of Manchester, United Kingdom

4:45 PM**(ICOTOM-S4-009-2008) Investigation of Variant Selection by using High Temperature in-situ EBSD Measurements**

I. Lischewski*, G. Gottstein, RWTH Aachen, Germany

5:00 PM**(ICOTOM-S4-010-2008) EBSD Analysis of Explosively Welded Aluminum**

C. C. Merriman*, D. Field, S. Freeze, Washington State University, USA

5:15 PM**(ICOTOM-S4-011-2008) Study of Texture Evolution at High Strain Rates in FCC Materials**

N. P. Gurao*, S. Suwas, Indian Institute of Science, Bangalore, India; R. Kapoor, Bhabha Atomic Research Center, India

5:30 PM**(ICOTOM-S4-012-2008) Technique for Texture Measurement Under Shock Loading**

B. El-Dasher*, J. Hawreliak, J. McNaney, Lawrence Livermore National Laboratory, USA; D. Milathianaki, University of Texas at Austin, USA; M. Butterfield, D. Swift, H. Lorenzana, Lawrence Livermore National Laboratory, USA

FINAL PROGRAM

Thursday, June 5, 2008

Recrystallization Texture: Retrospective vs. Current Problems**Recrystallization I**

Room: Rangos 2

Session Chair: Michael Kassner, University of Southern California

1:45 PM**(ICOTOM-S10-001-2008) Influence of Taylor Factor M Value on Recrystallization of the Cube and Cube-family Grains of FCC Metal**
H. Masui*, Teikyo University, Japan**2:00 PM****(ICOTOM-S10-002-2008) Influence of Grain Boundary Mobility on Texture Evolution during Recrystallization**
M. Winning*, D. Raabe, Max-Planck Institute for Iron Research GmbH, Germany**2:15 PM****(ICOTOM-S10-003-2008) Effect of External Constraint and Deviation from Ideal Orientation on Development of Rolling Texture in Pure Aluminum Single Crystal having {001} <100> Orientation**

K. Kashiwara*, Wakayama National College of Technology, Japan; H. Inagaki, INATEX, Japan

2:30 PM**(ICOTOM-S10-004-2008) Modeling Tandem Rolling in Commercial Aluminum Alloys including Recrystallization Simulation Using a Cellular Automata Method**

C. Schäfer*, V. Mohles, G. Gottstein, Institute of Physical Metallurgy and Metal Physics, Germany

2:45 PM**(ICOTOM-S10-005-2008) Simulation of Grain Coarsening Process Referring to Orientation Coordination at Encroaching Front**

K. Ito*, Nihon University, Japan

3:00 PM**(ICOTOM-S10-006-2008) Subgrain Coarsening as a Function of Texture Component in 3D Digital Microstructures in AA5005**

S. Wang*, A. D. Rollett, Carnegie Mellon University, USA

3:15 PM**(ICOTOM-S10-007-2008) Avoiding Roping and Ridging Phenomena in AA 6XXX Aluminium Sheet**

T. Bennett*, Netherlands Institute for Metals Research, Netherlands; R. H. Petrov, Ghent University, Belgium; L. A. Kestens, Delft University of Technology, Netherlands

3:30 PM

Break

4:00 PM**(ICOTOM-S10-008-2008) Texture Modification in Asymmetrically Rolled Aluminum Sheets**

J. Sidor*, A. Miroux, Netherlands Institute for Metals Research, Netherlands; R. Petrov, Ghent University, Belgium; L. Kestens, TU Delft, Netherlands

4:15 PM**(ICOTOM-S10-009-2008) Patterns of Deformation and Associated Recrystallization in Warm/Hot Deformed AA6022**

S. Raveendra*, S. Mishra, IIT Bombay, India; H. Weiland, ALCOA, USA; I. Samajdar, IIT Bombay, India

4:30 PM**(ICOTOM-S10-010-2008) Oriented Grain Growth Investigations in Annealed AlMn Alloys Using High Energy Synchrotron Radiation**

C. E. Tommaseo*, H. Klein, Friedrich August Universität, Germany

4:45 PM**(ICOTOM-S10-011-2008) Analysis of the Texture and Mean Orientation of Aluminium Alloy AA5052 Subjected to Forward and Reverse Hot Torsion and Subsequent Annealing**

O. Hernandez-Silva*, B. P. Wynne, M. Rainforth, The University of Sheffield, United Kingdom

5:15 PM**(ICOTOM-S10-013-2008) Evolution of {111} Recrystallization Texture in Al-Mg-Si Alloy Sheets Processed by Symmetric and Asymmetric Combination Rolling**

H. Inoue*, S. Kobayashi, M. Hori, Osaka Prefecture University, Japan; T. Komatsubara, Furukawa-Sky Aluminum Corp., Japan; T. Takasugi, Osaka Prefecture University, Japan

Texture Effects on Damage Accumulation**Damage Accumulation I**

Room: Connan

Session Chairs: Hasso Weiland, Alcoa Technical Center; Jean-Yves Buffiere, Universite de Lyon

1:45 PM**(ICOTOM-S13-001-2008) Experimental Characterisation of the Effect of Crystallography on the Three Dimensional Nucleation and Growth of Fatigue Cracks in Metals (Invited)**

J. Buffiere*, H. Proudhon, E. Ferrie, W. Ludwig, Universite de Lyon INSA-LYON MATEIS CNRS UMR5510, France

2:15 PM**(ICOTOM-S13-002-2008) Fatigue Crack Initiation Behaviour during Thermomechanical Cyclic Loading in Austenitic Stainless Steel**

M. Ramesh*, H. J. Leber, Paul Scherrer Institute, Switzerland; K. Kunze, M. Diener, R. Spolenak, Swiss Federal Institute of Technology (ETH), Switzerland

2:30 PM**(ICOTOM-S13-003-2008) 3D Observations of Fatigue Crack Initiation sites in 7075-T651 Aluminum Alloy**

S. D. Sintay*, T. Nuhfer, Carnegie Mellon University, USA; H. Weiland, ALCOA Technical Center, USA; A. Rollett, Carnegie Mellon University, USA

2:45 PM**(ICOTOM-S13-004-2008) Local Characterization of Void Initiation on IF Steel by FIB-EBSD Technique**

O. León García*, Netherlands Institute for Metals Research, Netherlands; R. Petrov, Ghent University, Belgium; L. Kestens, Delft University, Netherlands

3:00 PM**(ICOTOM-S13-005-2008) Determination of Geometrically Necessary Dislocation Densities Using Diffraction-based Orientation Determination Techniques: Application to Crack Tip/wake Plasticity**

V. K. Gupta*, Y. Ro, S. R. Agnew, University of Virginia, USA

3:15 PM**(ICOTOM-S13-006-2008) Reversible Texture Transition during Accumulative Roll Bonding**

N. Kamikawa*, X. Huang, G. Winther, N. Hansen, Risø National Laboratory Technical University of Denmark – DTU, Denmark

3:30 PM

Break

4:00 PM**(ICOTOM-S13-007-2008) Texture Evolution of Cold Rolled NC Nickel as Compared to the Tvolution in Cold Rolled CG Ni**

A. Kulovits*, S. X. Mao, J. M. Wiezorek, University of Pittsburgh, USA

4:15 PM**(ICOTOM-S13-008-2008) Deformation Mechanism on Submicron Pure Copper**

Y. Xusheng*, L. Yandong, Key Laboratory for Anisotropy and Texture of Material (Ministry of Education), China; J. Qiwu, Factory of Cold Rolling Silicon Steel, Anshan Iron and Steel Group Corporation, China; Z. Xiang, Z. Liang, Key Laboratory for Anisotropy and Texture of Material (Ministry of Education), China

Thursday - Friday, June 5–6, 2008

4:30 PM**(ICOTOM-S13-009-2008) Evolution of Grain Boundary Microstructures in Molybdenum by Thermomechanical Processing from Single Crystals**

S. Kobayashi*, Ashikaga Institute of Technology, Japan; S. Tsurekawa, Kumamoto University, Japan; T. Watanabe, Tohoku University, Japan

4:45 PM**(ICOTOM-S13-010-2008) Kinetic Measurements of Texture and Microstructural Evolution Using Orientation Distribution Function and Residual Stress Relaxation**

S. Saimoto*, J. Cooley, C. Gabryel, Queen's University, Canada

5:00 PM**(ICOTOM-S13-011-2008) Grain Growth and Texture Evolution in ECAP and Pre-aged Al-1.2% Hf Alloy**

O. Al-Buhamad*, M. Z. Quadir, M. Ferry, The University of New South Wales, Australia

5:30 PM**(ICOTOM-S13-020-2008) Comparative Analysis of Low-Cycle Fatigue Behavior of 2D-Cf-PyC/SiC Composites in Different Environments**

Y. Zhang*, L. Zhang, L. Cheng, Y. Xu, Northwestern Polytechnical University, China

Friday, June 6, 2008**Friction Stir Welding and Processing****Friction Stir Welding and Processing**

Room: Rangos 1

Session Chair: Paul Dawson, Cornell University

8:30 AM**(ICOTOM-S1-001-2008) Texture Development in Aluminum Friction Stir Welds (Invited)**

R. W. Fonda*, Naval Research Laboratory, USA; J. F. Bingert, Los Alamos National Laboratory, USA; A. P. Reynolds, W. Tang, University of South Carolina, USA; K. J. Colligan, Concurrent Technologies Corporation, USA; J. A. Wert, Risø National Laboratory, Denmark

9:00 AM**(ICOTOM-S1-002-2008) Effect of Texture on Fracture Limit Strain in Friction Stir Processed AZ31B Mg Alloy (Invited)**

Y. S. Sato*, A. Sugimoto, H. Kokawa, Tohoku University, Japan; C. Lee, Korea Institute of Industrial Technology, South Korea

9:30 AM**(ICOTOM-S1-003-2008) Texture Gradients in Friction Stir Processed Ti 5111**

D. P. Field*, Washington State University, USA; T. W. Nelson, Brigham Young University, USA; J. Miller, Washington State University, USA

9:45 AM**(ICOTOM-S1-004-2008) Texture as a Forensic Tool in Friction Stir Welding (Invited)**

A. P. Reynolds*, University of South Carolina, USA

10:15 AM**Break****10:45 AM****(ICOTOM-S1-005-2008) Texture Evolution during Friction Stir Welding of Stainless Steel (Invited)**

J. Cho*, Korea Institute of Materials Science, South Korea

11:15 AM**(ICOTOM-S1-007-2008) Microstructure and Texture Analysis of Friction Stir Welds of Copper**

T. Saukkonen*, K. Savolainen, J. Mononen, H. Hänninen, Helsinki University of Technology, Finland

11:30 AM**(ICOTOM-S1-008-2008) Microstructural Evolution in Titanium Friction Stir Welds**

K. Knipling*, R. W. Fonda, Naval Research Lab, USA

11:45 AM**(ICOTOM-S1-009-2008) Microstructural Studies of a Friction Stir Welded AA5052**

S. K. Sahoo, IIT Bombay, India; N. T. Kumbhar, Bhabha Atomic Research Centre, India; I. Samajdar*, IIT Bombay, India; R. Tewari, G. K. Dey, K. Bhanumurthy, Bhabha Atomic Research Centre, India

Texture Effects on Damage Accumulation**Damage Accumulation II**

Room: Connan

Session Chairs: Mukul Kumar, Lawrence Livermore National Lab; Antoinette Maniatty, Rensselaer Polytechnic Institute

8:30 AM**(ICOTOM-S13-013-2008) Effect of Grain Orientation on Fatigue Crack Nucleation (Invited)**

A. Maniatty*, D. Littlewood, D. Pyle, Rensselaer Polytechnic Institute, USA

9:00 AM**(ICOTOM-S13-014-2008) Dislocation based Finite Element Approach to Crystal Plasticity**

A. Alankar*, I. Mastorakos, D. P. Field, Washington State University, USA

9:15 AM**(ICOTOM-S13-015-2008) Physically based Approach for Predicting Damage Nucleation at Grain Boundaries in Commercial Purity Ti**

T. R. Bieler*, M. A. Crimp, Michigan State University, USA; P. Eisenlohr, F. Roters, D. Raabe, Max-Planck-Institut für Eisenforschung, Germany

9:30 AM**(ICOTOM-S13-016-2008) Influence of Crystallographic Texture on Fracture Resistance (Invited)**

F. Barlat*, Pohang University of Science and Technology, South Korea

10:00 AM**Break****10:30 AM****(ICOTOM-S13-017-2008) Role of Particles and Texture on Post-Necking Deformation in AA5754 Alloy**

X. Hu*, D. S. Wilkinson, M. Jain, P. Wu, McMaster University, Canada; R. K. Mishra, A. Sachdev, General Motors, USA

10:45 AM**(ICOTOM-S13-018-2008) Effects of Texture on the Growth Behaviors of Fatigue Cracks in High Strength Al Alloys**

T. Zhai, X. Jiang, J. Li, T. Li, Q. Zeng, University of Kentucky, USA; G. H. Bray, Alcoa Technical Center, USA; J. Li*, University of Kentucky, USA

11:00 AM**(ICOTOM-S13-019-2008) Experiment and Simulation Study on Texture and Bendability of AA5XXX Aluminum Alloys**

Y. Liu*, SECAT Inc., USA; Z. Long, X. Wen, University of Kentucky, USA; S. Ningileri, SECAT Inc., USA; S. K. Das, University of Kentucky, USA

FINAL PROGRAM

Friday, June 6, 2008

Texture and Anisotropy in Steels**Texture Analysis and Simulations**

Room: Rangos 3

Session Chairs: Bevis Hutchinson, KIMAB; Raul Bolmaro, Instituto de Física Rosario

8:30 AM**(ICOTOM-S3-038-2008) Quantitative Prediction of Transformation Texture in Hot-Rolled Steel Sheets by Multiple KS Relation**
T. Tomida*, M. Wakita, M. Yoshida, N. Imai, Sumitomo Metal Industries, Ltd., Japan**8:45 AM****(ICOTOM-S3-039-2008) Origins of "Texture Memory" in Steels**
B. Hutchinson*, KIMAB, Sweden; L. Kestens, TU Delft, Netherlands**9:00 AM****(ICOTOM-S3-040-2008) Effects of Preferred Orientation on Snoek Phenomena in Commercial Steels**
R. Gibala*, University of Michigan, USA; R. P. Krupitzer, American Iron & Steel Institute, USA**9:15 AM****(ICOTOM-S3-041-2008) Effect of Coating Texture on Powdering Behavior of Industrially Produced Galvannealed Coating on IF, IFHS and HSQ Grade Steels**
A. Chakraborty*, R. K. Ray, D. Bhattacharjee, TATA STEEL, India**9:30 AM****(ICOTOM-S3-042-2008) Method for Steels' Making Optimization**
A. Ioana*, University Politehnica of Bucharest, Romania**9:45 AM****(ICOTOM-S3-044-2008) On the Measurement of Residual Stress in Fe- Ni Based Alloy Sheet by X-ray Diffraction and Flexural Strain Gauge Techniques**
Q. Wu*, X. Hu, Z. Fu, W. Fang, Y. Wang, L. Li, Beijing Beiyue Functional Materials Co. Ltd., China; M. Xu, H. Zhao, Tsinghua University, China**10:00 AM****Break****10:30 AM****(ICOTOM-S3-045-2008) Effects of Strain and Strain Path on Deformation Twinning and on Strain Induced Martensite Formation in AISI 316L and 304L Austenitic Stainless Steel**
S. K. Mishra*, P. Pant, K. Narasimhan, I. Samajdar, IIT Bombay, India**10:45 AM****(ICOTOM-S3-046-2008) EBSD Textural Analyse of Deep Drawing Steels**
L. Hrabcakova*, P. Zimovcak, A. Lesko, U.S.Steel Kosice, Slovakia**11:00 AM****(ICOTOM-S3-047-2008) Comparison of Quantitative Texture Measurements via EBSD and X-Ray**
S. I. Wright*, EDAX-TSL, USA**11:15 AM****(ICOTOM-S3-048-2008) Practical Investigation into Identifying and Differentiating Phases in Steel Using Electron Backscatter Diffraction**
M. Nowell*, S. I. Wright, J. O. Carpenter, EDAX-TSL, USA**11:30 AM****(ICOTOM-S3-049-2008) Effect of Cold Rolling Reduction on the Texture and Plastic Strain Ratio of 2205 Duplex Stainless Steel**
C. Hou*, C. Liu, National Yunlin University of Science and Technology, Taiwan**11:45 AM****(ICOTOM-S3-050-2008) Texture and Deep-drawability of an Intermediately Annealed SUS430 Stainless Steel Sheet during Cold Rolling**
L. Chen*, Northeastern University, China; H. Bi, Baoshan Iron and Steel Co., Ltd., China; Y. Liu, H. Yu, Northeastern University, China**12:00 PM****(ICOTOM-S3-051-2008) Rolling and Annealing Textures in Low Carbon Steels**
R. E. Bolmaro*, A. Roatta, A. L. Fourty, Instituto de Física Rosario, Argentina**Recrystallization Texture: Retrospective vs. Current Problems****Recrystallization II**

Room: Rangos 2

Session Chair: Michael Kassner, University of Southern California

8:30 AM**(ICOTOM-S10-014-2008) Cube Texture due to Dynamic Recrystallization in Pb and PbSn Alloys under Equal Channel Angular Extrusion Processing (Invited)**
R. E. Bolmaro*, Instituto de Física Rosario, Argentina; V. L. Sordi, M. Ferrante, Universidade Federal de São Carlos, Brazil; W. Gan, Harbin Institute of Technology, China; H. Brokmeier, GKSS-Research Centre, Germany**9:00 AM****(ICOTOM-S10-015-2008) Studies on Texture and Microstructure of Cryorolled and Annealed Cu-5%Zn, Cu5%Al Alloys**
N. V.L., Indian Institute of Technology Madras, India; N. Gurao, Indian Institute of Science, India; U. Wendt, Otto von Guericke University, Germany; S. Suwas, Indian Institute of Science, India; S. S. Vadlamani*, Indian Institute of Technology Madras, India**9:15 AM****(ICOTOM-S10-016-2008) Function of Layer Thickness on the Microstructural Evolution in Copper of annealed Roll-Bonded Cu-Nb Composites**
C. Lim*, A. Rollett, Carnegie Mellon University, USA**9:30 AM****(ICOTOM-S10-017-2008) Development of Cube Texture in Cold-Rolled and Annealed Multilayer Tapes for Coated Superconductor Applications**
P. P. Bhattacharjee, Deakin University, Australia; R. K. Ray*, TATA Steel, India**9:45 AM****(ICOTOM-S10-018-2008) Rolling and Annealing Textures of Silver Sheets**
D. Lee*, H. Han, S. Kim, Seoul National University, South Korea**10:00 AM****Break****10:30 AM****(ICOTOM-S10-019-2008) Multi-cycle Pinch Welding of 304L Tubes: Inhomogeneities in Deformation and Recrystallization Textures and Microstructures**
C. T. Necker*, Los Alamos National Laboratory, USA; A. N. Marchi, New Mexico Tech, USA; M. G. Smith, Los Alamos National Laboratory, USA**10:45 AM****(ICOTOM-S10-020-2008) Ultra-fine Grain Austenitic Stainless Steels: Influence of Texture during Recrystallization**
A. Poulon*, Institut de Chimie de la Matière Condensée de Bordeaux, UPR CNRS 9048, France; S. Brochet, J. Vogt, Université de Lille I, LMPGM, UMR CNRS 8517, France; J. Glez, J. Mithieux, UGINE&ALZ Research Center, BP 15, France**11:00 AM****(ICOTOM-S10-021-2008) On the Stability of Recrystallization Textures in Low Alloyed Zirconium Sheets**
F. Gerspach*, N. Bozzolo, F. Wagner, LETAM, Université Paul Verlaine-Metz, France**11:15 AM****(ICOTOM-S10-022-2008) In-Situ SEM/EBSP Analysis during Annealing in Al-Mg Alloys**
Y. Takayama*, K. Morita, H. Kato, Utsunomiya University, Japan; Y. Ookubo, Sumitomo Light Metal Industries Ltd., Japan

11:30 AM

(ICOTOM-S10-023-2008) Effects of Elastic Modulus on Deformation and Recrystallization of High Purity Nb

D. C. Baars*, H. Jiang, T. R. Bieler, A. Zamiri, C. Compton, F. Pourboghrat, Michigan State University, USA; K. Hartwig, Texas A&M University, USA

11:45 AM

(ICOTOM-S10-024-2008) Nucleation and Growth of New Grains in Deformed Quartz Single Crystals

L. Lagoeiro*, P. Barbosa, Federal University of Ouro Preto, Brazil

12:00 PM

(ICOTOM-S10-025-2008) Effect of Solute Atoms on the Recrystallization Texture of Mg Alloys: In-Situ Annealing Experiments

R. Shahbazian Yassar*, Michigan Technological University, USA; S. Agnew, University of Virginia, USA; P. Kalu, National High Magnetic Laboratory, USA

**Monday, June 2 and
Tuesday, June 3, 2008****Posters**

Room: Rangos 2 & 3

(ICOTOM-P-001-2008) Texture Evolution in Dissimilar Al/Fe Welds: Influence of the Pin Position

I. Drouelle, A. Etter, T. Baudin, R. Penelle*, Université d'Orsay - Paris Sud, France

(ICOTOM-P-002-2008) Anisotropic Texture Evolution in Ti and Ni-based Alloys After Friction Stir Processing

O. M. Barabash, R. I. Barabash*, G. E. Ice, Z. Feng, S. David, Oak Ridge National Laboratory, USA

(ICOTOM-P-003-2008) Effect of Microstructure on Mechanical Properties of Friction-welded Joints between Aluminum Alloys (6061, 5052) and 304 Stainless Steel

S. K. Sahoo, IIT Bombay, India; N. T. Kumbhar, Bhabha Atomic Research Centre, India; I. Samajdar*, IIT Bombay, India; A. Laik, G. K. Dey, K. Bhanumurthy, J. Krishnan, D. J. Derose, R. L. Suthar, Bhabha Atomic Research Centre, India

(ICOTOM-P-004-2008) Grain Boundary Characteristics of the PED Nano-twin Copper Films

D. R. Waryoba*, FAMU-FSU College of Engineering, USA; B. Cui, National High Magnetic Field Laboratory, USA; P. N. Kalu, FAMU-FSU College of Engineering, USA

(ICOTOM-P-005-2008) X-Ray Microdiffraction Study of Grain-by-Grain Epitaxy of YBCO on Polycrystalline Ni

E. Specht*, A. Goyal, Oak Ridge National Laboratory, USA; W. Liu, Argonne National Laboratory, USA

(ICOTOM-P-006-2008) Epitaxial Substrates of Ni-based Ternary Alloys with Cr and W

I. Gervasyeva*, D. Rodionov, J. Khelebnikova, Russian Academy of Sciences, Russian Federation

(ICOTOM-P-007-2008) Texturing in Functional Thin Film Ceramic Battery Cathode Materials

J. Whitacre*, Carnegie Mellon University, USA

(ICOTOM-P-008-2008) Improvements in EBSD Data Analysis as Applied to Tantalum

D. Field*, Washington State University, USA; L. Maiocco, K. R. Ackley, Cabot, USA

(ICOTOM-P-009-2008) Microstructures and Microtextures of Au Flip Chip Bonds during Microelectronics Packaging

P. Yang*, C. Li, University of Science & Technology Beijing, China; D. Liu, M. Hung, M. Li, ASM Assembly Automation Ltd., China; W. Mao, University of Science & Technology Beijing, China

(ICOTOM-P-010-2008) Microstructure and Texture of Nb/SmCo₅ Bilayers

W. Skrotzki, R. Schaarschuch*, Technische Universität Dresden, Germany; S. Haindl, Leibniz-Institut für Festkörper- und Werkstoffforschung, Germany; M. Reibold, Technische Universität Dresden, Germany; V. Neu, B. Holtzapfel, Leibniz-Institut für Festkörper- und Werkstoffforschung, Germany; C. Oertel, Technische Universität Dresden, Germany; L. Schultz, Leibniz-Institut für Festkörper- und Werkstoffforschung, Germany

(ICOTOM-P-011-2008) On the Role of Nucleation during Microtexture Evolution in CVD Deposition of Diamond Thin Films

T. Liu*, S. Zaefferer, D. Raabe, Max-Planck-Institut fuer Eisenforschung, Germany

(ICOTOM-P-012-2008) Influence of the As-Cast Microstructure on the Evolution of the Hot Rolling Textures of Ferritic Stainless Steels with Different Compositions

P. Nnamchi*, D. Ponge, D. Raabe, Max-Planck-Institut fur Eisenforschung, Germany; A. Barani, G. Bruckner, J. Krautschik, ThyssenKrupp Nirosta GmbH, Germany

(ICOTOM-P-013-2008) Texture of Warm Rolled and Accumulative Roll Bonding (ARB) Processed Ferrite

A. Akbarzadeh*, Sharif Univ. of Technology, Iran; A. Kolahi, Sharif University of Technology, Iran

(ICOTOM-P-014-2008) Microstructure and Texture of Two Ferritic Stainless Steels

A. L. Pinto*, Instituto Militar de Engenharia, Brazil; C. S. da Costa Viana, A. L. Costa, Universidade Federal Fluminense, Brazil

(ICOTOM-P-015-2008) Effect of Tin on the Texture of Non-oriented Electrical Steels

C. Hou*, T. Lee, C. Liao, National Yunlin University of Science and Technology, Taiwan

(ICOTOM-P-016-2008) Combination of two X-ray Diffraction Settings for Determining the Texture of Small Sheared Samples

D. Barbier*, B. Bolle, J. Funderberger, C. Laruelle, A. Tidu, LETAM, France

(ICOTOM-P-017-2008) Analysis of the Formation and Growth of Recrystallizing Grains in IF Steels by In-Situ EBSD

H. Nakamichi*, Steel Research Lab., JFE Steel, Japan; J. F. Humphreys, University of Manchester, United Kingdom

(ICOTOM-P-018-2008) Primary and Secondary Recrystallization texture in Fe-3%Si Grain-Oriented Silicon Steels Containing Antimony

H. Joo*, J. Park, K. Han, J. Kim, Technical Research Laboratories, POSCO, South Korea

(ICOTOM-P-019-2008) Texture, Microstructure and Drawability of Frictionally Rolled AA 3003 Al Alloy Sheets

I. Kim*, S. Akramov, N. Park, J. Kim, Kum Oh National Institute of Technology, South Korea

(ICOTOM-P-020-2008) TEM study of the inhibition layer of Commercial Hot-Dip Galvanized Steels

J. Elia*, LETAM, France

(ICOTOM-P-021-2008) Texture Formation and Nucleation Observation during Recrystallization in Nonoriented Electrical Steels

J. Park*, K. Han, J. Kim, Technical Research Lab. POSCO, South Korea; J. A. Szpunar, McGill University, Canada

(ICOTOM-P-022-2008) Including Elastica Anisotropy of Welds in Finite Element Predictions of Residual Stresses

K. Decroos*, C. Ohms, JRC Petten, Netherlands; M. Seefeldt, F. Verhaeghe, mtm leuven, Belgium

(ICOTOM-P-023-2008) OBSERVATION OF SOLID-STATE WETTING MORPHOLOGY IN ABNORMALLY GROWING GRAIN OF FE-3%SI STEEL

K. Ko*, Seoul National University, South Korea; J. Park, J. Kim, POSCO, South Korea; N. Hwang, Seoul National University, South Korea

(ICOTOM-P-024-2008) Microstructural Characterization of Dual Phase Steels by means of Electron Microscopy

L. Barbe*, P. Pouteau, Centre for Research in Metallurgy (CRM), Belgium; K. Verbeken, Ghent University, Belgium

(ICOTOM-P-025-2008) Characterization of Mosaicity in a Mechanically Cycled Cu-13.1% Al-4.0% Ni Single Crystal Shape Memory Alloy

G. K. Kannarpady, University of Arkansas at Little Rock, USA; S. C. Vogel, Los Alamos National Laboratory, USA; A. Bhattacharyya*, University of Arkansas at Little Rock, USA

(ICOTOM-P-026-2008) X-ray Diffraction Studies on Texture Development in Aluminium Processed by Equal Angle Channel Pressing

J. te Nijenhuis*, PANalytical B.V., Netherlands; I. Cernatescu, PANalytical Inc., USA

(ICOTOM-P-027-2008) Correlation Between Austenitic and Martensitic Textures on Cu-Al-Ni-Ti Shape Memory Alloys

C. Sobrero, A. Roatta, J. Malarría, R. E. Bolmaro*, Instituto de Física Rosario, Argentina

(ICOTOM-P-028-2008) 3D-Orientation Microscopy in Electrodeposited CoNi

A. B. Fanta*, S. Zaefferer, D. Raabe, Max Planck Institute for Iron research, Germany

(ICOTOM-P-029-2008) 3D Microstructures and Textures of a Plane Strain Compressed {110}<112> Al-0.3%Mn Single Crystal

H. Paul*, Institute of Metallurgy and Materials Science PAS, Poland; J. Driver, C. Maurice, Ecole des Mines, France

(ICOTOM-P-030-2008) Grain Boundary Orientations in a Fe-Mn-Cu Polycrystalline Alloy

M. Takashima*, JFE Steel Corporation, Japan; P. Wynblatt, Carnegie Mellon University, USA

(ICOTOM-P-031-2008) Reconstruction of Three-Dimensional Microstructure of a Ni-based Superalloy and Its Grain Boundary Distribution

S. Lee*, G. S. Rohrer, A. D. Rollett, Carnegie Mellon University, USA; M. Uchic, AFRL/MLMD, USA

(ICOTOM-P-032-2008) Influence of Tape Casting Parameters on Texture Development in Alumina Ceramics

M. Snel*, J. van Hoolst, A. de Wilde, F. Snijders, J. Luyten, Flemish Institute for Technological Research, Belgium

(ICOTOM-P-033-2008) Influence of the Method of Ion Exchange and Copper Loading on the Physico-chemical of Cu-exchanged Pillared Clay Catalysts

R. Ben Achma*, A. Gorbil, Faculte des sciences de Tunis, Tunisia; F. Medina, A. Dafinov, University Rovira i Virgili, Spain

(ICOTOM-P-034-2008) Microstructural Studies of Solid Oxide Fuel Cell Cathodes by Orientation Imaging Microscopy

R. Petrova*, L. Helmick, P. A. Salvador, S. Seetharaman, G. Rohrer, Carnegie Mellon University, USA; R. Gemmen, K. Gerdes, U.S. Department of Energy, USA

(ICOTOM-P-035-2008) Fabrication of TiO₂-x by SPS and Improvement of the Thermoelectric Properties

Y. Lu*, M. Hirohashi, H. Yoshida, Chiba University, Japan

(ICOTOM-P-036-2008) Influence of Cold-Rolling in IF-Steel on Texture near Grain Boundaries

A. Wauthier*, CNRS, France; H. Regle, Arcelor Mittal R&D, France

(ICOTOM-P-037-2008) Crystallographic Investigation of Nitrided c-sapphire Substrate by Grazing Incidence X-ray Diffraction and Transmission Electron Microscopy

H. Lee*, J. Ha, Tohoku University, Japan; S. Hong, Chungnam National University, South Korea; S. Lee, H. Lee, S. Lee, T. Minegishi, T. Hanada, M. Cho, T. Yao, Tohoku University, Japan; O. Sakata, H. Tajiri, Japan Synchrotron Radiation Research Institute(JASRI), Japan; J. Lee, J. Lee, Korea Advanced Institute of Science and Technology, Japan

(ICOTOM-P-038-2008) Impurity Segregation Energy in fcc Al Determined from First Principles

M. Gao*, A. Rollett, Carnegie Mellon University, USA

(ICOTOM-P-039-2008) Quartzite Textures in the Córdoba Sierra (Argentina). The Guamanes Region

R. D. Martino, F.C.E.F. y N. Universidad Nacional de Córdoba., Argentina; A. L. Fourty, R. E. Bolmaro*, Instituto de Física Rosario, Argentina; H. Brokmeier, GKSS-Research Centre, Germany

(ICOTOM-P-040-2008) EBSD Study of Delamination Fracture in Al-Li Alloys

W. Tayon*, Old Dominion University and the Applied Research Center, USA; R. Crooks, National Institute of Aerospace, USA; M. Domack, J. Wagner, NASA Langley Research Center, USA; A. Elmustafa, Old Dominion University and the Applied Research Center, USA

(ICOTOM-P-041-2008) 5-Parameter Interfacial Boundary Character Distribution of Cu-Nb Composites

S. Lee*, C. Lim, Carnegie Mellon University, USA; A. Misra, Los Alamos National Laboratory, USA; A. D. Rollett, Carnegie Mellon University, USA

(ICOTOM-P-042-2008) Crystallographic Features during Martensitic Transformation in Ni-Mn-Ga Ferromagnetic Shape Memory Alloys

D. Cong, Northeastern University, China; Y. Zhang*, C. Esling, University of Metz, France; Y. Wang, X. Zhao, L. Zuo, Northeastern University, China

(ICOTOM-P-043-2008) Effect of High Magnetic Field During Annealing on Texture of Silicon Steel

H. Garmestani*, C. M. Bacaltchuka, Georgia Institute of Technology, USA

(ICOTOM-P-044-2008) Recrystallization Texture Development in Non-oriented Silicon Steel under Magnetic Annealing

W. Pei, Y. Sha*, S. Zhou, L. Zuo, Key Lab for Anisotropy and Texture of Materials, China

(ICOTOM-P-045-2008) Effects of Magnetic Field Direction on Texture Evolution in a Cold-rolled Interstitial-free Steel Sheet During High Magnetic Field Annealing

Y. Wu, X. Zhao*, S. C. He, L. Zuo, Northeastern University, China

(ICOTOM-P-046-2008) Lattice Reconstruction - A Crystallographic Model for Grain Reorientation in Basal Texture of HCP Magnesium

B. Li*, E. Ma, K. Ramesh, Johns Hopkins University, USA

(ICOTOM-P-047-2008) Effects of Alloying Elements on the Texture of Extruded Magnesium Alloys

J. Choi*, J. Hwang, K. Shin, Seoul National University, South Korea

(ICOTOM-P-048-2008) Analysis of the Formation of gamma-Massive Microstructures in a TiAl-based Alloy

A. Sankaran, E. Bouzy, M. Humbert*, A. Hazotte, UPVM, France

(ICOTOM-P-049-2008) Microstructure and Texture Evolution in Grain-refined α_2 +gamma Titanium Aluminides

S. Roy*, Indian Institute of Science, India; S. d. Waziers, Institut National Polytechnique de Toulouse, France; S. Suwas, Indian Institute of Science, India

(ICOTOM-P-050-2008) Bulk Texture Changes in Rolled Zr-1%Nb Alloy under Electron Irradiation

Y. Perlovich, M. Grekhov*, M. Isaenkova, O. Krymskaya, Moscow Engineering Physics Institute, Russian Federation; V. Lazorenko, V. Tovtin, Institute of Metallurgy RAS, Russian Federation

(ICOTOM-P-051-2008) Recrystallization Kinetics in Deformed Pure Copper

B. Zakaria*, B. Ghania, Biskra University, Algeria; G. Thierry, T. Isabelle, Rennes University, France

(ICOTOM-P-052-2008) Through-Process Texture Modeling of AA6016 from Hot Rolling to Final Annealing

C. Bollmann*, G. Gottstein, RWTH Aachen University, Germany

(ICOTOM-P-053-2008) Statistical Analysis on the Orientation Relationship between Recrystallized Grains and Deformed Grains in the IF Steel

D. Kim*, Korea Institute of Science and Technology, South Korea; K. Oh, H. Lee, Seoul National University, South Korea

(ICOTOM-P-054-2008) Investigation on Microstructure Evolution of Gold Bonding Wires during Annealing Using EBSD and MC Modeling

J. Cho*, Korea Institute of Materials Science, South Korea; S. Choi, Sunchon National University, South Korea; K. Oh, Seoul National University, South Korea

(ICOTOM-P-055-2008) Effect of Mg Concentration on the Texture Formation in Al-Mg Solid Solution Alloys during High Temperature Compression Deformation

K. Okayasu*, H. Takekoshi, M. Sakakibara, H. Fukutomi, Yokohama National University, Japan

(ICOTOM-P-056-2008) Comparison of the Texture Development During Static Recrystallization and Dynamic Recrystallization of Dilute Binary Mg-Y Alloys

R. Cottam*, J. Robson, G. Lorimer, University of Manchester, United Kingdom; B. Davis, Magnesium Elektron, United Kingdom

(ICOTOM-P-057-2008) Texture Evolution in α and β (B2) Phases of Ti-22Al-25Nb Alloy during Deformation in Two-phase Region and its Effect on α + β 2 \rightarrow β - α +B2 Transformation Texture

S. R. Dey*, Technische Universität, Germany; S. Suwas, Indian Institute of Science, India; J. Fundenberger, Université Paul Verlaine - Metz, France; R. K. Ray, Tata Steel, India

(ICOTOM-P-058-2008) Textural Inhomogeneity Effect during the Monte Carlo Simulation of the Abnormal Goss Grain Growth in Fe-3%Si Steel Grade HIB

T. Baudin, D. Ceccaldi, R. Penelle*, University of Paris Sud, France

(ICOTOM-P-059-2008) Study on Evolution of Partial Texture from Different Size Grains during Grain Growth in IF Steels

W. Tong*, Northeastern University, China; F. Wagner, Metz University, France; W. Chen, L. Zuo, J. He, Northeastern University, China

(ICOTOM-P-060-2008) Textures and Multistructure of Single to Multi-Layered Modern Brachiopod Shells

E. Grieshaber*, A. Götz, W. W. Schmahl, Ludwig-Maximilians Universität München, Germany; C. Lüter, Humboldt Universität, Germany; R. D. Neuser, Ruhr-Universität Bochum, Germany

(ICOTOM-P-061-2008) Texture and Ultrastructure of Brachiopod Shells: A Mechanically Optimized Material with Hierarchical Architecture

W. W. Schmahl, Ludwig-Maximilians-Universität München, Germany; K. Kelm, Rheinische Friedrich-Wilhelms Universität Bonn, Germany; E. Griesshaber*, Ludwig-Maximilians-Universität München, Germany; S. Enders, Max-Planck-Institut für Metallforschung, Germany

(ICOTOM-P-062-2008) Defect Structures in Block Copolymer/Nanoparticle Blends

H. Ryu*, M. R. Bockstaller, Carnegie Mellon University, USA

(ICOTOM-P-063-2008) Microtexture and Microstructure Evolution in High Purity and Particle Containing Aluminum Alloys Processed by Accumulative Roll Bonding

A. Akbarzadeh*, H. Pirgazi, Sharif Univ. of Technology, Iran; R. Petrov, Sharif University of Technology, Iran; L. Kestens, Ghent University, Belgium

(ICOTOM-P-064-2008) Effect of Dislocation Stress on the Surface Corrosion Behavior on (111) and (112) Plan of Aluminum Single Crystal

D. Pei, W. Mao*, University of Science and Technology Beijing, China

(ICOTOM-P-065-2008) Formation of Al₃Ti/AlB₂ in an Al-Ti/Al-B Master Alloy

D. G. Mallapur*, S. A. Kori, Basaveshwar Engineering College, India

(ICOTOM-P-067-2008) Influence of Shear Bands on Microtexture Evolution in Polycrystalline Copper

H. Paul*, Institute of Metallurgy and Materials Science PAS, Poland; J. Driver, Ecole des Mines, France

(ICOTOM-P-069-2008) Grain Coarsening Kinetic in ECAPed Al Containing 0.1%Sc

A. Bommareddy, M. Z. Quadir*, N. Burhan, O. Al-Buhamad, M. Ferry, The University of New South Wales, Australia

(ICOTOM-P-070-2008) Study of the Evolution of Texture and Microstructure during Different Modes of Rolling and Annealing of Two-phase ($\alpha+\beta$) Brass

R. Garg, N. Gurao*, S. Suwas, S. Ranganathan, Indian Institute of Science, India

(ICOTOM-P-071-2008) Processing-Texture-Property Relationship in ECAE Processed Two Phase ($\alpha+\beta$) Brass

A. Bhowmik, S. Biswas, S. Singh, N. Gurao*, S. Suwas, Indian Institute of Science, Bangalore, India

(ICOTOM-P-072-2008) Microstructure Sensitive Design of a Polycrystalline alpha-Ti Compliant Beam

T. Fast*, S. R. Kalidindi, Drexel University, USA

(ICOTOM-P-073-2008) Modeling Cube Texture Effects on Formability of FCC Sheet Metal

J. W. Signorelli*, M. A. Bertinetti, P. A. Turner, R. E. Bolmaro, IFIR - CONICET, Argentina

(ICOTOM-P-074-2008) Electroless Nickel Plating on Magnesium Alloys used in Space Applications

N. Dhawan*, Punjab Engineering College, India

(ICOTOM-P-076-2008) Simulation of Microstructure Evolution of Polycrystalline Ice: Model Set-up

A. Giera*, CNRS-Université Paul-Sabatier, France; R. Lebensohn, Los Alamos National Laboratory, USA; M. Jessell, CNRS-Université Paul-Sabatier, France; L. Evans, University of Melbourne, Australia

(ICOTOM-P-077-2008) Grain Interaction and Related Elastic Fields at Triple Junction in Low Deformed IF Steel: Micromechanical Model and Reconstruction from EBSD Orientation Data

A. Zisman*, V. Rybin, CRISM "Prometey", Russian Federation; M. Seefeldt, S. Van Boxel, P. Van Houtte, Kathollic University of Leuven, Belgium

(ICOTOM-P-078-2008) Two-Phase Microstructure Generation in 3D based on 2D Sections of a Nickel Alloy

C. Roberts*, Carnegie Mellon University, USA; L. Semiatin, Air Force Research Laboratories, USA; A. Rollett, Carnegie Mellon University, USA

(ICOTOM-P-079-2008) Study on Cold Drawing Texture of High-Strength Low-Expansion Fe-Ni Alloy

L. Chen*, University of Science and Technology Beijing, China; J. Zhang, Central Iron & Steel Research Institute, China; L. Zhang, University of Science and Technology Beijing, China

(ICOTOM-P-080-2008) Model of Plastic Spin Taking in Account Grain Interaction during Rolling

R. E. Bolmaro*, A. L. Fourty, J. W. Signorelli, Instituto de Física Rosario, Argentina

(ICOTOM-P-081-2008) Numerical Simulation of Mechanical Behavior and Failure Process for Heterogeneous Brittle Materials in Uniaxial Tension by use of Fast Lagrangian Analysis of Continua

W. Xue-bin*, Department of Mechanics and Engineering Sciences, Liaoning Technical University, China

(ICOTOM-P-082-2008) Simulating Recrystallization Texture Evolution in FCC and BCC Polycrystals

B. Radhakrishnan*, G. Sarma, Oak Ridge National Lab, USA

(ICOTOM-P-083-2008) Quantitative Texture Analysis Using Area Detector

N. Yang*, Bruker AXS Inc., USA; K. Helming, Bruker AXS GmbH, Germany; U. Preckwinkel, K. Smith, B. He, Bruker AXS Inc., USA

(ICOTOM-P-084-2008) Mechanism of Cube Grain Nucleation during Re-crystallization of Deformed Commercial Purity Aluminium

K. Kashyap*, C. S. Ramesh, PES Institute of Technology, India

(ICOTOM-P-085-2008) Effect of Thermomechanical Treatment on the Grain Boundary Character Distribution in a 9Cr-1Mo Ferritic Steel

T. Karthikeyan*, Indira Gandhi Centre for Atomic Research, India; S. Mishra, IIT Bombay, India; S. Saroja, M. Vijayalakshmi, Indira Gandhi Centre for Atomic Research, India; I. Samajdar, IIT Bombay, India

Abstracts

Monday, June 2, 2008

Plenary Session

Room: McConomy Auditorium

Session Chair: Anthony Rollett, Carnegie Mellon University

8:30 AM

(ICOTOM-PL-001-2008) Annealing Texture Evolution (Invited)

I. Dillamore*, Birmingham University, United Kingdom

The paper gratefully acknowledges receipt of the Bunge Award and reviews how views changed over the period of the author's experience concerning the debate concerning texture control by rolling and annealing.

Novel Texture Measurement Techniques Including 3D

Novel Methods Including 3D - I

Room: Rangos 1

Session Chair: Ulrich Lienert, Argonne National Laboratory

10:15 AM

(ICOTOM-S5-001-2008) Deformation Texture Evolution Observed at the Grain Scale (Invited)

G. Winther*, Technical University of Denmark, Denmark

Ideally, the community of polycrystal plasticity modeling would like input from experiments in the form of high resolution maps of deformed metals revealing the position and shape of each individual grain in the sample as well as its orientation spread. In addition such maps are desired as a function of deformation strain. Considering that the spatial coordinates of the sample span 3 dimensions, the crystallographic orientation space spans additional 3 dimensions, and that the strain adds 1 dimension, this is actually a 7D problem. Three dimensional X-ray diffraction (3DXRD) using high energy synchrotron radiation has the potential to yield 7D maps because it is non-destructive, relatively fast and penetrates well into the sample. The dynamic capability has been demonstrated by 4D+ measurements of rotation trajectories during deformation. This covers 3D crystallographic orientations as a function of strain (1D) and additional dimensionality of debatable dimension from knowing that the observed grain is in the central part of the sample. Knowing that the grain is deeply embedded in the bulk of the metal, i.e. free of potential surface effects, is an important quality of the data as it ensures that they are representative of the vast majority of grains. 6D maps with full spatial and orientational information have been constructed for undeformed samples. This has not yet been achieved for deformed samples although progress to do so is rapid. In the meantime, combination of 3DXRD in the undeformed state with serial sectioning and electron backscattering diffraction (EBSD) in the deformed state may be employed to add the 7th dimension. To illustrate the importance of multidimensional data, their emerging implications for polycrystal plasticity modeling are also briefly discussed.

10:45 AM

(ICOTOM-S5-002-2008) Local Crystal Rotations of Bulk Grains during Hot PSC in Al – 0.1 % Mn Polycrystals by High-Resolution EBSD

R. Quey*, D. Piot, J. Driver, Ecole des Mines de Saint-Etienne, France

There are relatively few studies which aim to characterize how individual grains actually deform and rotate during deformation, i.e. as a function of their initial orientations and locations. One of these, by Panchanadeeswaran et al. (1995), used a split sample of commercial purity Al deformed in hot plane strain compression. The sample was split in half normal to the transverse direction and a region on the "internal" surface was observed. Using the BKD technique, the orientations of 100 grains were measured before and after a one-pass de-

formation to determine how they actually changed — about 2 measurements per grain were done before deformation and 14 after. Agreement with standard Taylor models was the exception. In the present study, a similar sample of binary Al - 0.1 % Mn is used and a set of about 100 grains is observed on the internal surface. The bulk deformation is imposed at 400°C in several passes, up to 40 %. After each pass, the sample is quenched to avoid recrystallization, and the microstructure is analysed by high-resolution EBSD — about 5000 orientation measurements per grain were made. In this way, deformation features such as grain mean orientation changes or in-grain misorientations can be analysed accurately. Furthermore, fine-scale investigations on a smaller region provide information on the grain substructure development. This method enables us to study the evolution during hot plane strain compression of a representative set of grains embedded in a 3-D polycrystal, both at the grain and subgrain levels. The average grain reorientation, as measured in this set of grains, usually turns out to be significantly off the Taylor predictions in accordance with the conclusion of Panchanadeeswaran et al., and the rotation paths appear to be irregular. Moreover, large in-grain orientation spreads were measured, sometimes as high as 20 degrees.

11:00 AM

(ICOTOM-S5-003-2008) Three Laws of Substructure Anisotropy of Textured Metal Materials, Revealed by X-ray Method of Generalized Pole Figures

Y. Perlovich*, M. Isaenkova, V. Fesenko, Moscow Engineering Physics Institute, Russian Federation

Any metal material with a developed crystallographic texture shows the substructure anisotropy, i.e. different values of substructure parameters, measured along different external directions. Such anisotropy is responsible for various technological and operational properties of products and therefore is of the extraordinary interest, both scientific and practical. Processes of texture and substructure formation in metal materials under deformation treatment are tightly interconnected and require a joint experimental study, realizable by the new X-ray method of Generalized Pole Figures (GPF). This method combines the texture analysis with the X-ray line profile analysis and gives most detailed systematic data on the substructure anisotropy of material versus its texture. The method bases on the known principle, according to which the profile of X-ray line (hkl) characterizes the condition of crystalline lattice in irradiated grains along the normal to reflecting planes {hkl}. Application of the GPF-method by study of many textured metal materials resulted in discovery of three general laws, controlling the substructure anisotropy. The 1st law of substructure anisotropy: Residual deformation effects, i.e. grain fragmentation and lattice distortion, are minimal along directions, corresponding to maximal density of crystallographic axes, i.e. texture maxima, and increase up to highest values by passing to texture minima. The 2nd law of substructure anisotropy concerns variation of lattice parameters in metal products due to elastic microstrain: For each grain with crystalline lattice, extended along axis <hkl> by (+e), there is its pair with the symmetric orientation, where along axis <hkl> crystalline lattice is compressed by (-e), so that accompanying elastic microstresses are equilibrated. The 3d law: By passing from residual tension of the crystalline lattice to its compression, grain fragmentation becomes stronger, i.e. tensile elastic deformation is more uniform than compressing one.

11:15 AM

(ICOTOM-S5-004-2008) Tomographic 3D EBSD Analysis of Deformation and Rotation Patterns around Nanoindentations

D. Raabe*, N. Zaafarani, F. Roters, S. Zaefferer, Max-Planck-Institut für Eisenforschung, Germany

This study is about the origin of systematic deformation-induced crystallographic orientation patterns around nanoindentations (here: single crystalline copper; conical indenter) using the following approach: First, the rotation pattern is investigated in 3D using a high resolution 3D EBSD technique (EBSD tomography) which works by a serial sectioning and EBSD mapping procedure in a SEM-FIB cross

beam set-up. Second, the problem is modeled using a crystal plasticity finite element method which is based on a dislocation density based constitutive model. Third, the results are discussed in terms of a geometrical model which simplifies the boundary conditions during indentation in terms of a compressive state normal to the local tangent of the indent shape. This simplification helps to identify the dominant slip systems and the resulting lattice rotations and, thereby, allows us to reveal the basic mechanism of the formation of the rotation patterns. The finite element simulations also predict the pile-up patterning around the indents which can be related to the dislocation density evolution.

11:30 AM

(ICOTOM-S5-005-2008) Submicron-Resolution Mapping of Domains, Texture and Strain Using X-Ray Microdiffraction (Invited)

J. D. Budai*, B. Larson, G. Ice, Oak Ridge National Laboratory, USA; W. Liu, Argonne National Lab, USA; J. Tischler, Oak Ridge National Laboratory, USA; A. Rollett, Carnegie Mellon University, USA; K. Janssens, Swiss Federal Inst. of Tech., Switzerland; D. Norton, Univ. of Florida, USA; Z. Pan, Univ. of Georgia, USA; D. Sarma, Indian Inst. of Sci., India; G. Shenoy, Argonne National Lab, USA

Hard x-ray microbeam diffraction is emerging as a powerful tool to probe microstructures over lengths scales ranging from submicron to mm. At the UNI-XOR beamline at the Advanced Photon Source (APS), we have implemented a polychromatic, high-resolution scanning microbeam capability. This 3D structural probe has submicron spatial-resolution, and can alternate between polychromatic- and monochromatic-microbeam modes. Focusing is accomplished using elliptical Kirkpatrick-Baez (K-B) achromatic reflecting mirrors. Beam diameters of ~500 nm FWHM are typical, and 90 nm diameter focus has been achieved. In white-beam mode (~8-22 keV), a CCD area detector records the complete Laue diffraction pattern from each sample volume element, which is subsequently analyzed with automated indexing software. Spatially-resolved Laue diffraction patterns provide quantitative real-space maps of the local crystal structure, lattice orientation, and strain tensor. Conceptually, x-ray microscopy maps are similar to maps generated by electron backscatter diffraction, but do not require sectioning. Scanning x-ray microdiffraction has been used to investigate the microstructure and evolution of grain orientations in a variety of complex materials, including 1D, 2D and 3D systems. Using individual 1D nanowire devices, we have mapped the structure, orientation and crystal perfection along individual 200 nm diameter ZnO rods. In 2D studies, microdiffraction was used to quantitatively map the texture development of epitaxial oxide buffer-layer films grown on highly-textured metal substrates for superconducting applications. In 3D, structural investigations have included nondestructive studies of thermal grain growth in polycrystalline aluminum and local eutectic phase separation in complex, multiferroic manganite crystals. In each case, the ability to obtain spatially-resolved measurements represents a valuable new technique for probing material structures and dynamics. Support by DOE Office of Science, Division of Materials Sciences and Engineering under contract with ORNL, managed by UT-Battelle, LLC; UNI-CAT/XOR supported by ORNL, UIUC, NIST, UOP and DOE-BES; APS supported by DOE.

12:00 PM

(ICOTOM-S5-006-2008) 3D Measurements of Lattice Reorientation in the Near Surface Microstructures and Thin Layers Via Polychromatic Microdiffraction

R. I. Barabash*, G. E. Ice, Oak Ridge National Laboratory, USA

Three-dimensional (3D) measurements of the orientation (texture) distribution, lattice curvature and strain are now possible due to an emerging class of instrumentation: the 3D X-ray crystal strain microscope. This method is ideal for studies of mesoscale evolution of FIB and growth induced defects and lattice reorientation in thin layers. The spatial distribution of strain, misfit and threading dislocations, and crystallographic orientation in uncoalesced and coalesced GaN

layers grown on patterned substrates was studied by polychromatic x-ray microdiffraction, high-resolution monochromatic x-ray diffraction and scanning electron microscopy. Tilt boundaries formed at the column/wing interface depending on the growth conditions. Two kinds of crystallographic tilts are observed in the films. The measurements revealed that the free-hanging wings are tilted upward at room temperature in the direction perpendicular to the stripes. Finite element simulations of the thermally induced part of the wing tilt are presented. Moreover, a misorientation between the GaN(0001) and the Si(111) planes is observed in the parallel to the stripes direction. Its origin is discussed with respect to the strain of the epitaxial GaN on a miscut Si(111) surface and misfit dislocations formed at the interface. Lattice re-orientation in free and supported GaN films is compared. FIB induced lattice curvature and GNDs distribution in GaN layers is measured. Results are discussed in terms of the Nye tensor and deviatoric strain tensor components.

12:15 PM

(ICOTOM-S5-007-2008) Comparative Study of 3D Techniques for Microstructural and Texture Characterization

R. H. Petrov*, Ghent University, Belgium; O. León-García, Netherlands Institute for Metals Research, Netherlands; P. Gobernado Hernandez, Ghent University, Belgium; L. Kestens, Delft University of Technology, Netherlands

The microstructure of materials is of a 3-dimensional nature, but because the majority of the materials are opaque for either low-energy electron or light beams they are usually characterized on 2D sections by conventional light or scanning electron microscopy. For quantitative characteristics various methods are employed such as e.g. quantitative metallography, known also as stereometry. In many cases the obtained information is sufficiently precise to link the microstructure to the functional properties of the material, but in other cases such information is not complete. One example is the crack propagation in a material, which is by nature a 3D meso-scale feature. Also the grain boundary characteristics of the polycrystalline structures cannot be described completely in 2D only. Many of the processes during structure formation are dependent on the grain boundary or the phase boundary characteristics – like e.g. the nucleation behavior during phase transformation, or grain growth phenomena. Therefore, the 3D description of the microstructure is of crucial importance for a better understanding of the structure – properties relations. The application limits, advantages and disadvantages of two 3D EBSD techniques are compared and discussed in this work. The results obtained by the FEI dual beam FEG SEM NOVA600 system with an attachment for automated EBSD data collection are compared with the results obtained by a conventional serial sectioning technique by exactly controlled mechanical polishing. Both procedures were used for microstructural and microtextural characterization of three different type of materials: fine grained X80 pipeline steel (dav~5µm), coarse grained Fe-3%Si alloy (dav~120µm) and an IF steel with an average grain size of ~25µm. Various features like the grain shape directionality in the pipeline steel, grain boundary inclination in the Fe-3%Si and the deformation zones around Ti(CN) particles were described qualitatively and (semi) quantitatively. The quantitative 3D results are compared to the ones obtained by classical 2-D characterization of the same specimens and some restrictions for the optimal use of the techniques are outlined.

Novel Methods including 3D - II

Room: Rangos 1

Session Chair: Robert Suter, Carnegie Mellon University

1:45 PM

(ICOTOM-S5-008-2008) Statistically Reliable EBSD Analysis Method of Grain Boundary Characterization (Invited)

K. Oh*, J. Kang, E. Her, D. Kim, S. Kim, H. Han, SNU, South Korea; D. Kim, Korea Institute of Science and Technology, South Korea; H. Lee, SNU, South Korea

It is well known that the orientations of recrystallized grains or grain-grown grains are very closely related to that of deformed or original

Abstracts

grains. The orientation relation is believed to be dependent on time, temperature, deformation degree, initial deformed orientation, etc. To understand the physics of recrystallization or grain growth, the orientations of deformed grain and recrystallized grain should be characterized in a sense of the measurement accuracy and the statistically reliability. Recently EBSD (Electron Back Scattered Diffraction) technique was introduced to get the orientation relation with positional information. Modern digital computation technique can make the measurement speed in the range of hundreds frames per sec (fps), leading to get the information in the scale of X-ray measurement. To trace the change of the orientation relation during recrystallization, it is necessary to get out the orientation between the deformed and recrystallized grains. The grain growth characteristics also can be understood by obtaining the orientation relation at a certain grain size of the deformed grains. Also many various physical conditions are used to understand the grain growth characteristics from EBSD data. These statistically reliable EBSD analysis technique is used to the low carbon and IF steels. The developed analysis method can run under the public EBSD program REDS (Reprocessing of EBSD Data in SNU). Also an easy MDF space, o-MDF (Overlaid Misorientation Distribution Function) is introduced to understand the orientation easily. Also various criterions to discriminate recrystallised region from deformed region are analyzed to give statistical reliability of recrystallized fraction.

2:15 PM

(ICOTOM-S5-009-2008) Study on the Recrystallisation Nucleation Mechanisms of Heavily Deformed Fe36% Ni by High Resolution 3-Dimensional Orientation Microscopy

S. Zaeferrer*, Max-Planck-Institute for Iron Research, Germany

Fe 36 % Ni is an fcc alloy with high stacking fault energy. During rolling it develops a sharp copper-type cold rolling texture, during recrystallisation a sharp cube texture ($\{100\}\langle 001\rangle$). Using transmission electron microscopy the present author studied the origin of this recrystallisation component [1]. It was proposed that the cube orientation is formed by oriented nucleation from cube oriented deformed grains. The reason for preferred nucleation in these grains was found in the grain internal deformation structure. Using 3-dimensional (3D) orientation microscopy this subject was investigated again in order to study the 3D deformation structure and, in particular the nature of grain boundaries around the developing nuclei. 3D orientation microscopy is based on precise serial sectioning with a focused ion beam (FIB) and characterisation of the sections by EBSD (electron backscatter diffraction)-based orientation microscopy. It allows 3-dimensional characterisation of volume pixels as small as $50 \times 50 \times 50 \text{ nm}^3$, and maximum observable volumes in the order of $50 \times 50 \times 50 \mu\text{m}^3$. Using this technique the crystallography and morphology of cube-oriented recrystallisation nuclei in a 94 % cold rolled and in a shortly annealed sample of Fe 36 % Ni was studied. The technique revealed that nuclei form as small bubble-like areas, developing in the otherwise flat cube bands. A further important result which cannot be obtained by any other technique is the crystallography of the grain boundaries surrounding a growing nucleus, including not only the misorientation across boundaries but also the crystallographic indices of the grain boundary plane surrounding the nucleus. It was found that the well known $38^\circ \langle 111\rangle$ grain boundaries exist at growing cube nuclei but also other boundaries move quickly. [1] Zaeferrer S., Baudin T. and Penelle R., Acta Mater. 49 (2001) 1105 – 1122.

2:30 PM

(ICOTOM-S5-010-2008) Study on the Behaviours of Nucleation and Grain Growth in Deformed Ni and IF Steel by 3-D FIB-EBSD Tomography

W. Xu*, M. Ferry, University of New South Wales, Australia

The nucleation and grain growth behaviours in a cold rolled IF steel and a rolled SiO₂ particle containing Nickel single crystal were analyzed using 3-D FIB-EBSD tomography. It is revealed that the struc-

ture of nucleus can be divided into two parts: (1) nucleation core, having a dislocation containing subgrain structure, mainly bounded by low angle grain boundary, (2) newly grown part (NGP), having a dislocation free structure, mainly bounded by high angle grain boundary, in the very initial stage of nucleation. The formation process of nucleus is a combination of the NGP growing by strain induced boundary migration (SIBM) in a way of oriented pinning towards to high store energy areas such as high angle grain boundary, shear bands, and the nucleation core internally dislocation annihilation and externally expansion in its surrounding deformation substructures. Nuclei and their orientation are approved directly from deformation structures. The nuclei and recrystallizing grains grow faster toward to high store energy than low store energy deformation zone in heterogeneous deformation structures, causing a way of oriented pinning heterogeneous growth.

2:45 PM

(ICOTOM-S5-011-2008) 3D EBSD Texture Study on CVD Diamond Films

T. Liu*, S. Zaeferrer, D. Raabe, Max-Planck-Institut fuer Eisenforschung, Germany

A study of the nucleation and growth processes in chemical vapor deposition (CVD) diamond films was performed using a fully automated three-dimensional electron backscattering diffraction (3D EBSD) technique. The approach was conducted by a combination of a focused ion beam (FIB) unit for serial sectioning in conjunction with high-resolution field emission scanning electron microscopy and EBSD. The microstructures, microtextures, and grain boundary character distributions were characterized in full 3D. The low-index crystal planes, the twin boundary planes, and the twinning planes have been determined. The formation mechanism of lattice distortion and microtwinning during the growth process is discussed.

3:00 PM

(ICOTOM-S5-012-2008) 3D EBSD Investigation of Orientation Patterning Phenomena in Weakly Deformed Cu Single Crystals

O. Dmitrieva*, D. Raabe, Max-Planck-Institut fuer Eisenforschung, Germany

We present investigations on microscopic orientation patterning phenomena in single crystals after weak elastic-plastic deformations. The Cu single crystals were deformed under simple shear loading. During the shear experiment digital images were recorded from the crystal surface for photogrammetric analysis providing the von Mises strain distribution as well as the local strain tensors (strain determination via digital image correlation). The shear stress was applied along several crystallographic directions of the single crystals in order to investigate orientation patterning effects in dependence of the activated slip systems. Orientation gradients and 3D orientation patterns were in the weakly deformed single crystals investigated using three-dimensional orientation microscopy (3D EBSD). The fully automated 3D EBSD (electron backscattering diffraction) investigations were realized by a system which is a combination of a focused ion beam device for serial sectioning in conjunction with a high-resolution field emission scanning electron microscope which is equipped with a EBSD unit.

3:15 PM

(ICOTOM-S5-013-2008) 3D FIB-OIM of Ceramic Materials

S. J. Dillon*, G. S. Rohrer, Carnegie Mellon University, USA

Three-dimensional characterization of materials is important for understanding and predicting the microstructural evolution and properties of materials. Traditional serial sectioning of materials is difficult, tedious, and not well suited for fine grained materials. In recent years, the dual-beam focused ion beam microscope has allowed for three-dimensional characterization of fine grained materials to be performed more routinely. However, limited work has been performed on ceramic materials. This contribution discusses the application of this technique to obtaining

and reconstructing three-dimensional orientation data from ceramic materials. Results are presented for some cubic ceramic materials. Technical issues related to the sample preparation, experimentation, and three-dimensional reconstruction will be discussed.

4:15 PM

(ICOTOM-S5-014-2008) Measuring Strain Pole Figures and Distributions of Crystal Stresses in Deforming Polycrystals Using Synchrotron X-rays (Invited)

M. P. Miller*, J. Park, J. C. Schuren, Cornell University, USA

Motivated by quantitative texture analysis and pole figure inversion, we have developed methods for measuring lattice strain pole figures on specimens under load, then inverting the pole figures for the Lattice Strain Distribution Function (LSDF). Using single crystal moduli, the LSDF is then used to quantify the three-dimensional distribution of crystal stress over orientation space. In this talk, the experimental method, which includes monotonic and cyclic in-situ loading and synchrotron x-ray diffraction, is described. Experimental results from single and multiphase alloys are presented and some data are compared to simulation results. In particular, coefficients from spherical harmonic expansions of the stress component distributions from experiments and simulations are compared.

4:45 PM

(ICOTOM-S5-015-2008) Description of Plastic Deformation Substructure by Pair Correlations of the Dislocation Tensor

C. D. Landon*, J. Kacher, B. L. Adams, D. Fullwood, Brigham Young University, USA

Plastic deformation of crystalline materials is accommodated by crystallographic slip, and the formation and motion of dislocations. Of particular interest are the dislocation structures that form internal to grains, namely the cellular structure, because of their impact on the plastic behavior of the crystal. The motion of dislocations can be tracked by observing slip bands that form in a deformed material, and TEM micrographs can give qualitative measures of dislocation storage. For quantitative measures of dislocation content, Orientation Imaging Microscopy has been used to measure the orientation gradient in a material and determine the necessary dislocation content to accommodate the geometric crystal deformation. Recent advances in both Orientation Imaging Microscopy and dislocation characterization have overcome several of the limitations of the orientation based method. High resolution, cross correlation based Orientation Imaging Microscopy has increased angular resolution by a factor of 100 and is capable of recovering lattice strain, thereby increasing the resolution of dislocation densities without losing spatial resolution. Additionally, n-point correlations of the dislocation tensor provide a complete and compact representation of the dislocation densities and their interactions. Originally proposed by Kroner in 1970, correlations of the dislocation tensor are uniquely capable of identifying dislocation mesoscale structure, such as the plastic deformation substructure. A highly textured, near single-crystal, copper specimen was incrementally strain to known levels of plastic deformation. At each level of strain, the dislocation tensor pair correlations were evaluated and conclusions were drawn about the active mechanisms in plastic deformation substructure formation, specifically cell wall formation and grain fragmentation.

5:00 PM

(ICOTOM-S5-016-2008) Rapid Texture Determination Based on Two Dimensional X-Ray Detector

W. Mao*, University of Science and Technology Beijing, China

The rapid, non-destructive, continuous technology of on-line texture determination and corresponding deduction of texture related properties of industrial materials could serve for the instant and uninterrupted quality inspection and control on the production

line in modern material industry. High accuracy and high velocity are the two key factors of the on-line measurement technology. Two-dimensional X ray detector can collect very large amount of diffraction data instantaneously, and could be used to capture the necessary pole figure data which would be drastically reduced because of the symmetry and multiplicity of the pole figures. The corresponding accuracy of the texture measurement was obviously increased, while only the important diffraction data were selected and collected based on the known texture components of material products which were supposed to have Gaussian forms. The examination process and following texture calculation could be completed very rapidly with satisfied accuracy, which is suitable to the texture examination on stepwise or continuous materials production lines. A further transmission technique was proposed to ensure the representative texture expression in case of inhomogeneous texture through the material thickness. The on-line technologies for texture determination of pure aluminum, AA3104 aluminum alloy as well as interstitial free steel sheets were introduced as examples. It was also attempt to determine the texture related Lankford value of the interstitial free steel sheets based on the on-line technology.

5:15 PM

(ICOTOM-S5-017-2008) Development of a TEM-based Orientation Microscopy System and its Application to Study of Microstructure and Texture of Nanocrystalline NiCo Samples

G. Wu*, S. Zaefferer, Max-Planck-Institute for Iron Research, Germany

EBSD (electron backscatter diffraction)-based orientation microscopy is a powerful tool to study microstructure and texture of a wide variety of materials. On truly nanocrystalline bulk materials with grain sizes well below 50 nm, however, the technique cannot be applied because of its physical lateral resolution which, for the currently used technology, is in the order of 30 to 60 nm. For these materials TEM-based orientation microscopy might be a possible investigation technique. Nevertheless, the application of TEM techniques is not obvious: although the lateral resolution of TEM may be in the order of few nanometres (the size of the beam), its depth resolution is determined, compulsorily, by the thickness of the specimen which is very often in the order of 100 nm. A TEM technique for orientation microscopy on nanocrystalline materials therefore has to deal with superposition of several grains along the electron beam path and thus superposition of several diffraction patterns. Based on ideas of Rauch and Dupuy [1] and Dingley and Wright [2] and former developments of Zaefferer [3] we developed a TEM-based orientation microscopy system using a template matching algorithm to analyse spot diffraction patterns reconstructed from conical scanning dark field images. The system is designed to deal with overlapping diffraction patterns and is able to reconstruct grain structures and microtextures from nanocrystalline samples. We proof its capabilities by investigation of the texture and grain size of a nanocrystalline NiCo sample created by electrodeposition. The data are compared with those obtained by Bastos [4] using x-ray diffraction. [1] Rauch, E. F., Dupuy, L., Archives of Metallurgy and Materials 50 (2005) 87-99 [2] Wright, S. I. and Dingley, D. J., Mater. Sci. Forum 273-275 (1998) 209-214. [3] Zaefferer, S., Advances in Imaging and Electron Physics 125 (2002) 355 – 415 [4] Bastos, A., PhD Thesis, Max-Planck-Institute for Iron Research, Duesseldorf, Germany, to be defended end of (2007)

5:30 PM

(ICOTOM-S5-018-2008) New Method for Quantification of Texture Uniformity of Plate

P. Jepson*, H.C. Starck Inc., USA; R. S. Bailey, Tosoh SMD, Inc., USA

Since grains of different orientation sputter at different rates (in tantalum, a fast-sputtering orientation sputters at about twice the rate of a slow-sputtering orientation), control of texture in plate for sputtering targets is very important, particularly when the film to be deposited must be of very uniform thickness. In response to this situation, a

Abstracts

method is proposed to describe the texture, and particularly the degree of non-uniformity of the texture, quantitatively. The data-gathering is by EBSD, and the mathematics are simple, as the intent is to use the method in industry, for Quality Control purposes. The principles used may also have applications other than sputtering targets.

Effects of Magnetic Fields

Effects of Magnetic Fields

Room: Connan

Session Chair: Claude Esling, CNRS UMR 7078

10:15 AM

(ICOTOM-S8-001-2008) New Approach to Texturing and Grain Boundary Engineering by Magnetic Field Application (Invited)

T. Watanabe*, X. Zhao, L. Zuo, Northeastern University, China; S. Tsurekawa, Kumamoto University, Japan; C. Esling, Y. Zhang, University of Metz, France

Since the time of the introduction of a new concept of "Grain Boundary Design i.e. Grain Boundary Engineering" [1], basic and applied studies of "Grain Boundary Engineering" have been extensively attempted in connection with development of high performance structural and functional materials in the last two decades [2-6]. It has been found that there is a close relationship between characteristics of textures and grain boundary microstructures in textured materials [7,8]. It has been shown that the introduction of a sharp texture of a specific type of texture can generate unique orientation-dependent and grain boundary-controlled bulk properties and high performance of polycrystalline materials [5,7]. Quite recently, a new challenge of "Texturing and Grain Boundary Engineering by Magnetic Field Application" has been increasingly attempted and is now opening a new and highly potential area of Interface Science and Engineering, based on the control of textures and grain boundary microstructures by magnetic field application [9,10]. This plenary talk gives the background and state-of-the-art of "Grain Boundary Engineering by Magnetic Field Application" as a powerful non-contacting future processing for advanced materials. References: [1] T.Watanabe: Res Mechanics, 11(1984),47, [2] U.Erb, G.Palumbo (eds.): Proc. Karl Aust Intern. Symposium on "Grain Boundary Engineering", CIMMP,(1993), [3] G.Palumbo, E.M.Lehockey, P.Lin: J. Metals, 5(1998),40, [4] T.Watanabe, S.Tsurekawa: Acta Mater., 47(1999),4171, [5] T.Watanabe, S.Tsurekawa (eds.): J.Mater.Sci., 40(2005),Special Issue on "Grain Boundary Engineering", 817-932, [6] M.Kumar, C.A.Schuh: Scripta Mater.,54(2006), Viewpoint Set on "Grain Boundary Engineering", 961-1070, [7] T.Watanabe: Textures and Microstructures, 20 (1993), 195, [8] L.Zuo, T.Watanabe, C.Esling: Z.Metallkunde, 85(1994),554, [9] T.Watanabe, S.Tsurekawa, X.Zhao, L.Zuo: Scripta Mater.,54(2006),969, [10] T.Watanabe, S.Tsurekawa, X.Zhao,L.Zuo, C.Esling: J.Mater.Sci., 41(2006),7747-7759.

10:45 AM

(ICOTOM-S8-002-2008) Effect of Ultra-high Magnetic Fields on Grain Growth and Recrystallization in Metals

A. D. Sheikh-Ali*, H. Garmestani, Kazakh-British Technical University, Kazakhstan

Cold rolled pure Cu, Ti and Ni were annealed in a direct-current magnetic field of 25.5 MA/m. For comparison the samples from the same metals were annealed out of the field. The microhardness measurements reveal no effect of the field at the initial stages of recrystallization. A small difference in microhardness after annealing with and without field has been observed at the end of recrystallization and the beginning of grain growth following recrystallization. Annealing in the field preserves higher microhardness in comparison with annealing out of the field. The observed effect has been ascribed to the difference in magnetic free energy of recrystallized grains and grains with stored dislocations left after cold work.

11:00 AM

(ICOTOM-S8-003-2008) Eutectoid Point Shift and Orientation Relationships between Ferrite and Cementite in Pearlite in a High Magnetic Field

C. Esling*, Y. Zhang, University of Metz, France; X. Zhao, L. Zuo, Northeastern University, China

Thermodynamic calculation on phase transformation under high magnetic field B has been applied to FeX system [1,2]. In medium-C steels [3-5], the influence of B on microstructure [6] and crystallographic orientation relationships ORs of ferrite have been investigated. However, there is no experimental report on the shift of the eutectoid point by the application of B. Moreover, there is an argument about ORs determined by SAED. Therefore, experimental identification of the eutectoid point shift and clarification of the ORs between lamellar ferrite and cementite through modified eutectoid transformation by high B is a burning topic. Thus, a near eutectoid plain-C steel (0.81 C wt.%) was heat-treated without and with a high B. The influence of B on eutectoid point shift in composition and temperature is studied experimentally and theoretically. Its influence on the ORs between eutectoid ferrite and cementite was experimentally examined and analyzed. Results show that high B (12T) shifts the eutectoid composition from 0.77C%wt. to 0.84C%wt. Further calculation showed that this field increases the eutectoid temperature by 29 C. Without the field, there are mainly four ORs between pearlitic ferrite and pearlitic cementite that are Isaichev (IS), near Bagaryatsky (Bag) and two near Pitsch-Petch (P-P-1 and P-P-2) ORs, whereas with the field, there are mainly IS and P-P-2 ORs. Analysis shows that the selection of different ORs between ferrite and cementite in pearlite is dependent on the nucleation sequence of the two phases in pearlite. As the magnetic field promotes the formation of high magnetization phase, i.e., ferrite, as leading phase, in the field, the IS and P-P 2 are more frequent. [1] Zhang YD, He C, Zhao X, Zuo L, Esling C. Solid State Phenomena 2004;105:187 [2] Gao M C, Bennett T A, Rollett A D, Laughlin D E. J Phys D: 2006;39: 2890 [3] Zhang YD, He C, Zhao X, Esling C, Zuo L. Adv Eng Mater 2004;6:310 [4] Zhang YD, He C, Zhao X, Zuo L, Esling C, He J. J Magn Magn Mater 2004;284:287 [5] Zhang YD, He C, Zhao X, Zuo L. J Magn Magn Mater 2005;294:267 [6] Zhang YD, Esling C, Muller J, He C, Zhao X, Zuo L. Appl Phys Lett 2005;87: 212504

11:15 AM

(ICOTOM-S8-004-2008) Impact of a Magnetic Field on Recrystallization Texture Evolution in Non-Ferromagnetic Metals (Invited)

D. A. Molodov*, RWTH Aachen University, Germany

The current research on texture and grain structure evolution during recrystallization and grain growth in non-magnetic metals in high magnetic fields will be reviewed. As it is demonstrated in a series of experiments on polycrystalline zinc, titanium and zirconium, as well as by computer simulations, grain growth in magnetically anisotropic non-magnetic materials can be substantially affected by a magnetic field. This manifested itself by significant changes in the development of the grain growth texture during magnetic annealing compared to annealing at zero field. The magnetically induced texture changes are caused by the generation of an additional magnetic driving force which arises from a difference in magnetic free energy density between differently oriented grains. Owing to the orientation dependency of the magnetic driving force, a magnetic field possesses a remarkable property to produce preferred orientations during grain growth. The change of the driving force is not the only possible impact of a magnetic field on grain microstructure and texture evolution, but also the mobility of grain boundaries seems to be enhanced in the presence of a magnetic field. The influence of a magnetic field on the microstructure development, however, is not restricted by magnetically anisotropic metals but can also be observed in materials with magnetically isotropic properties. Moreover, a magnetic field can affect the microstructure evolution not only at the stage of grain

growth, but also at stages of recovery and primary recrystallization. In particular, the application of a magnetic field substantially enhances recrystallization in a cold rolled commercial aluminum alloy.

11:45 AM

(ICOTOM-S8-005-2008) Texture Development in Diamagnetic Ceramics Prepared by Slip Casting in a Strong Magnetic Field

T. S. Suzuki*, T. Uchikoshi, Y. Sakka, National Institute for Materials Science, Japan

Tailoring the crystallographic texture in ceramics is one way of effectively improving their properties, such as electrical, piezoelectric and mechanical properties. Many studies have been reported for the production of textured ceramics, such as by hot forging and the Templated Grain Growth method. On the other hand, recently, superconducting magnet technologies have been developed and used for various applications, and we reported that the successful control of the development of a textured microstructure in diamagnetic ceramics was achieved by a colloidal processing in a strong magnetic field and the crystalline orientation was seemed to be inseparably related to the microstructure. In this presentation, we report the relationship between the development of the crystallographic orientation and the microstructure in ceramics prepared using a strong magnetic field. The starting materials were commercially available ceramic powders, such as alumina, titania and so on. Each ceramic powder was dispersed in suspensions with dispersant to ensure dispersion by electrostatic repulsion between particles. The suspensions were homogenized with a magnetic stirrer and an ultrasonic horn was operated for 10 min to disperse the powders. The suspensions were consolidated by a slip casting in a strong magnetic field of 12 T. The green compacts after slip casting were isothermally sintered at the desired temperature for 2 h without applying a magnetic field. The sintered samples were polished and then thermally etched for microstructural analysis using SEM. The XRD and EBSD analysis were used for evaluation of the crystallographic orientation. The c-axes of alumina and titania were aligned parallel to the applied magnetic field. The degree of the crystalline orientation increased with increasing sintering temperature. The grains with the small tilting angle between the c-axis and the direction of a magnetic field increased as the grain growth occurred. The tilting angle of the large grains was smaller than that of the small grains. The degree of the development of crystalline texture can be controlled by the grain size of ceramics.

12:00 PM

(ICOTOM-S8-006-2008) Applications of Strong Magnetic Field to Materials Science

Y. Tanimoto*, Hiroshima University, Japan

Strong magnetic field is a useful tool to control various chemical and physical processes. We studied influence of strong vertical magnetic fields (maximum field; 15 T, 1500 T₂/m) on various processes. It is shown that many processes of diamagnetic materials are remarkably affected by magnetic force, as it changes effective surface gravity of earth. As an example, we examined the influence of magnetic fields on the surface phenomena of water [2,3]. The maximum mass of a water pendant droplet on the tip of a glass capillary are affected remarkably by magnetic fields: the mass of a droplet at -1500 T₂/m is six times larger than that at zero field, whereas the mass at 1200 T₂/m is one half. A droplet mass in magnetic field is determined by the balance of surface tension, earth gravity and magnetic force. A magnetic force at -1500 T₂/m cancels earth surface gravity, indicating that, in magnetically simulated microgravity, surface tension becomes a predominant factor for determining shape of water surface. Based on this observation, we attempted to make a water film of a large diameter using a magnetically simulated microgravity and succeeded to prepare a thin liquid water film of $\phi = 25$ mm, which cannot be prepared under earth surface gravity. Thin films of liquid ethanol, methanol, and benzene are prepared similarly. The above results encouraged us to prepare a thin solid polymer film using the simulated microgravity. So, we further attempted to prepare the solid film from a solution. By making a thin film of a polyvinyl alcohol (PVA) aque-

ous solution on a metal ring and evaporating the solvent under a simulated microgravity, a thin PVA film ($\phi =$ ca. 20mm) with two contactless, clean surfaces, which cannot be prepared under earth surface gravity, is prepared for the first time. It is concluded that magnetic force is a convenient tool in materials science to modify earth surface gravity which inherently affects chemical and physical processes. [1] A. Katsuki, K. Kaji, M. Sudea, and Y. Tanimoto, Chem. Lett., 36, 306 (2007). [2] M. Sueda, A. Katsuki, M. Nonomura, R. Kobayashi, and Y. Tanimoto, J. Phys. Chem. C, in press.

Hexagonal Metals

Deformation Mechanisms

Room: McConomy Auditorium

Session Chair: Thomas Bieler, Michigan State University

10:15 AM

(ICOTOM-S9-001-2008) Non-Schmid Behaviour of Twinning in a Magnesium Alloy (Invited)

M. R. Barnett*, Z. Keshavarz, A. G. Beer, Deakin University, Australia; X. Ma, SINTEF, Sweden

In magnesium alloys it is not uncommon for secondary twinning to occur in the interior of primary twins. The present work combines Electron Backscattering Diffraction and Schmid analysis to investigate the Schmid behaviour of primary and secondary twinning in magnesium alloy Mg-3Al-1Zn. It turns out that the tendency for twin formation follows the Schmid rule (applied assuming stress homogeneity) far more closely for primary than it does for secondary twinning. This is best demonstrated by comparing the Schmid factors calculated for the active twins with the value for the most heavily stressed system. For secondary twinning, the active twins frequently display a Schmid factor considerably less than the maximum. Such variation was not seen for primary twinning. Furthermore, a particular secondary twin variant is persistently favoured over others. It is suggested that the favoured variant occurs because it provides the closest match between the primary and secondary twinning planes thus minimizing the compatibility strain.

10:45 AM

(ICOTOM-S9-002-2008) Microstructure and Microtexture Evolution of Compression Twins in Magnesium

P. Yang*, University of Science & Technology Beijing, China

Basal slip and tension twinning of the {10-12} type are dominant deformation mechanisms of polycrystalline magnesium at low temperature. However, fracture originates mainly from compression twins or shear bands developed from compression twins. As both basal slip and tension twinning lead to basal texture which possesses high Schmid factor for compression twinning during compression or rolling, the formation of compression twins is inevitable. In addition, the (dynamic) recrystallization nucleation at compression twins or shear bands was observed to be more effective than that at tension twins or grain boundaries. Thus, the understanding of compression twinning has the significance of both preventing crack formation and optimizing annealing processing. In this work, the microstructures and (mis)orientations of compression twins with matrices during their formation, their evolution into shear bands and the recrystallization nucleation within them were analyzed by EBSD technique. Schmid factor analyses were applied to determine the orientation dependency of compression twins and the tendency for double twinning.

11:00 AM

(ICOTOM-S9-003-2008) Effect of Twinning on the Strain Hardening Behaviors of Two Mg Alloys Subjected to Different Strain Paths

L. Jiang*, J. J. Jonas, McGill University, Canada

The strain hardening behaviors of two Mg-based (+Al, Mn, Zn) alloys were investigated under the condition where twinning is the

Abstracts

dominant deformation mechanism. The results indicate that the combination of initial texture and a particular strain path determines the types of twins that form and their volume fractions. The different twinning behaviors are shown to be responsible for the sharply contrasting strain hardening characteristics of the experimental flow curves. Deformation twinning in Mg alloys can have both hardening and softening effects. When a certain volume fraction ($\geq 20\%$ in the present study) is reached, contraction and double twinning generate net softening effects. Nevertheless, when they interact with extension twins, hardening effects are reinforced. On the other hand, extension twinning generally introduces a net hardening effect. However, the extent of hardening depends not only on the volume fraction of extension twins, but also on the surface area per unit volume of the twin boundaries and the distribution of the twins.

11:15 AM

(ICOTOM-S9-004-2008) Development of Internal Strains and Texture during Cyclic Deformation of Extruded Mg AZ31B

D. W. Brown*, S. C. Vogel, Los Alamos National Lab, USA; S. R. Agnew, University of Virginia, USA

It has been shown that Mg AZ31B can twin reversibly during compression-tension cyclic deformation to relatively small strains ($\sim 4\%$). We have recently completed in-situ neutron diffraction measurements during strain controlled C-T cycling of extruded Mg AZ31B to failure to monitor the development of the twin volume fraction (as seen through the texture) and internal stresses. Twins appear with compressive deformation along the extrusion axis and withdraw with subsequent tensile deformation. The recovery (de-twinning) of the twins at the maximum tensile strain is observed to decrease with increased cycles, that is the overall twin volume fraction increases. In particular, parent grains which initially have their (11.0) plane normals parallel to the straining direction cease to de-twin completely at higher cycles. Despite this, no significant repartition of the internal stresses amongst the different grain orientations was observed.

11:30 AM

(ICOTOM-S9-005-2008) Dislocations in Textured Mg-4,5%Al-1%Zn Alloy: TEM and Statistical Studies

V. Serebryany*, V. Timofeev, Y. Zaliznyak, A.A. Baikov Institute of Metallurgy and Material Science, RAS, Russian Federation

Basal-textured samples of Mg-4,5%Al-1%Zn alloy cut at the right angle to rolling direction were examined in an effort to define the density of dislocations of the different types after warm rolling of the plates. The 22 different grains and their orientations were investigated in the transmission electron microscope JEM-1000 at the accelerating voltage 750 kV using a dark field-weak beam method of observation and the $g_b=0$ invisibility criterion as a basic method of the analysis of Burgers vectors. In the investigated samples the dislocations with Burgers vectors [a], [c] and [a+c] were found. The reaction showing decomposition a+c dislocation into a and c ones was experimentally observed. The [c] dislocations are as result of this reaction. The density of the [a] (basal and non-basal) dislocations does not depend on the grain orientations. The rare [c] and [a+c] dislocations arrange in the field of texture maximums. The statistical estimation of the density of the different types of dislocations in all material on the basis of small sample was introduced.

11:45 AM

(ICOTOM-S9-006-2008) Heterogeneous Deformation in Single-Phase Zircaloy 2

S. K. Sahoo*, V. D. Hiwarkar, I. Samajdar, P. Pant, IIT Bombay, India; G. K. Dey, D. Srivastav, R. Tewari, S. Banerjee, Bhabha Atomic Research Centre, India

Deformed single-phase Zircaloy 2 had shown clear patterns of heterogeneous deformation. The deformed microstructures could be generalized as grains/orientations which got fragmented and which did not. The presence of deformation twinning, observed only at low strains, does not explain this phenomenon – which existed even at

relatively higher (200-600°C) deformation temperatures where deformation twinning is absent. The source of this heterogeneous deformation appears to exist in the frame-work of differences in dislocations interactions at different crystallographic orientations. Though the exact source/origin of the heterogeneous deformation can still be debated, its effects on the deformed microstructures were apparent in terms of clear bi-modal distributions in grain size, in in-grain misorientation developments and in the patterns of stored energy of cold work and residual stress.

12:00 PM

(ICOTOM-S9-007-2008) Twinning and the Texture Changes in a Zr Alloy after Small Plastic Strains

J. Q. da Fonseca*, V. Allen, M. Preuss, The University of Manchester, United Kingdom

In this paper we investigate origins of the dramatic texture changes observed in a Zr alloy after only a small amount (~ 0.05) of plastic strain. Irradiation growth in Zr cladding is strongly anisotropic. This anisotropy is caused by the the strong texture characteristic of the product forms used. The need to control this anisotropy prompted a set of experiments aiming to understand the mechanisms responsible for deformation and texture evolution in Zirlo, a low Nb Zr alloy developed by Westinghouse. We carried out a series of uniaxial compression tests on hot rolled, recrystallised material. We used neutron diffraction and Electron Back Scattered Diffraction (EBSD) to characterise the texture evolution during deformation at room temperature, 450 K and 600 K. During testing, the samples exhibited softening just after yield. Associated with this phenomenon, we observed dramatic changes in texture, consistent with the operation of twinning. However, the changes observed could not be rationalised in terms of the twinning modes commonly observed in Zr alloys and implied the activation of compressive twinning in grains loaded in tension along the(c) axis. Further EBSD work confirmed the presence of twins that appear to be incompatible with the imposed deformation, and that their volume fraction increases with temperature. We attempt to explain this observation by considering the work done by twinning during deformation, which is highly anisotropic in nature, and the effect of temperature on the activation of $\langle c+a \rangle$ slip.

Texture Evolution During TMP

Room: McConomy Auditorium

Session Chair: S. Lee Semiati, Air Force Research Laboratory

1:45 PM

(ICOTOM-S9-008-2008) Textures in hcp Titanium and Zirconium (Invited)

N. Bozzolo*, F. Wagner, Université Paul Verlaine - Metz, France

Titanium and Zirconium are both hexagonal-close-packed metals at ambient temperature. The alpha (hcp) phase keeps predominant in many industrial alloys used in high performance fields such as aeronautics or nuclear industry. The crystallographic texture directly controls anisotropic mechanical properties like the elastic modulus, the yield strength or the ductility, but also controls other properties like the intergranular cracking resistance which is closely linked to the grain boundary character distribution, or the corrosion resistance which is sensitive to the crystallographic orientation of the crystal surfaces. In this paper, the texture evolution during cold-rolling and subsequent annealing will be described for hcp Ti and Zr. A special attention will be paid to the influence of deformation-twinning and the related texture components will be identified. The texture changes occurring during annealing will be quantified and attributed to the recrystallization or to the grain growth mechanisms, as a function of the initial strain and related texture. The recrystallization mechanisms and the corresponding texture changes are closely dependant on the spatial distribution of the orientations in the deformed microstructure. Grain fragmentation and its consequences on the global texture will therefore also be emphasized. The relationship between

the orientation distribution function (ODF) and the misorientation distribution function (MDF) will be discussed. It will be shown that the measured MDF can be significantly different from the one calculated from the ODF, especially in samples with a high twin density, but also in samples without twins. This is interpreted as a strong sign of local orientation correlations which may reveal special grain boundary types.

2:15 PM

(ICOTOM-S9-009-2008) Effect of Cooling Rate on Microtexture Heterogeneity during Hot Working of Titanium Alloys with a Duplex Microstructure

A. A. Salem*, M. G. Glavicic, S. L. Semiatin, Air Force Research Laboratory, USA

The hypothesis that slow cooling of alpha/beta titanium alloys from high temperatures leads to the retention of the primary alpha texture has been evaluated. For this purpose, the microtextures of primary and secondary alpha were established using EBSD of Ti-6Al-4V with a starting duplex microstructure. Samples were solution treated at 955°C followed by either water quenching (to retain the microtexture of primary alpha at high temperature) or slow (furnace) cooling to grow primary alpha and prevent secondary alpha from forming. High intensities of localized primary-alpha microtexture distinct from those in the WQ sample were revealed in the slow-cooled sample, suggesting that certain primary-alpha texture components grew much faster and eventually dominated the overall texture. The different texture components were correlated to the morphology of primary-alpha particles and the corresponding effect of size and shape on diffusional growth during cooling from high temperature.

2:30 PM

(ICOTOM-S9-010-2008) Texture Evolution during Casting, Rolling and Heat Treatment of Ti-Nb and Ti-Mo-based beta-Titanium Alloys

B. Sander, D. Ma, D. Raabe*, Max-Planck-Institut für Eisenforschung, Germany

The crystallographic microtexture and microstructure of various beta-titanium alloys based on Ti-Nb and Ti-Mo are studied after casting, warm rolling and recrystallization using EBSD. The main observations are fairly random casting textures, the evolution of partially recrystallized microstructures during warm rolling and the formation of strong through-thickness texture and microstructure gradients at larger strains. Both, the recrystallized volume fractions and the textures depend on the thickness reduction. At small reductions texture gradients are also small showing some alpha-fiber (crystallographic axis $\langle 110 \rangle$ parallel to the rolling direction) and gamma-fiber (crystallographic axis $\langle 111 \rangle$ parallel to the normal direction) texture components. At larger strains (70-90%) the texture and microstructure gradients are characterized by shear texture components and recrystallization particularly close to the surface layers and plane strain texture components which are typical of recovered grains in the center layers.

2:45 PM

(ICOTOM-S9-011-2008) Evolution of Transformation Texture in a Metastable β -Titanium Alloy

S. Suwas*, N. P. Gurao, A. Ali, Indian Institute of Science, India

Texture evolution in h.c.p. (α) phase derived from aging of a differently processed metastable b.c.c. (β) titanium alloy was investigated. The study was aimed at examining (i) the effect of different b.c.c. cold rolling textures and (ii) the effect of different defect structures on the h.c.p. transformation texture. The alloy metastable β alloy Ti-10V-4.5Fe-1.5Al was rolled at room temperature by unidirectional (UDR) and multi-step cross rolling (MSCR). A piece of the as-rolled materials were subjected to aging in order to derive the h.c.p. (α) phase. In the other route, the as-rolled materials were recrystallized and then aged. Textures were measured using X-ray as well as Electron Back

Scatter Diffraction. Rolling texture of β phase, as characterized by the presence of a strong γ fibre, was found stronger in MSCR compared to UDR, although they were qualitatively similar. The stronger texture of MSCR sample could be attributed to the inhomogeneous deformation taking place in the sample that might contribute to weakening of texture. Upon recrystallization in β phase field close to β -transus, the textures qualitatively resembled the corresponding β deformation textures; however, they got strengthened. The aging of differently β rolled samples resulted in the product α -phase with different textures. The (UDR + Aged) sample had a stronger texture than (MSCR + Aged) sample, which could be due to continuation of defect accumulation in UDR sample, thus providing more potential sites for the nucleation of α phase. The trend was reversed in samples recrystallized prior to aging. The (MSCR + Recrystallized + Aged) sample showed stronger texture of α phase than the (UDR + Recrystallized + Aged) sample. This could be attributed to extensive defect annihilation in the UDR sample on recrystallization prior to aging. The (MSCR + Aged) sample exhibited more α variants when compared to (MSCR + Recrystallized + Aged) sample. This has been attributed to the availability of more potential sites for nucleation of α phase in the former. It could be concluded that α transformation texture depends mainly on the defect structure of the parent phase.

3:00 PM

(ICOTOM-S9-012-2008) Evolution of the Texture and Microstructure in TiAl Alloys During Heat Treatments via Massive Transformation

A. Sankaran, E. Bouzy*, J. J. Fundenberger, A. Hazotte, Paul verline Université, France

Lamellar structures in the TiAl alloys, though have many good mechanical properties like high strength with low density, also have certain disadvantages like poor ductility due to high solidification texture. Hence, minimisation of the texture and grain size in these lamellar structures has been a study of major concern for a very long time. Multiple heat treatment is one of the solutions to this problem. Rapid cooling of these alloys produces many complex but more isotropic microstructures. One such structure is the massive structure. They are highly metastable structures and in our study we obtain them by high quenching experiments in the as-cast Ti 47 Al 2Nb 2Cr (GE Alloy) alloy. Multiple heat treatments are performed on these structures both below and above the alpha transus temperature. The microstructural and texture evolution is studied using Electron Microscopy, Electron Backscatter Diffraction and X-Ray Diffraction techniques. The final texture and the grain size of the sample is analysed and is compared with the lamellar structures obtained from the primary heat treatment obtained directly from the as-cast structure.

3:15 PM

(ICOTOM-S9-013-2008) Texture Evolution in Electron Beam Melted Boron Modified Ti-6Al-4V Alloy

S. Roy*, N. P. Gurao, S. Suwas, Indian Institute of Science, India; S. Tamirisakandala, Ohio University, USA; D. B. Miracle, Wright-Patterson AFB, USA; R. Srinivasan, Wright State University, USA

Owing to their high strength-to-weight ratio, excellent mechanical properties and corrosion resistance, titanium (Ti) and its alloys, especially ($\alpha+\beta$) alloys like Ti-6Al-4V, are the backbone materials for aerospace, energy, and chemical industries. Pure titanium has hcp (α) crystal structure at room temperature, which transforms to bcc (β) structure at $\sim 885^\circ\text{C}$ following specified orientation relationship. Based on this orientation relationship and the symmetries of cubic and hexagonal structures, a total of 12 crystallographically distinct variants of α phase can result from the transformation of single β grain. The basis for tailoring a suitable texture and microstructure during heat treatment of titanium alloys, therefore, depends strongly on the β to α transformation. The same is applicable for ($\alpha+\beta$) titanium alloys. Trace boron addition (~ 0.1 wt. %) to the alloy Ti-6Al-4V

Abstracts

produces a reduction in as-cast grain size by roughly an order of magnitude. Special attributes of Boron addition includes enhanced ductility, higher stiffness and strength in addition to good fracture resistance. Recently, Ti-alloys have been produced by electron beam melting (EBM) technique, which offers number of advantages in terms of improved ingot quality. Boron addition as well as EBM technique could affect the evolution of texture and microstructure in the material. A research program has been developed in order to study different aspects of texture evolution in EBM processed Boron modified Ti-6Al-4V. The solidification microstructure of Boron free as well as Boron containing Ti-6Al-4V after EBM processing are found to be almost homogeneous from periphery towards the center of as-cast ingot in terms of both α -colony size and distribution. Boron addition substantially reduces α -colony size (~50-80 μm). Needle shaped Ti-B particles segregate at the grain boundary. A gradual change in α -texture from periphery towards the center has been observed with orientations close to specific texture components suggesting the formation of texture zones. The mechanism of texture evolution can be visualized as a result of variant selection during solidification through ($\alpha+\beta$) phase field.

4:15 PM

(ICOTOM-S9-014-2008) EBSD Study of Orientation Relationships During the Dynamic Recrystallisation of Mg AM30 Deformed in the High Temperature Regime

<. Martin*, McGill University, Canada; S. Godet, Universite Libre de Bruxelles, Belgium; L. Jiang, A. Elwazri, McGill University, Canada; P. Jacques, Universite Catholique de Louva, Belgium; J. Jonas, McGill University, Canada

The orientation relationships that apply to the various DRX nucleation mechanisms were investigated in magnesium alloy AM30 using electron back-scattered diffraction (EBSD). Compression tests were carried out at 350°C and a strain rate of 0.001s⁻¹ on samples machined from extruded tubes. Three different types of nuclei were observed at this temperature (at bulges, triple junctions and those formed by means of CDRX) and their orientation relationships with respect to the matrix were determined and expressed in Rodrigues-Frank space. Specific misorientation relationships were found to apply to each of the three different types of DRX nuclei. The bulge nuclei are characterized by c-axis rotations, while rotation axes inclined at 45° to the c-axis are associated with CDRX nucleation. In both cases, low angle boundaries develop by means of the continuous mechanism. The triple junction nuclei, which are less common in the microstructure, developed relatively high angle misorientations around axes inclined at approximately 90° to the c-axis. A pole figure representation is also used to illustrate the contrasting features of the three different nucleation mechanisms.

4:30 PM

(ICOTOM-S9-015-2008) Texture Evolution During the Static Recrystallization of Three Binary Mg-Y Alloys

R. Cottam*, J. Robson, G. Lorimer, University of Manchester, United Kingdom; B. Davis, Magnesium Elektron, United Kingdom

The evolution of texture during the static recrystallization of three cold rolled binary Mg-Y alloys was characterised using electron backscattered diffraction (EBSD). It had been shown in previous studies that alloys that contain yttrium can develop more random texture, during thermo-mechanical processing and this can reduce or eliminate the yield asymmetry common to wrought magnesium alloy. The three alloys were initially hot rolled to break up the as cast structure then cold rolled using multiple passes of 1% reductions to avoid cracking and impart a high level of stored energy. The as rolled texture was a typical basal texture with a small component outside the basal ring formed as a result of {10-11} - {10-12} double twinning. Isothermal annealing was carried out in the temperature range 250 to 400°C to produce both partial and fully recrystallized structures. The texture produced after recrystallization was a weak basal texture. It was found that for all the alloys the orientations and

boundary misorientation of the double twins was carried through to the recrystallized texture due to preferential recrystallization of the twinned regions which were extensive throughout the structure.

4:45 PM

(ICOTOM-S9-016-2008) On the Role of Twin-Intersections for the Formation of the Recrystallisation Texture in Pure Magnesium

I. Schestakow, Max-Planck-Institute for Iron Research, Germany; S. Yi, TU Clausthal, Germany; S. Zaefferer*, Max-Planck-Institute for Iron Research, Germany

The rolling texture of pure magnesium with hexagonal closed packed crystal structure is characterized by the <0001>-crystal direction being oriented perpendicular to the main compression direction, i.e. parallel to the normal direction. Perpendicular to the normal direction the planes show an almost isotropic distribution. Surprisingly, this texture is also conserved during recrystallisation although it is related to large angle grain boundary movement. It has been found by use of EBSD-based orientation microscopy, that the recrystallised grains are related to the deformed matrix grains by an approximately 30° rotation about the <0001> crystal direction. We show in this contribution that at least a part of these 30° rotated crystals are created by an oriented nucleation mechanism in the intersection of particular tensile and compression twins. By means of conventional orientation microscopy and the newly developed 3D orientation microscopy (based on serial sectioning with a focused ion beam and EBSD-based orientation microscopy) we investigated the precise crystallography of the intersections. It is shown that the orientation of the intersection area is different from all three grains concerned (i.e. the matrix and the two twins) and shows exactly the above mentioned orientation relation. Conventional annealing series and in-situ annealing experiments show the evolution of these areas during the recrystallisation process. It is clear that the observed nuclei grow effectively and consume the surrounding structure.

5:00 PM

(ICOTOM-S9-017-2008) Texture Inheritance and Variant Selection through the α - β Phase Transformation in Zr-2.5Nb

M. R. Daymond*, R. A. Holt, Queen's University, Canada; S. Vogel, Los Alamos National Lab, USA

Zr-2.5Nb is used as the pressure-tube material in CANDU reactors, consisting of 90% α (hcp) phase and 10% metastable β (bcc) phase, analogous to the common microstructure of Ti-6Al-4V. Many of the properties of the material depend upon the crystallographic texture of the α -phase, which is developed during the extrusion stage of manufacturing. This is carried out at elevated temperatures in the two phase field where roughly equal volume fractions of the two phases are present. In addition, some manufacturers seek to use thermal cycling through the phase transformation as a way of 'randomizing' the texture. We have carried out in-situ transformation experiments on the HIPPO diffractometer starting with an extruded tube in order to investigate the α to β to α phase transformations. There is clear evidence of variant selection occurring during both the α to β and β to α transformations. The initial β texture is quite weak with several components. On first heating to the fully β phase field (975°C) the β inherits a strong (100)110 texture from the α phase, with a spread about the axial direction through the Burgers relationship. The variant selection occurring during this transformation can be explained through the anisotropic thermal stresses generated in the α phase. On subsequent cooling to 250°C, the α phase inherits its texture from the β phase, however, one preferred α variant develops which is quite different from the starting texture (a very strong axial (0002) component), while the texture seen in the β at high temperature is retained down to 250°C, with a reduction in the spread about the axial direction. Modeling of the texture change associated with the phase transformation, using a self-consistent approach, has been successful in describing the variant selection occurring during the α to β transformation, and gives insights into the selection occurring during the β to α transformation.

5:15 PM

(ICOTOM-S9-018-2008) Annealing Related Microstructural Developments in a Two-Phase Zr-2.5 Nb Alloy

V. D. Hiwarkar*, S. Sahoo, I. Samajdar, K. Narasimhan, IIT, Bombay, India; K. V. Mani Krishna, G. K. Dey, D. Srivastav, R. Tiwari, S. Banarjee, Bhabha Atomic Research Centre, India

Deformed/pilgered two-phase, 10-15% cubic second phase – rest being primary hexagonal phase, Zr-2.5 Nb alloy was subjected to various annealing treatments – treatments ranging from recovery to recrystallization and grain growth. Associated microstructural developments were monitored through combinations of characterization techniques - bulk crystallographic texture & microtexture measurements and estimations of lattice strain and residual stress. Significant texture changes were associated only with grain growth of the primary phase – a process facilitated by second phase coarsening. From nearly continuous presence at the primary phase grain boundaries, latter stages of grain growth had shown coarsened second phase present only at the tri-junctions. This process was associated with significant changes in phase-boundary nature. An effort was made to explain such changes from an 'extended', i.e. extended to phase boundaries, CSL (coincident site lattice) theory.

Biomaterials**Biomaterials**

Room: Connan

Session Chair: Stuart Wright, EDAX-TSL

1:45 PM

(ICOTOM-S11-001-2008) Crystallographic and Topological Textures of Biological Materials and the Resulting Anisotropy of the Mechanical Properties (Invited)

D. Raabe*, C. Sachs, H. Fabritius, Max-Planck-Institut fuer Eisenforschung, Germany; A. Al-Sawalmih, Max-Planck-Institute of Colloids and Interfaces, Germany; L. Raue, Max-Planck-Institut fuer Eisenforschung, Germany; H. Klein, Georg-August-Universität, Germany

The presentation gives an overview of crystallographic and topological textures of biological materials focusing on mineralized chitin-protein matrix nanocomposites (arthropod exoskeleton) and mineralized collagen-protein matrix nanocomposites (bone). The textures have been determined by synchrotron x-ray pole figure measurements and orientation distribution functions. The microstructures were investigated using electron microscopy. The study has two objectives: The first one is to elucidate crystallographic building principles via the preferred synthesis of certain orientations in crystalline organic tissue. The second one is to study whether a general design principle exists for the biological specimens which uses preferred textures relative to the local coordinate system. The first point, hence, pursues the question, to what extent and why natural nanocomposites reveal preferred textures at all. The second point addresses the question why and whether such preferred textures (and the resulting anisotropy) exist at different positions in a biological samples. Concerning the first aspect a strong preference of fiber textures of the crystalline polymer matrix of natural nanocomposites is often observed. The second question is tackled by studying samples from different parts of the same biological specimens. While the first aspect takes a microscopic perspective at the basic structure of the biological composite the second point aims at building a bridge between the understanding of the microstructure and the macroscopic design of a larger biological construction. We observe that the textures in the same biological specimen are often similar to each and have the same crystallographic axis parallel to the normal of the local tangent planes. Generally, it is found that the hierarchical microstructures of biological composites can be well described by surprisingly simple textures. Furthermore, we discuss preferred orientation relationships that we found between the crystalline polymer and minerals. Tex-

ture-property and microstructure-property correlations are also explored using nanoindentation and materials testing at different length scale.

2:15 PM

(ICOTOM-S11-002-2008) Peering into the Eyes of Trilobites Using EBSD (Invited)

M. Lee*, C. Torney, A. W. Owen, University of Glasgow, United Kingdom

Electron backscatter diffraction (EBSD) is a very powerful tool for elucidating the microtextures of rocks and their constituent minerals and here we describe an application in palaeontology, focusing on the crystalline eyes of trilobites. These extinct marine arthropods were the first group of animals to have evolved eyes, each of which was made up of tens to hundreds of calcite (CaCO₃) lenses. Over their 350 million year history the trilobites evolved three main eye types and we have concentrated on the schizochroal eyes, each of which contained a small number of millimeter-sized lenses. Initial work in the 1970s showed that lens calcite was oriented to minimize double refraction and light was focused using a complex doublet structure. This model has long been revered as an example of the elegance of biological design but was recently questioned and the doublet structure attributed to a fossilization artifact. As a comprehensive understanding of the crystallography and microtexture of the calcite is so critical for understanding lens function, we have used EBSD to reexamine trilobite eyes. This work has used a FEI Quanta 200F SEM equipped with a TSL EBSD system incorporating the Hiraki high speed detector, which enables rapid acquisition of scans containing data from up to several million indexed patterns. The results reveal that calcite lenses are microstructurally far more complex than previously realized and focused light by several mechanisms. Some species used a doublet structure and the lens elements were made from calcite of different compositions and refractive indices. In other species the light was channeled and focused via radiating arrays of individual calcite fibres that acted as 'light guides' or by using a single crystal of calcite of continuously varying crystallographic orientation so that its c-axis remained parallel to incident light. These results illustrate vividly how EBSD can help to understand very complex microtextures, in this case image formation by animals that thrived in the ancient oceans.

2:45 PM

(ICOTOM-S11-003-2008) Textures and Multi-Structure of Single to Multi-Layered Modern Brachiopod Shells (Invited)

E. Griesshaber*, A. Götz, W. Schmahl, LMU München, Germany; L. Carsten, Humboldt Universität, Germany; R. Neuser, Ruhr Universität, Germany

Magnesian calcites of biogenic origin are hierarchically structured, multifunctional materials. We have investigated the texture and shell microstructure together of the modern calcitic brachiopods of the genera *Kakanuiella chathamensis*, *Liothyrella uva* and *Liothyrella neozelanica* with SEM and EBSD as well as nano- and microhardness measurements. One of the most distinctive feature of the studied genera is the number of layers that compose the brachiopod shell. *Kakanuiella chathamensis* is built entirely of nano- to microcrystalline primary layer calcite. *Liothyrella uva* contains of a nanocrystalline outer primary and an inner fibrous secondary layer. *Liothyrella neozelanica* is composed of three layers, a nanocrystalline outer primary, a columnar secondary and an innermost fibrous tertiary shell layer. Even though *Kakanuiella chathamensis* is composed of primary layer material we observe some textural features and a pattern in the distribution of hardness within the shell. The texture of *Liothyrella uva* and that of *Liothyrella neozelanica* is significantly sharper than that of *Kakanuiella chathamensis*: The hardness distribution in *Liothyrella neozelanica* and *Liothyrella uva* is such that the outermost part of the shell is hard while the innermost part of it is soft: The secondary layer of *Liothyrella neozelanica* consists of calcite crystals that form long prisms which are perpendicular to the shell and parallel to the c-axis of calcite. Our observations on the interface

Abstracts

between the prismatic secondary and the fibrous tertiary layer of *Liothyrella neozelanica* suggest a mechanism by which the unusual texture of the fibrous layer may arise.

3:15 PM

(ICOTOM-S11-004-2008) Investigation of the Orientation Relationship Between α -Chitin and Calcite in Crustacean Cuticle Using Microbeam Synchrotron X-ray Diffraction

A. Al-Sawalmih*, Max-Planck-Institute for Colloids and Interfaces, Germany; H. Fabritius, S. Yi, Max-Planck Institute for Iron Research, Germany; C. Li, S. Siegel, Max-Planck-Institute for Colloids and Interfaces, Germany; D. Raabe, Max-Planck Institute for Iron Research, Germany; O. Paris, Max-Planck-Institute for Colloids and Interfaces, Germany

Crustacean cuticle contains α -chitin-protein organic fibers associated with crystallites of calcite and considerable amounts of amorphous biominerals. In this study, the crystallographic texture in edible crab *Cancer pagurus* and american lobster *Homarus americanus* cuticles was investigated using synchrotron x-ray diffraction (XRD). X-ray pole figure analysis was performed to evaluate the preferred orientation of crystalline calcite and α -chitin, with respect to their orientation relationship. The local texture was also investigated using vertical line scans of the cuticle section with a microfocused X-ray beam of 10 μm size. This allowed textural variations within the cuticle to be mapped. The importance of crystallographic texture in biological materials lies in a better understanding of the role of macromolecules in controlling the epitaxy of the minerals during the biomineralization process. This study shows that crab and lobster cuticles reveal a strong preferred orientation correlation between the orientation distribution of calcite and α -chitin. It was observed that the alpha-chitin-protein fibers occur in two components: the first is called the in-plane fiber component which shows the twisted plywood structure, and the second is composed of vertical fibers which penetrate the first toward the cuticle surface. Calcite orientation is related to the second component by revealing that the c-axis of the hexagonal calcite and the c-axis (chain axis) of the orthorhombic α -chitin of the vertically aligned fibers- are firstly preferentially aligned parallel to each other and secondly oriented along the surface normal. The synchrotron x-ray crystallographic texture results gave for the first time a description of the orientation relationship between the organic and inorganic components in arthropod cuticle, consistent with the analysis of fiber orientation in crab and lobster cuticle using SEM. This result strongly suggests that the in-surface fibers of α -chitin assists the growth of calcite crystals in crustacean cuticle by functioning directly or indirectly as a template for nucleation and subsequent growth of calcite.

4:15 PM

(ICOTOM-S11-005-2008) Crystallographic Texture in Calcium Phosphate Bioceramics (Invited)

R. P. Camata*, University of Alabama at Birmingham, USA

Naturally occurring apatite in human hard tissues often exhibits preferred crystallographic orientations. These textures strongly influence the biomechanical properties of bone and teeth and are also believed to affect key biochemical processes that mediate the interaction between these biomaterials and living cells including protein adsorption and folding. The occurrence of texture has also been observed in synthetic hydroxyapatite (HA) coatings applied to metallic implants. In this presentation we review the current knowledge on how the crystallographic texture of HA and other calcium phosphate materials can be controlled in energetic synthesis methods such as magnetron sputtering and pulsed laser deposition. We show how c-axis-textured HA coatings exhibit improved mechanical properties and present evidence that highly oriented surfaces may also improve the bioactivity of HA. Highly textured HA can be obtained by controlling the energy and direction of incidence of ionic species in energetic vacuum deposition. In pulsed laser synthesis, for example, variations in laser fluence, plume direction of incidence, and gas-phase hydroxylation

chemistry allow tailoring of the HA texture. X-ray pole figure measurements reveal that highly energetic deposition at normal incidence leads to HA grains with the c-axis preferentially aligned perpendicularly to the substrate. On the other hand, deposition under low laser fluences in rich OH- environment favors formation of grains with the a-axis aligned in the direction normal to the substrate. Nanoindentation results show enhancement of hardness and Young's modulus in c-axis-textured HA coatings, compared to randomly-oriented coatings. In addition, correlation of X-ray pole figure data and experiments using human mesenchymal stem cells suggest that cells attach in greater numbers to the HA coatings with c-axis texture, as compared with randomly-oriented coatings. Control of crystallographic texture in HA and other calcium phosphates may therefore lead to anisotropic bioaffinity that could be relevant for biomedical applications requiring bioceramics with tailored bioactivity and improved mechanical properties.

4:45 PM

(ICOTOM-S11-006-2008) Texture and Anisotropy of MP35N Wire for Conductor Leads

B. Li*, T. Steigauf, Medtronic, USA

MP35N alloy has composition of 35Co-35Ni-20Cr-10Mo. The wire made from MP35N alloy has a high strength, relatively low resistivity, high corrosion resistance and good fatigue property. Because of its good combination property MP35N wire has been used as conductor leads for medical device application for more than 20 years. However there is a little information about MP35N wire's texture and mechanical behaviour available. In this study, texture of four types of MP35N wires (D=0.178 mm) was analyzed to compare the difference of texture related with compositions, processes and manufacturers. The wire texture data was quantified by several texture components and the components were correlated to mechanical property and fatigue performance of wires. This study demonstrated that wire texture is a link between process and properties. The texture analysis was performed using an EDAX/TSL OIM system on a FEG SEM.

5:00 PM

(ICOTOM-S11-007-2008) Crystallographic Textures from the Exoskeleton of the Lobster *Homarus Americanus* and Calculation of the Mechanical Properties of the Calcite Phase

L. Raue, Max-Planck-Institute for Iron Research, Germany; H. Klein, University of Goettingen, Germany; D. Raabe*, Max-Planck-Institute for Iron Research, Germany

Some biological materials like the exoskeleton of the American lobster have been optimized over a period of ~600 million years by nature. Hence it is not astonishing that these natural constructions exploit the presence of structural anisotropy in a much more efficient and elegant way than usually encountered in man-made materials. The exoskeleton of the examined crustacean is a biological multiphase composite consisting of a crystalline organic matrix (chitin), crystalline biominerals (calcite), amorphous calcium carbonate and proteins. Variations in the composition and in the crystallographic arrangement can lead either to a rigid material serving as a protective armour layer or it can render the material highly flexible serving as a constructional element as in articular membranes at joints. Beside these properties the exoskeleton has a rather low density in view of the high stiffness it can provide in parts. One special structural aspect of this versatile biomaterial which has not yet been studied in detail is the occurrence of pronounced crystallographic orientations and the resulting anisotropic mechanical properties. Therefore crystallographic textures of chitin and calcite have been measured by wide angle Bragg diffraction, calculating the Orientation Distribution Function from pole figures using the series expansion method. Since the macroscopic properties of polycrystalline materials correspond to the spatial orientation of the single crystals, the macroscopic anisotropy can be calculated as a texture-weighted average of the single crystal anisotropy. Hence the

chitin phase shows similar textures for all examined parts of the lobster, it is very likely that the differences of the mechanical properties correspond to the calcite textures, which are different for every functional part. Under that assumption the anisotropic elastic modulus of the calcite phase has been calculated. As a result of the investigations a general strong relationship can be established between the crystallographic orientations and the resulting mechanical properties which suits the mechanical needs in lobster's live very well.

5:15 PM

(ICOTOM-S11-008-2008) Common Control of Texture in Calcite Biominerals of Bivalved Shells

M. Cusack, A. Pérez-Huerta, P. Dalbeck, M. Lee*, University of Glasgow, United Kingdom

For 550 million years, living systems have evolved to exercise exquisite control in the production of mineral structures that have precise morphology, mineralogy and crystallography. While the biosphere produces around 60 different types of minerals, calcium carbonate (CaCO₃) is the most abundant. From such a simple starting material, biology produces sophisticated structures that function in specific roles such as protection in corals and shells of marine organisms. The knowledge of how mineral-producing organisms exert precise control on their crystallographic orientation is one of the most fundamental questions of biomineralization. This understanding provides crucial information in revealing aspects of crystal nucleation, growth and emplacement in biomineral systems. The acquisition of crystallographic information within the structural context is challenging at high spatial resolution. These difficulties have limited our knowledge of processes involved in crystallographic control during the secretion of mineralized hard parts as in shells. Using an FEI Quanta 200F environmental SEM equipped with an EDAX-TSL EBSD system, we have characterised in exquisite detail the morphology and texture of carbonate crystals produced by a range of marine invertebrates. Here we present detailed crystallography in the context of shell ultrastructure in rhynchonelliform brachiopods and bivalve molluscs indicates that at the umbonal regions calcite crystals are oriented with the c-axis <0001> nearly parallel to the shell surface and progressively rotate during growth. Thus, these organisms construct bivalved shells via common mechanisms of controlling the crystallographic orientation of biominerals despite their different evolutionary history.

5:30 PM

(ICOTOM-S11-009-2008) Texture and Ultrastructure of Brachiopod Shells: A Mechanically Optimized Material with Hierarchical Architecture

W. Schmahl*, LMU München, Germany; K. Kelm, Universität Bonn, Germany; E. Griesshaber, LMU München, Germany; S. Enders, Stuttgart, Germany

Brachiopod shells consist of low-Mg calcite and belong to one of the most intriguing species for studies of marine paleoenvironments and variations in oceanographic conditions. We have investigated the texture and ultrastructure together with nano- and microhardness properties of modern brachiopod shells with SEM-EBSD, TEM and nanoindentation and Vickers microhardness analyses. The shells are structured into several layers. Next to the outermost organic lining, the shells consist of a thin, outer, hard, primary layer composed of randomly oriented nanocrystalline calcite, which is followed inward by a much softer shell segment built of long calcite fibres, stacked parallelly into blocks. While the crystallographic c-axes of the fibres are perpendicular to the shell vault, the morphological fibre axes run parallel to the shell vault with changing directions between different blocks or layers. The hardness distribution pattern within the shells is non-uniform and varies on scales as small as a few tens of microns. The maximum hardness in nanohardness indents has been ob-

served in the youngest part of the primary layer and in transverse cross sections through fibres of the secondary layer, while the lowest hardness in nanoindents within the shells has been measured in the longitudinally cut fibres of the secondary layer, predominantly those next to the soft tissue. Our results confirm that optimal mechanical performance and fracture toughness of the shell is given by structural features such as a distinct variation in crystal size and morphology, a varying degree of crystal orientation and the distribution of intracrystalline and intercrystalline organic matter.

5:45 PM

(ICOTOM-S11-010-2008) Wear Resistance and Microstructure in Annealed Ultra High Molecular Weight Polyethylenes

D. S. Li, H. Garmestani*, Georgia Institute of Technology, USA; A. O. Chu, H. Ahzi, G. Alapati, M. Khatonabadi, O. S. Es-Said, M. T. Siniawski, Loyola Marymount University, USA; L. Matriciano, MediTECH Medical Polymers, USA; S. Ahzi, University Louis Pasteur, France

To improve the wear behavior of UHMWPE, the correlation between microstructure and wear resistance was studied. In this study it was found that the relationship between wear volume and sliding distance fits a power law. The exponent was used to represent the wear property and crystal orientation distribution (texture) was used to represent microstructure. Texture analysis showed that four kinds of annealed UHMWPE sheets were all somehow isotropic. This correlates with the wear behavior of these four UHMWPE sheets.

Tuesday, June 3, 2008

Novel Texture Measurement Techniques Including 3D

Novel Methods including 3D - III

Room: Rangos 1

Session Chair: Matthew Miller, Cornell University

8:30 AM

(ICOTOM-S5-019-2008) Far Field Diffraction Studies of Individual Embedded Grains in Polycrystals (Invited)

U. Lienert*, J. Almer, D. Haefner, ANL, USA

It has recently been demonstrated that high-energy synchrotron radiation is a unique tool for the local (down to the micrometer scale) structural characterization within polycrystalline bulk materials. In the 'far field' regime orientation and strain information is obtained on individual diffracting domains within the illuminated gauge volume. The 1-ID beamline at the APS provides dedicated instrumentation to produce and utilize micro-focused high-energy synchrotron radiation. Major progress is anticipated when the commissioning of a fast large area detector (up to 30 frames per second) and hydraulic uni-axial load rig with high temperature capability will be completed. Gage volumes within bulk polycrystalline materials have been defined by a conical slit cell and by the position of a mechanical rotation axis. Applications so far include the ODF reconstruction of the mosaicity within a deformed Al grain, the identification of the austenite/ferrite phase transition under tensile load, domain reorientation in ferroelectric BaTiO₃, tensile twinning in Mg, and grain rotations in SrTiO₃ under compression. A suitable selection will be made. It is concluded that with instrumental and software advances statistically relevant data sets of a few hundred to thousands of grains can be obtained on a time scale suitable for in-situ characterization. Use of the Advanced Photon Source was supported by the U. S. Department of Energy, Office of Science, Office of Basic Energy Sciences, under Contract No. DE-AC02-06CH11357.

Abstracts

9:00 AM

(ICOTOM-S5-020-2008) Separating Coincident Electron Backscatter Diffraction Patterns near Interfaces

J. P. Kacher*, B. L. Adams, D. T. Fullwood, C. D. Landon, Brigham Young University, USA

A persistent difficulty with EBSD/OIM texture determination is the problem of overlapping EBSD patterns near grain boundaries or interfaces. More generally whenever the interaction volume of the electron beam (probe size) exceeds the scale of the microstructure, problems with overlapping EBSD patterns develop. Overlapping patterns can result in indexing problems; and in the case of cross-correlation-based high-resolution techniques errors can result in the determination of local elastic distortions. In this paper we describe a method for separating overlapping patterns. Its implementation is described in terms of EBSD scanning near grain boundaries. A sequence of EBSD patterns was obtained by stepping across the grain boundary. Cross correlation was then used to compare each image with an image from the interior of each of the two grains. The relative size of these cross correlations, taken at the 0-shift position, was used to estimate the fraction of each grain orientation component present in the image. The smaller component was then subtracted out, leaving only the dominant grain's pattern. These separated patterns were then used in the recovery of the elastic distortion tensor, and compared with those obtained without the separation of coincidence. The results suggest that significant errors can arise in recovery of the elastic tensor near grain boundaries when the effects of overlapping patterns are not removed.

9:15 AM

(ICOTOM-S5-021-2008) Semiautomatic Determination of Orientations and Elastic Strain from Kossel Microdiffraction

A. Morawiec*, Polish Academy of Sciences, Poland; R. Pesci, Ecole Nationale Supérieure d'Arts et Métiers, France; J. Lecomte, Université de Metz, France

There is a considerable interest in examination of materials at a local scale. In particular, there is a large demand for high resolution data on lattice orientations and lattice distortions (strains). These characteristics are important in analysis of a vast range of crystalline materials, from simple metallic samples, through alloys and intermetallics, ceramics and composites, to sophisticated electronic devices. High spatial resolution in strain determination can be achieved using divergent beam X-ray (Kossel) diffraction. This classical technique is now being revitalized by the use of scanning electron microscopes equipped with CCD cameras. Improvements in the Kossel technique are directed towards getting more reliable results faster and with less effort. In the case of orientations (which are necessary for determination of strain tensors), the key point is automation of measurements. The situation with strain is different: since the interest is in distortions of the magnitude < 0.001 , getting reliable values of strain tensor components is difficult even in the case of good quality patterns. Moreover, one faces the problem of computing the tensor from the geometry of Kossel conics. Due to the numerous free parameters, a "manual" matching of simulated and experimental patterns by trial and error is not possible. To address these issues, dedicated software has been developed. We will present a package of computer programs facilitating the determination of orientations and strains based on the Kossel diffraction patterns. The strain or lattice parameters are semi-automatically determined by matching geometric features of experimental and simulated patterns. To ensure good reliability of results, the program is capable of simultaneous matching of multiple patterns originating from the same sample location. User-specified strain components, sample-to-detector distances and locations of pattern centers can be fitted. The software is not limited to any particular material or structure. The use of two different strategies allows for the verification of results and for checking their consistency. Operation of the package is controlled via a Windows user interface.

9:30 AM

(ICOTOM-S5-022-2008) Three Dimensional Characterization of Timetal 21S Alloy by Combination of X-ray Microtomography with EBSD

S. R. Dey*, Technische Universität, Germany; E. M. Lauridsen, Risø National Laboratory, Denmark; W. Ludwig, European Synchrotron Radiation Facility, France; D. Rowenhorst, R. W. Fonda, U.S. Naval Research Laboratory, USA

For many decades X-ray microtomography has been quite effective in three dimensional morphological studies of polyphase materials. Impressive resolution of submicron has been reached with the establishment of third generation synchrotron at ESRF Grenoble, France. In addition with good temporal resolution of 10-3 - 1h, in-situ kinetics studies are also feasible. X-ray microtomography can only provide microstructural images/features but lacks in producing the crystallographic details for crystalline materials. In the present study Electron backscattered diffraction (EBSD) is utilized to study crystallography in addition with microtomography. Interesting areas in the specimens could be priorly noted through X-ray microtomography and then the electropolished specimens up to area specific depth are subjected under EBSD. To use this technique, phase transformation study mainly on Timetal 21S alloy were carried out. Timetal 21S alloy has only metastable β (disordered bcc) phase grains at room temperature which upon heating generated α (disordered hcp) precipitates. α precipitations occur at the prior β/β grain boundaries termed as α gb and inside the β grains termed as α laths. The precipitation of α from β phase follows Burgers orientation relationship: $\{1-10\}\beta // (0002)\alpha$ and $\langle 111 \rangle\beta // \langle 11-20 \rangle\alpha$. It has been reported earlier about the exact orientation relationship of the α laths and the relaxed orientation relationship of the α gb with the respective β grains. Few explanations of these are also given in the literature but there still lacks a thorough systematic study. With this combined X-ray tomography-EBSD technique, we would present the crystallographic studies of $\beta \rightarrow \alpha$ phase transformation carried out in Timetal 21S alloy.

9:45 AM

(ICOTOM-S5-023-2008) Continuous Pole Figure Measurements at the Materials Science Diffractometer STRESS-SPEC at FRM-II

U. Garbe*, GKSS, Germany; S. Flemming, C. Randau, HMI, Germany; M. Hofmann, TU-Munich, Germany; H. Brokmeier, TU-Clausthal, Germany

The Materials Science Diffractometer STRESS-SPEC at FRM-II is designed to be applied for phase specific texture analysis with neutron radiation by diffraction methods. The usual way for measuring pole figures with neutron radiation is to use a mesh of discrete c and j rotations. The step size for such a pole figure grid depends on the expected texture and is typically $5^\circ \times 5^\circ$ in c and j and at the moment has to be defined in advance on all neutron texture diffractometers. This is sufficient for most common applications except for texture measurements of materials exhibiting large grain sizes and/or sharp textures. A way to circumvent this problem is to take data continuously in all pole figure directions and to adapt the pole figure grid afterwards. The PSD detector system at STRESS-SPEC covers almost 15° in one pole figure direction. This allows already to manipulate the resolution in one direction afterwards via software. In order to do this for the complete pole figure area one has to combine the PSD system with a continuous rotation of the j circle while accumulating data in small time frames. As the readout time for the detector system on STRESS-SPEC is negligible compared to those time frames this then appears as a continuous scan. As our current instrument software (CARESS) is limited and not able to do this type of scans we are in the process of developing a new beamline control software (INSPIRE). The first part of the new software system is the continuous pole figure option. We have already measured selected samples, which are used as standards, with different grains sizes. We will present first results of continuous measured pole figures compared to stepwise measured pole figures.

10:45 AM**(ICOTOM-S5-024-2008) Watching Grains Anneal in Three Dimensions (Invited)**

C. M. Hefferan, Carnegie Mellon University, USA; U. Lienert, Argonne National Laboratory, USA; R. M. Suter*, Carnegie Mellon University, USA

We describe the evolution of an ensemble of grains in a three dimensional region of a high purity aluminum polycrystal as the sample is heated. Our measurements using high energy x-ray diffraction microscopy were carried out at beamline 1-ID at the Advanced Photon Source. The sample is a one millimeter diameter wire of 99.999% pure aluminum. At this purity, dynamics are observed at temperatures below 100 C; this makes thermal expansion a manageable experimental complication. Using a line focused x-ray beam of 2 μm height and 1.3 mm width, we collect data in a layer-by-layer fashion. Volume measurements span 80 microns in 10 micron steps. Complete volume measurements are done in stop action after anneals at different temperatures. During heating, we collect sub-sets of data from a sub-volume within the previously measured region. In this talk, we will describe the evolution of both the nature of scattering from the grains and the geometrical evolution of grain shapes.

11:15 AM**(ICOTOM-S5-025-2008) Texture and Microstructure Analysis Using 3D-EBSD**

A. Gholinia*, P. Konijnenberg, Oxford Instruments HKL A/S, Denmark

Electron backscatter diffraction (EBSD) analysis has become a routine tool for texture and misorientation analysis. The combination of focused ion beam (FIB) milling and EBSD analysis allows the user to obtain 3D-EBSD data. Successive layers of defined thickness are removed by FIB and 2D-EBSD data is gathered from each layer. The 2D-EBSD data are assembled to form a 3D-EBSD map. The 3D-EBSD data analysis opens up to new possibilities, which include analysis of the true grain size distribution and relate the grain shape to the texture analysis. A full description of a grain boundary geometry is possible, where all of the five parameters can be obtained. In this study the orientation of the grain boundary planes are analysed and their relationship to orientation of the lattice and misorientation to the neighbouring grain are discussed.

11:30 AM**(ICOTOM-S5-026-2008) Comparison of X-ray and EBSD Textures for Back-Annealed Al-Mg Alloys**

O. Engler*, Hydro Aluminium Deutschland GmbH, Germany

Despite the large number of single grain orientation data, which can nowadays readily be obtained by standard EBSD measurements, the number of grains encountered is still small compared to the number of grains contributing to X-ray pole figure measurements. In this paper, we will compare macrotexture results obtained for Al-Mg alloy AA 5005 in the cold-rolled and various back-annealed states. The accuracy of EBSD textures is assessed by way of the statistical parameter rho, which represents the relative mean square deviation between two textures. Furthermore, the impact of sampling step size on the statistical significance of EBSD texture measurements is investigated.

11:45 AM**(ICOTOM-S5-027-2008) Integration of Focused Ion Beam Serial Sectioning and Orientation Imaging Microscopy for 3-D Microstructure Reconstruction in a Ni-base Superalloy**

S. Lee*, E. B. Gulsoy, Carnegie Mellon University, USA; M. Groeber, Ohio State University, USA; G. S. Rohrer, A. D. Rollett, Carnegie Mellon University, USA; M. Uchic, J. P. Simmons, Wright Patterson Air Force Base, USA; M. De Graef, Carnegie Mellon University, USA

A new method for reconstructing a 3D microstructure using the focused ion beam-orientation imaging microscope (FIB-OIM) is introduced. The method acquires in an automated fashion a series of par-

allel sections with both topological and orientation information at the sub-micron scale. The method was applied to a fine-grained Ni-based superalloy, and results in cross-sectional ion-induced secondary electron (ISE) images and corresponding electron back-scattered diffraction (EBSD) maps. Both data series show small translational misalignments, which must be compensated for before combining the sections into a 3-D volume. For the EBSD map alignments, we developed a procedure based on the expectation that good alignment will result in minimal average disorientation between pixels in adjacent layers. After registration, the successive orientation maps were stacked using a voxel-based tessellation; individual grains were defined as collections of spatially contiguous voxels with nearest neighbor misorientation angles of less than 3 degrees. For each section, 4 EBSD images, at 6 degree sample tilt increments, were recorded, to maximize the fraction of grain boundaries imaged with high contrast. The 4 ISE images for each section were first aligned using convolution cross-correlation which produces sub-pixel accuracy and compensates for the tilt-induced image foreshortening. Then the entire stack of images was aligned using a similar algorithm. Finally, the images were aligned with respect to the orientation data volume. The final grain boundaries were obtained by employing an eroded orientation data volume combined with the 3-D Euclidean distance map of the image data as input for a 3-D watershed algorithm. This approach produces a high-resolution 3-D map of the microstructure, including local orientations. We will discuss the experimental and numerical methods developed for this approach, including a numerical method to approximate missing data sections. We will also present results of a quantitative analysis of the Ni-base superalloy microstructure, including the spatial distribution of carbide precipitates.

Complex Oxides and Other Compounds**Complex Oxides and Other Compounds**

Room: Connan

Session Chair: Keith Bowman, Purdue University

8:30 AM**(ICOTOM-S6-001-2008) Tentative Simulation of Crystal Rotation for NaCl Structural Type**

H. Masui*, Teikyo University, Japan

It is well known that crystals of NaCl type take $\{100\}\langle 011\rangle$ (cube) slip and $\{110\}\langle 110\rangle$ (dodecahedron) slip. Additively it is also reported that each of large sum of polarizability and large radius ratio above 0.63 between radius of cation and that of anion tends to cause $\{100\}\langle 011\rangle$ slip. Furthermore there is elaborate study that crystal rotation of NaCl is mainly caused by $\{100\}\langle 011\rangle$ slip. Another experimental study reported that $\{111\}$ orientation has maximum dislocation density which causes maximum hardenability in uni-axial deformation of NaCl structure. Present study tries to explain how $\{100\}\langle 011\rangle$ slip and $\{110\}\langle 110\rangle$ slip cause crystal rotation and form deformation texture of NaCl type structure based on the minimum total slip amount theory by Taylor. Simulation results are as follows. In NaCl structure, crystal rotation is theoretically caused solely by $\{100\}\langle 011\rangle$ slip and not caused by $\{110\}\langle 110\rangle$ slip. Nevertheless, effect of $\{110\}\langle 110\rangle$ slip is vital for a formation of deformation texture of NaCl structure. In selection of the minimum total amount of slip by Taylor, a case which considers the total amount by both $\{100\}\langle 011\rangle$ slip and $\{110\}\langle 110\rangle$ slip brings more realistic deformation texture than a case which considers only $\{100\}\langle 011\rangle$ slip, as follows. In uni-axial compression, final stable orientation shows $\{111\}$ and $\{100\}$ in the former case, while it shows such vague orientation spot as $\{24,31,31\}$ in the latter case. In cold rolling of NaCl structure, final stable orientation shows $\{100\}\langle 0hk\rangle$ in both cases. In pressforming bi-axial stretching of NaCl structure, however, the former case took $\{100\}\langle 0hk\rangle$ as final stable orientation, while the latter case showed rather diverged ori-

Abstracts

entation. There happens to be correlation between the minimum total amount of slip by Taylor and percentage of amount of $\{110\}\langle 110 \rangle$ slip in it in the former case. For example, in cold rolling of NaCl structure, smallest value of the minimum total amount of slip by Taylor in the ODF coordinates is indicated at the orientation of $\{100\}\langle 011 \rangle$, $\{110\}\langle 001 \rangle$ and $\{110\}\langle 110 \rangle$, but these orientations are removed from higher percentage (90%) distribution map of $\{110\}\langle 110 \rangle$ slip.

8:45 AM

(ICOTOM-S6-002-2008) Cast and Rolling Textures of NiMnGa Alloys

W. Skrotzki*, R. Chulist, Technische Universität Dresden, Germany; M. Pötschke, Leibniz-Institut für Festkörper- und Werkstofforschung, Germany; A. Böhm, Fraunhofer-Institut Für Werkzeugmaschinen und Umformtechnik, Germany; H. Brokmeier, GKSS Forschungszentrum, Germany; U. Garbe, ZWE FRM II, Germany; C. Oertel, Technische Universität Dresden, Germany

Off-stoichiometric Ni₂MnGa single crystals exhibit a maximum magnetic field induced strain (MFIS) of about 10%. Since for broad technical applications growth of single crystals is quite time consuming and cost intensive it is necessary to investigate polycrystalline samples on their usability for MFIS. To approach the MFIS of single crystals the crystallographic texture of polycrystalline samples is of particular concern. Therefore, the texture of coarse-grained cast and hot rolled NiMnGa alloys has been measured by diffraction of high energy synchrotron radiation and neutrons. The texture results will be discussed with respect to material, processing, phase transformations including variant selection, and MFIS.

9:00 AM

(ICOTOM-S6-003-2008) Texture of Hot-Rolled Rare Earth Metal-Containing Intermetallic Alloys

J. A. Wollmershauser*, M. C. Heisel, S. R. Agnew, University of Virginia, USA

The origin of the anomalous room temperature ductility in rare-earth metal containing CsCl type intermetallics has presently evaded the scientific community. The current study considers the crystallographic texture of certain copper and silver based rare-earth intermetallics and attempts to determine if crystallographic texture is a root of the anomalous ductility. Six intermetallics, including CuY, CuDy, CuEr, AgY, AgNd, and AgEr, were investigated. The alloys were manufactured using arc melting followed by canning, hot rolling and annealing within an inert atmosphere. Texture measurements were made using x-ray diffraction (XRD). Additionally, XRD and SEM based techniques were used to verify the phase content. It was conclusively determined from quantitative x-ray powder diffraction that all of the alloys under investigation were mainly comprised of the desired line compound. CuEr contained almost no additional phases, while CuY, CuDy, AgEr, and AgY contained 91%, 95%, 93%, and 88% CsCl type compound, respectively. The primary impurity in each of the alloys was the M₂R compound, where M is the transition metal and R is the rare earth component. Crystallographic texture measurements have revealed that the compounds are not consistently textured. CuY, in which literature has reported elongations of up to 11%, displays essentially random grain orientation, while AgY is shown to exhibit moderate texture. If a strong texture had been consistently observed, it would help to explain the apparent disregard for the Taylor criterion, which requires crystals to possess a minimum of 5 independent easy slip systems in order for them to exhibit significant homogeneous polycrystalline ductility. For example, some single crystalline materials can exhibit significant ductility along certain directions due to a single easy slip mode (e.g., basal slip in Zn), and if a strongly textured polycrystal were formed, it would be conceivable that all the grains could deform without developing incompatibilities at the grain boundaries. Currently, the underlying cause for the anomalous ductility has yet to be explained.

9:15 AM

(ICOTOM-S6-004-2008) Determination of Texture and Microstructure of Ordering Domains in gamma-TiAl

C. Zambaldi*, Max-Planck-Institute for Iron Research, Germany; S. I. Wright, EDAX/TSI, USA; S. Zaefferer, Max-Planck-Institute for Iron Research, Germany

TiAl is a widely studied intermetallic alloy with prospects for applications in jet engines, for example. The crystal structure of the gamma-TiAl phase in this alloy is tetragonal with a *c/a*-ratio of approximately 1.02, thus deviating only slightly from the cubic lattice. The order of Ti and Al atoms is such that successive layers of one set of (111) planes are either filled with Al-atoms or with Ti-atoms. This leads to the fact that domains of different order can develop which might have a significant influence on the mechanical properties of the material. The small *c/a* ratio and the order of the crystal structure make it very difficult to determine the correct tetragonal orientation of the crystal by electron backscatter diffraction (EBSD): the order leads to superlattice reflections which are difficult to detect automatically, while the small *c/a* ratio makes the distinction between the *c*- and the *a*-axis very imprecise. This is why, up to now, all researchers have used a fcc lattice structure to index the EBSD patterns. Consequently, the domain structure could not be revealed in any so far published EBSD-based investigations. Only TEM was able to reveal the domain structure but this technique suffers from the small investigable area, difficult sample preparation and little automation of the technique. We developed an EBSD-based technique which allows the reliable distinction of the *c*- and *a*-axis orientation and therefore the full characterization of the domain structure. Basis of our technique is a very precise measurement of the position of the diffraction bands using a high EBSD camera resolution, a highly resolved Hough transform and an accurate pattern centre calibration. The correct orientation is determined based on the angular deviation of the recalculated band positions and the experimental ones. We tested the correctness of the so determined solutions by means of manually detected superlattice reflections for a couple of critical cases. The technique was applied to sets of differently thermomechanically treated samples. We show that the domain structure is clearly revealed. Furthermore, the full, tetragonal microtexture of the material can now be determined.

9:30 AM

(ICOTOM-S6-005-2008) Effect of Texture on the Pore Exact Arrangement and Precision of AAO Nano-Template

I. Kim*, B. Park, Kum Oh National Institute of Technology, South Korea

The pores of anodic aluminum oxide (AAO) templates were hexagonal arranged pore domains in Al sheet. The AAO templates have many desirable characteristics, easy to change the pore diameter and length, good mechanical properties, thermal stability, and corrosion resistance. The thin porous AAO templates show the insulating, brittle and fragile properties. The exact arrangement and precision of AAO pores are very important to the filtering characteristics and nano wire making using by the AAO pore templates. The anodic aluminum oxide templates were prepared by a two step anodization process in a mixture phosphoric acid, sulfuric acid and chromic acid and oxalic acid in this paper. Ordered pores of AAO were prepared with the various types of textured Al sheets in single crystal and polycrystalline. The arrangement and precision of ordered pores were measured by SEM, and FIB. The (200) textured Al sheets showed better than (111) and (220) textured Al sheets in the exact arrangement and precision of ordered AAO pores.

9:45 AM

(ICOTOM-S6-006-2008) Lead-Free Textured Materials with Improved Dielectric and Piezoelectric Properties Fabricated Using Scalable Processing and Forming Techniques

M. Winter*, C. DiAntonio, N. Bell, M. Rodriguez, P. Yang, Sandia National Laboratories, USA

Lead zirconate titanate, PZT, has been established as the material of choice for many ferroelectric and piezoelectric applications; however,

increasing environmental restrictions surrounding lead use in industry have galvanized research seeking alternative materials with equivalent properties. Layer-structured perovskites offer a rich variety of potential alternatives, particularly the bismuth layered and alkali niobate-based solid solution ferroelectrics. Dielectric and piezoelectric properties are greatly improved by templated grain growth or reactive templated grain growth by producing preferably oriented microstructures. While it is of academic interest to explore alternative materials, the ultimate value to industry is the ability to fabricate these materials using scalable fabrication techniques. This work is focused on the production of textured layer-structure perovskites using the common industrial practices of screen printing and injection molding, as well as an aerosol deposition spray technique. The degree of texturing for each process was determined through microstructure, electron diffraction and x-ray diffraction analysis. The dielectric and piezoelectric properties of materials produced by scalable processing and forming techniques were determined, using PZT as a benchmark comparison. Sandia is a multiprogram laboratory operated by Sandia Corporation, a Lockheed Martin company, for the United States Department of Energy's National Nuclear Security Administration under contract DE-AC04-94AL85000.

10:45 AM

(ICOTOM-S6-007-2008) Domain Control Effect on Voltage-Strain Relation in BaTiO₃ Single Crystal

Y. Akimune*, K. Matsuo, R. Ooishi, AIST, Japan; A. Okada, Nissan Motor Co., Ltd., Japan

In recent years, non-lead ceramic materials like BaTiO₃ have been studied and developed as actuator elements. This paper investigates the effect of domain change in a BaTiO₃ single crystal. The effect of an electric-field-induced strain change was also examined. Commercially grown BaTiO₃ single crystals, cut in the (001) plane and with dimensions of 5x5x1mm³, were used in this experiment. The domain structure in single crystals was examined by an optical microscope. Obtained crystal has a head to tail domain constitution in an a-c domain zone. The photograph was taken by transmitted light; the dark area in the photograph is a head to tail domain from [001] and it is represented as a circle because it is not along a line of an a-c domain region on the surface. However, it exhibited stripes along the shared area in an a-a domain region. When a single crystal was aged in a furnace at 180 and 70 degrees Celsius (six hours), a comparatively large strain was obtained. There was no compression stress and the strain and polarization suddenly changed when the electric field exceeded ± 0.1 kV/mm. The results demonstrated the possibility of a reversible large displacement and these results suggested that the domain texture causes significant strain for an actuator.

11:00 AM

(ICOTOM-S6-008-2008) Effect of Crystallographic Texture on Ferroelectric Ceramics (Invited)

R. Garcia*, Purdue University, USA

Ferroelectric Lead Zirconate Titanate (PZT) films display physical behavior that makes them an important candidate for random access memories, actuators, and sensors. In such devices, ferroelectric domains are locally switched by the application of an electric field, thus fixing the polarization state of a volume element of material. Today's technological advancement, however, demands ever higher performances that makes the underlying microstructural features increasingly important. The local crystallographic orientation and the local grain-grain interactions play a critical role in determining the switching of domains. In particular, large spatial variations of the fields arise as a combined result of the stresses that develop due to the thermal expansion and lattice mismatch of the film-substrate system, the anisotropy of the properties of the involved materials, and the processing conditions. Simulations show that in-plane electromechanical interactions electrically shield some of the grains, while enhancing the polarization response in others. Additionally, grain

corners and boundaries become domain nucleation sites as well as domain pinning locations. The resulting local behavior will be a consequence of the local grain boundary misorientation, the underlying texture and the associated single-crystal properties. The local phenomenology observed in these simulations agrees macroscopically with the observed experimental behavior, and is used as a basis to propose microstructural mechanisms that explain the local in-plane and out-of-plane ferroelectric switching behavior.

11:30 AM

(ICOTOM-S6-009-2008) Enhanced Ferroelectric and Dielectric Property Relationships Induced by Textured Processing for Several Ceramic Compositions

C. DiAntonio*, N. Bell, M. Rodriguez, P. Yang, M. Winter, Sandia National Laboratories, USA

For a polycrystalline material, enhancements can be made to the anisotropic piezoelectric polar properties by fabrication of polycrystals that favor a preferred orientation. These oriented ceramics display improved and highly anisotropic properties when compared with randomly oriented ceramics. Many physical and electromechanical properties of crystalline materials are strongly dependent on the crystal orientation of the materials and could benefit enormously from textural modification. Texture allows for increased access to the more favorable single crystal properties, benefits the electromechanical performance of anisotropic piezoelectric ceramics and leads to easier poling. This work involves fabrication of a perovskite-type non-lead based polycrystalline ceramic by a template-induced texturing process using morphologically controlled platelets. The focus vehicle lies with the layer-structured perovskites, particularly the bismuth layered and alkali niobate-based solid solution ferroelectrics. Templated grain growth or "reactive templated grain growth" has been used to produce preferably oriented polycrystals and combined with a shear inducing tape casting process to produce textured bulk ceramics. The degree of texture development has been evaluated during the process based on the microstructure, determined by electron backscattering diffraction, and in terms of the 'Lotgering' factor, determined by x-ray diffraction analysis. The ferroelectric properties have been gauged by impedance analysis, hysteresis response and overall electromechanical behavior and compared based on random polycrystalline versus textured microstructures. The synthesis and fabrication technique will be discussed, including details of the templating, texturing, and forming processes, that result in enhanced functional ceramic components. Sandia is a multiprogram laboratory operated by Sandia Corporation, a Lockheed Martin company, for the United States Department of Energy's National Nuclear Security Administration under contract DE-AC04-94AL85000.

11:45 AM

(ICOTOM-S6-010-2008) Time-Dependent Changes to Preferred Orientation in Ferroelectric Materials and Implications to Macroscopic Properties

J. L. Jones*, University of Florida, USA

In ferroelectric materials, the movement of sub-grain microstructural features such as domain walls and interphase boundaries has a dramatic effect on the macroscopic properties. For example, domain wall motion is known to contribute to fatigue and aging, nonlinearity and hysteresis in the macroscopic electromechanical behavior, affect the mechanical deformation behavior, and influence the fracture mechanics. Such changes involve local crystallographic reorientations that occur uniquely in different grain orientations relative to the sample coordinate axes. We have therefore been using a textural framework in which to describe the preference of different crystallographic orientations relative to the electric field as a function of electric field amplitude, temperature, etc. This talk will highlight two novel applications of these approaches. First, because we are capturing the complete changes in crystallographic arrangement as a function of sample orientation, we can relate the microstructural changes to the

Abstracts

measured macroscopic behavior. Using orientation-averaging approaches, we calculate the respective domain reorientation and lattice strain contributions to the macroscopic strain as a function of electric field and mechanical compressive stress. Domain wall motion is found to contribute significantly to the macroscopic strain under both electrical and mechanical loading. Next, we demonstrate the time-dependence of these structural reorientations during dynamic, cyclic electric field application using time-resolved X-ray and neutron diffraction approaches. These measurements demonstrate that changes to the preferred orientation in different ferroelectric materials occur between the time scales of milliseconds and tens of seconds. These structural measurements have direct implication to the dynamic behavior of these materials in service conditions.

12:00 PM

(ICOTOM-S6-011-2008) Directionality and Anisotropy in Piezoelectric Materials with and without Crystallographic Textures

K. J. Bowman*, Purdue University, USA

Inherent to the microstructure of a polycrystalline material are orientations, orientation relationships and directional characteristics on multiple size scales. Aligned domains in a poled piezoelectric ceramic return to a random state after the material is heated to a temperature above the Curie temperature (TC) and the response is different for materials possessing crystallographic textures prior to poling. This thermal depoling leads to changes in electrical and mechanical properties of the material. Thermal effects on electrical poling or mechanical grinding induced texture in tetragonal lead zirconate titanate (PZT) and lead titanate (PT) have been investigated using ex situ and in situ X-ray diffraction (XRD) with an area detector. In situ thermal depoling experiments have been used to demonstrate the changing magnitudes of tetragonality (c/a ratio) and domain wall stability as a function of temperature and dopant. In contrast with electrical poling, surface grinding induced further increases in the ferroelastic polarization for both soft PZT and PT materials, across the whole temperature range. The in-plane compression of the surface layers and corresponding out-of plane expansion that are caused by grinding induce the same domain reorientation that electrical poling does, and therefore enhance the ferroelastic texture. In materials possessing an initial texture the response is different. Lead metaniobate ceramics tape cast with inclusions of acicular seed particles can be used to produce materials with inherent crystallographic textures prior to poling. Textures in poled and unpoled materials have been quantified using a combination of X-ray diffraction with the Lotgering factor and neutron diffraction with Rietveld refinement. The shear behavior of the individual slurries was linked to the amount of texture that is induced from a given slurry.

Interface Textures

Interface Textures I

Room: Rangos 1

Session Chairs: Greg Rohrer, Carnegie Mellon University; Valerie Randle, University of Wales Swansea

1:45 PM

(ICOTOM-S7-001-2008) Origin of Characteristic Grain Boundary Distributions in Polycrystalline Materials (Invited)

G. S. Rohrer*, Carnegie Mellon University, USA

It is widely recognized that the types of grain boundaries in a material and the manner in which they are connected affect a wide range of properties and, ultimately, a material's performance and lifetime. Understanding causal structure/property relationships relies on accurate descriptions of the grain boundary network, which is structurally complex. To distinguish one grain boundary from another, it is necessary to characterize five independent parameters. Furthermore, the

different types of grain boundaries are connected in non-random configurations. To capture this complexity, we have developed techniques to measure the five-dimensional grain boundary character distribution (the relative areas of different boundary types, distinguished by lattice misorientation and grain boundary plane orientation). Based on observations in a range of metals and ceramics (Al, grain boundary engineered Ni, Cu, and α -brass, Fe-1%Si, WC, MgO, SrTiO₃, TiO₂, MgAl₂O₄, and Al₂O₃), we are beginning to understand how the grain boundary character distribution evolves with time and is influenced by impurities and processing conditions. One general observation that will be described in this talk is that grains within polycrystals have preferred habit planes that correspond to the same low energy, low index planes that dominate the external growth forms and equilibrium shapes of isolated crystals of the same phase. A second topic will be the probable existence of a steady state grain boundary character distribution that is correlated to grain boundary energies and is established in the early stages of growth. A theory for the development of steady state, characteristic grain boundary character distributions will be described.

2:15 PM

(ICOTOM-S7-002-2008) Grain Boundary Patterns in Dynamically Recrystallized Quartz Aggregates

L. Lagoeiro*, C. Castro, Federal University of Ouro Preto, Brazil

The geometric and crystallographic nature of grain boundaries can be created and modified by deformation and temperature and therefore they can be used to interpret the deformation history of an aggregate. The purpose of this study is to show that in overall at different deformation conditions grain boundaries do not show any special crystallographic relationship. However, if the length of straight-boundary segments is taken into account some special relationships appear. Quartz aggregates from naturally deformed iron oxide-quartz rocks were selected to study the configuration of grain boundaries resulting from different deformation conditions. Using an optical microscope, with a mounted U-stage, grain boundary orientations were measured. In the SEM equipped with an EBSD the misorientation data was acquired. In the aggregates deformed at lower temperatures ($\sim 300^\circ\text{C}$), which have typical irregular contours made of short straight boundaries, grain boundaries show a wide range of combination between crystallographic planes, with a slightly predominance for rhombohedral-trapezohedral pairs. The misorientation axes for those aggregates spread with a weak concentration around $55\text{-}60^\circ$. In aggregates deformed at higher temperatures ($\sim 400^\circ\text{C}$) grain boundary segments increase in size and become preferentially oriented parallel to rhombohedral planes. An increase in segment length with temperature also corresponds to an increasing ratio of number of long to short boundary segments. For long boundary segments neighboring grains show limited possibilities for shared crystallographic planes with a predominant combination of rhombohedral-rhombohedral planes. Therefore, we conclude that for irregular grain contours of short boundary segments typically found in rocks deformed at low temperature, grain boundaries assume a broad range of crystallographic relationships between neighboring pairs. In aggregates deformed at higher temperatures grain boundaries occur in a narrow range of crystallographic relationships, with a slightly predominance for rhomb-rhomb interfaces between neighboring pairs for straight segments of long lengths.

2:30 PM

(ICOTOM-S7-003-2008) Orientation Effects in Liquid Phase Sintered Ceramics

J. L. Riesterer*, University of Minnesota, USA; J. K. Farrer, Brigham Young University, USA; C. Carter, University of Connecticut, USA

Lower processing temperatures of ceramic materials, and consequent reduction in production costs for industry can be achieved by liquid phase sintering (LPS). The behavior and redistribution of the liquid during cooling is not well understood but it is clear that the liquid

phase has a significant effect on the grain boundary migration and densification of the compact. Glassy films of $\text{CaAl}_2\text{Si}_2\text{O}_8$ (CAS or anorthite) and SiO_2 were deposited onto single and polycrystalline Al_2O_3 and rutile TiO_2 , respectively, using pulsed-laser deposition (PLD) at room temperature. Single crystals were joined to single crystals of different known orientation or to polycrystalline pieces by hot pressing at 1650°C for 30 min in air. These geometries allow for model grain boundary migration studies to be performed with an emphasis on the roll of orientation on the driving force. Additional heat treatments at 1650°C for varying times induced grain boundary migration. The local misorientation of grains was measured using electron backscatter diffraction (EBSD). This approach allows both normal (NGG) and abnormal (AGG) grain growth to be studied.

2:45 PM

(ICOTOM-S7-004-2008) Effects of Bi Segregation on the Grain Boundary Properties of Ni

F. Papillon*, P. Wynblatt, G. Rohrer, Carnegie Mellon University, USA

Bi is known to segregate strongly to both grain boundaries and surfaces of Ni. In order to assess the effects of Bi segregation on grain boundary properties, the grain boundary plane distribution has been studied by electron backscattered diffraction in high purity Ni, as well as in Ni saturated with Bi at 950°C . In addition, the distribution of relative grain boundary energy in both materials has been investigated by two approaches: atomic force microscopy studies of grain boundary grooving, which yields the ratio of grain boundary energy to surface energy, and grain boundary equilibrium configurations at triple junctions, which provides a more direct measure of the relative grain boundary energy distribution. The results of the changes produced by Bi segregation will be discussed.

3:00 PM

(ICOTOM-S7-005-2008) Possible Role of Complexions in Secondary Recrystallization of Silicon Iron

K. S. Rao*, Lehigh University, USA; A. D. Rollett, S. J. Dillon, Carnegie Mellon University, USA; C. J. Kiely, M. P. Harmer, Lehigh University, USA

An emerging insight in materials science is that interfaces, including grain boundaries and interphase boundaries, may be treated as distinct thermodynamic phases called complexions. This has been a useful new concept to explain abnormal grain growth in ceramic systems such as Al_2O_3 . The purpose of this study is to explore the possible existence of complexions in the Fe-Si system which exhibits some strong similarities in the grain growth behavior to that shown by Al_2O_3 . HRTEM and STEM-EELS analysis will be carried out to understand the nature of the grain boundaries and the existence of any possible complexions by comparing both abnormal and normal grain boundaries types in Fe-Si. We will also report kinetic studies on the nucleation density of abnormal grains in Fe-Si as a function of temperature since this has been found to be a strong indicator of the occurrence of complexions in ceramic systems.

3:15 PM

(ICOTOM-S7-006-2008) Role of Interface in Textured Development in Piezoelectric Ceramics made by Templated Grain Growth Process

T. Kimura*, K. Tsuzuki, T. Motohashi, T. Shoji, Keio University, Japan

Texture is necessary to develop lead-free piezoelectric ceramics. Piezoelectric ceramics belonging to the bismuth layer structure (BLS) and perovskite families have been textured by the templated grain growth process. In this process, green compacts containing aligned, platelike template grains and randomly oriented, equiaxed matrix grains are sintered. Sintering causes not only densification and grain growth but also texture development, which is directly related to microstructure development in the presence of interfaces. In this work, the role of interface on the texture development is examined for $\text{Bi}_4\text{Ti}_3\text{O}_{12}$ (BiT) with the bismuth layer structure and $\text{Bi}_0.5(\text{Na,K})_0.5\text{TiO}_3$ (BNKT) with the perovskite structure. In the

BiT case, (001) low energy surfaces develop in the matrix grains before the growth of template grains, and texture develops by the formation of parallel alignment of template and matrix platelike grains. In the BNKT case, on the other hand, the texture is developed by the growth of template grains and the formation of platelike template grains is controlled by the relative magnitude of (100) surface energy. It has been found that the anisotropy in surface energy and the presence of special interfaces are decisive factors determining texture development through microstructure in BiT and BNKT.

4:15 PM

(ICOTOM-S7-007-2008) Effect of Strain Path and Annealing on Development of Resistance to Intergranular Degradation in Austenitic Stainless Steels (Invited)

V. Randle*, R. Jones, University of Wales Swansea, United Kingdom; J. Marrow, D. Engleberg, University of Manchester, United Kingdom

There is much interest in measurement of grain boundary parameters in polycrystalline materials with a view to identification and exploitation of 'special' boundaries. It has become possible to produce 'grain boundary engineered' (GBE) materials which have an improved response to intergranular attack. Barriers to continued development of GBE include a lack of consensus on what constitutes a 'special' boundary and the need for more reliable data on the link between properties and grain boundary crystallography, and associated processing routes. This paper reports work on the distribution and properties of interfaces in austenitic stainless steels as a function of thermomechanical processing. A single step of 5% tensile strain was followed by annealing at temperatures between 950°C and 1050°C . The results showed an increase in S3 coincidence site lattice (CSL) boundaries, most of which were annealing twins. The largest increase was after annealing at 950°C for 24 hours. The texture was random. Selected data sets were investigated by the new 'five-parameter' analysis system, which allows all five parameters of a grain boundary, i.e. both the misorientation and the boundary plane, to be determined. Corrosion tests were also carried out to assess the effect of the thermomechanical processing on resistance to intergranular degradation. Finally, the misorientation data were compared with a parallel set of experiments where the deformation had been applied by cold rolling. There were significant microstructural differences in the two series of results. After processing which included rolling deformation, the S3 boundaries tended to break up the random boundary network, whereas after processing by tensile deformation the grain boundary network had been affected in other ways. The consequences of these findings for GBE are discussed.

4:45 PM

(ICOTOM-S7-008-2008) Rodrigues-Frank Space for Orientations, Misorientations and Orientation Relationships of Any Crystallographic Point Groups

Y. He*, Cornell University, USA; J. J. Jonas, McGill University, Canada

The fundamental zones of Rodrigues-Frank space for misorientations and orientation relationships between crystals of any two point groups are uniquely formulated in terms of quaternion algebra. Different reference systems are employed for these representations. For single orientations, the reference frame is the specimen coordinate system, which may possess monoclinic or orthorhombic symmetry. In the case of misorientations, the reference system is one of the two crystals and thus may have the symmetry of any of the 32 point groups. The representation of orientation relationships between different types of crystals is similar to that of orientations, but the parent crystal is usually taken as the reference frame and no parent symmetry is taken into consideration. The fundamental zones for all classes of crystals are constructed based on the associated symmetry operations and these can be classified into nine different geometric configurations. The "fundamental zones" that are unbounded are also tabulated. The maximum symmetry-reduced misorientation angles between crystals of any pair of point groups are evaluated and these are solely determined by the geometries of the fundamental zones.

Abstracts

Some examples are given to illustrate the usage of Rodrigues-Frank space for the representation of orientations, misorientations and orientation relationships of crystals with different symmetries, especially those with low symmetries.

5:00 PM

(ICOTOM-S7-009-2008) Correlation Between Grain Boundary Character and Intergranular Corrosion Susceptibility of 2124 Aluminum Alloy

L. H. Chan*, A. Rollett, G. Rohrer, Carnegie Mellon University, USA; H. Weiland, S. Cheong, Alcoa Inc., USA

The effects of grain boundary character on the intergranular corrosion susceptibility of 2124 aluminum alloy are examined. In the study, the alloy was subjected to different solutionizing heat treating temperatures and corrosion tested according to ASTM G110 standards. The samples that were heat treated at higher temperatures have shown susceptibility to intergranular corrosion. After obtaining grain orientations from the automated Electron Back-Scatter Diffraction (EBSD), both grain boundary character and grain boundary plane distributions were analyzed. Grain orientations were studied by measuring misorientations across the corroded boundaries. Grain boundary planes were studied by combining the results from a computer program that was created to correlate the corrosion boundary width with the grain boundary character and the analysis of grain boundary character based on the boundary planes. The relationship of grain boundary character and intergranular corrosion will be discussed.

5:15 PM

(ICOTOM-S7-010-2008) Fatigue Crack Dependence on Boundary Texture

J. LeDonne*, S. Sintay, R. K. Ray, A. D. Rollett, Carnegie Mellon University, USA

Tensile fatigue tests were conducted on thin sheet samples of an Interstitial-Free Low-Carbon Steel. The cyclic loading was terminated at the point where small surface cracks could be identified. The samples are examined using a Scanning Electron Microscope to identify crack initiating features. Preliminary results suggest that grain boundaries are the dominant source of cracks. In addition, micro-milling and ion milling are coupled with electron back scatter diffraction (EBSD) to obtain 3D microstructure observations of the fatigue crack initiation sites. The influence of texture and microstructure topology on fatigue crack initiation and short crack growth kinetics are explored.

5:30 PM

(ICOTOM-S7-011-2008) New Perspectives on Texture Evolution

K. Barmak, M. Emelianenko, D. Golovaty, D. Kinderlehrer*, S. Ta'asan, Carnegie Mellon University, USA

With the advent of rapid automated data acquisition in the laboratory, like the focussed ion beam microscope, an emerging issue is the interpretation of the vast body of information at hand. One important objective is the determination of the grain boundary character distribution. This is where accurate simulation and modeling has a role. We introduce a simplified model for evolution of interface texture based on simulation of a very large scale grain boundary network and whose main objective is to understand the role of topological reconfigurations. We then suggest several ways of formulating models for this simulation, some based on kinetic theory and some on 'random walk' descriptions. These models have advantages, for example, they all produce stable grain boundary character distributions, and disadvantages as well.

5:45 PM

(ICOTOM-S7-012-2008) Evolution of the Grain Boundary Plane Distribution in SrTiO₃ during Grain Growth

G. S. Rohrer, H. M. Miller*, Carnegie Mellon University, USA

The five-dimensional grain boundary character distribution (the relative areas of different boundary types, distinguished by lattice mis-

orientation and grain boundary plane orientation) has been measured in polycrystalline SrTiO₃ at different grain sizes. The samples were heated at 0, 1, and 3 hours in air at 1470 °C. The average grain size in the initial specimen was approximately 2 microns; the grain size increased to over 20 microns in the final heater treatment. The distribution evolves during growth and reaches a steady state as a function of grain size. One notable change is the initial decrease in the concentration of coherent sigma 3 boundaries and a related increase in the concentration of incoherent sigma three boundaries. Based on grain boundary groove measurements, we conclude that the coherent sigma three grain boundaries have higher than average energies and that the incoherent sigma three grain boundaries have lower than average grain boundary energies. Therefore, the observations presented here are consistent with the idea that grain boundary character distributions evolve to a steady state in which the populations of grain boundaries are inversely correlated to the grain boundary energy. The results will be discussed in the context of a theory for the development of steady state, characteristic grain boundary character distributions.

Hexagonal Metals

Texture Modeling

Room: McConomy Auditorium

Session Chair: Carlos Tome, Los Alamos National Lab

8:30 AM

(ICOTOM-S9-019-2008) Textures in Titanium Alloys: An Industrial Perspective on Deformation, Transformation and Properties (Invited)

D. Furrer, Rolls-Royce Corporation, USA; D. Rugg*, Rolls-Royce plc, United Kingdom

The development of texture within titanium alloys is often critical for the development of optimal final component mechanical properties. Alpha phase texture can lead to significant anisotropic behaviour, including directional strength, modulus and ultrasonic inspection capabilities. The formation of alpha phase textures can result from deformation and/or transformation from the higher temperature random or textured beta phase through a Burgers relationship. A summary of how alpha phase texture develops, the impact on mechanical properties and its implication for commercial application of titanium components will be provided. Understanding the formation of hexagonal close packed alpha phase texture within titanium alloys can lead to predictive models to guide engineers in material and process design methods.

9:00 AM

(ICOTOM-S9-021-2008) Grain Size and Orientation Distribution Function of High Purity Alpha-Titanium

B. S. Fromm*, B. L. Adams, S. Ahmadi, Brigham Young University, USA

A method to incorporate grain size effects into crystal plasticity is presented. The classical Hall-Petch equation inaccurately predicts the macroscopic yield strength for materials with non-equiaxed grains or materials that contain unequal grain size distributions. These deficiencies can be overcome by incorporating both grain size and orientation properties into crystal plasticity theory. Homogenization relationships based on a viscoplastic Taylor approach are introduced along with a new function, the grain size and orientation distribution function (GSODF). Estimates of the GSODF for high purity alpha-titanium are recovered through orientation imaging microscopy and the chord length distribution. A comparison between the new method and the traditional viscoplastic Taylor approach is made by evaluating yield surface plots based on deviatoric stress. The influence of grain size effects on the yield strength of alpha-titanium as recovered by the new GSODF is discussed.

9:15 AM

(ICOTOM-S9-022-2008) Elastoplastic Self-Consistent Modeling of Polycrystal Plasticity at Finite Strains

C. Neil*, University of Virginia, USA; B. Clausen, C. Tome, Los Alamos National Laboratory, USA; S. R. Agnew, University of Virginia, USA

The method of elastoplastic self-consistent (EPSC) polycrystal modeling is extended to the case(s) of finite strains and/or finite rotations. In practice, this generalization of the EPSC method incorporates the effects of texture evolution into its predictions, which are of particular utility for interpreting internal stress measurements made during plastic deformation. While the model does not rigorously enforce the principle of material frame indifference (objectivity), it applies corrections to the grain-level and aggregate constitutive models which approximate the effects of grain-level and macroscopic rotation the stress evolution. The model is bench-marked for two distinct cases: i) finite strain deformation of a cubic metal where the texture evolution is rather slow, and ii) moderate strain ($\epsilon \sim 0.1$) deformation of a low symmetry material (magnesium) where the texture evolution is rapid. In the former case, previously published simulation data from elastoplastic models, including finite element-based and self-consistent, are used to validate the approach because there is scant experimental data in the literature concerning the development of internal stresses at large plastic strains. In the latter case, the predictions of the model are compared with experimental internal strain data obtained using neutron diffraction during deformation of a magnesium alloy. These internal strain data had been previously interpreted using a model which is only rigorously correct in the range of infinitesimal strains and rotations. The results allow quantification of the effect of slip-induced grain rotation on internal strain development.

9:30 AM

(ICOTOM-S9-023-2008) Dependence of Deformation Mechanism in Polycrystalline Magnesium Alloys AZ31 and Textures Calculated by Sachs Model

Q. Xie*, P. Yang, University of Science and Technology Beijing, China

Magnesium is the lightest metallic structural material with high specific strength and is used in automotive, electronics and aerospace. However, magnesium often shows a poor formability at room temperature due to its hexagonal structure with less independent slip systems, which limits its use. Different slip systems have been detected in magnesium such as basal slip of $\{0001\}\langle 11-20 \rangle$, prism slip of $\{10-10\}\langle 11-20 \rangle$ and pyramid slip (including the a-type of $\{hkil\}\langle 11-20 \rangle$ and the a+c type of $\{hkil\}\langle 11-2-3 \rangle$). Besides, different types of twinning may also operate. Therefore deformation mechanisms may be complicated in magnesium. During deformation the orientation of a grain influences not only the deformation mechanisms (slip or twinning) and the specific selection of activated slip or twinning systems for that grain, but also the kinetics of different types of transformation. The orientation of a grain has a great influence on the deformation behavior of polycrystalline. This work aims to illustrate the dependence of deformation mechanisms in polycrystalline magnesium alloys AZ31 by using Schmid factor and X-ray diffraction analysis technique, the textures after deformation were also been calculated through Sachs model by alternating the ratios of the CRSS (Critical Resolved Shear Stress) of different deformation mechanisms in magnesium alloys. The results of Schmid factor calculation and textures simulations indicated the dependence of deformation mechanism in polycrystalline magnesium alloys AZ31. It was found that different deformation mechanisms proceeded according to theoretic prediction. Basal slip occurred when basal planes of grains were tilted toward ND around TD; Prism slip dominated when basal planes were perpendicular to TD. $\{10-12\}$ twinning was favored when basal planes were normal to RD and $\{10-11\}$ twinning was analyzed to be related to the basal orientation of grains. Basal orientations with TD- and RD-scattering can favor basal slip and tension twinning respectively after compression twinning based on the Schmid factor analysis.

9:45 AM

(ICOTOM-S9-024-2008) Comparison Between Non-Linear Intermediate and Self-Consistent Modeling for the Simulation of Large Deformation Behavior and Texture Evolution in HCP Metals

S. Mguil*, S. Ahzi, H. Youssef, University Louis Pasteur – IMFS, France; R. Lebensohn, Los Alamos National Laboratory, USA

Low symmetry crystalline structures usually lack the required five independent slip systems for the accommodation of an arbitrary plastic deformation and thus, the classical Taylor models are not applicable. Here, we consider hexagonal materials, such as magnesium, for which the pyramidal $\langle a + c \rangle$ slip has a much higher critical resolved shear stress than the basal and prismatic $\langle a \rangle$ slip. If the hard systems are not activated, the c-direction will not be able to plastically deform. The present work is restricted to modeling of deformation texture evolutions which have their origin in the crystallographic slip for the plastic deformation. In this work, we propose a comparison between two different approaches for the simulation of the large deformation response and crystallographic texture evolution in HCP polycrystals when all slip families are included. The first approach is the well-known viscoplastic self-consistent scheme. The second approach is based on a recently developed viscoplastic non-linear intermediate model. In a first part of the paper, we present a review of both the self-consistent and the intermediate models. In the intermediate approach, a single parameter is used to span the solutions from the upper bound (Taylor) to the lower bound (Sachs) estimates. For the comparison of these two approaches, we performed different tests such as axial tension and compression of hexagonal polycrystals. We considered isotropic hardening and used Voce law for the single-crystal hardening. Different values of the weight parameter for the intermediate modeling and different formulations of the macroscopic moduli used in the self-consistent model are selected to compute the results. Also, the viscoplastic Taylor model (when pyramidal slip is included) and the viscoplastic Sachs model were used to define the upper bound and lower bound estimates. We also compare the results to the modified viscoplastic Taylor model of Parks and Ahzi (1990) which is formulated for crystals lacking five independent slip systems. Specific applications to titanium and magnesium polycrystals are discussed.

10:45 AM

(ICOTOM-S9-025-2008) Prediction of Anisotropic Properties in Mg Alloy Sheets by Using Crystal Plasticity Finite Element Method

S. Choi*, D. Kim, Sunchon National University, South Korea; H. Kim, Korea Institute of Industrial Technology, South Korea

The effect of texture components typical in Mg alloy sheets on the anisotropic properties such as yield stress, r-value and earing profile was investigated using crystal plasticity finite element method (CPFEM). The Gaussian standard function was used to determine orientation distribution function (ODF) around a single ideal component. A predominant twin reorientation (PTR) scheme was successfully implemented to capture grain reorientation due to deformation twinning. For the polycrystal model, the material behavior is described using crystal plasticity theory where each integration point in the element is considered to be several grains of polycrystalline Mg alloy sheets. The experimental anisotropic properties for a polycrystalline AZ31 (Mg-3%Al-1%Zn-0.2%Mn) sheet were also compared to the anisotropic properties predicted by CPFEM.

11:00 AM

(ICOTOM-S9-026-2008) Introduction of Twinning into Cluster Type Deformation Texture Models

S. Mu*, V. Mohles, G. Gottstein, Institut für Metallkunde und Metallphysik RWTH, Germany

In many materials with low crystal symmetry or low stacking fault energies, plastic deformation is accomplished not only by crystallographic slip, but also by twinning. During deformation, twinning plays two important roles. On one hand, it changes the texture evolution associated with reorientation of the twinned portion of the grains. On the other hand, the twin boundaries act as barriers to the

Abstracts

propagation of slip and other twin systems. Therefore, to constitutively describe deformation texture evolution of the materials mentioned above, these two effects of twinning must be taken into account. The Grain-Interaction (GIA) model is one of the most advanced cluster type Taylor models, and has been successfully applied to predict deformation texture evolution of cubic materials, especially of Al and its alloys. The GIA model considers the next-neighbour grain interaction, but it only takes into account crystallographic slip as deformation mechanism, without twinning. In recent years, various attempts have been made to introduce twinning into deformation texture models. For example the Monte-Carlo approach proposed by Von Houtte and advanced by Tomé, reorients the selected grains fully by twinning. In the Volume Fraction Transfer (VFT) scheme, the Euler space is partitioned into equal cells, and the volume fractions are assigned to the respective cells and their evolution is recorded with progressing deformation. In both the Cherkaoui and 'Meso-Scale Composite Grain (CG)' approaches, the twins are treated as inclusions. Secondary twins and slip are allowed to be activated inside the primary twins in the latter approach. In this study, we test and compare two approaches to handle twinning in the GIA model. In the first one, grains are randomly sampled and fully reoriented by twinning; the twinned and untwinned-matrix grains are kept as neighbours. In the second approach, the orientations and volume fractions of the twinned portions are summed up for some simulation steps, and redistributed into the original 8-grain aggregates. The simulation results are compared with experimental data, and with predictions of other models.

11:15 AM

(ICOTOM-S9-027-2008) Grain Interaction Model Applied to Texture Predictions of Magnesium

T. Hochrainer*, H. Riedel, A. Prakash, D. Helm, Fraunhofer IWM, Germany

Hexagonal closed packed (hcp) crystals at low temperatures typically lack five independent deformation modes. According to the von Mises criterion the individual grains will therefore in general not be able to obey the prescribed macroscopic deformation as assumed in the Taylor model. Therefore texture predictions for hcp-metals are usually done by self-consistent schemes where each grain deforms in a visco-plastic effective medium comprising the average behavior of the polycrystal. Similar to the Taylor model, however, self-consistent schemes strongly over predict texture evolution, mainly because interactions between adjacent grains are not sufficiently taken into account. The available Taylor-based grain interaction models which model the individual grain interactions in two- or eight-grain aggregates, however, were so far not used to model hcp-metals. We use a grain interaction model where the polycrystal is divided into eight grain aggregates (each of which fulfilling the Taylor hypothesis) to simulate the texture evolution of Magnesium during rolling. Twinning is modeled as unidirectional pseudo slip which can occasionally lead to a reorientation of a grain as a whole. Recrystallisation is included as an effective softening mechanism. The texture predictions for rolling of Magnesium are compared to experimental data and results obtained by the VPSC model. We find that the grain interaction model provides good texture predictions and successfully slows down the prediction of texture evolution as compared to the self consistent scheme.

11:30 AM

(ICOTOM-S9-028-2008) Mechanism of Determining the Formability of AZ31 Near Room Temperature

H. Li*, E. Hsu, J. Szpunar, McGill University, Canada

In our previous studies, it was shown that basal slip and extension twinning were the primary deformation modes of AZ31 alloy at room temperature. In this paper, a mechanism that can be used to determine the formability of AZ31 at room temperature is explained in details. The mechanism assumes that the maximum amount of cold reduction that a specimen with a given initial texture can undergo coincides with the exhaustion of twin deformation. To verify the proposed mechanism, computer simulations with various initial textures

were carried out and the simulation results were compared with those of the experiments. The simulations were based on VPSC model. The effects of dynamic recrystallization and grain boundary sliding were not taken into account, which is reasonable for deformation near room temperature. In addition, maps of formability of AZ31 as a function of initial texture under both uniaxial compression and tension were generated by computer simulations. The simulated formability maps were presented in the inverse pole figure space and clearly demonstrated the relationship between the formability and the initial texture. The basal fiber texture exhibited the worst formability, random texture exhibited improved formability, and (10-11) fiber texture exhibited the best formability.

11:45 AM

(ICOTOM-S9-046-2008) Texture Modeling in Equal Channel Angular Extrusion Using a General Flow Line Function

L. S. Toth*, A. Hasani, Université Paul Verlaine de Metz, France

In 2003-2004, a new type of description was proposed to describe the material flow in Equal Channel Angular Extrusion ('ECAE'). It is based on an analytic flow line function using only one parameter. The value of the parameter was obtained by fitting the flow lines to finite element calculations. Then, this flow line model was applied to model the evolution of the texture of polycrystalline as well as monocrystalline materials. The first flow line model was developed for a 90° die without rounding of the corners. Then this flow line model was adapted also for the 120° die with successful simulations of the development of the texture in copper. The main interest of the flow line model is that several experimental texture effects are well reproduced which are not possible with the simple shear approach. These are: tilts of the texture components from their ideal positions, specific texture transitions and possibility to describe the gradient of the texture within the extruded samples. In the present paper, a general flow line function is presented which is capable to describe the material flow for any die angle between 90° and 180°. A specific feature of the new function is that it is capable to describe the asymmetrical shapes of the flow lines using only three parameters. These parameters are obtained from a good fit of the flow lines that are observed in finite element simulations of the process and also from experimental flow lines. Simulation results of the texture development on several materials and different die angles are presented with specific interest on the effects caused by the asymmetrical shapes of the lines as well as by the friction of the material with the die which alters also the flow line shape.

Texture Evolution and Severe Plastic Deformation

Room: McConomy Auditorium

Session Chair: Ayman Salem, Air Force Research Laboratory

1:45 PM

(ICOTOM-S9-029-2008) Evolution of Deformation Textures Under Dynamic Recrystallization in Hexagonal Metals During Large Strain Simple Shear (Invited)

B. Beausir*, University of Metz, France; S. Suwas, Indian Institute of Science, India; L. S. Toth, University of Metz, France; K. W. Neale, University of Sherbrooke, Canada; J. Fundenberger, University of Metz, France

Torsion experiments were carried out on pure magnesium (99.9%) having a non-axisymmetric initial texture under free end conditions of testing at 250°C [1]. Texture development in titanium during Equal Channel Angular Extrusion (ECAE) with a die angle of 90° has also been studied for Routes A, Bc and C up to three passes at 400°C. The so-obtained crystallographic textures were analyzed by EBSD (Mg) and by X-ray (Ti) measurements. The occurrence of dynamic recrystallization (DRX) was experimentally detected in titanium during the ECAE experiments as well as in the pure Mg. For both processes, the experimental textures will be compared to the simula-

tion results obtained by the viscoplastic self-consistent model and will be analyzed with the help of the ideal orientations for h.c.p. crystals in simple shear [2]. Taylor factor maps will be also presented for the two materials. Our finding is that the local minimum values of the Taylor factor coincide with the maximum intensities of the ODF in the recrystallized textures in both materials. Thus, it is proposed that the DRX process is controlled by the Taylor factor, which represents the stored energy in the crystal. The comparison of our deformation texture simulations with experiments combined with a suitable kinetics of the DRX process strongly supports our hypotheses.

2:15 PM

(ICOTOM-S9-030-2008) Texture of Magnesium Alloy Sheets Heavily Rolled by High Speed Warm Rolling (Invited)

T. Sakai*, H. Koh, S. Minamiguchi, H. Utsunomiya, Osaka University, Japan

Magnesium alloy sheets had to be rolled at elevated temperatures to avoid cracking. The poor workability of magnesium alloy is ascribed to its HCP crystallography and insufficient activation of independent slip systems. Present authors have succeeded in 1-pass heavy rolling of AZ31 and ZK60A magnesium alloy sheet below 473K by raising rolling speed above 1000m/min. Heavy reduction larger than 50% can be applied by 1-pass high speed rolling even at room temperature. The improvement of workability at lower rolling temperature is due to temperature rise of a material during rolling by plastic working. The texture of heavily rolled magnesium alloy sheet is investigated in the present study. The texture of AZ31B sheet rolled 60% at room temperature was <0001>//ND basal texture. At the rolling temperature above 373K, the peak of (0001) pole tilted 10-15 degrees along RD direction around TD axis to form a double peak texture. The texture varied through the thickness. At the surface, the (0001) peak tilted 10-15 deg along TD direction around RD axis. The direction of (0001) peak splitting rotated 90 degrees from the surface to the center of thickness. The texture of heavily rolled ZK60A sheets is almost similar to that of AZ31B sheets. Heavily rolled magnesium alloy sheets have non-basal texture. The sheets having non-basal texture are expected to show better ductility than sheets with basal texture.

2:45 PM

(ICOTOM-S9-031-2008) Texture Evolution during Multi-Pass Equal Channel Angular Extrusion of Beryllium

S. Li*, X. Liu, South China University of Technology, China

Equal channel angular extrusion (ECAE) is an effective means of grain refinement for metallic materials. The severe plastic deformation and strain path changes involved in the process can lead to significant changes in textures. Investigation of the texture evolution is important in understanding the simultaneous microstructure development and the resulting anisotropy of mechanical properties in the material. In this study, ECAE experiments were conducted for an AZ31 magnesium alloy via four different processing routes, using a 90-degree die. The deformation textures in the magnesium billets were determined by X-ray diffraction and analyzed with the aid of orientation distribution functions. The results reveal characteristic texture evolution associated with different processing route and pass number, and help to identify the conditions to weaken or strengthen the texture in the material. Meanwhile, polycrystal plasticity simulations were conducted using a visco-plasticity self-consistent model to seek elucidations of the texture evolution and the underlying mechanisms in the various cases.

3:00 PM

(ICOTOM-S9-032-2008) Texture Characteristics and Mechanical Properties in an AZ31 Magnesium Alloy Sheet Fabricated by Asymmetric Hot Extrusion

Y. Wang*, L. Chang, Dalian University of Technology, China; X. Zhao, Northeastern University, China

Mechanical properties such as yield strength as well as ductility strongly depends on the orientation of basal plane in magnesium

alloys, because the critical resolved shear stress (CRSS) for the non-basal slips are much higher than that for the basal slip near the room temperature. Primary processing such as hot rolling and hot extrusion generally gives rise to a strong basal texture, and this leads to a very limited ductility near the room temperature. Therefore, texture control during primary processing is important in order to enhance the ductility. For example, the great improvement of the room temperature ductility in some magnesium alloys would be obtained by adopting equal-channel angular press (ECAP) method, which could introduce shear strain inclined to ~ 45 degree against the extrusion. It is suggested that the great shear strain introduced by primary asymmetric mechanical processing can be effectively weaken the orientation of basal plane and enhance the room temperature ductility compared with normal (symmetric) mechanical processing. In the present study, the asymmetric hot extrusion performed at temperature of 400 degree was applied to fabricate AZ31 magnesium alloy sheet in order to introduce great shear strain during the primary processing. The texture characteristics along the extrusion planes from top layer to bottom layer, as well as mechanical properties at room temperature were examined. The experimental results showed that the asymmetric hot extrusion effectively weakens the orientation of basal plane in the extrusion plane and improve the room temperature ductility.

3:15 PM

(ICOTOM-S9-033-2008) Investigation of Texture and Microstructure Evolution During Asymmetric Rolling of Mg Alloys

J. Cho*, S. Kang, H. Kim, Korea Institute of Materials Science, South Korea

Asymmetric rolling (ASR) can be achieved either by changing the diameter of the rolls or changing the rotational velocity of each roll. Under these circumstances, the material was subjected to enhanced shear deformation, and it has been suggested that high-angle boundaries develop with increasing strain, and finer grains are formed by following recrystallization on annealing heat treatments. It is necessary to investigate the relationship between process parameters and shear deformation distribution through the thickness direction to increase the formability. Finite element modeling of conventional and asymmetric rolling processes has been carried out for an understanding of deformation and texture evolution. Using differential roll speed, asymmetric shear deformation was generated. Effects of various ratios of roll speeds on texture were investigated. Mechanical properties were also calculated from crystallographic textures.

4:15 PM

(ICOTOM-S9-034-2008) Microstructure and Texture Gradient in Titanium Severely Strained by Friction Roll Processing and Subsequent Annealing

M. Shi*, T. Umetsu, Y. Takayama, H. Kato, H. Watanabe, Department of Mechanical Systems Engineering, Utsunomiya University, Japan

The microstructure and texture evolution in titanium after severe plastic deformation using friction roll processing (FRP) followed by annealing has been investigated. FRP, which is a promising method to give severe strain in surface layers, was expected to obtain the grain refinement along with preferred orientation. Significant changes of strain were imposed into from the surface toward the interior of samples, and then the mechanism of deformation was proposed. All possible strain rates which are described by the rotation speeds of roll were used as a parameter for finding the optimum operating conditions. Other parameters including the feeding speed of sample and annealing temperature were experimentally set also for investigating effects on microstructure and texture evolution. Scanning electron microscopy/ electron back scatter diffraction pattern (SEM/EBSP) technique was used for observing texture evolution. In as processed sample, high density of dislocation was found at the surface layer, while both tensile and compression twins were mainly found between

Abstracts

the subsurface and center layers. After annealing, dependence of texture on the distance from the surface was observed. Different deformation modes accommodating by strain gradients was discussed as the reason for formation of microstructure and texture gradient.

4:30 PM

(ICOTOM-S9-035-2008) Texture and Mechanical Properties of Equiaxed Ultrafine Grained Zirconium Fabricated by Accumulative Roll Bonding

L. Jiang*, University of Southern California, USA; M. Pérez-Prado, O. Ruano, National Center for Metallurgical Research (CENIM), CSIC, Spain; M. Kassner, University of Southern California, USA

The texture and mechanical behavior of bulk ultrafine grained (ufg) Zr fabricated by accumulative roll bonding (ARB) are investigated by electron backscatter diffraction (EBSD) and tensile testing, respectively. A complex through-thickness texture gradient develops during ARB. In the areas subjected to pure plane strain deformation (located at the mid-thickness of inner layers), a typical rolling texture predominates, with basal planes slightly rotated away from the normal direction (ND) towards the transverse direction (TD) and with $\langle 10\text{-}10 \rangle$ directions aligned with the rolling direction (RD). At the surfaces a $\{0002\}\langle 11\text{-}20 \rangle$ texture develops due to the macroscopic shear strain imposed by friction with the rolls. At the mid-thickness of the outer layers the RD is still preferentially aligned with a $\langle 11\text{-}20 \rangle$ prismatic direction, but it tends to spread along the $\langle 11\text{-}20 \rangle\text{-}\langle 10\text{-}10 \rangle$ symmetry boundary of the stereographic triangle as a result of the simultaneous plane strain and shear deformation imposed. The areas in the vicinity of the inner interfaces are subjected first to shear strains and then to plane strain deformation during successive passes. In these areas the maximum in the RD inverse pole figure rotates away from the $\langle 11\text{-}20 \rangle$ pole toward the $\langle 10\text{-}10 \rangle$ pole along the $\langle 11\text{-}20 \rangle\text{-}\langle 10\text{-}10 \rangle$ symmetry boundary, so that the shear texture is replaced by a "rotated shear" component after one ARB pass and the latter by the rolling texture after two ARB passes. Since the "rotated shear" and rolling orientations in Zr are rather similar, a reasonably homogeneous texture is achieved in the bulk after 2 ARB steps. The yield stress and UTS values of ARBed Zr are nearly double those from conventionally processed Zr with only a slightly loss in ductility.

Texture in Materials Design

Texture in Materials Design I

Room: Connan

Session Chair: Brent Adams, Brigham Young University

1:45 PM

(ICOTOM-S12-001-2008) Microstructure Characterization and Localization Tensors Using 2-point Correlations (Invited)

S. Kalidindi*, S. Niezgodna, G. Landi, D. Fullwood, Drexel University, USA

This paper presents an efficient spectral framework, called Microstructure Sensitive Design (MSD), for building invertible microstructure-property-processing linkages. The methodology utilizes higher-order spatial correlations in the quantitative description of the microstructure. Combining this description with sophisticated homogenization theories, MSD formulates robust scale-bridging microstructure-property linkages. A salient feature of MSD is that it presents these linkages in an efficient Fourier space, which in turn allows treatment of inverse problems in materials design. In a similar manner, the processing-microstructure evolution linkages are formulated in MSD in the form of evolution laws for the higher-order statistics describing the microstructure. Combining all of these aspects into a single mathematical framework, MSD aims to facilitate a rigorous consideration of microstructure as a continuous design variable in a broad range of engineering design and optimization problems.

2:15 PM

(ICOTOM-S12-002-2008) Using ab initio Simulations in Texture Research

D. Raabe*, D. Ma, F. Roters, A. Counts, M. Friák, M. Petrov, J. Neugebauer, Max-Planck-Institut fuer Eisenforschung, Germany

In this contribution we discuss various strategies and examples for the use of ab initio simulations in the context of texture research. We show how parameter-free density functional theory calculations can be used to provide theoretical guidance in understanding the crystalline origin of mechanical anisotropy and how to use this information to design materials with tailored properties. Three strategies will be discussed in more detail, namely, the direct prediction of anisotropy coefficients which cannot be easily obtained otherwise (e.g. certain elastic constants); of structural transitions in dual-phase alloys in the context of texture research (e.g. volume portions of bcc and hcp phase in dual phase Ti alloys); and of constitutive parameters which can enter into internal variable formulations used in texture models (e.g. constitutive parameters used in crystal plasticity finite element simulations which are based on internal variables). A brief introduction to the applied theoretical methods will be given. Three material design examples for the direct application of such ab initio based strategies in texture research will be presented in more detail. The first one is about the optimal anisotropy design of Titanium based alloys, the second one is about the anisotropy of Magnesium based alloys, and the third one about the understanding of the microscopic origin of anisotropy in a biological structural composite material which is based on chitin, proteins, and calciumcarbonate.

2:30 PM

(ICOTOM-S12-003-2008) Hierarchical Multi-Level Modelling of Plastic Anisotropy Using Convex Plastic Potentials

P. Van Houtte*, S. K. Yerra, A. Van Bael, Katholieke Universiteit Leuven, Belgium

The plastic anisotropy of textured materials should be taken into account in finite element (FE) simulations of metal forming processes. The so-called hierarchical modelling scheme achieves by using an anisotropic constitutive model described by an analytical expression. Plastic potentials in either stress space (yield locus) or strain rate space are very suited for this. They contain a certain number of parameters which can be identified by fitting the expression to the predictions of a multilevel model. Van Houtte and Van Bael [1] have presented an expression for anisotropic plastic potentials in strain rate space which could be fitted to the predictions of Taylor model simulations of the plastic deformation of textured materials. However, these expressions were not automatically convex, which required an additional correction procedure. An entirely new analytical expression will be presented which is automatically convex anywhere in strain rate or stress space. Moreover, it is more flexible than the previous method, and can in principle be used with more advanced multilevel models than the Taylor theory. It will also be less difficult to use for anisotropy updates during a FE simulation. First results will be shown: strain rate space based equipotential surfaces for textured materials which will be compared to data points obtained directly by the Taylor theory, as well as to the results of older methods. It should be noted that in another presentation at the same conference, it will be shown how the new method can be used to generate analytical expressions of the plastic potentials in both strain rate and stress space, which allows for very high efficiency when implemented in engineering-type finite element codes for metal forming processes. [1] P. Van Houtte and A. Van Bael: "Convex Plastic Potentials of 4th and 6th Rank for Anisotropic Materials", Int. J. Plasticity 20 (2004) 1505-1524.

2:45 PM

(ICOTOM-S12-004-2008) Constitutive Modelling of the Dilatational Plasticity of Textured Aggregates

R. Lebensohn*, C. N. Tome, Los Alamos National Laboratory, USA; P. Ponte Castaneda, University of Pennsylvania, USA

In this work we consider the presence of ellipsoidal cavities inside polycrystals undergoing viscoplastic deformation. For this purpose, we make use of an implementation/generalization of the "second-order" non-linear homogenization method (P. Ponte Castañeda, *J Mech Phys Solids* 50, 737, 2002) into the general-purpose viscoplastic self-consistent (VPSC) code. Thus, the original VPSC formulation, which was based on a first-order linearization of the grain's behavior, has been extended to deal with porous polycrystals taking into account the dilatational deformation associated with void growth, and second-order statistical information in terms of average field fluctuations inside the constituent grains, which turn out to be significantly high in aggregates with strong contrast in local properties, like a voided polycrystal. Such extended model allows us to account for porosity evolution, while preserving the anisotropy and rate sensitivity capabilities of the VPSC formulation. We present several applications of this extended VPSC model, addressing the coupling between texture, plastic anisotropy, void shape, triaxiality, rate sensitivity and porosity evolution. We also discuss the implementation of a multi-scale calculation, using the extended VPSC model as a constitutive routine inside dynamic FEM codes, for the simulation of deformation processes in which both texture-induced anisotropy and cavitation become relevant aspects of the microstructural evolution.

3:00 PM

(ICOTOM-S12-005-2008) Spectral Representation of Higher-Order Localization Relationships for Elastic Behavior of Polycrystalline Cubic Materials

G. Landi*, D. T. Fullwood, S. R. Kalidindi, Drexel University, USA

In this study, we formulate an efficient higher-order spectral representation for calculation of elastic localization tensors for polycrystalline cubic material systems. The spectral basis is founded upon Generalized Spherical Harmonic Functions, and provides a framework for inverse design and rapid analysis of microstructure for the large class of the polycrystalline materials used in structural applications. The spectral representation presented in this study is developed in such a way as to effectively separate the microstructure morphology (i.e. structure) information from the fundamental material property information, facilitating independent search and optimization activities in the key design spaces. The spectral framework replaces complex integral relations for local stress and strain fields (derived from established composite theories) by algebraic expressions involving polynomials of structure parameters and morphology-independent influence coefficients. These coefficients need to be established only once for a given material system. We also formulated and demonstrated a viable approach to establishing the values of the second-order influence coefficients by calibration to the results of micromechanical finite element models.

3:15 PM

(ICOTOM-S12-006-2008) Texture-Based Plastic Potentials in Stress Space for Finite Element Simulations

A. Van Bael*, S. Yerra, P. Van Houtte, Katholieke Universiteit Leuven, Belgium

A new type of mathematical expressions [1] is employed to describe texture-based anisotropic yield loci. Their parameters are identified from the crystallographic texture and the Taylor polycrystal plasticity model. Various strategies are explored to construct the grids in strain rate space and the corresponding yield stresses that serve as basic information for these functions. In contrast with our previous formulation [2], the new flow laws are expressed in stress space, not in strain rate space. In addition they automatically guarantee convexity of the yield loci, without requiring additional modifications

of the parameters. The quality of these analytical approximations will be assessed for yield locus sections and r -values, using the results obtained directly with the Taylor model as reference solutions. Furthermore, it will be discussed how the analytical approximations are implemented through user-material routines in FE software, using similar constitutive integration algorithms as in [3]. Simulations of cup drawing of an IF-steel will be presented and compared to both experimental data and calculation results obtained with our previously developed explicit [3] and implicit [4] approaches. The direct use of yield loci in stress space allows for fast yield checks, and the corresponding effect on the required total simulation times is discussed. [1] P. Van Houtte and A. Van Bael: "Hierarchical Multi-Level Modelling of Plastic Anisotropy using Convex Plastic Potentials", submitted to this conference. [2] P. Van Houtte and A. Van Bael: "Convex Plastic Potentials of 4th and 6th Rank for Anisotropic Materials", *Int. J. Plasticity* 20 (2004) 1505-1524. [3] S. Ristic, S. He, A. Van Bael and P. Van Houtte: "Texture-based explicit finite-element analysis of sheet metal forming". In *Textures of Materials* (Proc. ICOTOM 14), Leuven, Belgium, July 11-15, 2005, P. Van Houtte and L. Kestens, Eds. *Materials Science Forum* 495-497 (2005) 1535-1540. [4] S. Li, E. Hoferlin, A. Van Bael, P. Van Houtte and C. Teodosiu: "Finite element modeling of plastic anisotropy induced by texture and strain path change", *Int. J. Plasticity* 19 (2003) 647-674.

4:15 PM

(ICOTOM-S12-007-2008) Using 3D Image-Based Finite Element Modeling to Investigate Interactions among Microstructure, Crystallography and Mechanical Response

A. C. Lewis*, Naval Research Laboratory, USA; M. A. Qidwai, SAIC, USA; A. B. Geltmacher, Naval Research Laboratory, USA

The three-dimensional microstructure of a single-phase beta Titanium alloy was reconstructed from serial sectioning and EBSD measurements, and used as input for image-based finite element modeling of mechanical response. This quantitative analysis of experimentally-derived 3D data in conjunction with finite element simulation results allows for the investigation of correlations of mechanical behavior with microstructure and crystallographic features. Using anisotropic elasticity and crystal plasticity constitutive models, the highest strains were observed at particular grain boundaries. The microstructural, morphological, and crystallographic features which correlate with these high strains were examined, including misorientation at the boundary, crystallographic grain boundary planes, crystallographic alignment with the loading axis, and boundary curvature. In addition, the effects of the simulation parameters such as meshing techniques, mesh density, simulation boundary conditions, and mesh resolution were considered. The ultimate goal of this research is to develop a simulation tool with the capability to take true 3D microstructures as input, and accurately and efficiently simulate the effects of 3D microstructure and crystallography on mechanical response.

4:30 PM

(ICOTOM-S12-008-2008) Plastic Heterogeneity Due to Grain Boundaries and Its Influence on Global Deformation Textures

A. K. Kanjarla*, P. Van Houtte, Katholieke Universiteit Leuven, Belgium; L. Delannay, Université Catholique de Louvain (UCL), Belgium

Plastic deformation in metals is heterogeneous in nature. This heterogeneity is induced by variety of factors at different length scales. The present study involves understanding the contribution of grain boundaries towards such a heterogeneous deformation field in a microstructure at mesoscopic scale. Finite element method coupled with crystal plasticity theory was used to deform a simple set-up of four grains. Each grain was discretised into large number of elements to effectively capture the complex nature of the plastic fields in the vicinity of the grain boundaries. Distribution of strain rates, both along and perpendicular to the grain boundaries was analyzed. The observations from above simulations were then used to enrich the

Abstracts

microstructural description and grain interaction effects in a Taylor-type micromechanical model. A new model, aimed at predicting deformation textures in face centred cubic materials, is presented. It takes into account the near neighbour interaction as well as the influence of global texture on the deformation behaviour of an individual grain. This is achieved by an iterative scheme for solving the field equations for a system consisting of a grain boundary segment (and its associated grain boundary zones) embedded in a homogenous media. Deformation textures predicted by the new model will be presented along with a quantitative comparison with both experimental and simulated textures from other micromechanical models.

4:45 PM

(ICOTOM-S12-009-2008) Modeling Rolling Textures of Beta Ti Alloys Using Constitutive Data From Ab-initio Simulations

D. Ma*, D. Raabe, F. Roters, M. Friak, J. Neugebauer, Max-Planck-Institut fuer Eisenforschung, Germany

In this study we present a new strategy for the incorporation of constitutive data which were obtained by a quantum mechanical approach in conjunction with experiments, into crystal plasticity finite element simulations for rolling texture simulations. The parameter-free density functional theory calculations were used to provide theoretical guidance in investigating and optimizing Ti-based body centered cubic alloys with respect to three constraints: (i) the use of non-toxic alloy elements for biomedical applications; (ii) the stabilization of the body centered cubic beta phase at room temperature; (iii) the reduction of the elastic stiffness compared to existing Ti-based alloys; and (iv) the creation of a beta phase Ti alloy with isotropic elastic properties. Owing to these constraints we focussed on a set of Ti-Nb and Ti-Mo alloys which were predicted as most promising by the ab initio calculations. The materials were then cast, rolled, annealed, and finally characterized. The simulations both, of the evolution of the rolling textures and of the resulting overall elastic anisotropy for a given texture, were conducted using a crystal plasticity finite element approach which uses ab initio and experimentally obtained constitutive input data.

5:00 PM

(ICOTOM-S12-010-2008) Texture Gradients in Hot-Rolled Al-Alloy Plates for Aeronautical Applications

D. J. Piot*, W. Robert, R. Quey, J. H. Driver, École des mines de Saint-Étienne, France; F. Eberl, Alcan centre de recherches de Voreppe, France

Some critical components of aircraft structures are directly machined from thick plates of 7xxx series Al-alloys. These plates are hot-rolled to the final gauge by a breakdown reversible mill. Thus, complex strain paths, incorporating plane strain compression and shears, occur through the plate and vary through the thickness. They develop deformation textures, which are retained, due to recrystallization inhibition, with through-thickness gradients, and lead to a spread of the mechanical properties due to anisotropy (direction) and gradients (position). Optimized design of such components implies the development of a well-suited texture (and its gradient) in the plate. In order to allow inverse method optimization, a rapid texture model derived from Taylor models has been developed integrating grain interactions. Details of the model are presented elsewhere [1–2]. In this study, the model is coupled with computations from standard commercial FEM codes simulating the entire industrial rolling schedule. A systematic study of texture gradients in aluminum thick plates is presented, notably the development of a rotated cube component due to alternating shear in the strain path. Through-thickness texture predictions and measurement are satisfactorily compared in order to validate the method. The results of the grain interaction model show that texture intensities are reduced compared to standard Taylor models with a better fit to the experimental data. Finally, the study illustrates an efficient on-line prediction tool using standard FEM simulation of the processing route with an integrated coupling using modified Taylor-type models. It is therefore a rapid, industrial pre-

dictive model, validated by experimental comparisons, and which allows an optimization of industrial rolling schedules for improved design, incorporating anisotropy and the through-thickness gradient, of aeronautical components. 1 Robert W., Piot D. and Driver J.H. – A rapid deformation texture model incorporating grain interactions, Scripta Materialia, 2004, vol 50, pp 1215–1219. 2 Quey R., Ringeval S., Piot D. and Driver J. H. – New grain interaction models for deformation texture simulations, Proceedings Thermec 2006.

5:15 PM

(ICOTOM-S12-011-2008) Numerical Modeling of Postnecking Deformation in AA5754 Aluminum Sheets

M. Gesing, A. Izadbakhsh, K. Inal*, University of Waterloo, Canada; R. K. Mishra, General Motors, USA

A new finite element analyses based on rate dependent crystal plasticity theory has been developed to investigate postnecking deformation in AA5754 aluminum sheets prepared by conventional rolling from direct chill-cast (DC) ingots. Microstructure of such a material consists of numerous intermetallic particles dispersed in the material which exhibits a rolling texture. The new model can incorporate electron backscatter diffraction (EBSD) maps into finite element analyses to capture texture information and incorporate experimentally measured second phase particle fields. The numerical analysis accounts for crystallographic texture (and its evolution) as well as grain morphologies. A unit cube (numerical model for three dimensions) approach has been adopted where an element or number of elements of the finite element mesh are considered to represent a single crystal within the polycrystal aggregate. Thus the full richness of localized deformation is investigated in three dimensions where often the stress state is tri-axial at necking. Experimentally measured particle fields are implemented in the form of finite elements with stiff elasticity properties within the unit cube. Numerical simulations of uniaxial tension, in-plane plane strain tension and balanced biaxial tension have been performed by models with and without second-phase particles. The predicted localized deformation patterns are compared with each other and some experimental data. The effects of various parameters such as second-phase particle distribution, texture evolution and strain paths on particle induced localized deformation patterns are investigated. The effects of texture evolution and second-phase particle distribution in postnecking deformations are studied.

5:30 PM

(ICOTOM-S12-012-2008) Rolling Parameters Governing the Evolution of Strain States and Textures during Asymmetrical Cold Rolling in AA 5052

H. Kang, M. Huh*, Korea University, South Korea; O. Engler, Hydro Aluminium Deutschland GmbH, R&D Center Bonn, Germany

Asymmetrical rolling was carried out in AA 5052 sheets with different velocities of upper and lower rolls. In order to study the major factors governing the evolution of texture during asymmetrical rolling, the ratio of upper and lower roll velocities, the friction between sample and rolls, the size of the rolls and the reduction per rolling pass were varied. Because these rolling parameters all affect the evolution of strain states and textures, the formation of uniform shear textures throughout the whole sheet thickness was obtained only by a proper control of the rolling parameters. The strain states associated with asymmetrical rolling were derived from simulations with the finite element method.

5:45 PM

(ICOTOM-S12-013-2008) The Variation Range of the Results of FCC Texture Simulations Based on {111}<110> SLIP

T. Leffers*, Risø National Laboratory, Technical University of Denmark, Denmark

The present work deals with the diversity of the results of texture simulations for fcc materials with normal {111}<110> slip depending

on the overall framework. To the author's best knowledge this is the first time such a comprehensive selection of results is presented together. The results are just going to be presented and compared with experimental textures without any discussion of the underlying physics. It so happens that all the published results are similar to existing experimental textures (or at least to components of existing experimental textures) – because those which are not have not been published, or because there is such a real limitation. The multitude of specific results is not to be recapitulated in this abstract. Only one extreme example will be quoted: Sachs-type models may simulate either the copper-type texture (with predominant $\{211\}\langle 111\rangle$ orientations) or the brass-type texture (with predominant $\{110\}\langle 112\rangle$ orientations) depending on the way slip is translated into lattice rotations, e.g. Leffers and Lebensohn in Proceedings ICOTOM 11, pp. 307-314.

Wednesday, June 4, 2008

Texture and Anisotropy in Steels

Low Carbon and IF Steels

Room: Rangos 3

Session Chairs: Leo Kestens, Delft University of Technology; Arunansu Halder, Tata Steel Ltd.

8:30 AM

(ICOTOM-S3-001-2008) Texture Control in Manufacturing Current and Future Grades of Low-Carbon Steel Sheet (Invited)

L. A. Kestens*, Delft University of Technology, Netherlands; R. Petrov, Ghent University, Belgium

Although there is still a lot of debate on the nature of texture forming transformations, in practice an increasing level of perfection was obtained in texture control for a number of steel grades of which the prime functionality depends on the texture. The two most pronounced examples are the deepdrawing grades for automotive applications and the electrical steel sheets for electromagnetic applications. By fine tuning the vast variety of manufacturing parameters, including the chemical composition, the intensity of the dominant components such as $\{001\}\langle 110\rangle$, $\{111\}\langle 110\rangle$, $\{111\}\langle 112\rangle$ and $\{110\}\langle 001\rangle$ can be controlled to a considerable extent. Nowadays deepdrawing steels are produced with a γ -fibre intensity ($\langle 111\rangle//ND$) of > 15 random levels which produces an average normal anisotropy well above 3.0 (average r-value). High quality grades of grain oriented electrical steels are manufactured in which nearly every single grain of the polycrystalline aggregate is confined to a narrow range of less than 3deg from the ideal Goss component ($\{110\}\langle 001\rangle$). In recent years new high strength steel grades are being developed. Some of them have already been commercialized such as TRIP steels (Transformation Induced Plasticity) and dual phase steels, whereas others, such as TWIP steels (Twinning Induced Plasticity) are still finding their way to the market. As the prime functionality of these new grades is to provide a superb combination of strength and ductility, texture is generally of minor concern for these steels. In the present review, though, it will be argued that a better understanding of the crystallographic features of these newly developed grades may also contribute to a further optimization of their performance. The crystallographic texture provides the preferred instrument for characterizing the microstructure of these complex grades (by orientation contrast microscopy) which may contribute to a deeper understanding of the rather complex physical metallurgy involved in the processing of these materials and a better control of various application aspects such as welding or forming.

9:00 AM

(ICOTOM-S3-002-2008) Importance of Dislocation Substructures in Texture Control of Low Carbon Steels (Invited)

H. Inagaki*, INATEX, Japan

In the past, the development of rolling and recrystallization textures has been discussed in terms of the Taylor type macroscopic crystal plasticity theory, or on the basis of the results obtained by macroscopic X ray ODF or EBSD analysis. However, in order to realize more precise and effective texture control, the development of rolling and recrystallization textures should be investigated in a much finer scale, i. e. at the level of dislocations. In the present paper, the development of dislocation substructures during cold rolling and the formation of recrystallization nuclei from these substructures during subsequent annealing were investigated in detail in high purity iron alloys by using TEM. It was found that, during cold rolling, formation of microbands occurred concurrently with the development of cold rolling textures. This indicated that, at the dislocation level, the formation of microbands played a decisive role in the development of rolling textures. The formation of these microbands was found to be strongly influenced by the alloying element. The largest effect was observed in the case of the interstitial carbon atom which interacts most strongly with dislocations in iron. In this case, cross slip was enhanced so frequently that, instead of microbands, dense dislocation tangles were developed homogeneously. This suppressed strongly the development of rolling textures. Also recrystallization textures observed after subsequent annealing were weak. The importance of dislocation substructure control was thus most clearly illustrated in this example. By using TEM, also origins of the most important recrystallization texture component in iron and low carbon steels, $\{111\}\langle uvw\rangle$, were investigated. Many examples could be obtained, which indicated that, $\{111\}\langle uvw\rangle$ recrystallized grains were originated from restricted $\{111\}\langle uvw\rangle$ deformed regions near grain boundaries.

9:30 AM

(ICOTOM-S3-003-2008) EBSD Investigation of Phase Transformations in Low Carbon Steels

S. Lubin*, Ecole des Mines de Paris, France; H. Réglé, Arcelor-Mittal Research, France; A. Gourgues, Ecole des Mines de Paris, France

This study presents the characterization of the mechanisms of phase transformation realized in low carbon steels during two kinds of experiments. First, in situ observations of the $\alpha \rightarrow \gamma \rightarrow \alpha$ phase transformation in a Titanium stabilised Interstitial Free steel using a specially designed Scanning Electron Microscope equipped with Electron Backscattering Diffraction system and a heating stage are presented. Local crystallographic orientation analyses were performed at high temperature where the material was fully austenitic and allowed accessing the austenite grain size. Crystallographic orientation maps of the same area of the sample performed in austenite and in ferrite after cooling down allowed comparing experimental to theoretical orientation relationships. On the other hand, we studied variant selection in a low carbon microalloyed steel during cooling down from deformed versus recrystallized austenite. For this purpose, samples were deformed by torsion at high temperature and cooled down directly or after a dwell time. We also determined the influence of various parameters of austenite such as temperature or strain rate.

9:45 AM

(ICOTOM-S3-004-2008) Texture Memory Effects in Low and Ultra Low Carbon Steels

A. Halder*, Tata Steel Ltd., India

According to the Kurdjumov – Sachs relationship, there are 24 variants which dominate the crystal orientation relationship between the austenite - Fe and ferrite - Fe lattices during ferrite to austenite or austenite to ferrite transformation. In this sense, one crystal orientation can be converted into 24 different orientations after transformation which results into weakening of texture present before transformation. But sharp transformation textures are sometimes observed

Abstracts

which indicates a mechanism which strongly reduces the number of variants. This texture memory effect, whereby the recrystallisation texture is completely or partially recovered after ferrite to austenite to ferrite transformation was found to occur in low and ultra low carbon cold rolled steels. The present paper describes the systematic investigation on texture memory effects in different steels with different initial microstructures. The steels were cold rolled and then annealed at different temperatures in two phase and austenitic regions with different time duration and cooled at different cooling rates including water quenching. This present paper summarizes the effect composition, initial microstructures, retention time at austenite and cooling rate on texture memory effect.

10:30 AM

(ICOTOM-S3-005-2008) Influence of the Al to N Ratio on the Texture of Batch Annealed Low Carbon Tin Plate for DWI Can Production

A. L. Pinto*, Instituto Militar de Engenharia, Brazil; C. S. da Costa Viana, Universidade Federal Fluminense, Brazil; P. R. Campissi, Companhia Siderúrgica Nacional, Brazil

The production of two-piece cans using the DWI (Draw Wall Ironing) technique is nowadays used worldwide. In the case of steels, it is well known that when a strong (111)<uvw>//DN fiber texture is present in the sheet the two-piece cans show reduced earing profiles, leading to reduced costs. In the present work, tinplates with different Al to N ratios (8, 11 and 17) were produced with the same finishing rolling temperature, coiling temperature after hot rolling, cold rolling reduction and batch annealing scheme. It was observed that a range of different microstructures, textures, microtextures and anisotropies can be obtained, all related to the Al/N ratio. DWI cans were produced with these materials and their drawing behaviour was observed. Optical microscopy, EBSD and OIM techniques were used in the analysis and texture quantification of the final products. When the Al/N ratio was equal to 8, a strong (111)<uvw>//DN fiber texture was observed to develop together with a pancake grain microstructure. The low earing and high R values were in expected accord. For the Al/N = 11 ratio material, the grains were slightly elongated and the relation between Delta R, earing and texture was not so clear. For the Al/N = 17 material the grains were equiaxed, the texture became weak, with stronger {001}<uvw> components and poorer relationship to deep drawing parameters. A better comprehension of the inter-relationship of all the data is attempted in the final conclusion.

10:45 AM

(ICOTOM-S3-006-2008) Development of Texture, Microstructure and Grain Boundary Character Distribution after Heavy Cold Rolling and Annealing in a Boron Added Interstitial Free (IF) Steel

R. Saha*, R. K. Ray, TATA STEEL, India

The mechanical properties of steels are strongly influenced by the microstructure and crystallographic orientation of grains or texture. Recently, it is being increasingly felt that grain boundary character distribution also plays an important role. It would be very interesting to understand the relationship between the above parameters and their influence in controlling material properties. These days interstitial free (IF) steels are in great demand for various purposes mainly in the automobile sector. Newer applications of IF steels, specially in the packaging industry, demand production of IF steels in much thinner gauges which may require levels of cold rolling higher than what is normally practised. However, industrial application of severe cold rolling (SCR) has been found to be very rare. Naturally, very little is known about the changes in microstructure, texture and grain boundary character distribution after very heavy cold rolling. Hence a systematic study has been carried out on the evolution of microstructure, texture and grain boundary character distribution during deformation and subsequent recrystallization in an industrially produced boron added interstitial free (IFB) steel which was severe cold rolled up to 98%. The steel sam-

ples were soaked at 1250°C and then hot rolled in the austenite region. These were further cold rolled up to 98% reduction in a laboratory rolling mill. Scanning and transmission electron microscopy were used to find out the microstructure of the cold rolled and annealed steels. EBSD was used to determine the texture and grain boundary character of the various samples. The cold rolled microstructure shows frequent formation of submicron to nanocrystalline grains. The intensity of the γ fibre has also been found to increase after annealing of the severely cold rolled steel. The deformation induced high angle grain boundaries appear to decrease gradually at the early stages of annealing and then again increases with the progress of recrystallization. It appears that texture, microstructure and grain boundary character of the steel are closely related.

11:00 AM

(ICOTOM-S3-007-2008) Effects of Composition and Coiling Temperature on Texture Formation in a Few Interstitial Free High Strength Steels

P. Ghosh, R. K. Ray*, TATA Steel, India

Interstitial free high strength (IFHS) steels are widely used in the automobile sector for their excellent deep drawability coupled with adequate strength. However, very often deterioration of drawability has been reported in these steels, as compared to the normal interstitial free (IF) steels. A few batch annealed IFHS steels with varying chemical composition and coiled at different temperatures have been chosen for the present study with a view to determining the effects of composition and coiling temperature on precipitation and texture formation after cold rolling and annealing. It has been observed that the final texture developed after batch annealing depends on precipitation which in turn can be related to the composition and processing history of the steels. In these steels P and Mn were added as solid solution strengthening elements, whereas Ti and Nb additions were made to scavenge the C and N in solid solution. It appears that P is taken out of the solution due to the formation of FeTiP, thus leaving behind insufficient Ti to form TiC. As a result C remains in solid solution thereby degrading the beneficial {111} texture formation during recrystallization annealing. However, when the same steel is coiled at a higher coiling temperature, precipitation of carbosulphides takes place during the coiling itself which in turn take the C out of solid solution leading to an enhancement of the favorable {111} texture formation during recrystallization anneal. Presence of FeTiP and absence of carbide type of precipitates have been identified as the key reasons for the deterioration of deep drawability in these steels when coiled at lower temperatures.

11:15 AM

(ICOTOM-S3-008-2008) Texture Development in Warm Rolled High Strength IF Steels Containing Cu, P and B

A. Haldar*, C. Ghosh, Tata Steel Ltd, India

Warm rolling or ferritic rolling of low carbon steels and interstitial free steels is gaining importance due to its potential to broaden the product range and reduce the production cost. The present paper discusses the evolution of microstructures and textures in Cu, B and P containing IF steels after multipass warm rolling with two finish rolling temperatures (FRT) and varying amount of deformation in ferritic region. The effect of warm rolling on Cu precipitation during ageing was also studied. It has been found that like cold rolling, warm rolling does not affect the kinetics of the Cu precipitation to that extent because of the occurrence of Cu precipitation during rolling and cooling. The activation energy for the Cu-precipitation in warm rolled condition was determined using DSC. Very strong gamma and alpha textures were developed after warm rolling in both the steels. In order to further strengthen the gamma texture and also to extract the maximum benefit of precipitation, both the steels were given special heat treatment. TEM study was carried out in order to characterize the microstructures and Cu precipitation.

11:30 AM**(ICOTOM-S3-009-2008) Relative Preference for Strain Localizations in Ultra Low Carbon Steel**

R. Khatirkar*, Visvesvaraya National Institute of Technology, India; L. Kestens, Delft University of Technology, Netherlands; R. Petrov, Ghent University, Belgium; I. Samajdar, Indian Institute of Technology Bombay, India

The deep drawability of low carbon steel is strongly enhanced by a strong γ -fiber (ND // $\langle 111 \rangle$) recrystallization texture. The preferred formation of the γ recrystallized grains, on the other hand, depends on the apparent preference for strain localizations in γ oriented deformed grains or bands. The present study involves plane strain deformation of ultra low carbon steel at different strain, strain rate and temperature. The deformation was followed by extensive EBSD (electron backscattered diffraction) measurements to bring out the relative preference of strain localizations and crystallographic orientations – a preference strongly affected by the deformation conditions. The occurrence of strain localizations could be explained in terms of textural softening. Textural softening, however, was strongly affected by the dislocation softening or relative recovery, as estimated from X-ray peak broadening. In a word, a combination of strain and relative recovery was critical in establishing the appropriate conditions for strain localizations.

Interface Textures**Interface Textures II**

Room: Rangos 1

Session Chairs: Peter Voorhees, Northwestern University; David Rowenhorst, U.S. Naval Research Lab

8:30 AM**(ICOTOM-S7-013-2008) Investigations of Interface Textures Using Advanced 3D Reconstructions (Invited)**

D. Rowenhorst*, A. Lewis, G. Spanos, U.S. Naval Research Lab, USA

In recent years there has been a significant improvement in the techniques used to collect 3D morphological and crystallographic information, including serial sectioning and x-ray tomography, which allows for detailed exploration of the properties of the interfaces within materials. We will discuss how the 3D imaging techniques can be leveraged to correlate the 3D shape of the interface with crystallographic information, specifically through the use of Crystallographic Interface Normal Distributions (CINDs). Two examples will be presented. The first will use the CIND construction to determine the full 3D crystallographic interface character of individual martensitic crystals in HSLA-100 steel, and their relation to the prior austenite orientation. The second example will look at the aggregate texture of the grain boundary interfaces within Ti-21S, a β -stabilized titanium alloy, using a 3D reconstruction of over 4000 grains. We will also briefly discuss relations between the grain boundary curvature and the crystallographic orientation of the interface.

9:00 AM**(ICOTOM-S7-014-2008) Microtexture of the PED Nano-twin Copper Films**

D. R. Waryoba*, FAMU-FSU College of Engineering, USA; B. Cui, National High Magnetic Field laboratory, USA; P. N. Kalu, FAMU-FSU College of Engineering, USA

Electron backscatter diffraction (EBSD) technique in the Zeiss XB1540 field emission gun scanning electron microscope (FEGSEM) has been used to characterize the microtexture development in the nano-twin copper films sensitized by the pulsed electrodeposition (PED) technique. The PDE was carried out using cold-rolled 304 stainless steel (304SS) and MP35N alloy as substrates in an electrolyte

of CuSO₄ solution with cathodic square wave pulses generated by turning on and off the current periodically. The microstructures of the deposited Cu films were characterized by columnar grains. These grains were subdivided further into a twin/matrix lamellar structure by a high density of twin boundaries (TBs). Closer to the interface, the microstructure was finer than other areas. A slight increase in grain size was found with increasing depth along the deposition growth direction. A detailed characterization of the microtexture variation across the interface is presented in this paper.

9:15 AM**(ICOTOM-S7-015-2008) Interface Texture in Cemented Tungsten Carbides and its Role in Microstructural Evolution during Sintering**

V. Kumar*, Z. Z. Fang, University of Utah, USA; S. I. Wright, M. M. Nowell, EDAX Inc., USA

An anisotropic nature of tungsten carbide exhibits faceted grains terminated by low energy planes and preferred grain boundaries in microstructure. In this study, a comprehensive microstructural analysis is performed to understand grain growth mechanisms by employing electron backscattered diffraction (EBSD) technique. A higher frequency of boundaries with 90° disorientation about [1 0 -1 0] and 30° disorientation about [0 0 0 1] is observed. These boundaries are supposed to be low energy boundaries due to their low coincidence site lattice (CSL) value. The evolution of these boundaries is studied during sintering in temperature range of 800°C (solid state sintering) to 1400°C (liquid state sintering). A decline in population of these boundaries during sintering is observed. A quantitative analysis of faceting is performed and correlated with grain coarsening and sintering temperature. The origin and role of preferred boundaries in sintering is also discussed.

9:30 AM**(ICOTOM-S7-016-2008) Thin Films on Single Crystal Substrates as Model Systems for the Study of Interphase Boundaries**

C. Detavernier*, K. De Keyser, Ghent University, Belgium; S. Gaudet, École Polytechnique de Montréal, Canada; J. Jordan-Sweet, C. Lavoie, IBM T. J. Watson Research Center, USA

The study of interphase boundaries in bulk materials presents a significant experimental challenge, since eight degrees of freedom need to be measured. In this contribution, we argue that thin films on single crystal substrates are interesting model systems, since one can characterize the crystallographic structure of the interphase boundary by only measuring the orientation of the grains in the film. Indeed, since the orientation of the single crystal substrate is fixed, and since the boundary plane is usually parallel to the original surface of the substrate, three degrees of freedom remain. We have used synchrotron XRD pole figure measurements and EBSD to characterize the texture of silicide and germanide films (e.g. NiSi, CoSi₂, CrSi₂, α -FeSi₂, PdGe, NiGe, Co₅Ge₇, CoGe₂), which were formed by a solid-state reaction between a metal film and Si or Ge, and consisted of a single layer of grains on top of a single crystal substrate. Many similarities could be observed in the types of texture present in these films, and thus in the nature of these interphase boundaries. For several materials, axiotaxy was observed. This is a recently discovered type of texture, characterized by a preferred alignment of lattice planes with similar d-spacing in film and substrate, resulting in periodicity along a single direction within the plane of the interface (1D periodicity). In some cases, epitaxial alignment (2D periodicity) was observed. Often, clear relationships could be determined between axiotaxial and epitaxial texture components. Our results suggest that interfacial periodicity is a major mechanism for texture selection in these materials. Periodicity within the boundary plane is highly advantageous, since it allows for an optimized bonding across the boundary by means of interfacial reconstruction, and hence for a low interfacial energy. According to our data, even periodicity along a single direction within the boundary plane (i.e. axiotaxy, or edge-

Abstracts

to-edge matching) is already sufficient to induce a preferred orientation relationship between film and substrate. Secondly, one also needs to consider the stability of periodicity with respect to interfacial roughness.

9:45 AM

(ICOTOM-S7-017-2008) Grain Boundary Character Evolution in Different Grain Growth Models

S. Wilson*, F. Uyar, J. Gruber, A. D. Rollett, Carnegie Mellon University, USA

The evolution of grain boundary character distributions (GBCDs) as a consequence of anisotropic grain boundary energy was determined using two different computational models. The two models used were a gradient-weighted moving finite element model and a phase field model. Identical inclination-dependent anisotropy functions were utilized in both models to search for model-dependence in the results and also to make detailed comparisons between the two models.

10:30 AM

(ICOTOM-S7-018-2008) Simulation of Anisotropic Grain Growth in Three Dimensions (Invited)

M. Gururajan, I. McKenna, P. Voorhees*, Northwestern University, USA

Recent advances in computational and experimental techniques allows for the routine visualization of the three-dimensional grain structure of materials. This opens new routes to explore the relationship between materials processing, structure, and properties. Using experimentally measured three-dimensional grain structures we have followed the evolution of grains using a phase field model that accounts for all five degrees of freedom that determine the grain boundary energy. We show that a multiorder parameter model can be used to explore the topological changes of individual grains during grain growth. This model employs quaternions to account for the dependence of the grain boundary energy on the misorientation and a tensor gradient energy coefficient to account for the change in grain boundary energy with boundary normal. We will also discuss a single order parameter phase field model for grain growth that leads to evolution equations that are free from singularities but still yields stable grain boundaries. Results of the simulations and the development of the models will be discussed.

11:00 AM

(ICOTOM-S7-019-2008) Microstructural Modification in a 15Cr-15Ni-2.2 Mo-Ti modified Austenitic Stainless Steel through Twin induced Grain Boundary Engineering

S. Mandal, S. Palle, Indira Gandhi Centre for Atomic Research, India; S. S. Vadlamani*, Indian Institute of Technology Madras, India

Grain boundary engineering (GBE) is based on the idea of grain boundary texture manipulation for enhancing material's performance. The main focus of GBE is to increase the fraction of low Σ coincidence sites lattice (CSL) boundaries as well as to disrupt the random grain boundary connectivity. In this study, we attempted to modify the grain boundary character in a 15Cr-15Ni-2.2Mo-Ti modified austenitic stainless steel (alloy D9) through thermo-mechanical treatment. The experimental methodology adopted in this investigation is based on the strain annealing approach, in which small amounts of strain (upto 15%) is imparted and subsequently annealed at various temperatures (1173-1323 K) for different time periods (0.5-2 h). Orientation Imaging Microscopy was used to determine the statistics of grain boundary character distribution. It has been observed that annealing without prior deformation results only in a marginal increase in the proportion of twins ($\Sigma 3$ and its variants). This increase in $\Sigma 3$ fraction was attributed to the formation of annealing twins during grain growth. However, a small amount of deformation prior to annealing has been found to be quite effective in increasing the fraction of CSL boundaries, especially twins and its variants. The maximum populations of CSL (~80%) have been obtained in the sample annealed at 1273 K for 1 hour with 15% pre-strain. In this condition, the fractions of $\Sigma 3, \Sigma 9$

and $\Sigma 27$ boundaries increased substantially in comparison to the as-received sample. Also, the well connected network of random grain boundaries present in the as received specimen was totally disrupted. The above results are discussed with reference to strain induced grain boundary migration (SIGBM) following straining and annealing.

11:15 AM

(ICOTOM-S7-020-2008) Use of Orientation Gradients for the Identification of Different Microconstituents in Multiphase Steels

P. Romano*, S. Zaefferer, D. Raabe, Max Planck Institute for Iron Research, Germany; F. Friedel, ThyssenKrupp AG, Germany

Multiphase steels are widely used, such as TRIP steels which are very important to the automotive industry. The microstructure of such steels is very complex, including ferrite, metastable austenite, bainite and in some cases, martensite. The correct identification and separation of all the different constituents is very important to predict and improve the mechanical properties of those materials. Ferrite and austenite with different crystal structure can be easily distinguished by the electron backscatter diffraction (EBSD) technique. However, bainite and martensite have the same crystallographic structure as ferrite and may be therefore more difficult to distinguish. Martensite can be identified due to its poor diffraction pattern quality but bainite requires a more careful analysis. During the bainitic transformation that is necessary to stabilize the metastable austenite, geometrically necessary dislocations (GND) are created in the bainitic area whereas the ferritic regions remain dislocation free. In order to find those areas with higher GND content (and hence, identify regions that are bainite) very detailed EBSD scans with a small step size have been carried out on electrochemically polished samples. Two different approaches were taken, grain reference orientation deviation (GROD) maps and kernel average misorientation (KAM) maps. Only the latter gave a reliable volume fraction of the different phases and situated them at the right position in the microstructure maps, when interpreted on the basis of known transformation mechanisms. This methodology is used on differently treated TRIP steels. The results are correlated with the mechanical properties of these materials.

11:30 AM

(ICOTOM-S7-022-2008) Nucleation of Primary Al phase on TiAl₃ during Solidification in Zn-11%Al-3%Mg-0.2%Si Coated Steel Sheet

K. Honda, K. Ushioda*, W. Yamada, Nippon Steel Corp., Japan

The newly developed Zn-11mass%Al-3 mass%Mg-0.2mass%Si coated steel sheet has excellent anti-corrosion properties. The refinement of solidification structure in alloy-coating layer is of great importance from the perspective of surface appearance. A small amount of Ti addition as much as 100massppm has the outstanding effect on the refinement of solidification structure. The mechanism on the Ti addition was investigated by means of EBSD. In the every center of the primary Al phase in alloy-coating layer, TiAl₃ was observed by scanning electron microscope, which suggests that TiAl₃ acts as the heterogeneous nucleation sites of the primary Al phase. The primary Al phase was revealed to have the perfect lattice coherency with the nucleus TiAl₃ phase. The crystal orientation relationships between TiAl₃ and primary Al are are $\{001\}\text{TiAl}_3//\{001\}\text{Al}$ and $\langle 100 \rangle \text{TiAl}_3//\langle 001 \rangle \text{Al}$, $\{100\}\text{TiAl}_3//\{001\}\text{Al}$ and $\langle 001 \rangle \text{TiAl}_3//\langle 001 \rangle \text{Al}$, $\{102\}\text{TiAl}_3//\{110\}\text{Al}$ and $\langle 201 \rangle \text{TiAl}_3//\langle 110 \rangle \text{Al}$, and $\{110\}\text{TiAl}_3//\{110\}\text{Al}$ and $\langle 110 \rangle \text{TiAl}_3//\langle 110 \rangle \text{Al}$, indicating that the primary Al phase grows in a manner of epitaxial growth from the nucleus TiAl₃ phase. The planar disregistry δ between the two phases was calculated to be less than 5% owing to this excellent lattice coherency. Furthermore, the dendrite of the primary Al phase was confirmed to grow in the direction of $\langle 110 \rangle$, not $\langle 100 \rangle$. The high content of Zn more than 60mass% in the primary Al phase was considered for this reason, because the increase of the Zn content in

Al-Zn alloy changes the growth direction of the primary Al from $\langle 100 \rangle$ to $\langle 110 \rangle$ through the change in the interfacial energy between the primary Al and the liquid. Consequently the TiAl₃ phase was considered to decrease the degree of undercooling necessary for the nucleation of the primary Al phase.

11:45 AM

(ICOTOM-S7-023-2008) Texture Development and Grain Growth during Annealing in Electrodeposited Ni/Fe-Ni Bimetals

J. Seo, J. Kang, J. Kim, Y. Park*, Sunchon National University, South Korea

Bimetal sheets consisting of Ni and Fe-Ni alloy were fabricated by using an electrodeposition method. The grains of electrodeposited Ni were columnar, while those of electrodeposited Fe-Ni alloy were nanocrystalline. These different parts of the bimetal underwent different evolution of textures and microstructures during annealing. In nanocrystalline part, i.e. Fe-Ni alloy, the as-deposited textures were of fibre-type characterized by strong $\langle 100 \rangle$ //ND and weak $\langle 111 \rangle$ //ND components, and the occurrence of grain growth resulted in the strong development of the $\langle 111 \rangle$ //ND fibre texture with the minor $\langle 100 \rangle$ //ND components. It was clarified using orientation imaging microscopy that abnormal growth of the $\langle 111 \rangle$ //ND grains in the early stages of grain growth plays an important role on the texture evolution. On the other hand, in columnar-structured Ni part, $\langle 112 \rangle$ //ND fibre texture strongly developed, and the textures and microstructures did not change after annealing up to 600°C. Second abnormal grain growth occurred at higher temperatures in Fe-Ni alloy part, and the growing grains were observed to cross over the interfaces between Ni and Fe-Ni alloy. These grain growth behaviors will be discussed in terms of their possible effects on the texture evolution of the bimetals.

12:00 PM

(ICOTOM-S7-024-2008) 3D-EBSD Study of Solid-state Nucleation in a Co-Fe Alloy

H. Landheer*, E. Offerman, Delft University of Technology, Netherlands; T. Takeuchi, M. Enomoto, Ibaraki University, Japan; Y. Adachi, National Institute for Materials Science, Japan; L. Kestens, Delft University of Technology, Netherlands

Nucleation has a strong influence on the overall kinetics of phase transformations and recrystallization processes that determine the final microstructure and thereby the mechanical properties of the material. During solid-state phase transformations heterogeneous nucleation takes place on grain corners, edges, and faces. Absolute predictions of the solid-state nucleation rates are very difficult, due to a limited understanding of the mechanism of solid-state nucleation. The interfacial energies involved in the nucleation process determine the chance that a potential nucleation site is activated. The energy of the interfaces depends among other factors on the difference in crystallographic orientation between neighboring grains. The relationship between the misorientation of the austenite crystallites and the favored sites for nucleation is investigated, as well as the orientation relationship between the austenite and ferrite crystallites. To determine the misorientation between the austenite crystallites in 3D, the microstructure of a Co-15Fe alloy was examined by SEM and EBSD through serial sectioning with a total of 50 sections and a depth of 18 µm. 7 sections were examined with EBSD to measure the crystallographic orientation of the individual grains. The alloy was solution-treated at 1273K for 30 minutes, subsequently cooled to 973K and was held at that temperature for 1 day. During this isothermal aging at 973K the bcc phase precipitated from the supersaturated fcc matrix. The preliminary results show ferrite formation on grain corners, edges and faces, involving both high and low angle grain boundaries and special boundaries like twins. It seems that many ferrite grains nucleated on grain faces have an orientation relationship with at least one of the austenite grains they originated from.

Hexagonal Metals

Texture-Property Relations

Room: Rangos 2

Session Chair: Matthew Barnett, Deakin University

8:30 AM

(ICOTOM-S9-036-2008) Characterization and Study of Texture Heterogeneities in Titanium Alloy IMI 834 in the Framework of Creep and Fatigue Investigations (Invited)

E. Uta*, UPVM, France; P. Bocher, ETS, Canada; N. Gey, M. Humbert, UPVM, France

Through ad-hoc processing, titanium IMI834 alloy is often designed to present bimodal microstructure, formed of equiaxed primary alpha grains and secondary alpha colonies, both of hcp structure. Such a microstructure is adapted for improved mechanical behaviours such as high fatigue and creep resistance for service temperatures up to 600°C. These properties make this alloy well suited for jet engine components. Nevertheless, after processing, the microstructure may present texture heterogeneities, (called macrozones) at the origin of a significant decrease of creep and fatigue performances leading to a strong reduction of secured service life of the product. In this contribution, we first present the results of our investigations in identification and characterisation of these heterogeneities, using the orientation maps (OIM) determined by Electron Back-Scattered Diffraction (EBSD) in a Scanning Electron Microscopy (SEM). In the second part, the results obtained on fracture surfaces of samples submitted to dwell fatigue are presented. Further, in the vicinity of the fracture initiation sites, local Schmid factor and Young modulus maps were calculated from the orientation maps. These data are used to analyse and discuss the links between the fatigue behaviour and the local microstructures.

9:00 AM

(ICOTOM-S9-037-2008) Strain Hardening Behaviour of an Initially Textured Ti6Al4V Titanium Alloy as a Function of Strain Rate and Compression Direction

F. Coghe*, L. Rabet, Royal Military Academy, Belgium; P. Van Houtte, KU Leuven, Belgium

This work shows the first results of a study aiming to determine the deformation mechanisms of a commercially available Ti6Al4V titanium alloy. More particularly, the work focuses on the strain hardening behaviour of the material during compression. The material originally came from a rod in the mill annealed condition. Microstructure consisted of an equiaxed hexagonal α -phase, with a majority of the c-axes of the α -phase parallel to each other aligned to one another and perpendicular to the longitudinal axis of the original rod, and a limited amount (4 wt%) of distributed body-centered cubic β -phase particles. Cylindrical samples were fabricated out of the rod along two directions. One set of cylindrical samples (LD) had its axis aligned to the axis of the rod, a second set (TD) had its axis aligned with the majority of the c-axes of the α -phase. Both sets of samples were tested under uniaxial compression for a wide range of strain rates (0.0005/s up to 1500/s) using a servo-hydraulic testing machine for the lower strain rates and a Split Hopkinson Pressure Bars setup for the higher strain rates. The LD-samples showed lower flow stresses than the TD-samples for the same amount of strain, as could be expected from the lower CRSS available slip systems. The LD-samples also could support much more strain before final fracture. Texture measurements (OIM) after testing showed for both sets of samples that the c-axes of the alpha phase were lined up with the compression axis. The strain hardening of the LD-samples showed a clear tendency to increase significantly during deformation. This was clearly illustrated in the concave-up true strain - true stress curves. This tendency was less clear for the TD-samples. Friction effects could be ruled out as being the source of this behaviour. In order to see which phenomenon is responsible for the increasing strain hardening (twinning, texture evolution, or a combination of both), TEM-work and plasticity modeling

Abstracts

are carried out. The onset of adiabatic shear localization for strain rates as low as 1/s will be briefly discussed.

9:30 AM

(ICOTOM-S9-039-2008) Texture Aspects of Delayed Hydride Cracking in Products from Zr-based Alloys

M. Isaenkova*, Y. Perlovich, Moscow Engineering Physics Institute, Russian Federation

Delayed hydride cracking (DHC) in products of Zr-alloys is a consequence of stress-oriented reprecipitation of hydrides under loading of the sample at the temperature of hydride formation, when primary hydrides dissolve and new hydride platelets form perpendicular to the tensile axes. DHC has a negative influence on operational properties of tubes from Zr-alloys for nuclear reactors. Though the study of DHC has already a many-years history, the relative importance of different factors, controlling this process, up to now was not established. In the given paper the problem of DHC is considered from the standpoint of texture analysis. It was shown that the texture controls the DHC development and proves to be the main factor, responsible for its anisotropy. The dependence of DHC from texture includes several aspects: existence of a definite texture in the product, different development of local plastic deformation at the tip of moving crack (slip or twinning, features of lattice rotation, size of the plastic deformation zone) depending on the orientation of tensile stress, reprecipitation of hydrides with definite preferential habit planes. New experimental data concerning DHC in Zr-2.5%Nb tubes were obtained by the X-ray diffractometric study of fracture surfaces, formed by testing of specimens after their charging with hydrogen. For the first time the reorientation of alpha-Zr grains by twinning in the plastic deformation zone near the surface of brittle fracture was revealed. Fractions of the hydride phase with different textures were observed by X-rays at the fracture surface of the sample experienced DHC. A new mechanism of DHC was proposed, including the twinning within the plastic deformation zone near the crack tip, formation of the distinct boundary between deformed and undeformed regions with the increased gradient of lattice distortion, the intensive diffusion of hydrogen to this boundary, the preferential precipitation of stress-oriented hydrides at its appropriately positioned sections, the growth of hydrides both inside and outside the plastic deformation zone till the next step of the crack between boundaries decorated by hydrides.

9:45 AM

(ICOTOM-S9-040-2008) Anisotropy, Twinning, and Texture Development in Rhenium

J. Bingert*, P. J. Maudlin, M. F. Lopez, Los Alamos National Laboratory, USA

Rhenium is a hexagonal close-packed, refractory transition metal that exhibits remarkable plastic anisotropy. The nature of this anisotropy was studied on rolled plate and hot isostatically pressed stock material. Microstructural analysis was performed on samples compressively deformed over a range of temperatures. Electron backscatter diffraction (EBSD) was used to track texture evolution and quantitatively identify and measure deformation twinning activity. The activation of the {11-21} tensile twin system as the dominant deformation twin mode was found to be a significant determinant in texture development, anisotropic response, and rhenium's extraordinary strain hardening behavior. The sensitivity of twinning at the grain level to initial orientation was observed and analyzed for both initial process conditions. Plastic yield surfaces were calculated and used to predict anisotropic behavior, while material instability was addressed through bifurcation theory incorporating plastic anisotropy.

10:30 AM

(ICOTOM-S9-041-2008) Electrochemical Behavior of {001}, {100} and {110} Ti Single Crystals under Simulated Body Fluid Condition

M. Azzi*, S. Faghihi, M. Tabrizian, J. Szpunar, McGill University, Canada

Titanium and its alloys have been widely used for biomedical applications due to their high corrosion resistance and biocompati-

bility. In this paper, the electrochemical behavior of single crystals Ti under simulated body fluid condition was investigated. {001}, {100} and {110} single crystals were used for this investigation. Electrochemical Impedance Spectroscopy (EIS) was used to characterize the electrochemical behavior of the interface between the substrate and the electrolyte. Potentiodynamic polarization tests were performed to compare the passive regions of the different Ti surfaces. The EIS spectra are presented in Bode plot and interpreted in terms of appropriate electrical circuits; it was shown that the resistance to charge transfer, R_{ct} , of the {001} single crystal was $5.37 \text{ M}\Omega\cdot\text{cm}^2$ compared to $3.28 \text{ M}\Omega\cdot\text{cm}^2$ and $3.46 \text{ M}\Omega\cdot\text{cm}^2$ for the {100} and {110} single crystals respectively. It should be mentioned that the resistance to charge transfer is inversely proportional to the corrosion rate. The Potentiodynamic polarization tests have also shown that the passive current was lower in the case of {001} plane compared to the other planes. These results have shown that the {001} basal plane which is the most densely packed plane had higher corrosion resistance compared to {100} and {110} planes which have lower planar atomic densities.

10:45 AM

(ICOTOM-S9-042-2008) Effect of Processing, Microstructure, and Texture on the Elevated-Temperature Creep Behavior of Ti-6Al-4V-XB Alloys

C. J. Boehlert*, W. Chen, Michigan State University, USA; M. Glavicic, UES, Inc., USA; S. Tamirisakandala, FMW Composite Systems, Inc., USA; D. Miracle, Air Force Research Laboratory, USA

This work investigated the effect of nominal boron additions of 0.1wt.% and 1wt.% on the elevated-temperature (400-455°C) tensile-creep deformation behavior of Ti-6Al-4V for applied stresses between 400-600MPa. The alloys were evaluated in the as-cast and cast-then-extruded conditions. Boron additions resulted in a dramatic refinement of the as-cast grain size and TiB whisker volume fractions of approximately 0.006 and 0.06 for the Ti-6Al-4V-0.1B(wt.%) and Ti-6Al-4V-1B(wt.%) alloys respectively. The creep resistance of the as-cast alloys significantly improved with increased boron concentration, where almost an order of magnitude decrease in the secondary creep rate was observed between the Ti-6Al-4V-1B(wt.%) and Ti-6Al-4V(wt.%) as-cast alloys. Grain refinement due to the boron addition did not deleteriously affect the creep resistance in the temperature and stress ranges considered, where dislocation creep was suggested to be the dominant secondary-creep mechanism. The enhanced creep resistance was attributed to load sharing by the TiB whiskers. For the same nominal boron contents, the cast-then-extruded alloys exhibited significantly greater creep resistance than the as-cast alloys. This was explained to be an effect of the alpha-phase texture, measured using both X-ray diffraction and electron backscattered diffraction, and the decreased lath spacing in the cast and extruded alloys compared with the as cast alloys. The cast-then-extruded alloys exhibited four times smaller lath widths than the as-cast alloys and the alpha-phase basal plane normal was preferentially oriented 0°, 60°, or 90° from the extrusion axis. The as-cast alloys exhibited a significantly weaker texture than the cast and extruded alloys. In the cast-then-extruded alloys, which were extruded in the beta-phase field, Ti-6Al-4V exhibited the greatest creep resistance. Thus the alpha-phase, which consisted of approximately 80% of the microstructure, texture appeared to be more dominant to the creep resistance than the small volume percent of TiB present in the microstructure.

11:30 AM

(ICOTOM-S9-045-2008) Role of Initial Texture in Low Temperature Plasticity of Mg-4.5%Al-1%Zn Alloy

V. Serebryany*, K. E. Mel'nikov, A.A. Baikov Institute of Metallurgy and Material Science, RAS, Russian Federation

It is known, magnesium alloys of system Mg-Al-Zn have deficient formability at temperatures below 200 degrees C. In the present re-

port one of the possible decisions of the problem of the plasticity increase in warm rolled Mg-4.5%Al-1%Zn alloy is considered at the expense of an initial texture change of a material. As an initial material for research the hot rolled plate of this alloy by thickness of 28 mm was chosen. In this plate as a result of the hot rolling the fine-grain equiaxed structure and the sharp basal texture were generated. For study of the initial texture influence on technological plasticity the plane samples cut out from a plate along hot rolling direction (the sample plane coincided with the plate one) (N 1) and along transverse direction (the sample plane was at right angle to plate one) (N 2) were subjected to the warm rolling on the laboratory rolling mill at temperature 180 degrees C. The warm rolling was finished at occurrence of the first cracks on lateral sample edge. In result the technological plasticity (the total deformations before occurrence of the first crack) was equal 37,1 % (for a sample N 1) and 66,2 % (for a sample N 2). Thus, the initial texture change had allowed almost twice to increase the technological plasticity at the warm rolling. For study of the possible reasons explaining such increase of plasticity mathematical simulation of the warm rolled texture using advanced thermal activation model in an approximation of a composite material was carried out. The rather good coincidence of the simulated and experimental results was achieved with account of the activation of (0001) <1120> basal slip and (1012) <1011> twinning in the central areas of grains and basal and (1122)<1123> pyramidal slip in the boundary areas of ones. On the basis of the received results it is possible to assume, that the plasticity increase of the given alloy is connected with the activation of the additional slip and twinning systems, as a result of the initial texture change before the warm rolling.

Texture in Materials Design

Texture in Materials Design II

Room: Connan

Session Chair: Surya Kalidindi, Drexel University

8:30 AM

(ICOTOM-S12-014-2008) Spectral Methods in the Statistical Description and Design of Microstructure (Invited)

D. Fullwood*, Brigham Young University, USA; S. Niezgodna, S. Kalidindi, Drexel University, USA; B. Adams, Brigham Young University, USA

Various tools are useful in the design of materials from texture and related higher order structure statistics. This paper presents recent results in two key areas – homogenization methods linking the material structure to its properties, and reconstruction techniques that produce material realizations from the statistics. Homogenization techniques that are based upon material statistics captured by correlation functions have been available for several decades. With recent increases in computational power, and with the added efficiencies of spectral methods, attention has returned to these methods as viable inputs to multiscale models. One such method that involves a more complex integration scheme than the typical Kroner-type approach, is the strong contrast formulation pioneered by Brown, and more recently developed by Torquato. In this paper we utilize spectral techniques to apply the strong contrast formulation to the computationally demanding case of polycrystalline materials, and discuss the potential benefits to material design. Another important capability in the statistical modeling, analysis and design of materials involves the reconstruction of statistical data in order to recover detailed realizations that can be used in deterministic models. Popular reconstruction techniques such as simulated annealing take large amounts of computational power and time to create relatively small realizations. Recent work, based upon image analysis methods, has resulted in dramatic increases in speed. These advances in reconstruction capabilities are presented and some of the issues inherent in the approach are discussed as they relate to material design.

9:00 AM

(ICOTOM-S12-015-2008) Two-point Orientation Coherence Functions: An Orthonormal Series Solution (Invited)

P. R. Morris*, retired, USA

An orthonormal series solution for the two-point orientation coherence function is proposed using functions orthonormal on the range $r = 0, 1$ with weight function corresponding to the distribution of r in a typical experimental procedure.

9:15 AM

(ICOTOM-S12-016-2008) Accessing the Texture Hull and Properties Closure by Rotation and Lamination

B. L. Adams*, B. Aydelotte, S. Ahmadi, C. Nylander, Brigham Young University, USA

New methodology for processing polycrystalline materials by rotation and lamination is presented. The processing is realized by ultrasonic consolidation that can achieve welded interfaces with negligible disturbance of the microstructure due to plastic deformation. Evidence of minimal plastic disturbance is presented for ultrasonic consolidations of Ni 201 and Cu 10100 polycrystals using orientation-imaging microscopy. The theory of rotation and lamination is presented in the Fourier space of orientation distributions (ODs). Rotations of polycrystals define the orbit of the OD, and convex combinations of the orbit describe the set of all ODs that can be achieved by lamination. These orbits and their convex combinations are described in the $l=4$ projection of the microstructure hull, and in the (yield strength versus inverse Young's modulus) properties closure. It is demonstrated that the span of the orbit for a Ni 201 material, which exhibits weak texture with some {100} cube component, is relatively small compared to that of the strongly {100} cube-oriented Cu 10100 material. The principal conclusion is that rotation and lamination is capable of accessing a substantial sub-set of the complete microstructure hull and properties closure when the initial polycrystal possesses a strong crystallographic texture. Strategies for determining the best rotations and laminations to achieve desired design properties are discussed.

9:30 AM

(ICOTOM-S12-017-2008) On the Correlation of Surface Texture and Strain Induced Surface Roughness in AA6xxx Aluminium Sheet

S. Kusters*, M. Seefeldt, P. Van Houtte, KULeuven, Belgium

The dependence of the strain induced surface roughness on the surface texture was investigated for cold-rolled and subsequently stretched AA6xxx aluminium sheet. To characterize the surface texture, EBSD scans (performed at the TUDelft by T. Bennett and L. Kestens) were analyzed and a statistical approach, based on two-dimensional correlation functions, was introduced to obtain quantitative information on the spatial arrangement of orientations and the possible clustering of similarly oriented grains. Clusters of grains exhibiting the Cube, the RD-rotated Cube or the Goss orientation are observed to align in the RD. Various qualitative micromechanical models were implemented and validated with experimental data to acquire knowledge on which texture components can cause surface roughness under which loading conditions. The developed micromechanical models all differ in the way the boundary conditions are implemented, to be able to investigate the influence of the mechanical constraints on the predicted surface roughness. Fourier analysis was applied to discriminate between low and high frequency surface roughness components and statistical methods were developed to correlate texture and predicted surface roughness profiles. This work is performed in the frame of the NIMR, Netherlands Institute for Metals Research.

Abstracts

9:45 AM

(ICOTOM-S12-018-2008) Microstructure-based Models to Predict the Formation of the Brass-type Texture

T. Leffers*, RISØ National Laboratory, Technical University of Denmark, Denmark; R. Lebensohn, Los Alamos National Laboratory, USA

Deformation twinning is always observed in materials which have developed a brass-type texture (with one exception not to be discussed here, viz. Cu-Ni). It is therefore an obvious assumption that deformation twinning is essential for the development of the brass-type texture. While it was early suggested that the brass-type texture is related with a volumetric effect due to twin reorientation, TEM investigations with the proper imaging conditions show that the volume fraction of twinned material is insufficient to explain the brass-type texture. Alternatively, looking at the microstructural effect of the closely spaced thin twins, it was shown that, inside the heavily twinned grains in brass rolled to about 40% reduction, slip was largely restricted to the slip plane parallel to the twin lamellae. It is generally accepted that the (minor) texture components with $\{111\}$ parallel to the rolling plane observed as part of the brass-type texture at reductions above 60% are extreme consequences of such overshooting. Sachs-type models, emphasizing primary slip relative to multiple slip, may be seen to represent the overshooting caused by the twin lamellae. And, as a matter of fact, various Sachs-type models do quite successfully simulate the brass-type texture at moderate reductions. These are multislip models but with fewer slip systems than the Taylor model. However, the above models do not consider the difference between grains with and without twins, of which only the former are known to be subject to overshooting. Recently, within the context of a second-order self-consistent calculation (Lebensohn et al., Phil. Mag. 87, 4287, 2007), the orientations most likely to twin were identified and assigned with a strong latent hardening. The resulting texture (up to 86% reduction) now has strong components with $\{111\}$ close to be parallel to the rolling plane – stronger than the experimental brass-type texture. In light of the above results, in this work we will discuss the necessity of more elaborate schemes for latent hardening and of considering grain-to-grain interactions via full-field solutions, in order to improve the simulation of the brass-type texture.

10:30 AM

(ICOTOM-S12-019-2008) Representation of Textures Using Quaternion Distributions

J. Mason*, C. A. Schuh, Massachusetts Institute of Technology, USA

Despite the rapidly increasing availability of orientation statistics, as well as models to relate texture information to material properties, there exists no completely satisfactory parameterization of orientation statistics within the literature. An ideal parameterization would allow for an intuitive interpretation, the manipulation of discrete orientations via a simple multiplication rule, presentation of orientation statistics in a non-singular and visualizable group space, and the ability to explicitly express an arbitrary orientation distribution as a series expansion. The quaternion parameterization is known to display most of these characteristics, but has one major drawback that has precluded its use in the texture community: a series expansion to represent textures as quaternion distributions has been lacking. Here we develop this expansion for the first time through use of the hyperspherical harmonics. We also present a refinement of this approach by developing symmetrized hyperspherical harmonics that allow an expansion conforming to the sample and crystal symmetries. The result is a more intuitive and powerful method of displaying texture information that the Euler angle presentation common in the literature today.

10:45 AM

(ICOTOM-S12-020-2008) Deformation Textures and Mechanical Properties of FCC and HCP Metals Predicted by Crystal Plasticity Codes

C. S. Hartley*, El Arroyo Enterprises LLC, USA; P. R. Dawson, D. Boyce, Cornell University, USA; S. R. Kalidindi, M. Knezevic, Drexel University, USA; C. Tomé, R. Lebensohn, Los Alamos National Laboratory, USA; L. Semiatin, T. J. Turner, Air Force Research Laboratory, USA; A. A. Salem, Universal Energy Systems, USA

Three crystal plasticity codes, the Material Point Simulator (MPS) developed at Cornell, the crystal plasticity codes developed at Drexel University and the ViscoPlastic Self-Consistent code (VPSC7b) developed at LANL, were compared by simulating the isochoric, free upsetting of a face-centered cubic (FCC) alloy, Type 304 Stainless Steel, and a hexagonal close-packed (HCP) material, unalloyed Ti. Deformation of an initially random sample of 5000 grains was carried out in compression at a constant true strain rate of 0.001 s^{-1} using strain increments of 0.02 to a true strain of 1.0. In all cases hardening on active slip planes was modeled by a Voce-type equation, and calculations were performed for non-hardening and linear hardening conditions. Deformation conditions appropriate to elevated temperature deformation were modeled by selecting a strain-rate sensitivity of 0.25 on all active slip systems. The Taylor linking hypothesis was employed for all codes, giving an upper bound calculation for the results. In addition, the MPS code was employed to calculate a lower bound for the same deformation conditions and the Affine mode of the VPSC7b code was employed to model grain interactions. Results of the calculations are expressed as von Mises effective stress-effective strain curves, normalized to the critical resolved shear stress (CRSS) on the slip plane, in the case of the FCC material. In the case of the HCP material, slip on basal $\langle a \rangle$, prismatic $\langle a \rangle$ and pyramidal $\langle c+a \rangle$ systems was permitted, with the ratio of the CRSS on the three systems equal to 1.0, 0.7 and 3.0, respectively. For these calculations the effective stress-strain curve was normalized to the CRSS on the basal $\langle a \rangle$ system. Pole figures of two or three principal crystallographic directions at the end of the deformation process are presented for all simulations. The effective Taylor Factor is also calculated as a function of strain using two different methods. The results demonstrate the equivalence of calculations performed with all codes using the Taylor hypothesis and the sensitivity of the calculations to the choice of linking hypothesis in other cases.

11:00 AM

(ICOTOM-S12-021-2008) Variance of the Orientation Distribution Function and the Yield Surface

S. Ahmadi*, B. L. Adams, B. S. Fromm, Brigham Young University, USA

Theoretical relationships for the variance of the orientation distribution function (ODF) and the yield surface are presented. Variance of interest here is due to the 'window size' of a representative statistical element, randomly taken from the material. It is illustrated that these require knowledge of the pair correlations of lattice orientation. These principles are illustrated by analysis of the ODF and the yield surface predicted for an alpha-titanium sputtering target. Pair correlations were recovered by orientation imaging microscopy on 13 oblique section planes. A Taylor viscoplastic theory was used to predict the yield surface, and its variance. Results obtained for the variance of the ODF are presented as an intensity profiles in the space of Euler angles. Results obtained for the variance of the yield surface are presented as a set of 2- and 3-dimensional yield surfaces in deviatoric stress space. Variance is predicted to reach a maximum when the window size shrinks to zero; it tends to zero when the window size exceeds the coherence limit. The implication of these results on the accuracy and reliability of texture-based properties predictions is discussed.

11:15 AM

(ICOTOM-S12-022-2008) Prediction of the Evolution of Polycrystalline Yield Surfaces in Deformed Metals Using a New Non-linear Intermediate Viscoplastic Model

S. Mguil*, S. Ahzi, F. Barlat, University Louis Pasteur – IMFS, France

In this paper, we propose a numerical computation of polycrystalline yield surfaces using a new non-linear intermediate model. First, we present this non-linear intermediate approach in the case of rigid viscoplasticity. It is formulated by the minimization of an error function, combining the local fields (strain rate and stress) deviations from the macroscopic ones in order to derive an intermediate interaction laws. The error function depends on a single weight parameter which can be selected between zero, which leads to a Taylor model, and unity, which leads to a Sachs model. Thus, the proposed interaction law allows spanning from the upper bound Taylor model to the lower bound Sachs model. Using this new intermediate approach, we compute the polycrystalline yield surface and its evolution for different loading cases such as plane strain compression and uniaxial loading. We analyze the change in the yield locus shape for different value of the weight parameter of the intermediate model. We consider both FCC and BCC metals and we discuss the results for each as they compare to the classical viscoplastic Taylor or Sachs models as well as to the experimental results in the literature. The effects of other parameters, such hardening, will also be addressed.

11:30 AM

(ICOTOM-S12-023-2008) Comparison of Twinning Modeling Approaches with Application to TWIP Steels

A. Prakash*, T. Hochrainer, H. Riedel, Fraunhofer Institute for Mechanics of Materials, Germany

Over the past couple of decades, there has been an enormous interest in the new age austenitic steels, also known as TRIP (transformation induced plasticity) and TWIP (twinning induced plasticity) steels. In particular, TWIP steels find a major interest in the automobile industry due to the excellent properties that they possess: high work hardening rate, high ductility and a high tensile strength along with a high wear and corrosion resistance. The high work hardening rate is attributed to the dynamic microstructure refinement resulting from the emergence of twins, which act as obstacles to the movement of dislocations. Not much study has been done towards understanding the influence of twinning towards texture and anisotropy development in TWIP steels. In order to predict the evolution of texture and the developing anisotropy accurately, texture models must account for the enhanced twinning activity. In this work, we compare two approaches towards modeling twinning, under the self-consistent framework. The central challenge in incorporating twinning in texture models is the exponential increase in new orientations, caused by the fact that the twinned region in a grain has a markedly different orientation with respect to the untwined part of the grain. To overcome this, two main modeling approaches have been proposed. Type (a) models do not increase the number of grains defining the polycrystal. Instead, a selection of grains is completely reoriented if a certain criterion is met. Thus, the number of grains under consideration remains constant. Type (b) models divide the grain into twin and non-twin parts, thereby increasing (virtually) the number of grains in the simulation. This increase in number can however, be limited through a few assumptions. Under the framework of the VPSC model, we evaluate these two modeling approaches. The results are compared with experimental data. The type (b) model provides better results with smaller number of grains (<1000 grains) and the results of both models seem to converge with increasing number of grains.

11:45 AM

(ICOTOM-S12-024-2008) Modeling Rolling Texture of Twinned Copper Single Crystals

K. J. Al-Fadhalah*, Kuwait University, Kuwait; A. J. Beaudoin, University of Illinois at Urbana-Champaign, USA; M. Niewczas, McMaster University, Canada

A polycrystal plasticity model is proposed to predict the rolling texture of twinned Cu single crystals. Prior to rolling, copper single crystals were deformed in tension at liquid helium temperature, with the tensile axis along [541], to induce twinning deformation. This resulted in ultra-fine structure of twin-matrix lamella. Two Cu samples were rolled to 70% reduction in thickness. The first sample is *as deformed* that has a texture of strong twin component, and the other sample is *recrystallized* at 400 K that gives two balanced texture components, nucleated originally from the twin and matrix components. X-ray texture measurements indicate that the rolling texture of the deformed sample preserves to a large degree the initial texture, suggesting a strong tendency for codeformation between the twin and matrix phases. For the recrystallized sample, the rolling texture partially preserves the initial texture, implying a weaker correlation between the coarse recrystallized layers. To include the effect of lamellar structure of twinned Cu samples on the rolling texture, the current model regards each lamella as a composite grain consisting of twin and matrix layers. The interaction at the lamella interface is accounted for by satisfying compatibility and equilibrium requirements across the interface. The aggregate response of composite grains is computed using a viscoplastic self-consistent (VPSC) scheme. In addition, codeformation is considered by imposing the average spin of the composite grain on both twin and matrix layers. This enables preserving the twin boundary orientation during rolling. With this continuum approximation, the simulated rolling textures show large similarities with the measured ones, keeping in mind no length scale has been considered in the model.

12:00 PM

(ICOTOM-S12-025-2008) Novel Spectral Approach for the Design of Deformation Processing Operations to Achieve Desired Textures in Polycrystalline FCC Metals

M. Knezevic*, D. Illson, Drexel University, USA; D. Fullwood, Brigham Young University, USA; S. R. Kalidindi, Drexel University, USA

In this paper, we present a novel spectral approach for formulating processing recipes that can potentially transform a given initial texture into one of the elements of a set of optimal textures (presumably identified to exhibit a desired combination of macroscale property/performance characteristics). The processing options considered here are currently restricted to deformation processing operations. This is accomplished by storing efficiently the results from the well established Taylor-type crystal plasticity framework in a spectral database for the complete range of deformation processing operations of interest. The algorithm explored in this study involves specifically selecting a limited number of available manufacturing options (from the complete set of feasible processing options) and delineating the subspace of the texture hull that can be realized by any combination of the selected processes. The spectral methods have proven to be computationally very efficient for such an approach. This novel spectral approach has been successfully applied to an aluminum alloy and a copper alloy, and these results will be presented and discussed in this paper.

12:15 PM

(ICOTOM-S12-026-2008) Micromechanical Modeling of Plastic Deformation and Texture Evolution in Semi-Crystalline Polymers: Self-Consistent vs. an Upper Bound Approach

O. Gueguen*, S. Ahzi, A. Makradi, IMFS, France; S. Belouettar, Research Center Henry Tudor, Luxembourg; S. Nikolov, Max-Planck Institut für Eisenforschung, Germany; R. A. Lebensohn, Los Alamos National Laboratory, USA

In this work we simulate the deformation behavior and texture evolution under large plastic deformation of polyethylene by using

Abstracts

micromechanically-based constitutive models. The morphology of this two phase material, consisting of crystalline lamellae and amorphous domains, is represented via a local stack of crystalline lamellae separated by interlamellar amorphous layers. The basic micromechanical modeling used is that developed in the work Ahzi et al. [1], Lee et al. [2] and Nikolov et al. [3]. In this, the interlamellar shearing (amorphous phase deformation) is assimilated to an additional slip system (Nikolov et al. [3]). Elasticity is neglected and both the viscoplastic self-consistent and a modified viscoplastic Taylor approach are considered. The results from both models, in terms of stress-strain behavior, texture evolution and phase contributions to deformation, are compared and discussed. The predicted texture evolution is compared to the experimental results for uniaxial tension, uniaxial compression and plane strain compression for high density polyethylene (HDPE). [1] S. Ahzi, D.M. Parks and A. Argon, "Modeling of Plastic Deformation and Evolution of Anisotropy in Semi-Crystalline Polymers", Computer Modeling and Simulation of Manufacturing Processes, Eds. B. Singh, Y. I. Im, I. Haque and C. Altan, ASME, MD-Vol. 20, pp. 287-292, 1990. [2] B.J. Lee, D.M. Parks, S. Ahzi. Micromechanical modelling of large plastic deformation and texture evolution in semi-crystalline polymers, 41 (1993) 1651. [3] S. Nikolov, R.A. Lebensohn, D. Raabe. Self-consistent modelling of large plastic deformation, texture and morphology evolution in semi-crystalline polymers, 54 (2006) 1350.

Thursday, June 5, 2008

Thin Films (Microelectronics, HTSC)

Thin Films

Room: Rangos 2

Session Chair: Jay Whitacre, Carnegie Mellon University

8:30 AM

(ICOTOM-S2-001-2008) Texture Development and Abnormal Grain Growth in Thin Films (Invited)

C. V. Thomspon*, MIT, USA; H. J. Frost, Dartmouth College, USA

Grains in polycrystalline films are rarely randomly oriented, even when deposited on amorphous substrates. Instead, the grains tend to have a fiber texture, in that specific crystallographic directions tend to be aligned normal to the plane of the film. Grain structures in polycrystalline films usually fall into two broad categories; non-equiaxed columnar structures, in which the average grain size normal to the plane of the film is much larger the average grain size in the plane of the film, and equiaxed columnar structures, in which the out-of-plane and in-plane average grain sizes are comparable. In both cases, most grain boundaries span the thickness of the film. Fiber texture does not generally develop during grain nucleation. In films with non-equiaxed structures, texture generally develops after nuclei have coalesced to form a continuous film and results from competitive growth processes that occur at the surface of the film during continued deposition. In films with equiaxed structures, texture usually results from grain boundary motion during as well as after growth and coalescence of nuclei. Post-deposition annealing of films with either type of structure can also lead to texture evolution, through abnormal grain growth. In this case, the grains that grow abnormally tend to have crystallographic orientations that minimize strain energy, the energy of the film-substrate interface, and/or the energy of the top surface of the film. However, it is notable that there are cases in which abnormal grain growth or recrystallization can not be explained in terms of minimization of these energies. Mechanisms of texture development in thin films will be reviewed, and examples of experimental systems that fit the understanding outlined above will be cited, along with examples that do not.

9:00 AM

(ICOTOM-S2-002-2008) Grain Growth and Texture Development in Lithium Fluoride Thin Films

A. King*, H. Kim, Purdue University, USA

A variety of different textures have been reported in polycrystalline lithium fluoride thin films. In this study, we observe the growth of grains with differing orientations and assess how they contribute to the texture development. In marked contrast with metal thin films, we find that a {111} texture develops by the preferred nucleation of {111}-oriented grains, but not by their growth. These grains do not coarsen significantly, and as other grains grow, the {111} component contributes to the formation of a bimodal grain size distribution in which they comprise the small-size peak. Continued nucleation increases the number of these grains, strengthening the texture, but their size is largely unaffected by annealing. We will discuss the mechanisms responsible for the preferred nucleation, and yet restricted growth of {111} grains in this material. This work is supported by National Science Foundation Grant # DMR - 0504813

9:15 AM

(ICOTOM-S2-003-2008) EBSD Analysis of the Texture Evolution of Rapidly Solidified Cu Thin Films

A. Kulovits*, R. Zong, J. P. Leonard, J. M. Wiezorek, University of Pittsburgh, USA

Excimer laser melting and lateral re-solidification is demonstrated in 200 nm thick Cu elemental metal thin films encapsulated between SiO₂ layers. Projection irradiation was used to selectively and completely melt lines 3 to 30 μm wide in the metal film. Rapid lateral solidification originated from unmelted sidewalls of the molten region. Three morphologically and in orientation different solidification zones have been identified, characterized and rationalized within the framework of rapid solidification theory. The orientation relationship between the solidified grains and the adjacent unmelted polycrystalline film, which acts as a seed for re-solidification, was investigated. TEM and SEM were used to characterize the resulting film morphology and typical solidification defect structures. EBSD measurements were used to characterize the solidification texture. Electron diffraction was used as a complementary tool to investigate grain misorientations on a local level.

9:30 AM

(ICOTOM-S2-004-2008) Microtexture Evolution in Free-standing CVD Diamond Films: Growth and Twinning Mechanisms

T. Liu*, D. Raabe, Max-Planck-Institut fuer Eisenforschung, Germany; W. Mao, University of Science and Technology, China; S. Zaefferer, Max-Planck-Institut fuer Eisenforschung, Germany

Three groups of free-standing diamond films deposited with variations in substrate temperature, methane concentration, and film thickness have been analyzed using a high-resolution electron backscattering diffraction (HR-EBSD) technique. The microstructures, microtextures, and grain boundary character distributions were characterized. The resulting textures consisted primarily of {001}, {110}, and {111} fiber textures. Furthermore, corresponding twinning and multi-twinning fiber textures were observed. The grain boundary distribution showed high angle grain boundaries (HAGB), primary twinning (PT) twin boundary, and secondary twinning (ST) twin boundary. Based on the characteristics of the diamond crystal lattice, a growth model and a twinning model have been proposed. The evolution of texture, microstructure, and grain boundaries as a function of the deposition parameters can be used for the optimization of chemical vapor deposition (CVD) diamond films.

10:30 AM

(ICOTOM-S2-005-2008) Microstructure Control in Formation of NiSi Thin Films (Invited)

K. Kozaczek*, NOVA Measuring Instruments, Inc., USA

NiSi is a material system commonly used for the gate and source-drain contacts of CMOS transistors. The current processing routes of

transforming Ni or Ni binary alloys and Si (single crystal or polycrystalline) into NiSi may result in formation of multiple phases and textures (axiotaxy and/or cyclic). Due to high degree of anisotropy of physical properties of a single crystal of NiSi, texture affects the quality and performance of the polycrystalline films. The presence of different phases of NiSi results in variation of electrical resistivity and mechanical properties of films. Tight control of NiSi phase and texture is important for producing films of consistent properties. X-ray diffraction is a metrology method providing the information about the phase and texture in time frames and with spatial resolution compatible with semiconductor industry requirements. This paper discusses the principles of automated texture and phase measurements of multiple phase systems. The implementation of a large area detector allows one to map significant sections of the reciprocal space. A novel analysis reduces the experimental data to texture, phase and grain size metrics usable for process development and monitoring. The effects of NiSi processing steps (doping, pre-amorphization implant, clean, form/anneal), Ni alloying and thickness on the final microstructure of NiSi in gate and source-drain applications are discussed.

11:00 AM

(ICOTOM-S2-006-2008) Texture of Thin NiSi Films and its Effect on Agglomeration

K. De Keyser*, C. Detavernier, R. Van Meirhaeghe, Ghent University, Belgium; J. Jordan-Sweet, C. Lavoie, IBM T. J. Watson Research Center, USA

Nickel silicide films are used as contacting materials in the micro electronics industry. It was recently [1] discovered that these films exhibit a peculiar type of texture, called 'axiotaxy', whereby certain lattice planes in the NiSi grains are preferentially aligned to (110)-type lattice planes in the single crystal Si substrate. In this contribution, we present a quantitative study of this phenomenon, using both XRD pole figure measurements and EBSD. Furthermore, we report a correlation between the texture of NiSi films and their morphological stability during annealing at high temperature. In spite of the small grain size in these films, EBSD could be used to determine the volume fractions of the various texture components. This provided quantitative support for the claim that axiotaxy is the main texture component in these films. A discussion of the techniques used during measurement and analysis of the EBSD data is presented, as this must be given special consideration in view of the peculiar type of texture encountered in these films. Secondly, EBSD was performed after annealing the NiSi films at various temperatures and durations. It is known that thin NiSi films have a strong tendency to agglomerate [2]. Our data indicates a correlation between the texture evolution and the agglomeration of the NiSi layer. Grains with axiotaxial orientation were observed to grow and thicken during the annealing process, by consuming neighboring randomly oriented grains. This suggests that the texture of the NiSi layer is a determining factor for the morphological stability of the film and can be related to the one dimensional periodicity at the interface, which lowers the interface energy and thus provides a driving force for the preferred growth of these grains. The agglomeration of NiSi films results in a significant increase of the sheet resistance, illustrating the importance of texture control for application of these films as contacts to micro-electronic devices. [1] Detavernier, C., A. S. Ozcan, et al. (2003). *Nature* 426(6967): 641-645. [2] Deduytsche, D., C. Detavernier, et al. (2005). *Journal of Applied Physics* 98(3).

11:15 AM

(ICOTOM-S2-007-2008) Control of Texture in Polycrystalline Thin Films used as Data Storage Media (Invited)

D. E. Laughlin*, H. Yuan, E. Yang, C. Wang, Carnegie Mellon University, USA

In current data storage systems the information is stored in polycrystalline thin film media which have a preferred crystallographic texture. The preferred texture is such that the easy axis of magnetization (or ferroelectricity) is either in the plane of the film or perpendicular

to the plane of the film. The texture of the media is obtained through polycrystalline epitaxy on layers that are deposited beneath the thin film media. In this paper we review the various schemes that have been and are being used to obtain preferred textures in magnetic and ferroelectric media. We will include descriptions of the control the texture of media made of close packed hexagonal Co based alloys, tetragonal FePt L10 phases and rhombohedral and tetragonal perovskite phases. Acknowledgments: This work has been supported by Seagate Research and the Data Storage Systems Center of Carnegie Mellon University.

11:30 AM

(ICOTOM-S2-008-2008) Determination of the Long Range Order Parameter in Fiber-Textured Films of L1₀ FePt

K. Barmak*, D. C. Berry, B. Wang, Carnegie Mellon University, USA

The combination of high magnetocrystalline anisotropy energy density and good corrosion resistance, the latter when compared with rare-earth based alloys, has resulted in significant interest in L1₀ ordered alloys of FePt for ultrahigh density (>1 Tb/in²) magnetic recording media. When deposited at room temperature, these alloys form in the chemically-disordered A1 state, requiring a post-deposition anneal to form the ordered L1₀ phase. It is of interest to determine the long-range order parameter of the L1₀ phase for the correlation of this parameter to the magnetic properties and performance of the recording medium. In this paper, we report on the determination of the long range order parameter in <111> fiber-textured films of FePt with a range of Pt concentrations. The films for our studies were 500 nm thick and were sputter-deposited from elemental targets onto oxidized silicon wafers coated with a few nanometers of an adhesion layer. The base pressure of the sputtering system was < 5×10⁻⁸ Torr. The films were deposited using 20 sccm flow rate of Ar-4%H₂ at 3 mTorr pressure. Film compositions were determined by energy dispersive x-ray fluorescence and were in the range of 39.3 to 55.3 at.% Pt. Using data from differential scanning calorimetry (DSC) experiments carried out on micron-thick free-standing films that had the same compositions as the films deposited on oxidized silicon wafers, each alloy film deposited on the oxidized silicon substrate was annealed to a temperature of 200 °C beyond the exothermic DSC peak temperature that marks the maximum rate of A1 to L1₀ transformation in the corresponding free-standing film scanned at 40 °C/min. Given the <111> fiber-texture in the film, the long range order parameter was determined from integrated intensities of related families of diffraction peaks such as 001/002/003 for samples tilted to suitable orientations. The peak intensities were corrected using a series of factors. This talk will address the determination of these correction factors in detail. The order parameter was found to increase with increasing Pt content; however, the increase was not monotonic.

11:45 AM

(ICOTOM-S2-009-2008) Epitaxial, Electrical/Electronic Devices via Reel-to-Reel Web-Coating in Kilometer Lengths on Flexible, Substrates with Strict Control of Crystallographic Texture and Grain Boundary Networks (Invited)

A. Goyal*, Oak Ridge National Laboratory, USA

For many energy and electronic applications, single-crystal-like materials offer the best performance. However in almost all cases, the single crystal form of the relevant material is too expensive. In addition, for many applications, very long or wide materials are required, a regime not accessible by conventional single crystal growth. This necessitates the use of flexible, large-area, long, single-crystal-like substrates for epitaxial growth of the relevant advanced material for the electronic or energy application in question. We report here a method to fabricate, low-cost, biaxially-textured, single-crystal-like, polycrystalline substrates, referred to as Rolling-assisted-biaxially-textured-substrates (RABiTS). The RABiTS technique employs simple and industrially scalable thermomechanical processing routes to obtain long lengths of near single-crystal-like, cube-textured substrates. Epitaxial buffer layers of various cubic oxides (of rock salt,

Abstracts

flourite, perovskite and pyrochlore crystal structures) are then deposited in a reel-to-reel configuration using web-coating employing electron-beam evaporation, sputtering or chemical solution deposition. Details of substrate fabrication, the texture quality of the substrates and the nature of grain boundary networks will be discussed. As an example of a material for energy and electronic applications, results will be presented for growth of superconductors on such substrates. Results will also be presented on the fabrication of single-grain, single crystal substrates of the same dimensional tolerance as RABiTS and on the deposition of epitaxial heterostructures on such substrates. Long lengths of epitaxial, high-temperature superconducting wires are now routinely deposited on kilometer long, single-crystal-like alloy substrates coated with an appropriate stack of epitaxial, multilayer buffer layers.

12:15 PM

(ICOTOM-S2-010-2008) Cube Texture Formation in Ni-Pd and Ni-Pd-W Alloys for HTS Coated Tapes

I. Gervasyeva*, D. Rodionov, J. Khlebnikova, Russian Academy of Sciences, Russian Federation; G. Dosovitskii, A. Kaul, Lomonosov Moscow State University, Russian Federation

During the last years, development of textured tape substrates from nickel-based alloys suitable for using in HTS cables has been carried out all over the world. The search for new alloys which are less subject to high-temperature oxidation during depositing buffer layers is of urgent topicality. It is important to exclude nickel penetration from the substrate material into the buffer and superconducting layers. From this point of view, it would be useful to use noble metals, such as palladium or platinum. However, in addition to the high cost, the disadvantage of these materials is their low strength properties. It was found [Michel A.C., et. all., Surf. Sci., 1998 and Derry G.N., et. all., Surf. Sci., 1995] that in the Ni-Pd single crystals after annealing the palladium concentration at polished faces can be increased in comparison of the volume content. The purpose of this work was to evaluate the possibility of producing a cube texture in nickel-palladium alloys and to investigate segregation processes at the surface of a textured tape after annealing. Tapes produced from Ni94Pd6 and Ni92.5Pd5W2.5 alloys after treatments by various rolling and annealing regimes have been investigated, and the possibility of formation of a sharp cube texture in such alloys as well as in pure palladium has been demonstrated. An increase in the degree of deformation during rolling of the binary alloy to 98.7% provides an optimization of the component composition of the deformation texture, which results in an increase in the intensity and a decrease in the scatter of the cube texture during primary recrystallization. The best parameters of the cube texture in the binary and ternary alloys are observed after annealing at 1000°C for 1 h. Tapes produced from the alloys investigated possess strength properties that exceed those of pure nickel by several times. Data testifying an enrichment of a surface layer of the tapes with Pd with respect to the average palladium amount in the alloy have been obtained. These factors provide favorable conditions for the use of such tapes as substrates for multilayered compositions with high-temperature superconductors.

Texture and Anisotropy in Steels

Stainless Steels and Electrical Steels

Room: Rangos 3
Session Chairs: Jerzy Szipunar, McGill University; Hugo Sandim, EEL-USP

8:30 AM

(ICOTOM-S3-010-2008) Microtexture Characterization of Duplex Stainless Steel after Hot Working

C. Herrera*, D. Ponge, D. Raabe, Max-Planck-Institut für Eisenforschung, Germany

Duplex stainless steels (DSSs) are based on the Fe-Cr-Ni system and formed by ferrite (30-70%) and austenite. Excellent combination of

mechanical properties and corrosion resistance under critical working conditions has made DSSs a good option to traditional austenitic and ferritic stainless steels. The processing of these materials demands special attention not only in hot deformation but also in cold deformation and annealing due to the low hot ductility and the precipitation of detrimental phases. During the hot working, the ferrite softens by dynamic recovery due to its high stacking fault energy (SFE). On the other hand, recovery in austenite is very sluggish due to the low SFE. The main softening mechanism of austenite during deformation is dynamic recrystallization. The different behaviour of both phases in hot deformation may result in cracks and low ductility. The ductility depends on different factors like temperature, strain rate, microstructure and chemical composition. EBSD is a powerful technique to characterize the microstructure and understand basic mechanisms such as dynamic recovery and recrystallization. The aim of the present work was to study the changes of the microstructure of the duplex stainless steel 1.4362 during hot deformation. The material was subjected to uniaxial hot compression tests at the temperatures range from 900 to 1250°C and a strain rate of 1 s⁻¹. Electron back scattering diffraction (EBSD) was employed to study the evolution of the microstructure during the hot deformation process in more details. The as cast microstructure is characterized by columnar grains of ferrite with austenite precipitates on the grain boundary and inside of the grains. The orientation relationship between ferrite and austenite is characterized by the Kurdjumov-Sachs (K-S) orientation relationship. The solidification texture of both phases, austenite and ferrite, is weak. The microstructures after deformation at all temperatures are heterogeneous. The ferrite shows dynamic recovery while the austenite is inhomogeneously deformed.

8:45 AM

(ICOTOM-S3-011-2008) Textures and Microstructures Evolution in Hot-Cold Rolling Microalloyed Ferrite Stainless Steel

L. Yandong*, Key Laboratory for Anisotropy and Texture of Materials (Ministry of Education), China; B. Hongyun, L. Weidong, Baosteel Research Institute, China; C. Liqing, J. Yongming, Z. Liang, Key Laboratory for Anisotropy and Texture of Materials (Ministry of Education), China

In this paper, the textures and Microstructures evolution of Ferrite Stainless Steel (FSS) are studied by XRD and EBSD technology. The macro texture evolution is analyzed by XRD for hot rolling and cold rolling FSS sheets with different techniques. Micro orientation and plastic deformation characters are observed by EBSD. The main cold rolling texture components are simulated and compared to the cold rolling IF steel sheets.

9:00 AM

(ICOTOM-S3-012-2008) Influence of Texture on Surface-Roughening during Press Forming in Ti Added High Purity Ferritic Stainless Steel Sheets

K. Kimura*, Nippon Steel Corporation, Japan; M. Hatano, A. Takahashi, Nippon Steel & Sumikin Stainless Steel Corporation, Japan

It is well-known that surface-roughening occurs during press forming in steel sheets having large grain size (approximately over 60µm). However, in high purity ferritic stainless, it often occurs in the sheets with relatively small grain size. Although it is considered that the texture of the sheets is related to surface-roughening phenomenon, details have not been made clear. In this study, the surface-roughening was investigated with emphasizing on the texture. The material used is high purity ferritic stainless steel sheets of 0.8 mm in thickness. Their grain size was 15 µm. Square shape blanks taken from the sheets were subject to drawing tests with cylindrical punches. Two types of the blanks having different initial textures were prepared by changing the directions in which the blanks were taken : one type of the blanks was that a side of the square blank was parallel to the rolling direction (RD), the other type of blanks was that a side and RD made an angle of 45 degree. As the surface-roughening appears at flange region during forming, micrographic observations were con-

ducted for a Laser optical microscope. Textures just under the surfaces were measured for the flange region of the blanks before and after the drawing tests. Major obtained results are as follows: (1) The magnitude of the surface-roughening was changed by initial textures. (2) Two types of shear-bands were observed on the surfaces. In the case that the shear-bands were uni-directionally stretched, the surface-roughening was remarkable. While in the case that the shear-bands were extended in two directions, the surface-roughening was smaller. (3) The grains at the flange region rotated during forming. It was recognized that the number of the directions of crystal rotation was consistent with that of the shear-bands described in (2). (4) From these results, it is considered that the initial texture influences the directions of crystal rotation during forming, resulting in the different shear-bands morphology depending on the texture, which should be the main factor for the surface-roughening.

9:15 AM

(ICOTOM-S3-013-2008) Effects of Texture and Microstructure on the Corrosion Resistance of SS304 Stainless Steel

M. Azzi*, J. Szpunar, McGill University, Canada

Stainless steels are well known for their high corrosion resistance properties. In this paper the effects of texture and microstructure of SS304 stainless steel surface on the corrosion resistance properties, in acidic and neutral solution, were studied. Different surface textures were produced for this study, namely $\{001\}\langle 100\rangle$, $\{110\}\langle 001\rangle$ and $\{111\}\langle 110\rangle$. For each type of texture, two different grain sizes were investigated. Electrochemical Impedance Spectroscopy (EIS) was used to characterize the general corrosion resistance of the stainless steel surfaces. Potentiodynamic polarization tests were performed to characterize the resistance to the local corrosion (Pitting) of the stainless steel surfaces. The poles figures were measured using x-ray diffraction technique and the orientation distribution functions (ODFs) were calculated using Resmat software. The grain size was found by the Orientation Imaging Microscopy (OIM). The results have shown that the corrosion resistance of the stainless steel was decreased when the grain size increased. It was shown also that $\{111\}\langle 110\rangle$ texture had the highest corrosion resistance compared to the other textures. An attempt has been made to correlate the corrosion resistance properties with the planar atomic density of the stainless steel surface.

9:30 AM

(ICOTOM-S3-014-2008) Texture of Nb-Containing Ferritic Stainless Steels after Secondary Recrystallization

H. R. Sandim*, S. P. Rodrigo, EEL-USP, Brazil; T. R. Oliveira, ACESITA S.A., Brazil

We present the results of the texture evolution of three Nb-containing ferritic stainless steels annealed at 1250°C for 2 h to promote secondary recrystallization (SR). Niobium is an important alloying element in the design of heat-resistant ferritic stainless steels (FSS). The steel sheets (4-mm thick) with 16 wt-% Cr and distinct Nb contents (0.31, 0.37, and 0.56 wt-%) were obtained by hot rolling. Carbon and nitrogen contents for the two first steels are 0.02 wt-%C and 0.02 wt-%N. The third steel (0.56 wt-%Nb) contains 0.03 wt-%C and 0.03 wt-%N. The crystallographic textures were determined by conventional X-ray texture analysis. Microstructural characterization was performed in hot-rolled and annealed samples using scanning electron microscopy (SEM) and electron-backscatter diffraction (EBSD). Microtexture was evaluated in a TSL 4.5 system interfaced to a Philips XL-30 SEM operating at 20 kV with a LaB6 filament. The hot-rolled sheets display partial recrystallization with most Goss grains close to the surface and recovered grains (pancake morphology) at the center layer. The hot-rolled sheets exhibit strong $\{011\}\langle uvw\rangle$ and $\{4\ 4\ 11\}\langle 11\ 11\ 8\rangle$ texture components at the surface layer. These components were also reported for others bcc materials such as Fe-3%Si and low-carbon steels. In the center layer, strong α -fiber (mainly $\{001\}\langle 011\rangle$) and weak γ -fiber components are present. Grain size after SR varies no-

ticeably with alloying. For the annealed samples (after SR), the center layer displays $\{001\}\langle 120\rangle$, α -fiber shifted to higher $\phi 1$ angles, and γ -fiber components. The γ -fiber becomes sharper with increasing Nb content. In the surface layer, sharp $\{001\}\langle uvw\rangle$ and weak $\{021\}\langle 100\rangle$ texture components are observed for lower Nb, C, and N contents. However, texture changes significantly for the highly alloyed steel. In this case, the $\{001\}\langle uvw\rangle$ component becomes less pronounced whereas the $\{011\}\langle uvw\rangle$ texture component becomes sharper (Goss-to-Brass). Surface texture observed in the highly alloyed Nb-containing FSS after SR is similar to the one reported in Fe-3%Si. These results show important composition effects in texture of FSS sheets after secondary recrystallization.

9:45 AM

(ICOTOM-S3-015-2008) Control of Rotated Cube Texture of $\{001\}\langle 110\rangle$ in 2.7Si-Electrical Steels

S. K. Chang*, S. I. Lee, D. N. Lee, POSTECH, South Korea

The aim of the control of rotated cube (R-cube) texture is to acquire a large amount of this texture and thus to improve the magnetic properties such as the magnetic flux density and iron loss. Multi-steps of cold rolling and annealing are designed as the first sequence of 1st cold rolling (CR1) and subsequent annealing (AN1) and the second sequence of 2nd cold rolling (CR2) and subsequent annealing (AN2) to control and obtain the significant amount of $\{001\}\langle 110\rangle$ orientation. The texture development was investigated by using EBSD and XRD techniques. From the pole figures of $\{110\}$, $\{200\}$ and $\{112\}$ measured by series expansion method the ODFs were calculated to further access the texture intensity and volume fraction quantitatively. The results obtained are as follows; (1) CR1 shows the volume fraction of R-cube 0.8% for 50% reduction and 7.9% for 80% reduction. For the subsequent annealing (AN1) at 700°C, R-cube revealed 10.8% and 8.5% for 50% and 80% cold reduction, respectively, which are a significant increase especially for 50% reduction of cold rolling. R-cube texture can be developed well by larger strain than lower strain because large strain produces more shear strain resulting in more rotated cube texture. (2) the second cold rolling of 20% for the first annealed sheets revealed R-cube 13.1% for 50% CR1 and 11.5% for 80% CR1. R-cube volume was enlarged to significant level by the light cold reduction but has a little difference between the first cold rolling of 50% and 80%. (3) The subsequent annealing at 700°C for 1000 minutes for the second cold rolled sheets shows a significant decrease in R-cube volume fractions. In case of small reduction 20% of 2CR, R-cube decreased significantly when annealed at 700°C. That is, stored energy obtained by 20% reduction can not provide sufficient energy for the growth of R-cube and thus it is swept away by migration of γ grains. The conclusions obtained in the work are (1) R-cube volume fraction increases with increasing the first cold reduction ratio but a little difference after the subsequent annealing, (2) R-cube after the second cold rolling increases again to a remarkable extent but decreases significantly after the subsequent annealing.

10:30 AM

(ICOTOM-S3-016-2008) Texture and Microstructure Evolution in a Fe-Si Sheet during the Processing Route before Secondary Recrystallization

F. Cruz-Gandarilla, National Polytechnic Institute, Mexico; R. Penelle*, T. Baudin, University of Paris-Sud Orsay, France; H. Mendoza-Leon, National Polytechnic Institute, Mexico

The present work deals with the origin of the Goss grains present at the primary recrystallized state. Consequently, the filiation of the main texture components and their associated microstructure was studied from the hot rolled to the primary recrystallized state at each step of the route. The texture was characterized by neutron, X-ray diffraction and by EBSD. The different microstructures were studied by EBSD coupled to the OIM™ software. At the hot rolled state, the microstructure is made up of bands showing subgrains or recrystallized grains. Near the surface the texture presents a strong Goss component

Abstracts

whose sharpness decreases till the thickness quarter. Conversely the α fiber reinforces at the center. After the first cold rolling, the Goss orientation present in subsurface drops down at the benefit of the orientations (111)[1-21] and (111)[-1-12] and the α fiber including the orientations (111)[1-10] and (111)[0-11]. From EBSD characterizations, it turns out that the Goss grains only rotate either towards the orientation (111)[-1-12] or (111)[0-11], volume fractions are equal to 18 and 16% respectively, whereas that of the two orientations (111)[1-21] and (111)[1-10] is equal to 4 and 2%. Let us remark that some Goss grains residues are observed between the lamellar grains, but not under the form of shear bands. The subsequent annealing does not modify the sharpness between the components. The second cold rolling is translated into an increase of the (111)[1-21] and (111)[-1-12] orientations and a decrease of the α fiber from the surface to the sheet quarter. The γ grains present shear bands inclined by 35-40° relative to the rolling plane. The main feature is that the shear bands present in (111)[1-21] grains have either the (111)[1-10] orientation or that of Goss, conversely the grains (111)[0-11] only present (111)[1-21] shear bands. After the last annealing, the α fiber decreases at the benefit of the (111)[1-21] orientation. Regarding the Goss grains, their volume fraction is about 0.1%.

10:45 AM

(ICOTOM-S3-017-2008) Measurement of the Texture Sharpness in Grain-oriented Electrical Steels

M. Frommert*, C. Zobrist, Max-Planck-Institute for Iron Research, Germany; L. Lahn, A. Böttcher, ThyssenKrupp Electrical Steel, Germany; D. Raabe, S. Zaefferer, Max-Planck-Institute for Iron Research, Germany

Grain-oriented Fe-3%Si steels are used as cores in electrical transformers due to their specific soft-magnetic properties. They are characterised by a very large grain size in the range of millimetres to centimetres and a sharp Goss texture developing at the end of a complex production process. The measurement of the texture sharpness is a challenging task due to the immense grain size and no sophisticated investigation with an appropriate statistical relevance is known to the authors. In this work, X-ray diffraction and large-area EBSD-based orientation microscopy (EBSD: electron back scatter diffraction) were both used for texture analysis and orientation determination, in order to estimate the Goss orientation spread of different grades of grain-oriented steels. For X-ray diffraction measurements a stack of samples containing about one hundred sheets was mounted in a holder for texture analysis on the cross-section. This setup allowed probing of grains from more than 400 square centimetres thus providing excellent statistical data. In contrast to the calculated orientation distribution function (ODF) obtained by X-ray diffraction, the EBSD technique directly *measures* the ODF, therefore avoiding possible calculation errors. The use of a large scan EBSD setup allows for the rapid acquisition and accurate analysis of the diffraction patterns and permits scans on the sheet surface in the order of several square centimetres to be determined within reasonable measurement time. First results show that both measurement techniques deliver comparable values for the Goss orientation spreads which lie in the range of about 3 to 4 degrees for high permeability grades (HGO) and about 6 degrees for conventional grades (CGO). Furthermore, slight variations of the magnetic properties could be correlated with differences of the texture sharpness which suggests that the proposed XRD technique is an accurate and convenient tool for the determination of the texture.

11:00 AM

(ICOTOM-S3-018-2008) Stability of Secondary Recrystallization in Grain Oriented Silicon Steel

E. Namba*, S. Arai, H. Homma, Nippon Steel Corporation, Japan

Secondary recrystallization stability of grain-oriented silicon steel sheets containing AlN and MnS precipitates was investigated by changing the gas atmosphere during secondary Recrystallization annealing. The secondary recrystallization was incomplete when the

surface grains grew excessively through the thickness caused by inhibitor drop before the completion of the secondary recrystallization. It is effective for secondary recrystallization stability to decrease the excessive grain growth in the surface layer by increasing N₂ partial pressure. In addition the suitable texture components to sharpen the Goss orientations were strengthened by the grain growth of matrix grains. Therefore, in order to make the stability of secondary recrystallization compatible with sharp Goss secondary recrystallization texture, the grains in the surface layers should be controlled to adequate sizes by N₂ partial pressure during secondary recrystallization annealing.

11:15 AM

(ICOTOM-S3-019-2008) Effect of Tin on the Recrystallization Behavior and Texture of Grain Oriented Electrical Steels

L. Chun-Chih*, H. Chun-Kan, National Yunlin University of Science and Technology, Taiwan

Influence of tin on the recrystallization behavior and texture of grain oriented electrical steels has been investigated. Tin is easy to segregates at grain boundary and on the surface that pinning the grain boundary mobile. The steel ingots had tin content range from 0 to 0.31wt%, and were reheated to 1200°C and finished rolled at 820°C. Annealed hot bands in 2.3mm were cold rolled to 0.35 mm in one-stage cold rolling. Then, cold-rolled sheets were decarburization annealed at 800°C for 5 minutes in wet H₂-N₂ atmosphere. During secondary recrystallization specimens were heated to 900°C~1200°C and soaked 12 hours with a heating rate 12°C per hour after 700°C. Both of X-ray and EBSD were conducted to examine the grain orientation. It was found that the intensity of (110)<001> texture increased with increasing tin content. Both of grain size and intensity of (111)<1-21> texture were decreased with increasing tin content after primary annealing. The tin promotes the number of (110)<001> nuclei during primary annealing. However, the pinning effect of tin was very strong for secondary recrystallization. The specimens containing less than 0.05wt% tin reached secondary recrystallization completing at 1000°C, but the specimens containing higher than 0.1wt% tin have pool secondary recrystallization and have lower magnetic properties. Specimen containing 0.05wt% tin has maximum flux density and minimum iron loss.

11:30 AM

(ICOTOM-S3-020-2008) Evolution of Recrystallization Texture in Asymmetrically Rolled Non-Oriented Silicon Steel

W. Pei, Y. Sha*, C. Sun, L. Zuo, Key Laboratory for Anisotropy and Texture of Materials, China

Non-oriented silicon steel was asymmetrically cold rolled with various speed ratios, and primarily annealed at different temperatures. The recrystallization texture as well as cold rolling texture and microstructure were investigated. Asymmetric rolling was found to produce through-thickness shear bands with a larger inclination angle to the rolling plane, and the cold rolling alpha (<011>//RD) and gamma (<111>//ND) fibers were weakened. After annealing, asymmetric rolling significantly increased its fiber (<001>//RD) and somewhat decreased gamma fiber. The effect of asymmetric rolling on recrystallization texture was explained from the change in cold rolling texture and shear bands.

11:45 AM

(ICOTOM-S3-021-2008) Influence of Precipitate Distribution on Grain Growth Simulation: Case of the MnS and AlN Precipitates in a Fe-3%Si Electrical Steel HiB

C. Sekkak, N. Rouag, Université Mentouri Constantine, Algeria; R. Penelle*, Université Paris-Sud, France

It is well known that the presence of second phase particles permits to control grain size and orientation distribution during the growth stage. The influence of these second phases depends on their size, shape, volume fraction and distribution. Indeed, the introduction of

particles in the growth simulation permits to control the grain growth inhibition by pinning. Various distributions of particle size are taken into consideration in the present work to study the effect of a bimodal distribution on grain growth simulation in comparison with that of the real distribution (MnS (30-50 nm) and AlN (5-8 nm)) in a Fe₃Si alloy grade HiB. So, the stagnation of normal grain growth and the presence of special grain boundaries around the potential Goss grains embedded in a textured matrix are fundamental parameters for their abnormal growth during the secondary recrystallization annealing. Moreover, the grain boundary energy and mobility are introduced in the Monte Carlo simulation so as the dissolution of precipitates after the stagnation stage which allows the grain growth process to start again.

12:00 PM

(ICOTOM-S3-022-2008) Influence of Grain Orientation and Additional Cementite Precipitation on the Magnetic Aging of a Non-Oriented Silicon Steel

L. Xu, W. Mao*, P. Yang, H. Feng, University of Science and Technology Beijing, China

One of the factors inducing magnetic aging is the additional precipitations of tiny cementite and other particles during the active operation of non-oriented silicon steels, while the working temperature increases in certain extent initiated by the instinct core loss of the sheets. However, the orientation relationship between cementite particles and the ferrite matrix could lead to non-equiaxed cementite particles precipitated additionally because of the possible supersaturated carbon atoms, which might act as anisotropic obstacles against the wall movement of magnetic domains during the magnetization process. Therefore, the grain orientations as well as the sheet texture could influence the effect of magnetic aging in silicon steels, which need to be investigated in details. Two samples of a commercial non-oriented electrical steel sheet 50W800 with 0.002~0.003 %C and similar average grain size were taken and annealed at 200°C for 24h in vacuum to simulate the aging process. The magnetic properties along the rolling direction before and after the aging treatments as well as the sheet textures were measured. It was observed that the core loss increment appeared higher as the sheet texture was a little less favorable for the magnetization, while the magnetic induction kept basically constant. It was indicated that the relative orientations of the non-equiaxed cementite particles to the directions in wall movement of 180° magnetic stripe domains are the same for all grains. However, the driving force for the wall movement is grain orientation dependent, which would lead to different energy expense during the magnetization process and therefore different core loss increment after the magnetic aging. The average orientation factor for the wall movement were introduced and calculated according to the texture of the two sheet samples based on the phenomenological theory of magnetic anisotropy energy, which implied that the sheet texture could exhibit certain influence on the magnetic aging of non-oriented silicon steels, of which the contribution fraction to the core loss increment was discussed.

High Strength Steels

Room: Rangos 3

Session Chairs: Dierk Raabe, Max-Planck-Institut für Eisenforschung; Martin Cernik, U.S.Steel Kosice

1:45 PM

(ICOTOM-S3-023-2008) Microstructure and -Texture Evolution during Intercritical Annealing with and without Deformation in the Production of Ultrafine Grained Ferrite/Martensite Dual Phase Steels

M. Calcagnotto*, D. Ponge, D. Raabe, Max-Planck-Institut für Eisenforschung, Germany

An ultrafine grained ferrite/martensite dual phase steel was fabricated by use of large strain warm deformation and subsequent intercritical annealing. During annealing, a one-step deformation pass was applied imposing variable strains. The final microstructure consists of

fine martensite islands embedded in an ultrafine grained ferrite matrix. The steel exhibits an excellent combination of high strength, considerable strain hardenability and high uniform elongation. The microstructure and -texture evolution during intercritical annealing was studied by means of electron backscatter diffraction (EBSD). The analysis revealed important information about the processes being active during heat treatment and plastic deformation. The effect of intercritical annealing conditions without and with deformation on microstructure and -texture is discussed in detail.

2:00 PM

(ICOTOM-S3-024-2008) Inhomogeneity of the Crystallographic Texture in Hot Rolled High-manganese TWIP Steels

D. Raabe*, Max-Planck-Institut für Eisenforschung, Germany; H. Hofmann, ThyssenKrupp Steel AG, Germany; G. Frommeyer, K. Verbeke, Max-Planck-Institut für Eisenforschung, Germany

The ever increasing demand for energy-saving engineering design strategies requires the use of advanced light weight materials. Steels are in terms of their optimal combination of strength, ductility, formability, and price the dominant materials class in the realm of light weight engineering solutions. In this context TWIP steels are currently under intense investigation ("TWIP" refers to the mechanism of twinning-induced plasticity). Particular emphasis in the current study is placed on a better understanding of the underlying mechanisms of the evolution of texture during warm rolling using different rolling and coiling strategies. In particular the through-thickness homogeneity of the hot band texture is addressed in detail.

2:15 PM

(ICOTOM-S3-025-2008) Microstructural and Textural Evolutions in a Cold Rolled High Mn TWIP Steel

K. Verbeke*, Max-Planck-Institut für Eisenforschung, Germany; L. Bracke, Corus Research, Development and Technology, Netherlands; L. Kestens, Delft University of Technology, Netherlands; J. Penning, Ghent University, Belgium

A fully austenitic TWIP steel was cold rolled. During cold rolling, the evolution of the crystallographic texture was monitored. The development of a brass type of texture was found, which is typical for low SFE materials. Intensive electron microscopic observations, TEM and SEM, revealed four deformation mechanisms to be active: micro twinning, dislocation slip, the formation of stacking faults and microscopic shear banding. The effect of macroscopic shear banding was expected to be minimal. Putting together all the results showed that both micro twinning and slip play a role in the development of the observed brass texture.

2:30 PM

(ICOTOM-S3-026-2008) On the Role of Mechanical Twinning in Microstructure Evolution of High Manganese Steels: Experiments and Modelling

L. A. Hantcherli*, P. Eisenlohr, F. Roters, D. Raabe, Max-Planck-Institut für Eisenforschung, Germany

Twinning-induced plasticity (TWIP) steels have received increased interest during the last decade owing to their high strength coupled with good ductility which renders them attractive for a large number of applications. However, since continuum-scale simulation techniques do not yet account precisely enough for mechanical twinning as potential deformation mode, accurate prediction of forming operations and texture evolution by e.g. finite element method (FEM)-based tools still remains challenging. Published statistical models—in the framework of crystal plasticity FEM (CPFEM)—to describe deformation twinning differ in many respects, like twin volume evolution or slip-twin interactions or twin-twin interactions, but share the phenomenology of the dependence of twin nucleation rate on resolved stress on the habit plane. A variety of such models has been implemented into a CPFEM framework. The validity of different assumptions in those models is checked by comparing in-situ SEM observations of oligocrystalline samples under tension with respective direct CPFEM simulations in terms of twinning/dislocation slip activity.

Abstracts

2:45 PM

(ICOTOM-S3-027-2008) Crystallographic Characterization of a Phosphorus Added TRIP Steel

K. Verbeke, L. Barbé*, Ghent University, Belgium; D. Raabe, Max-Planck-Institut für Eisenforschung, Germany

Texture and crystallographic orientation relationships, active during the transformation of austenite to bainite, are studied for two TRIP steels by means of Electron BackScattering Diffraction (EBSD). The texture measurements showed that the maximum intensity for the retained austenite was on the Brass component with the intensity gradually decreasing along the alpha and the beta fibre. The intensity of both BCC phases was comparable and the bainite texture displayed clear transformation products that could be related with the dominant Brass component of the intercritical austenite. The study of the crystallographic orientation relationships showed that the Kurdjumov Sachs relationship was dominant and no strong indication for variant selection could be retrieved from the studied data. It was, however, also demonstrated that some precautions are necessary since a clear distinction between the evaluation of a small region of the microstructure and conclusions made for the complete material is required.

3:15 PM

(ICOTOM-S3-029-2008) Quantitative Analysis of Variant Selection and Orientation Relationships during the γ -to- α Phase Transformation in Hot-Rolled TRIP Steels

M. Loic, Université Libre de Bruxelles, ULB, Belgium; P. J. Jacques, Université catholique de Louvain, UCL, Belgium; S. Godet*, Université Libre de Bruxelles, ULB, Belgium

The orientation relationships that apply to the fcc (γ) – bcc (α) phase transformation in high-performance hot-rolled TRIP-aided steels were characterised by EBSD techniques. The use of Rodrigues-Frank space enables straightforward comparison to be made with orientation relationships proposed in the literature. A statistical treatment of the experimental data allows the most accurate orientation relationship to be determined. The variant selection phenomenon was quantitatively characterized at the level of individual austenite grains. The crystallographic features of the bainite packets were also investigated.

4:00 PM

(ICOTOM-S3-030-2008) Stored Energy Evolution in a Cold-Rolled IF Steel

A. Wauthier*, Arcelor Mittal R&D, France; B. Bacroix, T. Chauveau, O. Castelnau, CNRS, France; H. Regle, Arcelor Mittal R&D, France

During the deformation of low carbon steel by cold-rolling, the shape and the orientations of the grains change relative to the direction of the applied stress and some dislocations are continuously created. Two different synchrotron experiments, for quantitative and statistically representative analysis, have been led to measure the dislocation densities via the analysis of the broadening of the X-ray diffraction lines. Different cold-rolling levels have been considered from low to high (30% to 95% thickness reduction) and in different states: deformed or restored ones. One experiment was dedicated to the study of some specific crystallographic orientations and the other one to get a mapping of a complete pole figure in stored energy. Comparisons of these two kinds of results will be given with also some EBSD data to make links between misorientation, dislocation densities and stored energy. The advantage of the gamma fiber grains during the recrystallisation is quantified, with a stored energy two times higher than the alpha fiber grains.

4:15 PM

(ICOTOM-S3-031-2008) Monte Carlo Algorithm for Ziner Drag Effect in the Fe-3%Si Magnetic Alloys

M. Noureddine*, Université du 20 août 55-Skikda, Algeria; P. Richard, B. Thierry, E. Anne-laure, Université de Paris Sud, France

In Monte-Carlo simulation of grain growth [1], particles are randomly distributed on such a theoretical microstructure. This assumption is not representative of real materials like Fe-3%Si sheets. The

presence of AlN and MnS precipitates which are inhibitors of normal grain growth, permits the development of the Goss texture by a sudden and fast growth of grains possessing the $\{110\}<001>$ orientation. The interaction between particles and grain boundaries occurs in a selective way [2]. In the present study, a model for classical Monte-Carlo simulation is developed where local effect is considered by introducing a critical radius R_n of neighbourhood in relation with the nearest neighbouring of the growing grain [3]. In order to introduce the influence of the morphological and crystallographic using as starting state a real microstructure of grain oriented Fe-3%Si sheet neighbourhood inhomogeneities around Goss grain on its AGG, the simulation procedure has been implemented characterised by Orientation Imaging Microscopy (OIM). References 1-D.J. Srolovitz, G. S. Grest and M. P. Anderson, *Acta Metall.* 33 N° 12 (1985) 2233. 2-E.H. Aigeltinger and H.E. Exner, *Metall. Trans. A* 8A (1977) 421. 3-N. Maazi, N. Rouag, A.L. Etter, R. Penelle and T. Boudin, *Scripta Mat.* 55 (2006) 641.

4:30 PM

(ICOTOM-S3-032-2008) Evolution and Relation between Texture-Microstructure-Mechanical Behaviour of a FeMnC TWIP Steel during Tensile Test

D. Barbier*, N. Gey, B. Bolle, M. Humbert, LETAM, France; S. Allain, Arcelor Research, France

Austenitic Fe-Mn steels have outstanding mechanical characteristics, combining a very high mechanical strength and an important ductility notably at room temperature. This remarkable behaviour is due to the interaction between dislocation glides and twinning, which is named TWIP effect (TWinning Induced Plasticity). The twins formed during deformations become obstacles to the dislocation motions and reduce their mean free path. These combined mechanisms are known to act as a dynamic Hall-Petch effect which sensitively influences the texture and the microstructure evolutions. Therefore, we particularly studied the microstructure and texture evolutions during a tensile test at local and global scales. In parallel, the mechanical behaviour of the steel was analyzed. In this contribution, we present and discuss the textures, microstructures / micro-textures of samples deformed during a tensile test for different strains. The local characteristics of textures and microstructures were obtained by EBSD technique using a SEM FEG. The different sets of the twinning microstructure and the strong local deformation heterogeneities in the austenitic matrix are analysed with the high resolution orientation maps. The evolutions of macroscopic textures determined by x-rays diffraction are examined by considering the local microstructural characteristics. These texture evolutions are then analysed in relation to the mechanical behaviour of the alloy and especially to the different strain hardening stages.

4:45 PM

(ICOTOM-S3-033-2008) Grain Subdivision in Niobium during ECAP: EBSD Characterization and Multiscale Modeling

M. Seefeldt*, B. Verlinden, P. Van Houtte, K.U. Leuven, Belgium

Grain subdivision in niobium during Equal Channel Angular Pressing (ECAP) at homologous temperatures of 0.1 and 0.25 is studied by Electron Back Scatter Diffraction (EBSD) and multiscale modeling of the substructure and texture evolution. EBSD indicates that during the first pass, at 0.1 T/T_m, shear banding is a major deformation mechanism, while at 0.25 T/T_m, the microstructure evolution resembles the one in f.c.c. materials with high stacking fault energy (like Al or Ni) at room temperature. After several passes, the microstructure arising from deformation at 0.25 T/T_m resembles very much the one known from deformation at room temperature, i.e. 0.1 T/T_m. The model starts from an imposed velocity gradient tensor (the one for simple shear as a first approximation, the one proposed by L.S. Tóth, based on flow field analysis, in a second stage) that drives a Taylor full constraints (FC) texture model. The slip rates predicted by this texture model drive balance equations for the mobile, immobile and excess screw and edge dislocations in the involved slip systems. The

storage and recovery terms of the balance equations are based on the underlying elementary processes and take the different mobilities of the two dislocation characters into account. From the excess dislocation densities, the arising misorientations are estimated. Grains where the misorientation has exceeded a critical value after fixed deformation intervals are considered as split and re-enter into the texture model as separate elements.

5:00 PM

(ICOTOM-S3-034-2008) Texture Component Model for Predicting Recrystallization Textures

A. Brahme*, M. Winning, D. Raabe, Max-Planck Institut für Eisenforschung, Germany

We will present an analytical model for predicting crystallographic textures and the final grain size during primary static recrystallization of metals using texture components. The model uses a subset of texture components instead of using the entire set of orientations needed to represent the material. The recrystallization kinetics and the texture evolution are governed by the tensorial variant of the Johnson-Mehl-Avrami-Kolmogorov (JMAK) equation. The number of components determines the order of this tensor. Each entry in the tensors represents coupling between the recrystallizing and the deformed components. The growth of a recrystallizing component in to a given deformed component is dependent on various factors like activation energy of nucleation, activation energy for boundary mobility and stored energy (in the deformed region). All of these factors along with the texture components can be obtained from precise and directed experiments. Main aim of this work is to present a fast and physically based process for simulation of recrystallization texture with respect to processing. We will present a comparison with experimental data and the predictions of our model for low carbon steel.

5:15 PM

(ICOTOM-S3-035-2008) Relationship Between Microstructure and Texture Evolution during Cold Deformation of TWIP-Steels

A. B. Fanta*, S. Zaeferrer, Max Planck Institute for Iron Research, Germany; I. Thomas, ThyssenKrupp Steel, Germany; D. Raabe, Max Planck Institute for Iron Research, Germany

The low stacking fault energy of austenitic Fe-Mn-C steels promotes extensive mechanical twinning along with dislocation gliding during deformation. The rapid formation of fine twins during straining results in a decrease in the mean dislocation path which favors a uniform work hardening. This hardening effect is known as twinning-induced plasticity (TWIP). TWIP-steels reveal high ductility and high plasticity and reach very high strength during straining. We present a study on the evolution of microstructure and texture of TWIP steels during tensile deformation by means of EBSD-based orientation microscopy. Aim of this study is to advance the understanding of the microstructural reasons for the high tensile ductility of the material. Indeed, the uniform elongation in a tensile experiment may exceed 50 %. With increasing strain the density of twins increases and after a tensile deformation of 10% twinning in multiple systems occurs. Twinning is strongly related to the grain orientation. Grains with a $\langle 100 \rangle$ direction parallel to the tensile direction do not develop twins even after 50% of tensile strain. Furthermore, the presence of both single and multiple twin variants are also related to the grain orientation. A particular effect observed in this material is the absence of intense slip localization inside of individual grains. Rather, the grains deform homogeneously all over the grain interior. Complementary to EBSD analysis, transmission electron microscope (TEM) investigations are currently been performed to study in more detail the interaction between twins and dislocations.

5:30 PM

(ICOTOM-S3-036-2008) Texture of Non-oriented Rolled Steels by X-ray and Electron Diffraction

M. Cernik*, M. Predmersky, A. Lesko, U.S.Steel Kosice, Slovakia

Strong magnetic properties of non-oriented cold rolled silicon steels depend on suitable microstructure and texture. The alternative tech-

nological techniques were applied to achieve the textural changes. Also the effect of silicon and antimony additions on textural parameters and magnetic properties was studied. The standard industrially produced steel sheets and experimentally treated materials in heat cycle simulator were used for textural investigations. The textural data were measured by X-ray radiation on 3D goniometer and by electron beam with EBSD system. ODF – orientation distribution function was calculated using popLA, LaboTex and TSL OIM programs with different estimation algorithms (Bunge, iterative). Very good coincidence of X-ray and Electron Diffraction modes analyses results were achieved on measured and calculated textural characteristics for selected grade of non-oriented steels.

5:45 PM

(ICOTOM-S3-037-2008) Texture Development during Cold Ring Rolling of 100Cr6

K. Rytberg*, M. Knutson Wedel, Chalmers University of Technology, Sweden; P. Dahlman, SKF Sverige AB, Sweden; L. Nyborg, Chalmers University of Technology, Sweden

The past years' steadily increasing steel prices have acted as an incentive to apply near-net-shape manufacturing processes in production. Cold ring rolling is such a manufacturing method that exhibits a great potential in terms of material waste reduction. In this process waste reduction is achieved by expanding a pre-turned ring (a blank) into the final shape employing incremental forming by radial compression during rotation. Even though the process has been applied in ring production for several decades the approach has been of a deterministic nature regarding process parameters such as applied forces, shape after rolling, tool design and rolling speed and feed. The very large deformation associated with cold ring rolling is accompanied by a development of texture. Knowledge of the texture in the material at different stages of deformation, linked to material properties, permits development of improved models of the material behaviour during cold ring rolling. By applying the improved models in simulations of the process it would be possible to predict the texture development depending on process parameters and thereby the final distortion of the rings. Material allowance after rolling can thus be reduced resulting in material waste reduction. Furthermore, an improved knowledge of the development of texture could make it possible to control the grain structure and thereby achieve enhanced material properties. In the current project the microstructural texture development throughout the cross-section of cold rolled rings made of spheroidise-annealed 100Cr6 steel is being evaluated by the use of X-ray diffraction (development of macrotexture) and electron microscopy (development of microtexture). By interrupting the rolling process at specified intervals resulting in varying amount of deformation the successive development of texture in the material can be determined. Near the surface of the inner circumference of the ring strains were found to be as large as 500 %. A substantial grain refinement had been achieved resulting in increased hardness in this area.

Texture at Non-Ambient Conditions

Texture at Non-Ambient Conditions

Room: Rangos 1

Session Chairs: Sven Vogel, Los Alamos National Laboratory; Bjorn Clausen, Los Alamos National Laboratory

1:45 PM

(ICOTOM-S4-001-2008) High Pressure Deformation Mechanisms from In Situ Texture Measurements (Invited)

S. Merkel*, CNRS - University Lille 1, France

The diamond anvil cell (DAC), when used in radial diffraction geometry, emerges as a powerful tool for investigation of plasticity and texture of materials at high pressures. In those experiments, the sample is located within a DAC, which has a directional loading component,

Abstracts

and can be plastically deformed, in-situ, up to pressures above 100 GPa (1 MBar). Stress and texture in the sample can also be measured in-situ using synchrotron x-rays and later compared to results of visco-plastic self consistent calculations to infer deformation mechanisms. This technique has now been used for several years and applied to study textures and deformation mechanisms in many Earth-related materials such as the epsilon phase of iron, silicate perovskite, or silicate post-perovskite. Moreover, the application of the technique is not limited to the field of geophysics and it can be used for most materials. Here, I will present the radial diffraction technique and how it can be used to measure textures in samples up to megabar pressures. Examples will be given for the study of deformation mechanisms in various minerals and iron. I will also present new results demonstrating how this technique can be used to study texture evolution and memory effects during phase transformations.

2:15 PM

(ICOTOM-S4-002-2008) High Pressure Deformation Study of Zirconium and Beryllium

S. C. Vogel*, D. W. Brown, Los Alamos National Laboratory, USA; N. Nishiyama, APS, USA; H. Reiche, T. A. Sisneros, H. M. Volz, Los Alamos National Laboratory, USA; Y. Wang, APS, USA; J. Zhang, Y. Zhao, Los Alamos National Laboratory, USA

In situ deformation studies of polycrystalline materials using diffraction are an established method to understand elastic and plastic deformation of materials. Parameters studied by diffraction are typically lattice strains and texture evolution, which in combination with the macroscopic flow curve allow improvements of predictive models. In situ uni-axial deformation at ambient conditions has been established over 10 years and in the last 5 years uni-axial deformation at temperatures above and below ambient have become routine. However, only few devices exist which allow deformation at high pressure and only a few investigations using these devices are reported in the literature. Here, we report results on a study of the uni-axial deformation of Zirconium alloy (Zircaloy-2) at 2 and 5 GPa as well as pure beryllium at the BM13 beamline at the Advanced Photon Source. The deformation-DIA apparatus generates a confining hydrostatic pressure using a cubic anvil setup. Two differential rams allow to increase (compressive) or decrease (tensile) the uni-axial loading in the vertical direction, resulting in plastic deformation at high pressures. The stress is measured from the lattice response while the macroscopic strain is measured using the beam line in radiography mode. In diffraction mode, diffraction of a monochromatic beam (wavelength 0.1901 Å) is detected using a CCD detector. Deviations from Debye rings allow derivation of the lattice strains resulting from the uni-axial deformation. Intensity variations along the ring allow quantitative texture analysis. Both quantities are compared with our previous studies at ambient conditions for the same material.

2:30 PM

(ICOTOM-S4-003-2008) Texture Development in Copper after Cryogenic Rolling and Heat Treatment

A. Haldar*, Tata Steel Ltd., India; D. Das, P. P. Chattopadhyay, Bengal Engineering and Science University, India

Present study aims at investigating the texture evolution and mechanical properties of bulk nanocrystalline / ultra fine grained pure Cu after heavy cold deformation (86%) at cryogenic temperature (liquid nitrogen) and recrystallisation at different temperatures. Cryogenic rolling of Cu has been used to produce nano-grain sizes with bimodal distribution so that total elongation is improved along with strength. A few fold increments in tensile properties were observed in this study. Both bulk and micro textures were determined using XRD and EBSD. In as rolled sample, the strongest texture components were found to be S with a volume fraction of as high as 26% and Brass components with volume fraction of 14.3 %. All other components like Cube, Copper, and Goss etc were also present with less intensity. During heat treatment (180- 300 degree C), bulk textures showed a

very high stability of S components and almost no changes in the volume fraction could be observed. EBSD study showed that deformed structures were still present after heat treatment. The S components belonged to these deformed structures. In the recrystallisation region texture got randomized in all the cases. This shows a clear difference between cryogenically rolled Cu and room temperature rolled Cu in developing recrystallisation texture. Significant dependence of mechanical property on grain size has been recorded. Present study indicates that conventional rolling at subzero temperature followed by controlled recrystallisation may be utilised as an effective method for development of bulk Cu, with two to three fold improvement in yield strength in comparison to its coarse grained counterpart with moderate ductility and toughness.

2:45 PM

(ICOTOM-S4-004-2008) Texture Changes during Phase Transformations Studied In-Situ with Neutron Diffraction (Invited)

H. Wenk*, University of California, USA

Advantages of using neutron diffraction for texture analysis are that large volumes can be investigated and statistically representative data are obtained, particularly for coarse-grained samples. With multidetector time-of-flight diffractometers quantitative orientation information can be obtained efficiently within minutes. Furthermore with furnaces texture changes in bulk materials during recrystallization and phase transformations can be studied in situ. Here the TOF diffractometer HIPPO at Los Alamos National Laboratory is used to investigate zirconium (Acta Mat. 52, 1899), titanium (Acta Mat. 55 in press), iron (Met. Trans 32A, 261) uranium and quartz (Phys. Chem. Min. 36, in press) to assess orientation changes during heating. Heating of single-phase hcp cold-rolled metals (Ti and Zr) produces recrystallization around 500 degree C and conversion to bcc around 850 degree C. During recrystallization c-axes do not change significantly, but a-axes transform to a texture with (110) poles in the rolling direction. During the hcp-bcc transformation this grain growth component nucleates first according to Burger's relation with variant selection. During the reverse bcc-hcp transition again Burger's relation applies but selecting common variants between adjacent bcc grains. In iron, both the bcc-fcc and fcc-bcc transformation obeys the Kurdjumov-Sachs relation, but again with significant variant selection and increase in texture strength. More complex is the situation in uranium that changes from orthorhombic to tetragonal and bcc. In this case twinning plays a significant role. Another low-symmetry material quartz with a trigonal-hexagonal-trigonal transformation at 573 degree C displays a perfect texture memory if the initial texture is strong and grains are non-equiaxed, suggesting that stresses from neighboring grains have a significant influence. In situ texture measurements with neutrons are becoming a routine and results on various systems reveal complexities that are of particular interests for interpreting shape memory systems.

3:15 PM

(ICOTOM-S4-005-2008) Texture Memory and Modeling In A NiTi Shape Memory Alloy

B. Ye, B. S. Majumdar*, New Mexico Tech, USA

NiTi alloys are known for their shape memory effect, which enables the alloy to be permanently (plastically) deformed in the martensite state and fully recover the original shape on subsequent heating to austenite. Here, we draw attention to near-reversible strain hysteresis during thermal cycling of a nominally equiatomic NiTi alloy at a stress that is below the yield strength of the stable martensite. The transformation strain (up to 3.5%) is found to depend almost linearly on the applied stress. In order to probe the strain evolution, in situ thermal cycling experiments were conducted at constant applied stress on the SMARTS neutron diffraction apparatus at Los Alamos. The diffraction data were used to develop inverse pole figures (IPF) either parallel or perpendicular to the tensile axis. In addition, com-

plete pole figures were developed for the martensite following thermal cycling. We demonstrate that the strain hysteresis occurs due to a stress-dependent crystallographic texture of the martensite during cool-down from the austenite, and thereafter 'remembered' during subsequent thermal cycling. We designate this the 'texture memory effect', and prove its manifestation by mapping texture evolution during thermal cycling under sub-yield stresses. We suspect that the low stress requirement is a result of the sharp drop in shear modulus as the sample is cooled through the martensite start temperature. Finally, we quantitatively relate the observed texture to the experimental strain by developing a calculated strain-texture map, which is similar to a pole figure except that strain rather than preferred pole-intensity is represented at any pole location. Excellent agreement is obtained between the calculated strain-texture map and the texture and strains observed at different applied stress levels. The model is also shown to be applicable in other martensitic transformations, including superelastic deformation of shape memory alloys. Partial funding came through NSF grant DMR-0413852, and we thank Drs.D.Brown, S. Vogel and B. Clausen of LANL for their help. Relevant reference: B. Ye, B.S. Majumdar and I. Dutta, Applied Physics Letters, 91, 06198 (2007)

4:00 PM

(ICOTOM-S4-006-2008) Texture Development during Compressive Loading of Extruded Magnesium

B. Clausen*, C. N. Tome, D. W. Brown, Los Alamos National Laboratory, USA; S. R. Agnew, University of Virginia, USA

Neutron diffraction allows for in-situ non-destructive measurements of texture and internal strains within crystalline materials. In the present study, texture and internal strain development was followed during compressive loading of extruded magnesium alloy. The axisymmetric nature of both extrusion and uniaxial compression results in axisymmetric textures in the sample throughout the deformation. Thus, we can use the two diffraction patterns recorded simultaneously on SMARTS together with the assumption of axisymmetry to fully determine the texture in-situ during deformation. The initial and final textures were also measured on HIPPO without any symmetry constraints, and it was verified that they were indeed axisymmetric. The measured in-situ textures were used to determine the twin volume fraction during deformation. Together with the measured texture and internal strains the determined twin volume fraction was used to validate a new twinning scheme in an Elastic-Plastic Self-Consistent (EPSC) polycrystal deformation model.

4:15 PM

(ICOTOM-S4-007-2008) In Situ Observation of Texture Evolution in Ti-10-2-3

S. L. Raghunathan*, R. J. Dashwood, M. Jackson, D. Dye, Imperial College, United Kingdom

The near- β titanium alloy Ti-10V-2Fe-3Al is often isothermally forged in the $\alpha+\beta$ condition at 760C for aircraft landing gear applications. It has been established that during isothermal forging the prior β microstructure consisting of α plates and grain boundary α within large β grains evolves into an equiaxed grain structure with spheroidised α within a β subgrain matrix. While the dependence of microstructure development on forging conditions in this alloy has received much attention, macro- and microtextures evolution have not been investigated. In situ synchrotron X-ray, neutron and ex situ electron backscatter diffraction (EBSD) were utilised to characterise the evolution of macrotexture and microtexture during $\alpha+\beta$ forging of Ti-10-2-3. EBSD was used to determine the subgrain misorientation distribution at a strain of 0.8 and strain rates of 0.1 and 0.01s⁻¹. The measured distributions were found to be similar, with an average misorientation of 2.2 σ . Macrotexture evolution was studied using time of flight neutron diffraction. Interrupted testing was performed at 0.01s⁻¹ to a strain of 0.2, 0.4, and 0.6 and 0.8. It was found that the moderate cube macrotexture of the parent material was converted into a

moderate fibre texture more typical of deformation of the α phase, with the major change occurring between strains of 0.4 and 0.6. It is suggested that at low strains the β phase dominates the behaviour whereas at higher strains the α deformation behaviour has more influence. The in situ synchrotron diffraction studies allowed the orientation evolution of individual grains (observed as spots / streaks in the diffraction pattern) to be characterised. At the highest strain rate of 0.1s⁻¹, this indicated a change in behaviour from dispersion of the crystal mosaic (peak angular spread) at low strains, to convergence of the crystal mosaic at larger strains. At lower strain rates, only convergence of the crystal mosaic was observed. These results appear to indicate a change in mechanism between deformation-controlled behaviour during the early stages of deformation and a strain rate of 0.1s⁻¹ and diffusional, recovery-controlled behaviour lower strain rates and higher strains.

4:30 PM

(ICOTOM-S4-008-2008) Texture Evolution of Zirconium Alloys During Processing on the High Temperature Beta Phase

J. Romero*, J. Q. da Fonseca, M. Preuss, The University of Manchester, United Kingdom

The purpose of this study is to use synchrotron X-ray diffraction to perform time-resolved in-situ texture studies during the allotropic phase transformation in a zirconium alloy. Although several thermo-mechanical processing routes that exploit the allotropic phase transformation undergone by zirconium at high temperatures are being developed to produce random textures, there is no consensus about the fundamental processes responsible for texture development and evolution during zirconium alloys processing. A time-resolved in-situ experiment was carried out on the high-energy beamline ID15B at the European Synchrotron Radiation Facility (ESRF). Zircaloy-2 samples were studied in transmission mode with a monochromatic X-ray beam during in-situ thermal and mechanical cycling. The aim was to investigate and distinguish the effects of maximum temperature, heating/cooling rates and stress on the phase transformation in terms of preferential crystallographic orientation. In a first stage one 2-D diffraction pattern was obtained every 4 seconds during complete temperature cycles from room temperature to above the transformation temperature. Different maximum temperatures and heating/cooling rates were applied. Stress was applied in three different schemes: during the whole process, during heating and during cooling. Higher time resolution was then employed to study the alpha-to-beta transformation in detail, acquiring images every 0.4 seconds. From a detailed qualitative analysis of the diffraction patterns obtained, it was found that there is indeed variant selection during the phase transformation, which is modified by the different heating/cooling and stress conditions. Crystallographic orientation relationships between the phases have been seen, influencing orientation in the beta phase, and thereby the inherited alpha texture. Further analyses of the data are being carried out in order to quantify the changes in texture observed, as well as post-mortem microstructural characterisation of the samples tested in-situ, with laboratory X-Rays and Electron Backscatter Diffraction (EBSD). The information obtained from such analyses will be presented in due course.

4:45 PM

(ICOTOM-S4-009-2008) Investigation of Variant Selection by using High Temperature in-situ EBSD Measurements

I. Lischewski*, G. Gottstein, RWTH Aachen, Germany

A novel concept for a laser powered heating stage for commercial SEMs is introduced. By utilizing the energy of an infrared diode laser as heating source in combination with automated EBSD-data acquisition more information about microstructure and orientation changes during grain growth, recrystallization, recovery and phase transformations can be achieved. The new laser powered heating stage was developed for commercial SEMs with the capacity to heat specimens up to a temperature of 1000°C. Data acquisition utilizes a

Abstracts

combination of the well established electron back-scatter diffraction (EBSD) technique and orientation contrast (OC) imaging. Most investigations into microstructure and texture evolution are restricted to post-mortem analysis. Due to this limitation there is a need for experimental setups permitting the in-situ observation of microstructural changes of polycrystalline materials. Besides in-situ deformation the main focus lies on the in-situ observation of thermally activated processes like grain growth, recrystallization, recovery and phase transformations. An example is the α - γ - α phase transformation in low carbon steels. The observation of this phase transformation by using the EBSD technique is limited to the low temperature regime since it is a reversible process and cooling down instantaneously leads to a back transformation to the low temperature phase. New results of the α - γ - α phase transformation in steel relating to the texture memory effect and the unequal behaviour of variant selection of different mother orientations will be shown. Also the role of the orientation relation between the phases regarding to the kinetic of phase transformation will be discussed.

5:00 PM

(ICOTOM-S4-010-2008) EBSD Analysis of Explosively Welded Aluminum

C. C. Merriman*, D. Field, S. Freeze, Washington State University, USA

Explosive welding is a unique welding process through which high pressure produced by a detonation joins two or more metal plates together. Historically optical micrographs and descriptions of the local bond character using TEM images have been the extent of microstructural studies, thus excluding non-local and grain interaction effects. The current study uses EBSD to investigate the local texture and microstructure at and surrounding the bond line between two plates of AA 6061-O. Gradients in the deformation character are described by excess dislocation density measurements from the EBSD data. Local deformation and grain interactions along the bond line are analyzed with respect to the wavy nature of the interface. The developed textures give an indication of local metal flow during the bonding process. These are analyzed using standard crystal plasticity techniques.

5:15 PM

(ICOTOM-S4-011-2008) Study of Texture Evolution at High Strain Rates in FCC Materials

N. P. Gurao*, S. Suwas, Indian Institute of Science, Bangalore, India; R. Kapoor, Bhabha Atomic Research Center, India

Plastic deformation in polycrystalline materials is accommodated by glide on specific slip systems, the choice of which is assumed to be rate insensitive but not rate-independent. Hence, the evolution of texture turns out to be rate insensitive. However, recent investigations showed that texture changes under dynamic conditions depending on the strain hardening response. With these results in perspective, FCC materials present an interesting case as the hardening response of FCC materials varies with the SFE. Evolution of crystallographic texture for FCC materials with different SFE was studied over 7 orders of magnitude of strain rate. Polycrystalline Ni, Cu, and Cu-10Zn were compressed at strain rates ranging from 3×10^{-4} to 1×10^3 s⁻¹. A thorough characterization of these samples was carried out using XRD, EBSD and TEM. The texture evolved in FCC materials at low rates show little dependence on the SFE and the amount of strain. There is a strong $\langle 101 \rangle$ component forming in all the three materials under quasi-static conditions indicating that the SFE has little effect on the texture evolution of FCC materials. Under dynamic conditions, the texture in case of Cu-10Zn and Ni tends to be random and shows weak $\langle 101 \rangle$ while Cu maintains a strong $\langle 101 \rangle$. Detailed microstructural investigation showed the presence of newly recrystallized grains and a necklace type microstructure in Cu that is a characteristic of continuous Dynamic Recrystallization (cDRX); while no such microstructural modification was observed in case of Cu-10Zn and Ni. These results are further established by using a unique

scheme to model grain fragmentation in Los Alamos Polycrystalline Plasticity code. To summarize, deformation texture evolution in FCC materials does not depend on SFE under quasi-static conditions; while under dynamic conditions it determines the onset of a restoration mechanism. Ni & Cu-10Zn having distinctly different SFE exhibit similar texture after high strain rate deformation. Cu is an exception in terms of texture evolution under dynamic conditions. This is attributed to the ease of cross slip that helps in attaining optimum recovery rate for the onset of cDRX under experimental conditions.

5:30 PM

(ICOTOM-S4-012-2008) Technique for Texture Measurement Under Shock Loading

B. El-Dasher*, J. Hawreliak, J. McNaney, Lawrence Livermore National Laboratory, USA; D. Milathianaki, University of Texas at Austin, USA; M. Butterfield, D. Swift, H. Lorenzana, Lawrence Livermore National Laboratory, USA

Understanding the behavior of materials under shock loading has been of interest for some time, with the majority of the work focused on the study of bulk material behavior using suitable diagnostics (e.g. laser interferometry) as well as sample recovery studies. While this work has been instrumental in advancing our understanding of the field, none of it was capable of elucidating crystal behavior during the shock process. Recently however, the advent of in-situ X-ray diffraction (XRD) has allowed the probing of material behavior at the lattice level under shock loading, and for the first time providing crystallographic information during the shock process. In this work we present a technique that builds upon the temporal and spatial advantages of in-situ XRD by combining it with a cylindrical pinhole camera. We demonstrate how texture measurements are obtained from in-situ XRD shock experiments, and how they relate to electron backscatter diffraction (EBSD) data obtained from the original specimen material. We anticipate that this technique will allow the detection of texture changes that may occur during shock loading due to grain rotations and/or defect generation, allowing us to probe lattice level deformation mechanisms in-situ. This work was performed under the auspices of the U.S. Department of Energy by University of California, Lawrence Livermore National Laboratory under Contract W-7405-Eng-48. The project (06-SI-004) was funded by the LDRD Program at LLNL.

Recrystallization Texture: Retrospective vs. Current Problems

Recrystallization I

Room: Rangos 2

Session Chair: Michael Kassner, University of Southern California

1:45 PM

(ICOTOM-S10-001-2008) Influence of Taylor Factor M Value on Recrystallization of the Cube and Cube-family Grains of FCC Metal

H. Masui*, Teikyo University, Japan

It is known that main recrystallization texture of fcc metal (aluminum, copper, brass, etc.) after cold rolling is $\{100\}\langle 001 \rangle$ (cube). One of recent studies of mechanism for the cube recrystallization is related with existence of the cube oriented bands with the cube and cube-family oriented grains in hot band which may remain as a nucleus in cold band. This theory seems to be supported by many observations with EBSP method which showed that around the recrystallized cube grains there are still abundant cube-family recrystallized grains of such indiscrete orientation as $\{100\}\langle 013 \rangle$, $\{100\}\langle 012 \rangle$ and further $\{015\}\langle 100 \rangle$, $\{013\}\langle 100 \rangle$, $\{012\}\langle 100 \rangle$ and $\{034\}\langle 100 \rangle$, etc. One of the reasons why the cube oriented and the cube-family grains more easily recrystallize than other orientation grains was so supposed that subgrains within the cube bands have a size advantage

compared with subgrains of other orientations. Why do they recover sooner than other orientations? The present study calculated Taylor orientation factor M value which is defined as M i.e. $\sum \gamma$ divided by $d\epsilon$ (here, γ : shear strain, ϵ : normal strain) and is believed to indicate how much dislocation density generates at unit normal strain in cold rolling. In this study, it has been made clear that the distribution of the smallest M value of fcc metal under cold rolling is spotted just on the cube $\{100\}\langle 001\rangle$ orientation in ODF coordinates. For example, the cube $(010)[001]$ ($\phi_1=90, \Phi=90, \phi_2=0$) has the least M value of 1.7 in fcc metal under cold rolling and M value indiscretely increases up to 2.2 from the cube, $(010)[001] \rightarrow (010)[106] \rightarrow (010)[103] \rightarrow (010)[102] \rightarrow (010)[203] \rightarrow (010)[9,0,11]$ with increase of ϕ_1 and $(010)[001] \rightarrow (160)[001] \rightarrow (130)[001] \rightarrow (6,13,0)[001]$ with increase of ϕ_2 . The result that the cube and the cube-family have indiscrete lower M value than other orientation may support partly the fact that each of the cube and cube-family recovers sooner than other orientation in annealing. M value in fcc metal under cold rolling increases finally up to 4.7 with $\{110\}\langle 110\rangle$ orientation. The present report also introduces the distribution of M value of bcc metal in the ODF coordinates under cold rolling for comparison.

2:00 PM

(ICOTOM-S10-002-2008) Influence of Grain Boundary Mobility on Texture Evolution during Recrystallization

M. Winning*, D. Raabe, Max-Planck Institute for Iron Research GmbH, Germany

Recrystallization is one of the most effective ways to change the microstructure as well as the properties of crystalline materials. On one hand primary static recrystallization is defined by nucleation and growth, whereas the growth takes place by the motion of high angle grain boundaries. On the other hand it is known that even low angle grain boundaries are able to move and therefore able to contribute to microstructural changes. But although there is some experimental evidence that low angle grain boundaries can play a role during recrystallization the influence of low angle grain boundaries are usually not taken into account neither in experimental investigations nor in simulations of the recrystallization process. In general, recrystallization models discriminate between three different types of grain boundaries: low angle grain boundaries which are immobile, random high angle grain boundaries which are mobile and sometimes also some special grain boundaries with a higher mobility than the random grain boundaries. The aim of this study is to investigate the influence of different mobilities for low and high angle grain boundaries on the microstructure and texture evolution during recrystallization of deformed Al single crystals by using a cellular automaton model.

2:15 PM

(ICOTOM-S10-003-2008) Effect of External Constraint and Deviation from Ideal Orientation on Development of Rolling Texture in Pure Aluminum Single Crystal having $\{001\}\langle 100\rangle$ Orientation

K. Kashiwara*, Wakayama National College of Technology, Japan; H. Inagaki, INATEX, Japan

The development of rolling texture was studied by an X-ray diffraction method using two kinds of aluminum single crystal specimens, which had an initial crystal orientation of $\{001\}\langle 100\rangle$ and an initial crystal orientation deviated by 5° about the rolling direction from the ideal $\{001\}\langle 100\rangle$. These specimens were embedded in polycrystalline aluminum frames to apply constraint in the transverse direction. These were unidirectionally cold-rolled to obtain rolling thickness reductions between 30% and 95%. The other specimens were cold-rolled without the external constraint to the same thickness reductions. In specimens having the $\{001\}\langle 100\rangle$ orientation rolled without constraint, both clockwise and counterclockwise crystal rotation with respect to the transverse direction took place in the mid-thickness region, resulting in the change in the main component to $\{102\}\langle 201\rangle$ after 70% thickness reduction. Upon further cold

rolling, crystal rotation occurred about both the rolling and the normal directions, such that after 90% cold rolling $\{112\}\langle 312\rangle$ became the main orientations. In the specimens having the same orientation rolled with constraint, such rotation was suppressed and only crystal rotation toward $\{102\}\langle 201\rangle$ was observed. In both cases, the orientation density of $\{001\}\langle 100\rangle$ decreased dramatically with increasing rolling thickness reduction and the texture became random after 95% thickness reduction. The texture of the specimens deviated by 5° from the ideal $\{001\}\langle 100\rangle$ rolled without the constraint was composed of two main orientations at 50% thickness reduction, which were characterized by resultant rotations about the transverse, rolling and normal directions with respect to the initial orientation. The two main orientations reached $\{123\}\langle 634\rangle$ at 95% thickness reduction without passing through $\{110\}\langle 001\rangle$ and $\{110\}\langle 112\rangle$. In order to realize crystal rotation from $\{001\}\langle 100\rangle$ to $\{123\}\langle 634\rangle$ in rolling, the $\{100\}\langle 001\rangle$ single crystal should have the initial orientation deviated by 5° from the ideal orientation, and in addition be rolled without constraint.

2:30 PM

(ICOTOM-S10-004-2008) Modeling Tandem Rolling in Commercial Aluminum Alloys including Recrystallization Simulation Using a Cellular Automata Method

C. Schäfer*, V. Mohles, G. Gottstein, Institute of Physical Metallurgy and Metal Physics, Germany

The aim of this work was to model the texture and microstructure evolution during tandem hot rolling of commercial Al-alloys. A recrystallization model simulating the progress of recovery and recrystallization and the accompanying texture and microstructure changes is linked to deformation and microchemistry models. For the simulation of recrystallization a cellular automaton (CORE) code is used, which provides a spatially resolved microstructure consisting of cells. Hence, it enables data transfer on the grain scale between deformation and recrystallization cycles. That makes CORE a preferred choice to model the interstand recrystallization between subsequent tandem hot rolling passes. Since CORE is a pure growth model, separate nucleation models are required to describe the occurring nucleation mechanisms. The deformation behavior is modeled by means of the advanced deformation texture model GIA-3IVM, based on a multi-grain approach which incorporates further the work hardening behaviour described in terms of the evolution of dislocation densities. The influence of precipitation during annealing is considered by linking the recrystallization model to the precipitation model ClaNG, which allows tracking potential changes in Zener drag and solute drag. The material softening due to recovery can be modeled by the same evolution equations that are used in the hardening model 3IVM. Further, the influence of heating rates on recovery has been addressed, which is important especially for low heating rates e.g. during batch annealing, when a considerable amount of recovery takes place, which can dramatically reduce the driving force. The presented recrystallization model CORE allows the exchange of microstructure and texture related information on a grain scale, which yields improved predictions of the Cube texture strength. The presented modeling setup enables a virtual complete thermo-mechanical process cycle by computer simulations. In the present work the through-process model scheme has been successfully applied for the prediction of recrystallization texture evolution during hot rolling in the alloy AA3103.

2:45 PM

(ICOTOM-S10-005-2008) Simulation of Grain Coarsening Process Referring to Orientation Coordination at Encroaching Front

K. Ito*, Nihon University, Japan

The development of recrystallization textures must be controlled by movement of multiple junction points of boundaries. A simulation of the process has been tried by a current personal computer. A specimen was presented by a two dimensional array of points with or without translational symmetries. A point possessed one of eight orientation numbers and one grain number. Its energy was expressed by

Abstracts

a number of neighbouring points different in orientation in the first nearest and the second nearest neighbourhood of the square lattice and a number of dissimilar orientation numbers there. The specimen was fulfilled by initial grains uniform in size and spatial orientation distribution. When points belonging to grain A and possessing non zero energy, or points on the A side front line, happen to be adjacent to points on the B grain side front line, a point in the A side may replace with its orientation and grain number those of one of neighbouring points in the B side. Points on front lines were list-upped. A target point was selected in random order from this list. A counter point different in orientation from it was in random order sought in its neighbourhood. The occupation or replacement of the target point by a candidate point selected from possible counter points was decided after change in energy of a local area. Either if the occupation was not allowed for zero energy change or when both occupation and energy of point were considered in the first nearest neighbourhood only, structures fell into a net work of traps of local energy minimum. The trap can be mostly destroyed by relaxing the occupation conditions. Unbreakable trapping structures, however, have been found that reflect symmetries of the model. The computing time can be reduced if points are dynamically thinned with coarsening of grains. In the model, the occupation process that represents details of the multiple junction points is expressed by orientation distribution in the local area containing $(5 \times 5 =) 25$ points. Development of the orientation distribution in a specimen is realized by a sequence of probability events being controlled both by its initial pattern and the occupation process.

3:00 PM

(ICOTOM-S10-006-2008) Subgrain Coarsening as a Function of Texture Component in 3D Digital Microstructures in AA5005

S. Wang*, A. D. Rollett, Carnegie Mellon University, USA

Monte Carlo simulations were performed on 3D digital microstructures based on hot-rolled AA5005 aluminum alloy EBSD observations, such as subgrain size distribution, subgrain aspect ratio statistics, texture components, misorientation distribution function (MDF) and orientation distribution function (ODF). From EBSD characterization, subgrain sizes and shapes vary between the different texture components. Cube components (cube bands) have the largest subgrains, followed by Brass and S. Therefore, different texture components are likely to exhibit different rates of subgrain coarsening, which in turn can lead to different rates of nucleation of recrystallization, especially if abnormal grain growth takes place. In addition to simulating the behavior within individual texture components, combinations of different texture components are modeled.

3:15 PM

(ICOTOM-S10-007-2008) Avoiding Roping and Ridging Phenomena in AA 6XXX Aluminium Sheet

T. Bennett*, Netherlands Institute for Metals Research, Netherlands; R. H. Petrov, Ghent University, Belgium; L. A. Kestens, Delft University of Technology, Netherlands

Roping and ridging phenomena are investigated in AA 6XXX sheet alloys. Microstructural and textural characterization via electron backscatter diffraction (EBSD) was conducted on samples of four classes of alloys in the as-received condition, with the objective of determining the mechanisms that lead to the occurrence of the surface peaks and valleys characteristic of these phenomena. Profilometry measurements reveal that samples of the low roping material have lower surface roughness values compared to high roping materials. Comparison of low roping material with and without 15% stretching revealed no significant differences in the grain size distributions. The same is true for high roping materials with and without 15% stretching. However, a detailed analysis of the surface texture of each of these materials reveals bands of $\{100\} \langle 001 \rangle$ Cube-oriented grains parallel to the rolling direction (RD) and which propagate along the transverse direction (TD). The population of the bands decrease with 15%

stretching in the low roping materials. The converse is true in the case of the high roping materials, where the population of Cube-oriented grains in the bands increases with 15% stretching, consistent with an increase in the Cube intensity in the $f_2 = 0^\circ$ section of the orientation distribution. These findings suggest, as previously shown in the literature, that the roping and riding phenomena in these AA 6XXX sheets are controlled by the banding of Cube-oriented grains in the initial (pre-deformed) material.

4:00 PM

(ICOTOM-S10-008-2008) Texture Modification in Asymmetrically Rolled Aluminum Sheets

J. Sidor*, A. Miroux, Netherlands Institute for Metals Research, Netherlands; R. Petrov, Ghent University, Belgium; L. Kestens, TU Delft, Netherlands

The plastic anisotropy of flat metal products is strongly affected by the crystallographic texture. In textured materials, such as commercial aluminum alloys, the Lankford value (r-value) is highly anisotropic while the average still remains below 1 which is quite low compared to that of steel. Theoretical calculations based on crystal plasticity programs show that material with a FCC crystal structure produces a strong $\{111\}/ND$ fibre texture during shear deformation with average r-values comparable to steel. The shear deformation in flat products can be imposed by asymmetric rolling (ASR). This is a rolling process in which the diameters of working rolls are different and in this way could provide an alternative process for texture control of a rolled sheet. The possibilities of the asymmetric rolling process are modeled by crystallographic texture models and confronted with experimental results. It is shown that ASR process completely transforms an initially strong cube texture into a new one consisting of shear texture components at relatively low thickness reductions. The microstructure of the asymmetrically rolled and subsequently recrystallized sheets is fine grained and the recrystallization texture is considerably weaker than that of conventionally rolled sheets. Both the fine microstructure and the presence of rotated shear texture orientations developed during the recrystallization process should improve strength and the plastic anisotropy of aluminum sheets.

4:15 PM

(ICOTOM-S10-009-2008) Patterns of Deformation and Associated Recrystallization in Warm/Hot Deformed AA6022

S. Raveendra*, S. Mishra, IIT Bombay, India; H. Weiland, ALCOA, USA; I. Samajdar, IIT Bombay, India

Samples of AA 6022 were deformed at different temperatures, strain and strain rates through channel die compression. Deformed samples, though quenched immediately after deformation, had both deformed grains/bands and recrystallized grains. Using a simple criterion of grain size and in-grain misorientation developments, respective deformed and recrystallized regions could be distinguished. Deformation temperature/strain rate, or the so-called Zener-Holloman (Z) parameter, had clear effects on the deformed microstructure – in terms of orientation stability or textural changes and in terms of in-grain misorientation developments. These, in turn, strongly affected the associated recrystallization behavior – including relative contributions from particle stimulated nucleation and contributions from deformed grains/bands of different ideal orientations.

4:30 PM

(ICOTOM-S10-010-2008) Oriented Grain Growth Investigations in Annealed AlMn Alloys Using High Energy Synchrotron Radiation

C. E. Tommaseo*, H. Klein, Friedrich August Universität, Germany

Annealed AlMn alloys with different amounts of manganese (0.4; 0.7; 1 wt-%) were analysed with unique texture and microstructure imaging techniques with high orientation and location resolving power using high-energy synchrotron radiation in combination with an area detector [1,2,3]. Results obtained from the location and orientation scanning methods allowed to get grain size measurements in dif-

ferent crystallographic directions with good statistic and texture measurements with high angular resolving power. The grain size distribution analyses from the location scans reveal finally information about grain shape and grain size frequency in the different crystallographic directions and make it possible to deduce information about oriented grain growth. The measurements with high orientation resolving power, in comparison to conventional texture goniometer measurements, allow to determine the orientation of single grains. The different strong texture components in the orientation distribution functions could be mathematically transformed [4] to backtrack all grains in reflection under two specific pole figure angles $\{\omega, \gamma\}$ in order to analyze in which correlation the grain growth and the changing texture components could be put. The combination of the location and orientation scanning methods allow beneath measurements with high location and orientation power, a good statistic of grain size distributions in different crystallographic directions, resulting in grain growth in correlation with the changing texture components with increasing annealing time and manganese content, which could be relevant for the determination of material properties. [1] H.J. Bunge, H. Klein, L. Wcislak, U. Garbe, W. Weiss, J.R. Schneider, *Textures and Microstructures* 35, 253-271 (2003). [2] H.J. Bunge, L. Wcislak, U. Garbe, J.R. Schneider, *J. of Applied Cryst.* 36, 1240-1255 (2003). [3] H. Klein, A. Preusser, H.J. Bunge, L. Raue, *Mat. Science Forum*, Vol. 467-470, 1379-1384 (2005) [4] H.J. Bunge, H. Klein, *Z. Metallkd.* 87, 465-475 (1996).

4:45 PM

(ICOTOM-S10-011-2008) Analysis of the Texture and Mean Orientation of Aluminium Alloy AA5052 Subjected to Forward and Reverse Hot Torsion and Subsequent Annealing

O. Hernandez-Silva*, B. P. Wynne, M. Rainforth, The University of Sheffield, United Kingdom

In commercial thermomechanical processing metals and alloys are often subjected to complex deformation histories, including changes in the strain rate, temperature and strain path. In this work we have investigated the effect of strain path on microstructure and texture evolution of the aluminium alloy AA5052 under hot working conditions using forward and reverse torsion. The material was deformed at 300°C at a strain rate 1s⁻¹ to a total equivalent strain of 0.5 in two steps. In the first test the material was deformed to a forward strain of 0.25 followed by dropping the torque to zero followed by and forward step of strain of 0.25. In the second test the second straining direction was reversed leading to a net strain of zero. Material from both tests was subsequently annealed for 1 hour at 300°C. The microstructure and texture was then studied using electron backscattered diffraction (EBSD). We determined the mean orientation of each grain using quaternion geometry which enabled the calculation of the spread of disorientation in each grain from the mean. For the as-deformed forward/forward sample the disorientation spread was significant in each grain though no greater than 15°, whilst for the forward/reverse sample the disorientation spread was bimodal with some grains exhibiting virtually no orientation spread and others having spreads similar to the forward/forward case. This analysis has then enabled an analysis of the orientation of grains having no spread compared to those with significant spread. A similar analysis for the annealed samples will also be presented.

5:15 PM

(ICOTOM-S10-013-2008) Evolution of {111} Recrystallization Texture in Al-Mg-Si Alloy Sheets Processed by Symmetric and Asymmetric Combination Rolling

H. Inoue*, S. Kobayashi, M. Hori, Osaka Prefecture University, Japan; T. Komatsubara, Furukawa-Sky Aluminum Corp., Japan; T. Takasugi, Osaka Prefecture University, Japan

In recent years, a trend of weight reduction in automobiles is rising from the viewpoint of reducing fuel consumption and exhaust gas emission. To apply aluminum alloys to automotive body panels, it is necessary to vastly improve deep drawability of the sheet materials. In

the present study, a new rolling process consisting of conventional symmetric rolling and subsequent asymmetric rolling at relatively low reduction was adopted to increase r-value of 6xxx series aluminum alloys. The aim of this rolling process is to rotate the β -fiber texture developed during symmetric rolling around the TD-axis with shear strain by asymmetric rolling, and to form the TD-rotated β -fiber texture including {111} components favorable for improving r-value. Hot-rolled AA6022 (Al-0.55%Mg-1.1%Si) plates were cold rolled to 75-80% reduction in thickness and then asymmetrically warm rolled at 473 K to 21-33% reduction with roll-speed ratio of 1.2 to 2.0. These rolled sheets were solution treated at 813 K for 90 s and followed by water cooling (T4-treatment). Recrystallization textures of the T4-treated materials varied significantly depending on roll-speed ratio and reduction in asymmetric warm rolling. On the appropriate rolling conditions, a {111}<110> orientation was formed as a main component of recrystallization texture from the TD-rotated β -fiber rolling texture. Although deformed microstructure showed orientation distribution ranging from shear texture components to β -fiber components, the proportion of {111} and {001} oriented subgrains and recrystallized grains increased with the progress of recovery and recrystallization. From the comparison of recrystallization behavior among materials rolled under different conditions, it is suggested that a sample with smaller {001} oriented regions in deformed microstructure is more favorable for the growth of {111} recrystallized grains.

Texture in Materials Design

Texture in Materials Design III

Room: Connan

Session Chair: David Fullwood, Brigham Young University

8:30 AM

(ICOTOM-S12-027-2008) Earing, Texture and Drawing Ratio in Deep Drawing of Orthorhombic Sheets of Cubic Metals (Invited)

M. Huang, Nanchang University, China; C. Man*, University of Kentucky, USA; T. Zheng, Nanchang University, China

We examine the effects of texture and drawing ratio in the forming of four-ear cups in deep drawing of orthorhombic sheets of cubic metals. Consider a circular blank of radius R_b placed symmetrically under a blank-holder over a die with a circular aperture of radius $r_a < R_b$. A flat-headed punch of circular cross-section is forced down onto the blank, which is allowed to slip under the blank-holder and formed into a cylindrical cup. The material originally located in the annular region over the die makes up the wall of the cup. At the base of the cup we choose a polar coordinate system (r, θ) with the origin located at the center of the original circular blank and the polar axis agreeing with the rolling direction of the sheet metal (i.e., $\theta = 0$ corresponds to the rolling direction). Let $v = R_b/r_a$ be the drawing ratio and let $h(\theta)$ be the height of the cup rim above the cup base at (r_a, θ) . We define the earing-value or earing of a four-ear cup by $\varepsilon = (\sum_{k=0}^7 (-1)^k h(k\pi/4)) / (8r_a)$. We assume that the blank be rigid-plastic and observe the quadratic yield function proposed by Man (1994) for orthorhombic sheets of cubic metals, namely that which explicitly carries two material parameters and three texture coefficients. Under the assumption of plane stress in the deformation of the metal flange, we obtain an expression for $h(\theta)$ that shows explicitly the effects of v and the three texture coefficients on the angular dependence of the cup height. From this expression for $h(\theta)$ follows an explicit formula for the earing ε , where the drawing ratio v , one material parameter, and only one texture coefficient appear. The validity of this formula for ε was examined against results of cupping tests conducted on batches of commercially pure (L2Y2) aluminum blanks that had undergone various heat treatments. The texture coefficient in the formula was given the value corresponding to its through-thickness integral average as obtained by applying Simpson's rule to the five

Abstracts

values measured by X-ray diffraction at the surface and at depth $H/8$, $H/4$, $3H/8$, and $H/2$, respectively, where H is the thickness of the sample. The formula for the earing ε was largely corroborated by the experimental results.

9:00 AM

(ICOTOM-S12-028-2008) Texture Development in a Nanocrystalline Al-alloy

B. Ye, B. S. Majumdar*, New Mexico Tech, USA; S. Vogel, Los Alamos National Laboratories, USA; V. Seetharaman, T. Watson, Pratt & Whitney, USA

Rapidly solidified powders of a nominal Al-4Y-4Ni alloy were consolidated by extrusion. Microstructural analysis showed that the alloy contained approximately 70 volume percent of pure Al of around 200 nm grain size, 25% of orthorhombic Al₁₉Ni₅Y₃ phase, and about 5% of Al₃Y phase. The ternary Al₁₉Ni₅Y₃ phase was in the form of platelets of 40-60 nm thickness, and in-plane dimension of 100-150 nm. The lattice parameters of this phase were: $a=4.06\text{\AA}$, $b=15.91\text{\AA}$, $c=27.12\text{\AA}$, and the [001] axis aligned along the thickness direction of the platelets. The extruded material revealed a fairly strong texture (~ 3.5 mrd) for the ternary phase, with the (100) pole preferentially aligned along the extrusion axis and the (001) pole perpendicular to the axis. In contrast, the Al-phase exhibited a relatively weak texture (1.6 mrd), with the (111) pole along the extrusion direction. Nevertheless, the (111) texture is in agreement with known fiber texture for Al-alloys. The extruded material was further forged at about 350 C by simple compression along the original extrusion direction. Texture measurements using neutron diffraction technique showed that the (001) pole now aligned along the compression direction. The reason for this rotation is not clear, although it may be mentioned that the platelet size decreased following forging, suggesting that some fracture may have occurred. Perhaps the most intriguing aspect of the texture was the development of a cube texture for the Al-phase with the (100) pole along the compression axis, which is different from the ideal {110} texture in fcc materials under simple compression. Cube texture is only observed in Al-alloys following recrystallization of cold worked material. It has also been observed in Al-2Mg alloys when compressed at 400 C at low strain rate, and this has been attributable to dynamic recrystallization. On the other hand, there is no report of dynamic recrystallization in pure Al. Thus either the nano size of the grains or the nano size of the relatively high volume fraction of precipitates appear to alter the normal texture evolution in such nano-crystalline alloys. Results from ongoing research in understanding the texture evolution will be presented.

9:15 AM

(ICOTOM-S12-029-2008) Texture Development of Molybdenum Sheets during Last Steps of Heat Treatment

W. Skrotzki, C. Oertel*, I. Hünsche, W. Knabl, A. Lorich, Technische Universität Dresden, Germany

Molybdenum is a refractory metal with special properties, like an excellent high temperature creep strength, a low coefficient of thermal expansion and a high Young's modulus. In sheet or ribbon form molybdenum is widely applied as electrodes, heating elements and ideal substrate material for many technological applications, such as electronics, electric power, lighting technology, nuclear energy and even aerospace engineering. To produce workpieces the material has to be thermomechanically processed producing characteristic deformation and recrystallization textures depending on the deformation and/or annealing conditions. The present work concentrates on the influence of annealing during the last steps of heat treatment on the texture development of selected sheets and strips of molybdenum. Usually, unidirectional cold rolling in the last stage of production leads to a strengthening of the main texture component, which for molybdenum is the rotated cube component. This component leads to a strong anisotropy of the mechanical properties in the sheet plane. Therefore, for three intermediate annealings four final heat treatments were done in

each case in order to change the texture. The texture development during these annealing stages is discussed on the basis of microstructure investigations, texture and EBSD measurements. A model explaining the microstructural and textural changes observed will be presented.

9:30 AM

(ICOTOM-S12-030-2008) Development of High Strength, Low Magnetism and Strongly Cube-textured Composite Ni-7%W/Ni-10%W Substrate for Coated Superconductor

D. Liu*, Beijing University of Technology, China

Ni-W alloys are preferred as substrates for the preparation of YBa₂Cu₃O_{7- δ} tapes due to its reduced magnetization losses and improved mechanical strength. It has been confirmed that the magnetization intensity decreases strongly with the addition of W. Curie temperature is suppressed to below 77 K at W content more than about 9.5at.% and hysteretic losses are negligible at W content about 7.5 at.% at 77 K. However, the cube fraction in structure was found to decrease with W content >5 at.%. This is attributed to the transition in the rolling texture from copper type to brass type caused by the SFE decreasing with increasing W content. In addition, the low tensile yield strength of Ni-W alloy with low W content (3~5at.%) limits the processing to produce thin tapes. For these reasons the preparation of substrate material with low magnetism and high strength is important. In this paper, we studied on the development of Ni-7at.%W/Ni-10at.%W composite substrates fabricated by Spark Plasma Sintering, a new kind of powder metallurgy technique. After heavy cold-rolling and recrystallization annealing, sharp cube-textured Ni-7at.%W/Ni-10at.%W composite foils with high strength and low magnetism were obtained. Deformation and recrystallization textures of composite foils were studied systematically. The magnetic and mechanical properties of Ni-W composite foils were also reported.

9:45 AM

(ICOTOM-S12-031-2008) Effect of Deformation Constraints on the Texture Formation in Al-5mass%Mg Solid Solution at High Temperatures

K. Okayasu, M. Sakakibara, H. Fukutomi*, Yokohama National University, Japan

The authors have been investigated the deformation behavior and texture formation of Al-3mass%Mg solid solution by the high temperature uniaxial compression. The main component of the fiber texture was {011} (compression plane) in the early stage of deformation, followed by {011}+{001} and finally {001}, when the viscous motion of dislocations is the dominant mechanism of deformation. It was suggested that the development of {001} component should be attributed to the preferential grain boundary migration effective for the growth of {001} grains. In this study, the effect of deformation constraints on the texture development is investigated, in order to understand the preferential growth of {001} grains in the uniaxial deformation. Uniaxial compression deformation and plane-strain compression deformation was conducted on Al-5mass%Mg alloy at 673K and 723K in air. The strain rate was 0.0005/s and true strains were in the range between -0.3 and -1.2. Texture measurements were conducted on the mid-plane section of the specimen by the Schulz reflection method using Cu K α radiation. Orientation distribution function (ODF) was calculated by the Dahms-Bunge method. Textures were examined on the basis of pole figures and inverse pole figures derived from ODF. EBSD measurements were conducted to evaluate the spatial distribution of the texture component. The measurements were performed in four micrometers interval. The results are summarized as follows. 1) Uniaxial compression deformation results in the development of {001} (compression plane) component with the pole densities more than eight times of their average pole densities at 673K and 723K. 2) Plane-strain compression deformation at 673K generates the preferential alignment of <001> along the rolling direction at the beginning of deformation, followed by the development of <001> along the normal direction.

10:30 AM

(ICOTOM-S12-032-2008) Multiscale Modeling of Equal Channel Angular Extruded Aluminium with Strain Gradient Crystal Plasticity and Phenomenological Models

L. Duchêne*, University of Liège, Belgium; M. Geers, M. Brekelmans, Eindhoven University of Technology, Netherlands; A. Habraken, University of Liège, Belgium

The ECAE process (Equal Channel Angular Extrusion) is utilized to modify the microstructure of the AA1050 material in order to process an ultra fine grained material. This contribution assesses the performance of different numerical models for an accurate modelling of ECAE processed aluminium. Due to the severe plastic deformation undergone by the material during the ECAE process, the subsequent behaviour of the material is non-conventional and difficult to model with classical constitutive laws (e.g. ECAE aluminium presents a large initial back-stress which must be adequately incorporated in the model). In order to identify the mechanical properties of the produced material, several mechanical tests were carried on. Several monotonic loading paths have been investigated: torsion, compression and tensile tests. Complex strain paths were also analysed: tensile test followed by compression and tensile test followed by torsion. A polycrystalline texture based computational model with and without texture evolution is investigated. This model is coupled with the Teodosiu and Hu hardening model. The anisotropy and the particular hardening of the ECAE aluminium can be captured by this model. A single crystal strain gradient plasticity model is also scrutinized in this research. This model uses as internal variables the densities of statistically stored dislocations (SSD) and geometrically necessary dislocations (GND). The evolution of the SSD densities is based on a balance between dislocation accumulation and annihilation rates depending on the slip rates. The GND densities on the other hand result from the incompatibilities in the crystal lattice due to gradient of the dislocation slip. Both GND and SSD densities are taken into account for the isotropic hardening of the material. The GND densities naturally induce a physically based kinematic hardening through their internal stresses (i.e. the back-stress, computed as a function of the GND densities gradient). The results provided by these numerical models are compared to the experimental results.

10:45 AM

(ICOTOM-S12-033-2008) Simulation of Texture Development in Pure Aluminium Deformed by Equal Channel Angular Pressing

M. Hoseini*, L. Hualong, J. Szpunar, McGill University, Canada; M. Meratian, Isfahan University of Technology, Iran

Texture simulation procedure for multi-pass equal channel angular pressing (ECAP) was studied by using a computer texture simulation based on Visco Plastic Self Consistent modeling. The program inputs were initial texture and loading condition and the output was texture after deformation. The simulation was done for each individual pass of ECAP and the results were compared with experimental texture results of commercially pure aluminum processed by ECAP. For simulation of first pass, X-ray measured texture of aluminum rod before ECAP was used as input data. Simulation of each pass after that was carried out by using input data from previous simulation and rotating this texture for different routes in ECAP. There was good agreement in peak position between experimental and simulated pole figures after first and second passes.

11:00 AM

(ICOTOM-S12-034-2008) Texture Evolution in Tantalum Processed by Equal Channel Angular Pressing

J. W. House*, P. J. Flater, Air Force Research Laboratory, USA; J. M. O'Brien, O'Brien and Associates, USA; W. F. Hosford, University of Michigan, USA

Current ingot refinement and solidification techniques used in pure tantalum processing often result in a heterogeneous microstructure which produces inconsistent mechanical properties.

An example of the heterogeneous structure is the texture banding observed in forged tantalum disks. These bands alternate between regions that are dominated by $\langle 100 \rangle$, or $\langle 111 \rangle$, oriented grains relative to the plate normal. The current study examined how severe plastic deformation of pure tantalum via equal channel angular pressing (ECAP) effects the physical and mechanical properties. The materials of interest are 63 mm (2.5-inch) diameter round bar of pure tantalum supplied by H.C. Starck and Cabot Supermetals. Three metallurgical conditions were examined for each material: as worked, fine-grain annealed, and large-grain annealed. Prior to annealing, each bar was processed eight times through a 135-degree ECAP die using route C (180 degrees rotation between each pass) and then forged into 6.3 mm (0.25-inch) thick plates. Specimens were subsequently removed from the plates for low and high strain rate mechanical properties experiments. Orientation dependence was characterized by orienting specimen load axes through the thickness or in the plane of the forged plate. The crystallographic texture was characterized by orientation imaging microscopy. These data showed the effects of thermo-mechanical processing on the texture evolution. The texture analysis is used to interpret the anisotropic mechanical properties that are observed in the material.

11:15 AM

(ICOTOM-S12-035-2008) Textures in Nb Processed by Equal Channel Angular Extrusion

S. Balachandran*, K. T. Hartwig, R. B. Griffin, Texas A&M University, USA; T. Bieler, D. Baars, Michigan State University, USA; R. E. Barber, Shear Form Inc., USA

High purity niobium (Nb) is fabricated into large aperture bellows-shaped tubular cavities for superconducting radio frequency particle accelerators. For this application, the microstructural characteristics of the Nb strongly influence the quality of the product. Conventionally processed materials commonly have significant textural and microstructural gradients that can cause unusual and irreproducible anisotropic behavior. A fine-grained and uniform microstructure with favorable texture translates into better formability and product performance. In order to obtain such material, 25 mm square bars of niobium were processed via a severe plastic deformation process (SPD) called equal channel angular extrusion (ECAE), rolled into sheets and annealed. The SPD processing was done to refine the grain size, reduce microstructure and texture inhomogeneities, and enable development of a preferred texture. Texture results are reported for as-processed and recrystallized bar and sheet at different stages of processing. The variables examined include Nb purity, ECAE route and heating rate of recrystallization annealing.

11:30 AM

(ICOTOM-S12-036-2008) Solute, Superplasticity and Texture change in Aluminium Alloys

K. Sotoudeh*, P. Bate, J. Humphreys, The University of Manchester, United Kingdom

There are several aluminium alloys which exhibit high tensile ductility at slow strain rates and elevated temperatures. This superplasticity is due principally to a high sensitivity of flow stress to strain rate. It is well known that a fine grain size is needed for this to occur, but in addition it appears that a relatively high level of solute, such as copper or magnesium, is also required. This has been investigated in Al-Cu-Zr alloys with different copper contents and Al-Mg-Mn alloys with different magnesium contents. In both cases, low solute materials were not superplastic. They also exhibited texture change during uniaxial tension essentially consistent with that expected with simple octahedral slip as the deformation mechanism. In the high solute, superplastic, alloys there was a significant divergence of preferred orientation. This orientation divergence is the main microstructural characteristic associated with the superplasticity: other factors such

Abstracts

as dynamic grain growth occurred in non-superplastic alloys. The degree of boundary sliding and relative grain translation was very limited and did not differentiate the superplastic alloys either. The possibility that rate sensitive dislocation slip can explain the texture changes is discussed.

11:45 AM

(ICOTOM-S12-037-2008) Effect of Microstructure in Thermoelectric Nanodots, Nanowire Composites, and Polycrystalline Materials

R. Garcia*, Purdue University, USA

Thermoelectric generators are devices that can directly convert heat into electricity. While these devices have been historically used in niche applications such as satellites and nuclear reactors, potential applications include the optimization of gas engines, solid oxide fuel cells, etc., by harvesting the heat that these devices dissipate and transforming it into useful work. The response of thermoelectrics is characterized through ZT, the figure of merit, which is a function of several bulk material properties: the thermal conductivity, the electrical conductivity, and the Seebeck coefficient. For most materials, these properties are a function of temperature, can be strongly anisotropic, and highly dependent on their underlying topology. Features such as grain size, texture and grain boundaries all impact the associated macroscopic ZT. Some of these mesostructural features can be controlled by using novel processing techniques, leading to structures of dramatically different dimensionality and thus potentially enhanced properties. Such structures include nanodots (zero-dimensional), nanowires (one-dimensional), films (two-dimensional), and bulk (three-dimensional). In this paper, the effect of geometrical confinement on the thermoelectric figure of merit is analyzed in an effort to understand the relations of size and dimensionality to the macroscopic response. The effect of crystallographic texture and grain size was studied. Optimal microstructures and morphologies are proposed.

12:00 PM

(ICOTOM-S12-038-2008) Drawability and Texture Change of Asymmetry Rolled Al Alloy Sheets

I. Kim*, S. Akramov, H. Jeoung, Kum Oh National Institute of Technology, South Korea

The preferred crystallographic orientations (texture) of the metals are related to the physical, mechanical properties, and drawability of sheet metal forming. In this study, texture evolution and drawability are investigated after asymmetry rolled and subsequent heat treated various types of aluminum alloy sheets. The specimens after asymmetry rolling showed a very fine grain size and the specimens after asymmetry rolling and subsequent heat-treatment were increased the ND // <111> texture component. One of the most important properties in sheet metals is drawability. The r-value or plastic strain ratio has been used as a parameter that expresses the drawability of sheet metals. The change of the plastic strain ratios after asymmetry rolling and subsequent heat-treatment conditions have been investigated and it were found that they were about two times higher than those of the original Al sheets. These could be attributed to the formation of ND // <111> texture components texture components through asymmetry rolling in Al sheets.

12:15 PM

(ICOTOM-S12-039-2008) Processing of Straight and Sheared Layers in Alternating Al and Al(0.3%Sc) ARB Sheets

M. Z. Quadir*, O. Al-Buhamad, L. Bassman, M. Ferry, The University of New South Wales, Australia

High purity Al sheet was roll bonded with Al containing 0.3% Sc in super saturated solid solution (and plus aged) condition. A controlled post ARB heat treatment produced lamellar structures containing 32 alternating layers of recrystallized and recovered substructures in 0.5mm thick sheet. Massive through thickness shear bands were oper-

ated in Aged ARB sheet and the amount is quantified and explained by the relative hardening rate of the candidate materials. Coarse lamellar bands of 0.7-1.00 μm was produced in Al layers in either ARB sheets, whereas the lamellar bands in Al(Sc) is relatively finer <0.30 μm . Annealing at 350C of both ARB sheets lead to complete recrystallization in Al layers and kept the Al(Sc) layers with a relaxed structures comprised of submicron grains. The recrystallization textures of Al layers in super saturated ARB sheet was measured as Brass free β fibre texture, which is more randomized in Aged ARB sheet. The deformation and annealed microstructures and textures were investigated using focused ion beam (FIB) channelling contrast imaging, electron backscatter diffraction (EBSD) and transmission electron microscopy (TEM).

Texture Effects on Damage Accumulation

Damage Accumulation I

Room: Connan

Session Chairs: Hasso Weiland, Alcoa Technical Center; Jean-Yves Buffiere, Universite de Lyon

1:45 PM

(ICOTOM-S13-001-2008) Experimental Characterisation of the Effect of Crystallography on the Three Dimensional Nucleation and Growth of Fatigue Cracks in Metals (Invited)

J. Buffiere*, H. Proudhon, E. Ferrie, W. Ludwig, Universite de Lyon INSA-LYON MATEIS CNRS UMR5510, France

This paper presents results on the experimental characterisation of the influence of crystallography on fatigue crack nucleation and growth in the interior of metallic materials. Synchrotron X ray tomography has been used to study fatigue mechanisms leading to crack initiation and growth inside various aluminium alloys. Classical surface observations have been complemented by three dimensional (3D) post mortem and in situ characterization. Thanks to a Gallium infiltration technique it is possible to obtain 3D images of grains in the interior of the material, allowing to study the interaction of the fatigue cracks with the local microstructure on the crack front. Experimental data on the configuration of the front of a crack as it enters new grains have been obtained: a tilt and twist of the crack plane seems to delay the crack front propagation as compared to a simple tilt. Moreover, grain boundaries also appear to act as efficient barriers for crack retardation. Quantitative data can be extracted from the reconstructed images of the propagating crack such as the crack growth rate at different positions along the crack front. It is also shown that the influence of grains on the crack path can be strongly dependent of the local stress state.

2:15 PM

(ICOTOM-S13-002-2008) Fatigue Crack Initiation Behaviour during Thermomechanical Cyclic Loading in Austenitic Stainless Steel

M. Ramesh*, H. J. Leber, Paul Scherrer Institute, Switzerland; K. Kunze, M. Diener, R. Spolenak, Swiss Federal Institute of Technology (ETH), Switzerland

Fatigue and fracture behaviour of austenitic stainless steel (ASS) under relevant light water reactor (LWR) conditions evoked consistent interest through the years. Many components of nuclear power plants made of ASS like primary coolant circuits are subjected to very sharp thermomechanical loadings, due to incomplete mixing of flows at different temperatures. Most studies deal with this problem under isothermal conditions which is not the case in service, and less attention has been paid to thermomechanical fatigue (TMF). This work concerns the micromechanics of fatigue crack initiation during thermomechanical cyclic loading of these materials. The aim of this study is to understand better the interactions between grains in a polycrystalline specimen under thermal-mechanical cyclic loading by investi-

gating strain heterogeneity at macroscopic and microscopic level after deformation. Particular attention is placed on micromechanics at grain scale prior to and during fatigue crack initiation. Specimens prepared from commercial tube and pipe ASS are characterized for surface relief evolutions via atomic force microscope (AFM). The microstructure is analyzed by scanning electron microscope (SEM) in conjunction with electron backscatter diffraction method (EBSD) in order to correlate crack initiation with crystallographic orientations of concerned grains.

2:30 PM

(ICOTOM-S13-003-2008) 3D Observations of Fatigue Crack Initiation sites in 7075-T651 Aluminum Alloy

S. D. Sintay*, T. Nuhfer, Carnegie Mellon University, USA; H. Weiland, ALCOA Technical Center, USA; A. Rollett, Carnegie Mellon University, USA

Several two-hole fatigue specimens of 7075-T651 Aluminum were subjected to spectrum loading with sufficient cycles to initiate fatigue cracks. The fatigue loading was stopped prior to final failure and the specimen fractured under tension such that the fracture surface can be observed. Overloads in the spectrum act effectively as marker loads and many of these are characterized with SEM microscopy. In addition, micro-milling and ion milling are coupled with OIM to obtain 3D microstructure observations of the fatigue crack initiation sites. The influence of texture and microstructure topology on fatigue crack initiation and short crack growth kinetics are explored.

2:45 PM

(ICOTOM-S13-004-2008) Local Characterization of Void Initiation on IF Steel by FIB-EBSD Technique

O. León García*, Netherlands Institute for Metals Research, Netherlands; R. Petrov, Ghent University, Belgium; L. Kestens, Delft University, Netherlands

The rigid and well-bonded cubically shaped titanium-nitride or carbo-nitride particles have been identified as void initiation sites for the ductile failure process of IF steels. A three-dimensional characterization of the particle deformation zone prior and after the void initiation is conducted using the novel FIB-EBSD technique which allows acquiring three-dimensional information of the crystal orientation coupled with 3D spatially resolved data of the microstructure. The particles and their surrounding zone were investigated in tensile test samples. There was no evidence of void initiation after an elongation up to a strain of 0.3. At a tensile strain of 0.34 ferrite/particle debonding was observed close to one corner of the cubical particles. A geometrical and crystallographic description is reported of the substructures appearing in the particle deformation zone giving rise to the nucleation of microvoids.

3:00 PM

(ICOTOM-S13-005-2008) Determination of Geometrically Necessary Dislocation Densities Using Diffraction-based Orientation Determination Techniques: Application to Crack Tip/wake Plasticity

V. K. Gupta*, Y. Ro, S. R. Agnew, University of Virginia, USA

Recently, diffraction-based techniques such as electron back-scattered diffraction (EBSD) and micro-Laue diffraction have been employed to measure localized lattice curvatures in plastically deformed materials. Fundamental continuum dislocation theory can be used to link measured lattice curvatures and elastic strain fields with the dislocation density (Nye) tensor. Notably, the dislocation densities measured are denoted geometrically necessary dislocations, but the authors stress that this is a scale-dependent terminology that must be carefully qualified for a given problem (i.e., size of Burgers circuit.) With that caveat, an examination of the potential to extract the geometrically necessary dislocation densities of particular slip systems/character using the components of Nye dislocation density tensor will be presented. As an application of the developed approach, we consider the geometrically necessary dislocations at the crack tip/wake. Recent experimental results obtained using EBSD,

micro-Laue and transmission electron microscopy (TEM) techniques from fatigue cracked aluminum alloy 2024 have shown the grain-to-grain variation in plasticity in the vicinity of crack wake. These variations are presently considered to arise due to the orientation dependence of slip system activation during fatigue loading, however, more subtle causes related to dislocation interactions during strain hardening/cycling are also considered.

3:15 PM

(ICOTOM-S13-006-2008) Reversible Texture Transition during Accumulative Roll Bonding

N. Kamikawa*, X. Huang, G. Winther, N. Hansen, Risø National Laboratory Technical University of Denmark – DTU, Denmark

Accumulative roll bonding (ARB) is designed to apply high strains to metal sheets, which introduces a fine microstructure and a high strength. A cycle of ARB process consists of cutting, stacking and rolling. As a result, the process involves complicated changes in strain path and strain level, where the surface layers in each cycle are subjected to extensive shear deformation while the central part experiences moderate deformation by rolling. The complexity of the ARB process further increases with the number of cycles because one of the surface layers in cycle $i-1$ becomes the center layer in cycle i while the center layers in cycle 1 to $(i-1)$ approaches the surface again. The through-thickness texture variation therefore changes in a systematic way as a function of the number of cycles. This is analyzed by electron back scatter diffraction in pure aluminum deformed by ARB from low to high strains. It is found that the texture can change reversibly between shear and rolling components, i.e., it quickly adapts to the local changes in deformation conditions. The microstructure is found to correlate with the local texture and this correlation is the basis for discussion of the subsequent annealing behavior.

4:00 PM

(ICOTOM-S13-007-2008) Texture Evolution of Cold Rolled NC Nickel as Compared to the Tvolution in Cold Rolled CG Ni

A. Kulovits*, S. X. Mao, J. M. Wieszorek, University of Pittsburgh, USA

The importance of dislocation based plasticity mechanisms has been questioned in nanocrystalline metals (NC) with average grain sizes around a critical grain size, the grain size beyond which the yield stress deviates from the commonly known Hall Petch behavior. In this study we compared the evolution of texture changes of NC Ni and coarse grained (CG) Ni with similar starting textures during cold rolling. As the texture evolution during cold rolling of CG FCC metals can be explained using dislocation mechanism based models we discuss similarities and differences in texture evolution in terms of importance of the role of dislocation mediated plasticity processes in NC vs. CG Ni. EBSD and XRD – texture measurements were used to determine the global texture in NC and CG Ni. TEM results on changes in morphology and local orientation relationships of grains were combined with findings from the texture evolution comparison.

4:15 PM

(ICOTOM-S13-008-2008) Deformation Mechanism on Submicron Pure Copper

Y. Xusheng*, L. Yandong, Key Laboratory for Anisotropy and Texture of Material (Ministry of Education), China; J. Qiwu, Factory of Cold Rolling Silicon Steel, Anshan Iron and Steel Group Corporation, China; Z. Xiang, Z. Liang, Key Laboratory for Anisotropy and Texture of Material (Ministry of Education), China

The paper studied diversities of deformation mechanism between submicron grains and conventional grains, by means of Orientation Distribution Function (ODF) and Electron Back Scatter Diffractions (EBSD), using submicron grain pure copper obtained by severe plastic deformation by means of the equi-channel angular technique and conventional grain pure copper acquired without the equi-channel angular technique as experimental materials. The experimental results showed that main components of deformed textures in the submicron grain pure copper were {-

Abstracts

110} <-1-14> and {-225} <2-32>; while main components of deformed textures in the conventional grain pure copper were {-110} <001> and {-225} <6-65>. The orientation density of them was increasing with increases of cold-rolled reduction; yet, the orientation density of the latter was smaller than that of the former. At the same time, variations of the grain boundary were differential in the two kinds of the coppers. What's more, distributions of differential angels' grain boundary existed different. Through the analysis of results above, mechanisms of the conventional grain copper were dislocation slip and twin, while mechanisms of the submicron grain copper include grain boundary sliding except for dislocation slip and twin.

4:30 PM

(ICOTOM-S13-009-2008) Evolution of Grain Boundary Microstructures in Molybdenum by Thermomechanical Processing from Single Crystals

S. Kobayashi*, Ashikaga Institute of Technology, Japan; S. Tsurekawa, Kumamoto University, Japan; T. Watanabe, Tohoku University, Japan

Fracture of brittle polycrystalline materials is predominantly caused by intergranular brittleness. The studies using molybdenum bicrystals have revealed that the intergranular fracture strongly depends on grain boundary character [1]. We have confirmed that both grain boundary connectivity and triple junction distribution (TJD) make a significant influence on crack nucleation and propagation in molybdenum [2]. Control of grain boundary character distribution (GBCD) and TJD will be essential to improvement in toughness and workability of brittle polycrystals. Improvement in bulk properties by twin-related grain boundary engineering (GBE) has been extensively reported for fcc metals with a low stacking fault energy [3]. However experimental studies on GBE of bcc metals have been little reported. The purpose of this study is to obtain a clue to GBE of bcc metals by thermomechanical processing. Molybdenum single crystals with <110> and <111> orientations were grown by a r. f. floating zone method. These specimens were uniaxially compressed at room temperature up to 80%. The deformed specimens were annealed at 1773K and 1873K for 7.2ks. The SEM/EBSD/OIM was applied to analyze recrystallized GB microstructure. It was composed of some grain-orientation clusters, in which grains possessing a similar orientation were assembled, and the orientation of clusters changed according to the initial surface orientation. The frequency of low-angle boundaries was considerably high in the grain-orientation clusters. The lower annealing temperature induced a higher frequency of low-angle boundaries in the clusters except in the {100} cluster. The frequency of percolation-resistant triple junctions against intergranular fracture increased with increasing CSL boundaries, and the connectivity of them drastically increased when the frequency exceeded about 60%. The importance of GB microstructure to control of intergranular brittleness is discussed. [1] H. Kurishita, A. Ōishi, H. Kubo and H. Yoshinaga, Trans. JIM 26 (1985), 341. [2] S. Kobayashi, S. Tsurekawa and T. Watanabe, Phil. Mag. 86 (2006), 5419. [3] S. Tsurekawa, S. Nakamichi, T. Watanabe, Acta Mater. 54 (2006), 3617.

4:45 PM

(ICOTOM-S13-010-2008) Kinetic Measurements of Texture and Microstructural Evolution Using Orientation Distribution Function and Residual Stress Relaxation

S. Saimoto*, J. Cooley, C. Gabriel, Queen's University, Canada

Recovery (ReC) and recrystallization (ReX) processes of cold rolled products were highly investigated in the 20th century but, due to the assumed complexity of the cold-worked state, systematic examination using modern texture analysis has rarely been undertaken. Although crystallite by crystallite examination will reveal the diversity of microstructure and its complexity, the evolution of a distinct ReX texture strongly suggests that statistically specific mechanisms under specific dislocated environment prominently manifest itself. Based on this premise, systematic isochronal and isothermal examination using

orientation distribution function (ODF) and line broadening determinations would reveal the primary mechanisms responsible for the resulting ReX texture. A kinetic study of an Al-Mg-Si alloy used for auto body panels reveals that cube grain nucleation and growth is highly affected by the amount of Fe solute in the matrix. The cube volume fraction decreases as the ReX temperature is increased from 250 °C to 275 °C. This type of study has been extended to AA1100 with varying amounts of Fe in solution and with nominally pure Al with varying amounts of H₂. The results reveal that the cold-worked state recovers over 70 % prior to ReX grain growth under conditions of continuous ReX when the solute content of matrix approaches the solubility limit. These findings extend the industrial means to reliably alter the resulting ReX texture.

5:00 PM

(ICOTOM-S13-011-2008) Grain Growth and Texture Evolution in ECAP and Pre-aged Al-1.2% Hf Alloy

O. Al-Buhamad*, M. Z. Quadir, M. Ferry, The University of New South Wales, Australia

A sub-micron grained (SMG) microstructure of an Al-1.2wt%Hf alloy was produced utilizing the well known severe plastic straining (SPD) technique of Equal Channel Angular Pressing. This alloy was subjected to solution heat treatment preceded the ECAP deformation process, followed by aging at different temperatures up to 500 oC. This generated very fine grained microstructures that contains a large fraction of high angle grain boundaries (HAGB) associated with a good dispersion of submicron/nanosized Al₃Hf particles. The evolutions of microstructure, texture as well as the grain stability study were investigated in details using Nova FEG-SEM system equipped with an Electron Back Scatter Diffraction (EBSD) detector and Phillips CM-200 Transmission Electron Microscopy (TEM). The grain size distribution has been statistically measured from EBSD data at different stages, and growth exponent was measured and compared to well known pure Al and Al(Sc) systems. The role of fine Al₃Hf particles was evaluated in preventing grain growth, and the study showed their ineffectiveness at the temperature range covered in this investigation.

5:30 PM

(ICOTOM-S13-020-2008) Comparative Analysis of Low-Cycle Fatigue Behavior of 2D-Cf-PyC/SiC Composites in Different Environments

Y. Zhang*, L. Zhang, L. Cheng, Y. Xu, Northwestern Polytechnical University, China

Ceramic matrix composites such as the carbon fiber reinforced silicon carbide composites have received considerable attentions in their application of hot load-carrying structures for the aircrafts. However, the thermo-mechanical properties as well as the failure mechanism in specific environment such as in high-speed and high-enthalpy gaseous flows must be understood before its use. In this paper, a carbon/silicon carbide composite with protective silicon carbide coating was prepared by chemical vapor infiltration. Low-cycle fatigue behavior at room temperature and at high temperatures up to 1800°C in a combustion environment was investigated on the composites. The combustion environment simulates severe heat flux with rich oxygen, water vapor, carbon dioxide and some nitrogen. Fatigue tests were conducted at the same maximum stress level of 180MPa but at various temperatures and cycles. Residual tensile strength of pre-fatigued specimen was tested in controlled environment. Finally, the microstructure of the damaged specimen was characterized by scanning electron microscopy. Analysis of damage mechanisms showed that interfacial bonding and oxidation of carbon fibers was the major difference between the room and high temperatures. Oxidizing atmosphere in combustion environment speeded and enhanced the failure of composites by decreasing the load-carrying ability of fibers suffered from oxidation damage. The

strength enhancement at room temperature but the significant strength degradation in high-temperature combustion environment was obtained after fatigue.

Digital Microstructures

Digital Microstructures

Room: Rangos 1

Session Chair: Marc DeGraef, Carnegie Mellon University

8:30 AM

(ICOTOM-S14-001-2008) Predictions and Experimental Validation of the Development of Intragranular Misorientations in Copper under Tension Using Direct Input from OIM Images (Invited)

R. Lebensohn*, Los Alamos National Laboratory, USA; R. Brenner, O. Castelnau, Universite Paris XIII, France; A. D. Rollett, Carnegie-Mellon University, USA

We present results of a numerical formulation based on Fast Fourier Transforms (FFT) to obtain the micromechanical fields in plastically deformed 3-D polycrystals using direct input from a digital image of their microstructures. The FFT-based formulation provides an exact solution of the governing equations in a periodic unit cell, has better performance than a Finite Element calculation for the same purpose and resolution, and can use voxelized microstructure data as input and for validation. To illustrate the capabilities of this model, we first discuss the construction of a 3-D unit cell using 2-D orientation maps obtained by means of Orientation Imaging Microscopy (OIM), and we then show FFT-based predictions, together with the corresponding OIM measurements, on the subgrain texture evolution in a recrystallized Cu polycrystal deformed in uniaxial tension. The average misorientations, whose orientation-dependence can be explained in terms of grain interaction, are well reproduced by the FFT-based model.

9:00 AM

(ICOTOM-S14-002-2008) Accurate Texture Reconstruction with a Set of Orientations Based on Integral Approximation of the Scaled Orientation Distribution Function

P. Eisenlohr*, F. Roters, Max-Planck-Institut für Eisenforschung, Germany

We are concerned with the reconstruction of textures—given as discrete, i.e. piecewise constant, orientation distribution functions (ODFs)—by a limited number, N^* , of equally weighted orientations. The N^* orientations are sampled from those N central orientations for which the respective Euler space boxes overlap with the fundamental zone of the discrete original ODF. Taking strong and intermediate experimental and random artificial textures as test-case, probabilistic and deterministic reconstruction schemes are compared. The quality of ODF reconstruction is quantified by the root mean squared deviation as well as by the correlation factor of a linear regression between the probabilities in the original and reconstructed ODF. A scaling with N^*/N is found for the quality of both reconstruction schemes. In terms of both quality measures, the deterministic sampling scores higher than probabilistic sampling for given N^*/N . However, if $N^* \ll N$, then deterministic sampling progressively sharpens the reconstructed texture with decreasing N^*/N due to systematic over-weighting of orientations with originally high probability at the expense of low-probability ones. Therefore, a combined method is proposed, which for $N^* \ll N$ draws a random subset of N^* orientations from a population containing N orientations, where this population is itself generated by prior deterministic sampling from the discrete ODF. The reconstruction quality achieved by this hybrid method is naturally identical to deterministic sampling for $N^* \geq N$ and asymptotically declines with decreasing N^* to settle at the levels of probabilistic sampling for $N^* \ll N/10$ —without systematic sharpening of the reconstructed texture.

9:15 AM

(ICOTOM-S14-003-2008) Adaptive Mesh Refinement in Crystal Plasticity Finite Element Simulations of Large Deformations in Polycrystalline Aggregates

H. Resk*, M. Bernacki, T. Coupez, ENSMP, France; L. Delannay, Université catholique de Louvain UCL, Belgium; R. Logé, ENSMP, France

The objective of this work is to study the deformation of large grain structures subjected to important strains comparable to those encountered during forming processes. The capability of the simulations to predict the evolution of the microstructure in terms of grain shape, texture distribution and stored energy is illustrated. The effect of mesh refinement and anisotropy on the local response of the polycrystal is investigated. The grain structures are generated by the DigiMicro software using Voronoi tessellations. The orientations are assigned either randomly or distributed so as to represent the texture of a real material. The grain boundaries are represented using the level set approach. Automatic isotropic or anisotropic meshing, based on the level set representation, is used to mesh the structure initially and as often as needed during the simulations. Material behaviour is governed by a classical crystal elasto-viscoplastic constitutive law. This latter is coupled to a mixed stabilized finite element formulation based on the mini-element P1+/P1 in an updated Lagrangian framework. Massive parallel computations based on the CIMLIB library are used. The implemented approach is validated by comparing the predicted crystallographic orientations to experimental data. The heterogeneity across the grains and within individual grains, in terms of crystallographic orientation, stress, strain and stored energy, is demonstrated. The results with and without remeshing are comparable, thus validating the remeshing approach. The effect of different strategies of mesh refinement and anisotropy is shown to have an impact on the local mechanical response and distributions. This study validates our crystal plasticity based finite element modelling. The automatic remeshing allows for the deformation of large three dimensional grain structures up to important strain levels. Such levels are necessary if we want to provide reliable quantitative data to be used for the detailed modelling of recrystallization which can take place upon heat treatment, after the deformation step.

9:30 AM

(ICOTOM-S14-004-2008) Interfacing Finite Element Simulations with Three Dimensional Characterizations of Polycrystalline Microstructures via the 3D Materials Atlas (Invited)

P. Dawson*, D. E. Boyce, M. P. Miller, Cornell University, USA

Experimental methods to characterize the microstructural state of polycrystalline samples have progressed rapidly in recent years. Automated serial sectioning, combined with diffraction measurements, provides digital renditions of the crystalline microstructure of material samples in three dimensions. These complement x-ray tomography and bulk diffraction measurements to give both detailed spatial definition of specific samples and statistically-based distributions of microstructural attributes. The organizing and archiving of such a diverse and large array of data with the intent of facilitating scientific collaborations present interesting challenges. In this presentation, we describe a new system, called the 3D Materials Atlas, which combines a database (for describing material structure and the data set pedigree) with a file storage management capability (for archiving and retrieving the associated data files.) The database schema defines which material and data characteristics are of interest and how they are related. At the level of the user, there is graphical software for entering data, for querying the database, and for retrieving the desired data sets, as well as the capability to interface other software with the atlas via plugins. From a modeling perspective, the availability of spatially-resolved microstructures of real samples offers fresh opportunities for investigating the links between the microstructural state of a material

Abstracts

and its derivative mechanical behaviors. In this presentation we discuss simulations using virtual samples that have been instantiated directly from data in the atlas. We discuss aspects of the response to mechanical loading. The first is the evolution of intracrystalline textures, especially the correlation between intragrain lattice misorientation and the spatial position within a deforming grain. The second is the evolution of load sharing in polycrystals as the stress level is elevated and the material progresses through the elastic-plastic transition.

10:30 AM

(ICOTOM-S14-005-2008) CPFEM Investigation of the Effect of Grain Shape on the Planar Anisotropy and the Shear Banding of Textured Metal Sheets (Invited)

L. Delannay*, M. A. Melchior, Université catholique de Louvain (UCL), Belgium; A. K. Kanjarla, P. Van Houtte, K.U.Leuven, Belgium; J. W. Signorelli, Fac. de Ciencias Exactas, Ingeniería y Agrimensura, CONICET-UNR, Argentina

The alloy under consideration is an austenitic steel grade with low stacking fault energy. Upon plastic yielding, mechanical twins are created, taking the form of very thin lamellae. Twins act as obstacles against dislocation slip in the parent grain, which increases the hardening capacity of the metal and, hence, its formability. The phenomenon also tends to promote dislocation movement on slip systems having a Burgers vector parallel to the twinning plane relative to the other slip systems. Such anisotropic hardening of the grains has, in turn, a potential effect on the formation of localised shear bands. In the present study, the onset of shear banding is investigated using crystal plasticity based finite element modelling (CPFEM) and a statistical representation of the polycrystalline aggregate. The sensitivity of shear band formation to several parameters of the simulation is assessed. From a purely numerical viewpoint, shear banding is influenced by the degree of mesh refinement, the number of grains included in the digital microstructure, and the type of boundary conditions. Material parameters, such as texture, grain shape and anisotropic hardening of the slip systems, also have an influence which is revealed by CPFEM.

11:00 AM

(ICOTOM-S14-006-2008) Linking Plastic Deformation to Recrystallization in Metals, Using Digital Microstructures

R. E. Logé*, M. Bernacki, H. Resk, H. Dignonnet, Y. Chastel, T. Coupez, Ecole des Mines de Paris, France

Procedures for synthesizing digital polycrystalline microstructures are illustrated, either from 2D statistical data or from 3D deterministic data. The obtained digital microstructures can be meshed anisotropically and adaptively, with refinement close to the grain boundaries. Digital mechanical testing can then take place using crystal plasticity finite element simulations, which provides an estimate of the spatial distribution of strain energy within the polycrystalline aggregate. The latter quantity is used as an input for modelling subsequent static recrystallization, grain boundary motion being described with a level set framework. The kinetic law for interface motion accounts for both stored strain energy and grain boundary energy. The possibility to include nucleation events within the level set framework is discussed, as well as the evolving topology of the grain boundary network.

11:15 AM

(ICOTOM-S14-007-2008) Multiscale Model for Anisotropic Work Hardening of Aluminium Including Transient Effects during Strain Path Changes

S. Van Boxel*, M. Seefeldt, B. Verlinden, P. Van Houtte, Katholieke Universiteit Leuven, Belgium

A multiscale texture-work hardening model for aluminium is presented which captures both the changes of the anisotropy and the transient behaviour in the work hardening after strain path changes in order to obtain a better prediction of the flow stress in

forming operations with complex strain paths. At the macroscale, texture information is incorporated by selecting a representative set of discrete orientations. The advanced Lamel model of Van Houtte et al.(1) is used to make the transition to the mesoscopic level, calculating the shear rates on the active slip systems and predicting texture changes. At the mesoscopic level, evolution equations for the critical resolved shear stresses of all slip systems are formulated in an incremental form. The substructural anisotropy is incorporated in these equations by attributing a high hardening for low and non active slip systems and a low hardening to the reverse directions of active slip systems. The former is motivated by the observation that substructural elements are favourably oriented towards the most active slip planes, the latter by the back stresses inherent to a substructure built up of stored dislocations. The transient effects in the work hardening are modelled by exponentially decaying softening or hardening contributions if an abrupt change in the shear rate of a slip system occurs. The model is used for simple shear tests on AA3103 plate samples prestrained by simple shear or cold rolling in order to have different strain path changes. Textures are measured at different stages of the deformation and compared to results of the advanced Lamel model with and without the model for hardening anisotropy. It is shown that including hardening anisotropy due to strain path changes improves the modelling predictions of the flow stress anisotropy significantly, while the evolution of the shear textures is not captured as good as by the advanced Lamel model without hardening anisotropy, but still to a better extend than with a FC Taylor model. 1. Van Houtte, P., Li, S., Seefeldt, M. and Delannay, L. Int. J. Plasticity 21 (2005) 589-624

11:30 AM

(ICOTOM-S14-008-2008) Gradient Matrix Method to Image Crystal Curvature with Discrete Orientation Data: Case Study of Triple Junction in Deformed IF Steel

A. Zisman*, CRISM "Prometey", Russian Federation; M. Seefeldt, S. Van Boxel, P. Van Houtte, Catholic University of Leuven, Belgium

In order to derive the lattice orientation gradient (curvature) from orientation data acquired over a discrete grid, the gradient matrix for the latter has been introduced. This approach notably facilitates the fitting of both the dimensions and shape of differentiation domains when selecting the best compromise between the spatial resolution and noise reduction. EBSD orientation data around a triple junction in a low deformed IF steel, as a case study, is considered, where conventional methods of treating such data could not discern weak dislocation substructures of involved grains. The gradient matrix method, when applied to the same raw data, proves to reveal a distinct low-angle boundary extending from the junction line on the background of dim dislocation cells. Further perspectives of the curvature mapping, indicative of low angle substructures, are discussed; particularly in application to 3D orientation data.

11:45 AM

(ICOTOM-S14-009-2008) Representative Volume Elements for the input into Structure-Property-Processing Relationships

S. R. Niezgodá*, D. Fullwood, S. Kalidindi, Drexel University, USA

In this paper we develop the concepts underlying the definition of a representative volume element (RVE) based on higher-order microstructure statistics or property information gathered from an ensemble of samples. Through the development of a formal mathematical definition of the RVE, it is shown that it is often impossible to identify a single realization of a microstructure as an RVE. Instead, the RVE is defined in a statistical sense and is considered to be equivalent of a weighted combination of specific realizations. The concept of an RVE is central to building robust microstructure-property-processing relationships. A clear and precise definition of RVE is the essential first step in the formulation a rigorous mathematical framework for building such relationships.

12:00 PM

(ICOTOM-S14-010-2008) Moment Invariant Shape Descriptors for 2-D and 3-D Microstructure Representation

J. MacSleyné*, Carnegie Mellon University, USA; J. P. Simmons, Wright Patterson Air Force Base, USA; M. De Graef, Carnegie Mellon University, USA

The digital representation of a two-phase microstructure is facilitated by the binary nature of the problem: a randomly chosen point belongs either to phase A or to phase B. If the secondary phase B precipitates as isolated particles, as is the case, for instance, in many superalloys, then one can employ a moment-based description of the precipitate shape. We restrict the discussion to second order moments. In the center-of-mass reference frame, one can always orient an object so that there are only three non-vanishing second order moments. From these moments one can construct (in 3-D) two quantities which are invariant under similarity transformations, and one quantity which is invariant under affine transformations. In 2-D, there are two invariant quantities, one w.r.t. similarity transformations and the other w.r.t. affine transformations. In this contribution we will show how these invariants can be used as sensitive shape discriminators both in 2-D and 3-D. After defining the invariants and providing examples based on simple shapes, we will introduce the concept of moment invariant space, and illustrate how all possible shapes reside within a finite region in this space. Then we will provide applications of invariants, such as the quantitative representation of shapes and shape changes of precipitates that develop in real 3-D microstructure observations as well as in microstructure evolution simulations. The equilibrium particle shape is an attractor in moment invariant space, so that the general trajectories of particles proceed towards this attractor. When particle trajectories collide or when one particle bifurcates, this results in a discontinuity in the particle trajectory, making these events easily detectible. Since particle shapes are characteristic of microstructures, this technique can be used to quantify the "closeness" of two microstructures by the statistics of their moment invariants. Finally, as an example of 3-D moment invariants, we will present an analysis of the shapes of complex (dendrite-like) precipitates in a Rene-88DT alloy. We will show that the precipitate shapes lie along a curved surface in the moment invariant space.

12:15 PM

(ICOTOM-S14-011-2008) Minimally Supervised Segmentation Algorithms for Serial Section Image Data

P. Chuang, M. L. Comer*, Purdue University, USA; J. P. Simmons, AFRL/MLLMD, USA; M. De Graef, Carnegie Mellon University, USA

The integration of computer controls and the increased detector capacity of modern electron microscopes have enabled serial section image acquisition at a rate that outpaces the human resources on any given project to fully analyze the data. It appears that data collection is limited by two factors: the ability to analyze and readily store data. Current trends in dataset size indicate roughly a doubling every year, with current dataset sizes being on the order of 8-10GB. These datasets typically consist of hundreds of images or image montages, sometimes including information from multiple signal sources, such as alternate imaging conditions, chemical spectra, or orientational data. In order to be used in property simulations, image data must be converted to feature-based representations of grains, particles, laths, and the like. Historically, the supervised image processing techniques developed in the 1970's have been used in order to extract features of interest. To keep pace with the production of image data, we have turned to algorithms requiring minimal supervision, such as those developed for computer vision applications in the 1990's. In this contribution, we will present results of several of these applications towards feature extraction from serial section image stacks of metallic systems. Alloy systems under consideration include Ni-based superalloys and Ti α - β alloys. Serial sectioning data sets of these systems reveal either polycrystalline grain configurations, multi-scale lath and precipitate structures, or isolated second phase particles. Automated segmentation methods based on Bayesian segmentation with a simu-

lated annealing component will be compared to conventional techniques, such as Gaussian deconvolution and standard histogram thresholding. We will illustrate the use of these methods both for 2-D and 3-D segmentation.

Friday, June 6, 2008

Friction Stir Welding and Processing**Friction Stir Welding and Processing**

Room: Rangos 1

Session Chair: Paul Dawson, Cornell University

8:30 AM

(ICOTOM-S1-001-2008) Texture Development in Aluminum Friction Stir Welds (Invited)

R. W. Fonda*, Naval Research Laboratory, USA; J. F. Bingert, Los Alamos National Laboratory, USA; A. P. Reynolds, W. Tang, University of South Carolina, USA; K. J. Colligan, Concurrent Technologies Corporation, USA; J. A. Wert, Risø National Laboratory, Denmark

This presentation will be an overview of research programs at the Naval Research Laboratory on the development of texture in aluminum friction stir welds, from the initial deformation of the base material ahead of the tool to the deposition of the weld in the wake of the tool. Stop action friction stir welds were prepared in both polycrystalline and single crystal aluminum specimens by immediately quenching the weld upon completion to preserve the microstructure surrounding the tool. Plan view sections of these weld terminations reveal the microstructural and textural evolution that occurred around the tool during welding. These studies have revealed that slight variations in the crystallographic orientation of grains in the base material ahead of the tool can engender different susceptibilities to the shear deformation induced by the rotating tool. The resulting flow localization takes the form of misoriented grains, which develop in both size and misorientation as they approach the tool. Rotation of these misoriented grains continues until they approach an ideal shear orientation with either $\langle 101 \rangle$ aligned with the shear direction or $\langle 111 \rangle$ aligned with the shear plane normal, after which no further rotation is observed. The corresponding continuous development of misorientation at the (sub)grain boundaries indicates that grain subdivision occurs by a continuous dynamic recrystallization process. As this material approaches the rotating tool, the increased temperatures and shear deformation transition the observed texture to consist predominantly of the B and -B components of the simple shear texture. This material is swept around the tool and then deposited in the wake of the tool. The deposited weld also exhibits a simple shear texture, but it varies with a periodicity of the tool advance per revolution between a pure B/ -B component and a mixture of the B/ -B and C components. Thus, the development of textures ahead of the tool can be correlated directly to the increasing temperature and shear deformation of those regions, while the periodic texture variations of the deposited weld indicate a systematically varying component in the friction stir welding process.

9:00 AM

(ICOTOM-S1-002-2008) Effect of Texture on Fracture Limit Strain in Friction Stir Processed AZ31B Mg Alloy (Invited)

Y. S. Sato*, A. Sugimoto, H. Kokawa, Tohoku University, Japan; C. Lee, Korea Institute of Industrial Technology, South Korea

Mg alloy has a poor formability at room temperature because of lack of the active slip systems. However, it has been reported that the grain refinement improves its ductility, thus it would be expected that friction stir processing (FSP) enhances the formability of Mg alloys because FSP can create homogeneous microstructure consisting of fine grains in Mg alloys. The present authors examined effect of grain size

Abstracts

on formability in FSPed Mg alloy in previous papers, and reported that the finer grains resulted in the higher formability in AZ91 and AZ31B Mg alloys. However, FSP leads to not only the grain refinement, but also the strong accumulation of crystallographic texture in Mg alloy. The texture formed during FSP also affects the formability significantly in Mg alloy, but effect of texture on formability in FSPed Mg alloy has not been examined yet. In this study, the effect of microstructure, especially grain size and texture, on fracture limit major strain under the uniaxial tension was examined in only the stir zone of the FSPed AZ31B Mg alloy. This study applied FSP to AZ31B Mg alloy, 2 mm in thickness, at several FSP parameters. The various stir zones with the different grain sizes were obtained. All stir zones exhibited the strong accumulation of (0001) basal plane near the plate surface, whose formation was attributed to shear deformation along the tool shoulder during FSP. However, the $\langle 0001 \rangle$ direction was not exactly parallel to the normal of the plate surface, and the angle between them was different in the FSPed Mg alloys produced at the different parameters. In the present stir zones, the finer grains resulted in the lower fracture limit strain. The fracture limit strain increased with increasing the grain size up to 10 microns, beyond which it decreased. On the other hand, the fracture limit strain was higher when the angle between $\langle 0001 \rangle$ direction and the direction perpendicular to the tensile direction was smaller in the stir zones. This result would be explained by activation of $\langle a \rangle$ slip on the non-basal slip system. This study clarified that the texture is also a major microstructural factor governing the formability in the FSPed Mg alloy.

9:30 AM

(ICOTOM-S1-003-2008) Texture Gradients in Friction Stir Processed Ti 5111

D. P. Field*, Washington State University, USA; T. W. Nelson, Brigham Young University, USA; J. Miller, Washington State University, USA

Non-uniform plastic flow during friction stir welding or processing gives rise to rather severe gradients in the crystallographic texture in the processed region as well as in the intermediate zone between the base metal and the weld nugget. Although the metal undergoes a rather tortuous flow path in some instances, the texture is defined predominantly by the deformation just before plastic flow stops. In alpha and near alpha titanium alloys such as Ti 5111 (5% Al, 1% Sn, 1% Zr, 1% V, and 1% Mo), the metal may be processed either in the BCC beta phase or in the HCP alpha phase depending upon the weld parameters that govern the metal temperature during processing. Analysis of the local crystallographic textures gives a clear indication of the phase just prior to the termination of metal flow, typically the point at which the metal temperature is at a peak. Process zones using various weld parameters indicate regions of either alpha or beta structure. In addition, the textural gradients in these materials is described.

9:45 AM

(ICOTOM-S1-004-2008) Texture as a Forensic Tool in Friction Stir Welding (Invited)

A. P. Reynolds*, University of South Carolina, USA

Textures in metals are normally studied in order to understand the effects that known deformations have in the production of preferred orientations or in order to understand how anisotropy arises in polycrystalline aggregates. In the field of friction stir welding, the study of texture serves another purpose. In FSW, texture is used as a forensic tool to aid in understanding the kinematics of material flow and the mechanisms by which the final friction stir weld microstructure is established (e.g. static, or various dynamic recrystallization mechanisms). While certain aspects of the deformations associated with FSW are (purportedly) understood, many key details are not, and the restorative mechanisms operating during the process are not by any means well established (and probably vary depending on the chosen welding parameters and material being welded). In this paper, the current understanding of FSW kinematics will be described and several key questions related to, for example, the effects of tool features,

will be addressed. The role of texture study in elucidating deformation fields etc. will be reviewed and specific important questions to be addressed will be formulated.

10:45 AM

(ICOTOM-S1-005-2008) Texture Evolution during Friction Stir Welding of Stainless Steel (Invited)

J. Cho*, Korea Institute of Materials Science, South Korea

Texture evolution during friction stir welding (FSW) of stainless steel was investigated using both experimental measurements and model predictions based on a polycrystal plasticity. Material undergoes heating and deformation sufficient to substantially alter its microstructural state during friction stir welding (FSW). Texture evolution is quite complex in FSW, owing in particular to its dynamics under the induced stirring motion. Modeling approaches help to better understand how the stirring can both strengthen and weaken textures, which is an essential element in a complete description of texturing during FSW. In a two-dimensional way, texture stability is addressed from the computed velocity gradients along streamlines of the flow field. The texture is assumed to be uniform initially and shows monoclinic sample symmetry after deformation. Upstream and downstream of the tool, the deformation is nearly monotonic, causing little change of the texture. Around the tool pin, the texture strengthens, weakens, and restrengthens. The repeated strengthening and weakening of the texture are explained with the aid of an idealized, circular streamline path and consideration of the relative magnitudes of the deformation rate and spin along the streamline. The mixture of pure and simple shear textures was found. The effects of frictional conditions with the tool pin and shoulder on the complicated flow and texture evolution in the through thickness were examined with a three-dimensional approach. Trends in regard to strengthening and weakening of the texture were discussed in terms of the relative magnitudes of the deformation rate and spin. The computed textures were compared to EBSD measurements and were discussed with respect to distributions along orientation fibers and the dominant texture component along the fibers.

11:15 AM

(ICOTOM-S1-007-2008) Microstructure and Texture Analysis of Friction Stir Welds of Copper

T. Saukkonen*, K. Savolainen, J. Mononen, H. Hänninen, Helsinki University of Technology, Finland

Copper is readily joined by friction stir welding (FSW) due to its relatively low melting point. The stacking fault energy (SFE) of copper is comparatively low, resulting in a discontinuous dynamic recrystallization (DRX) mechanism operating in the temperature and strain rate range typical for FSW. Because of DRX the weld nugget (centre area of the weld) has an equiaxed, homogeneous grain structure with only a weak texture. Small variations in e.g. welding parameters or geometry of the parts to be welded can cause temperature changes in the weld due to the high thermal conductivity of copper. As a result, the microstructure near the weld nugget can clearly differ from that in the nugget. In these regions also the texture is usually much stronger than in the weld nugget. A notable texture gradient has been detected in the very narrow zone of the weld, in which the texture changes from typical to DRX (no texture) in the nugget to texture typical to static recrystallisation annealing texture in the heat affected zone (HAZ). To study the textures in the weld area, several FSW welded copper (Cu-OFEP) samples with different thickness were studied in detail. Also some "cold" welds were prepared to verify the hypothesis that the occurrence of notably different areas characterized by very small grain size, typically close to the bottom of the nugget, can be explained in the terms of hot working processing maps (related to the change of the rate controlling mechanism of hot deformation). The mechanism may change from grain boundary self diffusion at higher temperatures to dislocation core diffusion at lower temperatures affecting the microstructure and the texture.

11:30 AM**(ICOTOM-S1-008-2008) Microstructural Evolution in Titanium Friction Stir Welds**

K. Knipling*, R. W. Fonda, Naval Research Lab, USA

The deformation mechanisms occurring during friction stir welding of a near-alpha titanium alloy, Ti-5111, are examined by scanning electron microscopy (SEM), electron backscatter diffraction (EBSD), and transmission electron microscopy (TEM). The undeformed baseplate consists of coarse lamellar α colonies within large equiaxed prior β grains (up to 8 mm in diameter). The microstructure surrounding the tool was preserved by immediately quenching the weld upon completion. EBSD analyses of the weld end reveal that $\{10\text{-}11\}$ twinning is the predominant deformation mechanism in the outer regions of the thermomechanically affected zone (ca. 1.5 mm from the tool), where the frictional heating and shear stress generated during welding are relatively small. In addition to accommodating small strains at the weld periphery, deformation twinning also acts to reorient the grains of the parent baseplate material into orientations more favorable for slip. Much of the plastic deformation in the α (hcp) phase is accommodated by dislocation glide, concentrated within a narrow banded region (200–300 μm wide and 1 mm from the tool) which is composed of regularly-spaced 35–50 μm bands of alternating crystallographic orientations. The mechanisms of slip within these bands are studied by EBSD and TEM. The microstructure within 1 mm of the tool, as well as within the deposited weld, consists of small, equiaxed α grains. In these regions the material exceeded the beta transus, and deformation occurs while the material is in the high-temperature β (bcc) phase. The crystallographic texture of the deposited weld is studied by EBSD, and the role of variant selection during the $\alpha \rightarrow \beta \rightarrow \alpha$ phase transformation is discussed.

11:45 AM**(ICOTOM-S1-009-2008) Microstructural Studies of a Friction Stir Welded AA5052**

S. K. Sahoo, IIT Bombay, India; N. T. Kumbhar, Bhabha Atomic Research Centre, India; I. Samajdar*, IIT Bombay, India; R. Tewari, G. K. Dey, K. Bhanumurthy, Bhabha Atomic Research Centre, India

Partially recrystallized AA 5052 plates were successfully joined through friction stir welding. Combinations of optical microscopy, micro-hardness, electron probe microanalysis (EPMA), electron backscattered diffraction (EBSD) and transmission electron microscopy (TEM) were used to bring out a composite picture of microstructural developments. Different regions of the weld were generalized as advancing side (AS), retreating side (RS) and nugget – using standard terminologies. AS showed evidence of shear and of grain fragmentation, while RS indicated initial stages of geometrical dynamic recrystallization. The nugget region, on the other hand, had nearly equiaxed grains, with strong in-grain misorientation and presence of grain-interior dislocation structure ruling out contributions from static recrystallization. The nugget also had typical onion rings; each ring had a single/dominant orientation. The process of plastic deformation, solid-state stirring and dynamic recrystallization are the possible mechanisms behind the nugget microstructure.

Texture Effects on Damage Accumulation**Damage Accumulation II**

Room: Connan

Session Chairs: Mukul Kumar, Lawrence Livermore National Lab; Antoinette Maniatty, Rensselaer Polytechnic Institute

8:30 AM**(ICOTOM-S13-013-2008) Effect of Grain Orientation on Fatigue Crack Nucleation (Invited)**

A. Maniatty*, D. Littlewood, D. Pyle, Rensselaer Polytechnic Institute, USA

In this work, the effect of grain orientation on fatigue crack nucleation in aluminum alloy 7075 is examined by modeling discretized

polycrystals. In AA7075, cracks initiate at fractured second-phase particles. The nucleation of microstructurally small cracks from these cracked particles depends on the local microstructure in the vicinity of the cracked particle. In this work, the effect of the grain orientations near particles is examined through finite element simulations of polycrystals. A constitutive model, on the grain scale, that captures the precipitation strengthening through the Orowan looping mechanism is developed and used in this work. Fatigue crack nucleation metrics are proposed and computed for a set of polycrystals with cracked particles. The results are compared against experimental observations to evaluate the quality of the proposed metrics.

9:00 AM**(ICOTOM-S13-014-2008) Dislocation based Finite Element Approach to Crystal Plasticity**

A. Alankar*, I. Mastorakos, D. P. Field, Washington State University, USA

Deformation of crystalline materials is an inhomogeneous process. The deformation process includes the evolution of statistical dislocations and that of geometrically necessary (or excess) dislocations as well. In the present effort, a framework of a dislocation density based model which uses the evolution of different dislocation densities for determination of stress evolution is adopted. The finite element code ABAQUS with user interface UMAT subroutine is used to predict deformation in polycrystalline aluminum. The model incorporates evolution laws for each type of dislocation, based upon the kinematics of crystal deformation, and dislocation interaction laws. To make the model useful for high strength Al alloys, the constitutive laws in the crystal plasticity formulation are modified using the results of dislocation dynamics simulations (DD) to include the effects of solute and precipitates.

9:15 AM**(ICOTOM-S13-015-2008) Physically based Approach for Predicting Damage Nucleation at Grain Boundaries in Commercial Purity Ti**

T. R. Bieler*, M. A. Crimp, Michigan State University, USA; P. Eisenlohr, F. Roters, D. Raabe, Max-Planck-Institut für Eisenforschung, Germany

The ability to predict damage nucleation and evaluate whether it will lead to the fatal flaw is commonly based upon the assumption of pre-existing flaws or cracks, such that modeling approaches developed so far predict the growth rather than the nucleation of damage. To identify fundamental rules for identifying strong and weak grain or phase boundaries in the context of a deformation path, quantitative measurements of (i) the orientations of crystals on either side of interfaces, (ii) the boundary orientation, (iii) the activated deformation systems on either side of the boundary, and (iv) the local strain history within the grains on either side of an interface are made on 4-point bend specimens of commercial purity titanium. Combined use of digital image correlation to measure local strains, orientation imaging microscopy to track grain orientations, and electron channeling contrast imaging to detect dislocation activity are used for the characterization of local deformation phenomena in the vicinity of grain boundaries. Using methods developed in prior studies of equiaxed (duplex) TiAl alloys, a fracture initiation parameter capable of predicting strong and weak boundaries is developed, using metrics associated with Burgers vectors of highly activated slip and twinning systems, grain boundary inclinations, c-axis misorientations, and slip transfer criteria. These metrics are combined in a probability statement that predicts weak vs. strong boundaries for a given deformation state. Computational modeling of highly characterized microstructural regions is used in comparison with experiments to evaluate the accuracy of crystal plasticity finite element models (CP-FEM), and provide slip based information that is otherwise difficult to obtain experimentally. Progress towards implementing fracture initiation parameters into CP-FEM will be presented.

Abstracts

9:30 AM

(ICOTOM-S13-016-2008) Influence of Crystallographic Texture on Fracture Resistance (Invited)

F. Barlat*, Pohang University of Science and Technology, South Korea

In this work, the effects of macroscopic properties as well as some aspects of the material microstructure are assessed. The influence of macroscopic properties and damage in plane strain fracture toughness is investigated using experimental correlations between toughness and other macroscopic properties, as well as numerical simulations of the testing of a compact tension specimen. Predicted values of plane strain fracture toughness K_{Ic} for aerospace materials are compared with experimental results. Moreover, the influence of plastic anisotropy and crystallographic texture on the plastic zone size and shape near the tip of a plane stress crack is investigated using finite element modeling. Based on the findings of these investigations and other critical studies, the influence of crystallographic texture on fracture resistance is discussed.

10:30 AM

(ICOTOM-S13-017-2008) Role of Particles and Texture on Post-Necking Deformation in AA5754 Alloy

X. Hu*, D. S. Wilkinson, M. Jain, P. Wu, McMaster University, Canada; R. K. Mishra, A. Sachdev, General Motors, USA

For light-weight AA5754 Al alloys to replace steels more widely in automotive structures, its cost must be reduced. In this regard, the alloy produced by continuous cast (CC) is promising, since this significantly lowers processing costs as compared with more conventional direct chill (DC) casting. The formability of the CC alloy is similar to that of the DC alloy in terms of the onset of localized necking. The post-necking deformation and fracture limit, however, are greatly reduced. These observations were linked to microstructure, in particular grains and particles. A plane stress FE analysis for the onset of localization showed that the grain structure dominates over particle distribution because particles are much smaller and more dilute compared to the matrix grains in the alloys. An edge-constrained plane strain model consisting of only particles was used to study the post-necking behavior. In this paper, the incorporation of grain structures will be reported. A simple user material model is developed, where the Taylor factor of each material point is formulated into an isotropic elasto-plastic constitutive law. The evolution of Taylor factor and crystal spin can be tracked by a coupled Taylor-Bishop-Hill model. Simulations with or without considering the evolution are performed. The results show that particle distributions dominate grain structures in controlling post-necking deformation if the evolution is allowed while the opposed occurs if it is not. To further understand this problem, a 3D FE model with homogeneous cube elements is studied for uniaxial tension. Each element represents a grain with an orientation randomly assigned from the orientations of one EBSD measurement. It is found that the Taylor factors of elements outside the localization band slowly evolve up to the end of the simulation. The Taylor factors inside the band evolve slowly during the uniform deformation stage, but change much more rapidly once localization starts. This observation indicates that the results of plane strain post-necking models are not valid if the Taylor factor evolution is not allowed, since there is excessive deformation and crystal spin in the localized region.

10:45 AM

(ICOTOM-S13-018-2008) Effects of Texture on the Growth Behaviors of Fatigue Cracks in High Strength Al Alloys

T. Zhai, X. Jiang, J. Li, T. Li, Q. Zeng, University of Kentucky, USA; G. H. Bray, Alcoa Technical Center, USA; J. Li*, University of Kentucky, USA

High cycle fatigue tests were carried out on some new generation Al-Li and Al-Cu alloys under constant stress amplitude control in air at 20 Hz and room temperature. It was found that the geometry of grain boundaries had significant effects on the behaviors of short crack growth in these alloys. The commonly observed behaviors (such as deflection, branching and retardation at grain boundaries, etc.) of fa-

tigue crack growth were caused by twist and tilt of crack plane deflection across grain boundaries. These twist and tilt angles were the major resistance from the boundaries to crack growth in planar slip alloys. Texture and grain structure controlled the statistics of the possible twist and tilt angles, when a crack propagated across a boundary, thereby the resistance of the alloy to crack growth. With this model, it could be explained why a finer layered grain structure with a strong b fiber texture exhibited faster growth rate of a fatigue crack than that in a coarse fibril grain structure with a $\langle 111 \rangle$ fiber texture of a Al-Cu alloy. The fibril grain structure led to multiple crack deflections within each grain across its boundary, hence giving rise to higher resistance to crack growth, despite the grains were much coarser than the layered grains. The grain orientation also had a strong effect on crack initiation and early growth in these alloys. The results from this work pave a way to developing a model that incorporates texture and grain structure to quantify the behaviors of short fatigue cracks.

11:00 AM

(ICOTOM-S13-019-2008) Experiment and Simulation Study on Texture and Bendability of AA5XXX Aluminum Alloys

Y. Liu*, SECAT Inc., USA; Z. Long, X. Wen, University of Kentucky, USA; S. Ningileri, SECAT Inc., USA; S. K. Das, University of Kentucky, USA

Texture and bendability of sheet aluminum alloys was investigated. Experiment was performed by bending test coupon in different angles from rolling direction. Bending was simulated by Abaqus explicit. The effect of initial texture and particle structure on bending behavior and failure initiation is discussed. It is concluded that particles volume fraction has significant effect on bendability. Texture also plays an important role in governing bendability in different direction.

Texture and Anisotropy in Steels

Texture Analysis and Simulations

Room: Rangos 3

Session Chairs: Bevis Hutchinson, KIMAB; Raul Bolmaro, Instituto de Física Rosario

8:30 AM

(ICOTOM-S3-038-2008) Quantitative Prediction of Transformation Texture in Hot-Rolled Steel Sheets by Multiple KS Relation

T. Tomida*, M. Wakita, M. Yoshida, N. Imai, Sumitomo Metal Industries, Ltd., Japan

Although it is well known that the texture in hot-rolled steel sheets should be determined by the γ texture before transformation to α , KS orientation relationship between γ and α , and variant selection rules, the texture in hot-rolled steel has been barely explained quantitatively. The purpose of this article is to demonstrate that the quantitative explanation of the texture in hot-rolled steel becomes possible if a noble variant selection rule is taken into account. The selection rule to be considered is that the α nucleated on high angle grain boundaries in γ prefers to have KS relation with not only a γ grain but also another (or more) adjoining γ grain(s); let us call this selection rule the double (or multiple) KS relation. This variant selection rule modifies the transformation texture correlating with the prior γ texture. To examine this selection rule, the textures of α and retained γ of a hot-rolled 0.2%C-2.5%Mn-1.3%(Si+Al) steel sheet were measured by x-ray. Then the measured α texture was compared with the calculated one from the texture of retained γ by the MODF method combined with the double KS relation. In the calculation, the following assumptions have been made; (1) the α nucleated on a boundary grows into the γ on one side of the boundary with exact KS relation, (2) such the α variant tends to have near KS relation with the γ on the opposite side, (3) the possibility at which such the α variant nucleates (or grows) is linear to the possibility at which the γ on the opposite side has the orientation that is nearly KS-related to the α variant. The

agreement between the measured and calculated α textures was remarkable through the entire orientation space. The measured α texture that had large orientation density in the range from $\{311\}\langle 011\rangle$ to $\{332\}\langle 113\rangle$ was quantitatively well reproduced by the calculation using the retained γ texture that had a Cu-type rolling texture, although the parameter in the calculation is only the coefficient of the linearity in the assumption (3). The averaged deviation in orientation density from the measured texture was only about ± 0.29 . The results of untransformation ($\alpha \rightarrow \gamma$) calculation will be also presented.

8:45 AM

(ICOTOM-S3-039-2008) Origins of "Texture Memory" in Steels

B. Hutchinson*, KIMAB, Sweden; L. Kestens, TU Delft, Netherlands

Texture memory is the phenomenon whereby the original texture is restored after a metal has been heated through a solid state phase transformation and then cooled back to its initial structure. In the case of steels it can occur after heating into the austenite temperature range and then cooling back to the original ferritic state. Crystallographic relationships between the two phases have high multiplicity so that the double transformation would be expected to produce many possible products from a single starting orientation, and this should result in a very weak product texture. However, it is commonly observed that the original texture of the ferrite is restored to a significant extent, implying that certain transformation variants are selected preferentially. Probably, all steels show this phenomenon to some extent but, in some cases, restoration of the original texture may be essentially perfect. The best known case occurs in interstitial free steel that is alloyed with manganese. A remarkable aspect of this behaviour is that there is no corresponding memory of the initial microstructure; the final structure may be of an altogether different scale and type from the initial one. Three different explanations have been proposed in the literature to explain the texture memory effect. These are: 1. Residual stresses resulting from the alpha to gamma transformation on heating, bias the selection of variants on cooling so that the forward and reverse transformations are identical 2. Thin layers of the prior ferrite are stabilised adjacent to carbo-nitride particles of the alloying elements, Ti, Nb(C, N), and these act as ready-made nuclei for new ferrite on cooling 3. Certain grain boundaries created in the austenite on heating have especially favoured character for nucleating ferrite having the original grain orientations on cooling The presentation will discuss these viewpoints and present results of new critical experiments designed to clarify the mechanism involved. It will also consider the role of steel chemistry and the nature of the phase transformations as these affect the tendency for texture memory to exist in steels.

9:00 AM

(ICOTOM-S3-040-2008) Effects of Preferred Orientation on Snoek Phenomena in Commercial Steels

R. Gibala*, University of Michigan, USA; R. P. Krupitzer, American Iron & Steel Institute, USA

The dependence of the Snoek peak height on preferred orientation has been examined in two aluminum-killed and two silicon-treated steels. Internal friction measurements were made in torsion at approximately 1 Hz over the temperature range 240 K to 400 K. Inverse pole figure measurements based on ten selected crystallographic planes were made along the sheet-normal direction and along the axis of each torsion pendulum specimen. Texture variations were produced by cold rolling and annealing and by varying the direction in the plane of the sheet along which the internal friction specimens were cut. The crystallographic texture of these low-carbon steels was described by measuring volume fractions associated with the ten different single-crystal orientations and defining for polycrystals deformed in torsion a texture factor which ranges from zero for a 'perfect' $\langle 100 \rangle$ texture to a value of 100 for an axial texture of $\langle 111 \rangle$. Use of this texture factor predicts that a polycrystal of randomly oriented grains should have a peak height of 0.68 of the $\langle 111 \rangle$ single-crystal value. Comparable values of 0.74 and 0.66 are predicted by the uniform-stress and uniform-strain approximations, respectfully. By

using this description of texture, the Snoek phenomena in the low-carbon steels were shown to correlate with the inverse pole figure measurements. A linear relationship was found between the Snoek peak heights and the texture factor for these steels. Some of the specific experimental results include: (1) the Snoek peak height was found to vary appreciably with angle in the plane of the sheet for both aluminum-killed and silicon-treated steels, with a nominal 3% silicon steel showing the largest variation in both peak height and texture factor; (2) the amount of cold reduction prior to annealing was found to have little effect on either the Snoek peak height or the texture factor. The results of this investigation are compared with other results in the literature, and the interactive effects of texture and grain size on Snoek peak heights are discussed briefly.

9:15 AM

(ICOTOM-S3-041-2008) Effect of Coating Texture on Powdering Behavior of Industrially Produced Galvannealed Coating on IF, IFHS and HSQ Grade Steels

A. Chakraborty*, R. K. Ray, D. Bhattacharjee, TATA STEEL, India

Among the Zinc and Zinc alloy coated steels used in automotive bodies, galvannealed coated steel sheets are the most widely accepted due to their superior spot weldability, corrosion resistance, paintability and improved resistance against scratch. In this process the preheated steel sheet is first immersed in a liquid zinc aluminum bath which is called Galvanizing, and then given a post coating heat treatment. The entire process is known as Galvannealing. The heat treatment causes the zinc in the coating to inter-diffuse with the substrate iron to form several iron-zinc intermetallic phases, namely gamma (Γ), gamma 1 (Γ_1), delta (δ) and zeta (ζ) which are subsequently stacked over the steel substrate. The present study deals with the effect of the coating texture on its formability and powdering behavior with respect to three industrially produced galvannealed steels, an Interstitial Free (IF), an Interstitial Free High Strength (IFHS) and a Low Carbon High Strength Quality (HSQ). The coating formability decreases and the powdering tendency increases from IF to IFHS to HSQ. An attempt has been made to correlate this phenomenon with the observed increasing degree of discontinuity of the $\{01.3\}\langle uv.w \rangle$ fiber found in the textures from the IF to the IFHS to the HSQ steel. The increasing amounts of iron present in the coated layers of the above three steels in that order are also supposed to contribute to the observed effects.

9:30 AM

(ICOTOM-S3-042-2008) Method for Steels' Making Optimization

A. Ioana*, Univesity Politehnica of Bucharest, Romania

This paper shows an original method for steels' making optimization. This method is based on the analysis of the functional and technological performances of the electric arc furnace (EAF), using mathematic modelling of respective processes. The papers has as a starting point main principles of mathematical modelling of EAF process on the basis of these modelling principles the optimization possibilities of steel elaboration in the EAF are analysed. The main results presented in the papers are based on the modelling flow chart of the EAF technological process, which is thoroughly described in the paper. The modelling system's central element of the EAF processes conceived consists of the system's criteria function. Knowing that the technological processes study for EAF is subordinated to high quality steel obtaining, the modelling system's criteria function (CF) is the ratio between Quality and Price (equation 1): $CF = (QUALITY/PRICE)_{max} (1)$

9:45 AM

(ICOTOM-S3-044-2008) On the Measurement of Residual Stress in Fe- Ni Based Alloy Sheet by X-ray Diffraction and Flexural Strain Gauge Techniques

Q. Wu*, X. Hu, Z. Fu, W. Fang, Y. Wang, L. Li, Beijing Beiye Functional Materials Co. Ltd., China; M. Xu, H. Zhao, Tsinghua University, China

The Fe-Ni alloy sheet exhibits excellent mechanical properties compared to the conventional Fe-Ni. Inevitably there will be strong texture, weak texture, nanograin and large grain in Fe- Ni based alloy

Abstracts

sheet during cool rolled process. It introduces some challenging obstacles for their evaluation only by x-ray diffraction (XRD) subject to large residual biaxial macroscale stresses, which are difficult to resolve using conventional XRD technique. Flexural strain gauge technique was developed to be combined with XRD technique to investigate the residual stress in Fe- Ni based alloy sheet during cool rolled process. The texture strength and composition was analyzed with orientation distribution function (ODF). The rationale behind the combination method is presented that enable the calculation of residual stress and strain-free lattice parameter from asymmetric and symmetric XRD data. The combination method has been applied to inspect Fe- Ni based alloy sheet during cool rolled process.

10:30 AM

(ICOTOM-S3-045-2008) Effects of Strain and Strain Path on Deformation Twinning and on Strain Induced Martensite Formation in AISI 316L and 304L Austenitic Stainless Steel

S. K. Mishra*, P. Pant, K. Narasimhan, I. Samajdar, IIT Bombay, India

AISI 304L and 316L austenitic stainless steel were deformed at different strain and strain path using LDH (limiting dome height) method. Deformed microstructures had two interesting features- deformation twins and strain induced martensite. The former originated from decay of prior annealing twins as well as through formation of new deformation twins. Assuming that rotations of grains, specifically grains on both sides of a twin boundary, are responsible for the twin decay, a simple model was proposed to distinguish between domains of twin formation and decay. Strain induced martensite formation was strongly affected by the strain and strain path. This was generalized in terms of nucleation and growth advantage – a classification based purely on martensite grain size. The nucleation advantage was related to the presence of microstructural heterogeneities, while the growth advantage appears to originate from relative tolerance around 45degree <001> Bain orientation relationship.

10:45 AM

(ICOTOM-S3-046-2008) EBSD Textural Analyse of Deep Drawing Steels

L. Hrabcakova*, P. Zimovcak, A. Lesko, U.S.Steel Kosice, Slovakia

Deep drawing IF steels dedicated for galvanizing should have the crystallographic texture with high ratio of {111} type planes and low ratio of {100} type planes with the suitable microstructure. The hot and cold rolling history and the annealing mode and parameters are the main factors influencing the final texture. The continuous annealing parameters influence on texture formation in cold rolled Ti- alloyed and re-phosphorized IF-steel sheet from real industrial production were EBSD analysed. Complex microstructural and textural data were elaborated in form of textural images, ODF, and fibres diagrams.

11:00 AM

(ICOTOM-S3-047-2008) Comparison of Quantitative Texture Measurements via EBSD and X-Ray

S. I. Wright*, EDAX-TSL, USA

Shortly after the introduction of the Electron Backscatter Diffraction technique to the texture community, several studies were undertaken to compare textures measured using manual measurements of individual grain orientations using EBSD with those obtained using the conventional X-Ray diffraction pole figure technique. The primary object of these studies was to ascertain the number of grains required to reach the same statistical reliability as the X-Ray technique. Shortly after the full automation of the EBSD technique, several follow up studies were performed as well. Since those early studies, the speed of modern EBSD systems has increased dramatically making it practical to measure many more grains than the early manual and automated systems. In view of these advances, we revisit the question of statistical reliability of

textures measured using EBSD relative to X-ray diffraction. The focus of the study is on textures measured in rolled stainless steel and in threaded steel rods. Several parameters for comparison have been considered including comparing Orientation Distribution Function (ODF) intensities, volume fractions of specific texture components and the degree of sample symmetry. In addition, the selection of appropriate values for the variables used in the EBSD texture calculations will be discussed. The results from these comparisons suggest that approximately 10,000 individual grain orientations are needed to accurately characterize materials of moderate texture strength.

11:15 AM

(ICOTOM-S3-048-2008) Practical Investigation into Identifying and Differentiating Phases in Steel Using Electron Backscatter Diffraction

M. Nowell*, S. I. Wright, J. O. Carpenter, EDAX-TSL, USA

While Electron Backscatter Diffraction (EBSD) has proven useful for differentiating phases in steels such as austenite from ferrite, other constituent phases such as bainite, martensite, cementite and pearlite are considerably more difficult. Often these difficulties arise due to similarity in the crystallographic structure between constituent phases. For example, martensite is body-centered tetragonal. However, it typically has a c/a ratio of 1.06 depending on carbon content. This is very close to a standard body-centered cubic structure, making it difficult to distinguish martensite from ferrite based on analysis of individual EBSD patterns. Even in the case of austenite and ferrite which differ substantially in crystal structure, the morphological scale can be quite different, making it difficult to get accurate volume fractions of retained austenite in a ferritic matrix. This work explores different approaches to differentiating separate steel phases and structures including integrating EBSD with X-Ray Energy Dispersive Spectroscopy (XEDS). The results from these approaches are compared to those obtained using complementary characterization techniques.

11:30 AM

(ICOTOM-S3-049-2008) Effect of Cold Rolling Reduction on the Texture and Plastic Strain Ratio of 2205 Duplex Stainless Steel

C. Hou*, C. Liu, National Yunlin University of Science and Technology, Taiwan

The effect of cold rolled reduction, range from 52.4 % to 67 % and annealing temperature from 1025- 1100 °C on the annealing texture and plastic strain ratio of 2205 duplex stainless steel have been studied. The predominant δ phase texture components in cold rolled state were (001)[1-10] and (111)[-1-12]. Both texture intensities increased with increasing cold rolled reduction and reached a maximum value at cold rolled reduction 61.9% and then became level off. The predominant γ phase texture components in cold rolled state were (011)[3-11] and (112)[-1-11]. The intensity of (011)[3-11] increased with increasing cold rolled reduction. After cold rolled sheet annealing, the predominant δ phase texture components were (001)[1-10], (011)[0-11], and (111)[-1-12]. The intensity of (001)[1-10] increased with increasing cold rolled reduction. The effect of temperature on texture was not obvious. The predominant γ phase texture components after annealing were (011)[3-11] and (113)[-3-32]. Both intensities of (011)[3-11] and (113)[-3-32] increased with increasing cold rolled reduction. Furthermore, the intensity of (113)[-3-32] increased with increasing annealing temperature in the specimens with cold rolled reduction larger than 61.9%. After cold rolled sheet annealing, r value increased with increasing cold rolled reduction. However, r value decreased with annealing temperature and reached a minimum at 1075 °C. Besides, plane anisotropy Δr value decreased with increasing cold rolled reduction. Moreover, Δr value decreased with increasing annealing temperature in the specimens with cold rolled reduction less than 57%. Conversely, Δr value increased with increasing temperature and reached a maximum at 1075 °C in the specimen with 67% cold rolled reduction.

11:45 AM**(ICOTOM-S3-050-2008) Texture and Deep-drawability of an Intermediately Annealed SUS430 Stainless Steel Sheet during Cold Rolling**

L. Chen*, Northeastern University, China; H. Bi, Baoshan Iron and Steel Co., Ltd., China; Y. Liu, H. Yu, Northeastern University, China

The cost-effective stainless steel has received worldwide attention. For the deep drawing application of this kind of steel, the deep-drawability is a critical criterion. Homogeneously distributed and textured fine grains are required to be considered. In this paper, a processing route of intermediate annealing during cold rolling for a hot-rolled ferritic stainless steel sheet SUS430 has been adopted to attain this. Textures in different stages of annealing and cold rolling have been examined and the relationship between texture and anisotropy of final product has been correlated and analyzed in detail.

12:00 PM**(ICOTOM-S3-051-2008) Rolling and Annealing Textures in Low Carbon Steels**

R. E. Bolmaro*, A. Roatta, A. L. Fourty, Instituto de Física Rosario, Argentina

The current work shows applications of texture development simulation techniques to the processing of low carbon steels. The final textures in steel sheets are influenced by their alloy chemistry as well as by the processing parameters by consecutive application of hot rolling, cold rolling and annealing. Some textures are difficult to find in the literature and hardly obtainable by the current development of measurement techniques. High temperature phase textures are certainly impossible to measure immediately after hot rolling. Holding the material at high temperature, with the sole purpose of measuring, will not guarantee having the same material afterwards. Those textures are only available by back simulation from texture measurements at low temperature after phase transformation or are inferred from measured analog materials. Textures of high and low temperature phases after high temperature rolling and low temperature rolling and recrystallization textures are addressed in the current presentation. For the simulation of deformation processes a polycrystalline viscoplastic self-consistent code is employed. The prediction of recrystallization textures is carried out by the analysis of the deformation micromechanical variables, stored energy, nucleation and grain growth. The martensitic transformation phenomenon is described by using the empiric Kurdjumov-Sachs model with variant selection activated by taking in account different mechanisms. The results are compared with experimental values from literature when available. The work attempts to be a whole process analysis intended to fill blanks on both experiments and simulations. The results are conclusive in some aspects of the interaction between experiments and simulations.

Recrystallization Texture: Retrospective vs. Current Problems**Recrystallization II**

Room: Rangos 2

Session Chair: Michael Kassner, University of Southern California

8:30 AM**(ICOTOM-S10-014-2008) Cube Texture due to Dynamic Recrystallization in Pb and PbSn Alloys under Equal Channel Angular Extrusion Processing (Invited)**

R. E. Bolmaro*, Instituto de Física Rosario, Argentina; V. L. Sordi, M. Ferrante, Universidade Federal de São Carlos, Brazil; W. Gan, Harbin Institute of Technology, China; H. Brokmeier, GKSS-Research Centre, Germany

ECAE has been one of the most prolific techniques in the study of severe deformations of metallic alloys. The case of severe deforma-

tion on low melting temperature alloys has not been studied due to the high dynamic recrystallization effects they usually present. In the current presentation we show ECAE deformation experiments performed in a 120° tool at room temperature in pure Pb and near eutectic composition PbSn alloy. The samples were passed 5 times in a route A. After each pass they showed a completely recrystallized structure under metallographic observation. Due to the high absorption presented for X-rays by Pb the sample textures were measured by neutron diffraction. Because of their high penetration and superior statistical capabilities the textures showed well defined patterns even in the cases when the strengths were rather weak. The textures presented a well defined cube texture rotated between 20 and 25 degrees around an axis coincident with the transversal direction. Even on the two-phase PbSn samples the cube component was clearly the major and better defined one. Despite Pb is a low stacking fault energy FCC metal, that orientation shows a recrystallization behavior resembling the regular static recrystallization texture presented by high stacking fault FCC materials after rolling processing. The nature of the recrystallization process is discussed taking in account the texture results. Because of the severe deformation it is possible that the subgrain size due to fragmentation might have reached a value close to the grain thickness and geometrical dynamic recrystallization is the most probable mechanism. That hypothesis is difficultly testable because of the readily occurring recrystallization.

9:00 AM**(ICOTOM-S10-015-2008) Studies on Texture and Microstructure of Cryorolled and Annealed Cu-5%Zn, Cu5%Al Alloys**

N. V.L., Indian Institute of Technology Madras, India; N. Gurao, Indian Institute of Science, India; U. Wendt, Otto von Guericke University, Germany; S. Suwas, Indian Institute of Science, India; S. S. Vadlamani*, Indian Institute of Technology Madras, India

There is a growing interest in bulk ultra fine grained (ufg) metals and alloys due to their improved mechanical properties. Much of the research on bulk ufg metals and alloys synthesis is by severe plastic deformation (SPD) techniques like Equal Channel Angular Pressing (ECAP) and High Pressure Torsion (HPT). However, plastic deformation (rolling) at cryogenic (liquid nitrogen) temperature and low temperature annealing has also been shown to produce ufg microstructures. In the present work, we report the development of texture and microstructure in Cu-5 wt.% Zn and Cu-5 wt.% Al alloys following cryorolling (true strain of $\epsilon \sim 2$) and annealing. Texture was studied using X-ray diffraction and Electron Back Scatter Diffraction in the scanning electron microscope. In-situ Young's modulus (E) measurements (using resonance technique) at temperatures from 298-573K revealed that E is lowest in both the alloys in the as-rolled condition and recovers to the isotropic value after heating to 523-573K. This could be correlated to the rolling and annealing textures that develop in both the alloys. Cu-Zn and Cu-Al alloys were found to develop a strong brass texture component after cryorolling and the texture weakens considerably following annealing in the range 523-573K. The texture randomization could be attributed to the recrystallisation twinning, which occurs in low SFE materials. After annealing at 523K for 15 min., a recrystallized ufg microstructure with an average grain size in the range of 0.5- 1 μm was obtained. A finer grain size and a high density of annealing twins with a spacing of few tens to hundreds of nanometers is obtained in the recrystallised condition in Cu-Al alloy.

9:15 AM**(ICOTOM-S10-016-2008) Function of Layer Thickness on the Microstructural Evolution in Copper of annealed Roll-Bonded Cu-Nb Composites**

C. Lim*, A. Rollett, Carnegie Mellon University, USA

The annealed microstructure and texture of any material govern its mechanical properties in composites just as in single-phase materials.

Abstracts

Nevertheless few studies on the annealing of deformed Cu-Nb layered composites have been performed as compared to the strengthening mechanisms involved. In order to investigate the annealing response in such materials, recrystallization textures of monolithic pure Cu and alloyed Cu - C19210, with and without Nb reinforcement were investigated. Roll-bonded samples of different layered length scales were deformed to reductions of 70-90% and annealed at temperatures between 300°C and 800°C for 0.5 hours. We found that the Cube and $\{215\}\langle 211\rangle$ orientations were the dominant components in the recrystallized texture of monolithic pure Cu and alloyed Cu respectively. However, rolling texture was retained for the sub-micron Cu layers of the composites. X-ray analysis and EBSD was used to study the recrystallization evolution of the Cu in the composites. EBSD in particular was also used to observe recrystallization for the sub-micron Cu layers. We also propose a term – “confined recrystallization” to explain the effect of the length scale of the Cu layer thickness on the recrystallization texture and microstructural evolution especially in the sub-micron range.

9:30 AM

(ICOTOM-S10-017-2008) Development of Cube Texture in Cold-Rolled and Annealed Multilayer Tapes for Coated Superconductor Applications

P. P. Bhattacharjee, Deakin University, Australia; R. K. Ray*, TATA Steel, India

A simple powder metallurgy route has been investigated to prepare multilayer tapes having configurations Ni(outer)/Ni-5at.%X (core) and Ni/Ni-5at.%X(core)/Ni (X=W or Mo) for use as mechanically strong and textured substrate for coated superconductor applications. Development of cube texture ($\{001\}\langle 100\rangle$) following heavy cold rolling (~95%) and annealing has been studied in the Ni side(s) of these multilayer tapes and has been compared to a stand-alone Ni tape. The deformation textures in the Ni side of the tapes are found to be quite similar to that of Ni strained to similar level of deformation. However, the cube texture upon annealing is found to be significantly stronger in the Ni side(s) of the multilayer tapes as compared to pure Ni after different annealing treatments. This trend is also observed when all the materials are prepared using a less purity Ni powder as starting material. Cross sectional EDS analyses of the multilayer tapes show significant diffusion of the alloying elements (e.g. W or Mo) from the alloy side to the Ni side. All these facts indicate the beneficial role of the alloying elements W or Mo on the development of cube texture in Ni. Finally, the mechanical properties of the multilayer tapes have been evaluated to ascertain their suitability in the actual application scenario.

9:45 AM

(ICOTOM-S10-018-2008) Rolling and Annealing Textures of Silver Sheets

D. Lee*, H. Han, S. Kim, Seoul National University, South Korea

Texture studies of rolled silver sheets have been motivated by its potential use for substrates of high temperature superconductors, of which textures are influenced by those of substrates. However, the evolution of the textures is not well understood. The purpose of this paper is to review and discuss the deformation and annealing textures. Extensive data of measured rolling and annealing textures for thermomechanically processed silver samples have been reported with little explanation. We simulate the rolling textures, through which active slip systems and their activities are calculated. The slip data are used to calculate corresponding recrystallization textures using the strain-energy-release-maximization model. When silver is processed so that the dislocation density decreases rapidly during annealing, the annealing texture is discussed based on the grain boundary mobility. The rolling texture of silver varies with the purity of silver, annealing atmosphere (vacuum, Ar, air) before rolling, annealing temperature and time, grain size, rolling reduction, and rolling temperature. Various annealing textures such as $\{236\}\langle 385\rangle$, $\{110\}\langle 110\rangle$, $\{023\}\langle 032\rangle$, $\{100\}\langle 001\rangle$, etc. are observed depending

on annealing atmosphere, temperature, and time. The phenomena are attributed to changes in the stacking fault energy due to small amounts of interstitial and substitutional elements, which influence the deformation texture and in turn the annealing texture. When the stacking fault energy is small, the $\{110\}\langle 112\rangle$ deformation texture is dominant, and as the stacking fault energy increases, the $\{112\}\langle 111\rangle$ and $\{123\}\langle 634\rangle$ textures develop. Specimens with the $\{110\}\langle 112\rangle$ deformation texture can have different annealing textures, and the $\{112\}\langle 111\rangle$ and $\{123\}\langle 634\rangle$ textured specimens usually bring about the $\{100\}\langle 001\rangle$ recrystallization texture. The $\{236\}\langle 385\rangle$ annealing texture can be explained based the grain bound mobility, and other annealing textures can be explained by the strain-energy-release-maximization model for recrystallization texture.

10:30 AM

(ICOTOM-S10-019-2008) Multi-cycle Pinch Welding of 304L Tubes: Inhomogeneities in Deformation and Recrystallization Textures and Microstructures

C. T. Necker*, Los Alamos National Laboratory, USA; A. N. Marchi, New Mexico Tech, USA; M. G. Smith, Los Alamos National Laboratory, USA

Solid-state resistance closure welds, referred to as pinch welds, are used to seal tubes after gas filling operations. Seals were produced by mechanically confining (0/180°) and pinching (90/270°) 304L tubes while passing up to 12 cycles of current across the pinching electrodes. The evolution of local texture and microstructure across the welded region was evaluated using electron backscatter diffraction (EBSD). The initial texture was a weak $\langle 111\rangle$ fiber while the grain size was 30 μm and equiaxed. The pinching operation partially closed the tube leaving the opening shaped like a high aspect ratio oval with pinched ends. Material across the minor axis showed little evidence of deformation, having retained the initial texture and microstructure. The texture near the pinch points was a strong $\langle 111\rangle$ component, however the texture was no longer fibrous. The microstructure was angular with grain aspect ratios in the range of 2:1 to 3:1. After 5 weld cycles the tube was closed. Material along the minor axis retained the initial microstructure and texture. Material near the pinched regions was completely recrystallized with a weak $\langle 100\rangle + \langle 111\rangle$ mixed fiber component. The local grain size was about 5 μm. After 12 weld cycles, the material along the minor axis near the weld interface was recrystallized with a 30 μm - 40 μm grain size while the texture was dominated by a non-axisymmetric $\langle 100\rangle$ fiber. Material along the major axis changed little after the additional weld cycles. The presence of localized misorientations in the near-weld material after 12 cycles suggests that the loading maintained during the welding operation continued to strain the heated material sufficiently to drive recrystallization along but not across the weld interface. The near equivalence of the recrystallized grain size to that of the initial material along with the localized strong recrystallization texture suggests recrystallization mechanics similar to recrystallization of heavily rolled high stacking fault FCC materials that yield cube, $\langle 100\rangle\langle 001\rangle$, textures through selective nucleation and growth controlled by orientation pinning.

10:45 AM

(ICOTOM-S10-020-2008) Ultra-fine Grain Austenitic Stainless Steels: Influence of Texture during Recrystallization

A. Poulon*, Institut de Chimie de la Matière Condensée de Bordeaux, UPR CNRS 9048, France; S. Brochet, J. Vogt, Université de Lille I, LMPGM, UMR CNRS 8517, France; J. Glez, J. Mithieux, UGINE&ALZ Research Center, BP 15, France

Ultra-fine grains about 1 μm have been obtained in a metastable austenitic stainless steel by a repetitive thermomechanical process consisting of non-conventional warm rolling and annealing in order to avoid formation of martensite. In this case grain refinement is linked to strain-hardened austenite. Decorrelation between martensite reversion and grain size refinement is done. The use of the Gleeble thermomechanical simulator combined with information from

EBSD characterization helps to answer the questions which are the limitations in term of grain size refinement based on the texture evolution during recrystallisation.

11:00 AM

(ICOTOM-S10-021-2008) On the Stability of Recrystallization Textures in Low Alloyed Zirconium Sheets

F. Gerspach*, N. Bozzolo, F. Wagner, LETAM, Université Paul Verlaine-Metz, France

It has been recognized since many years that the texture evolves only very slightly during primary recrystallization in low alloyed titanium and zirconium sheets subjected to severe cold rolling reduction. This retention of the deformation texture, despite the complete regeneration of the microstructure, has been explained by the non oriented nucleation in very fragmented grains and, up to a limited extent, by extended recovery. However the stability of the texture during the primary recrystallization is not a general rule. In this presentation we will give examples of texture evolution occurring in low alloyed Zr sheets submitted to different cold rolling schedules up to a limited thickness reduction (40 to 60%). In such cases the recrystallization texture is somewhat different from the deformation one. This is shown to be linked to the various deformation microstructures which exhibit distinctive heterogeneity in the distribution of the strain. Careful examinations have been conducted using EBSD mapping after deformation as well as at different stages of the annealing process. X-Ray diffraction and quantitative texture analysis have been used also to characterize the global change of the orientation distribution. In the deformed samples, orientations of the most deformed areas could be identified by comparing EBSD and XRD textures. These comparisons allow to understand the particular texture of the nuclei which grow the fastest. Once these most deformed areas have disappeared, the new grains grow in a more homogeneous way –and with very weak selection of orientation– so their texture leads to the one seen at the end of primary recrystallization. The present investigations provide a more complete overview of the recrystallization process and the mechanisms of texture change in cold rolled Zr.

11:15 AM

(ICOTOM-S10-022-2008) In-Situ SEM/EBSP Analysis during Annealing in Al-Mg Alloys

Y. Takayama*, K. Morita, H. Kato, Utsunomiya University, Japan; Y. Ookubo, Sumitomo Light Metal Industries Ltd., Japan

In-situ SEM/EBSP analysis has been performed in pure aluminum, Al-1mass%Mg and Al-3mass%Mg sheets. These sheets were cold rolled with 50%, 70% or 90% reduction for each material after the process of casting, homogenizing and hot rolling. The sheet sample was analyzed by the EBSP technique at a constant temperature, which was step-heated repeatedly by 20K or 50K from a room temperature to 673K. Recrystallized grains appeared earliest in pure aluminum among three materials with 90% reduction. However, the grains appeared in Al-3mass%Mg earlier than in Al-1%Mg, because the grains in former involved many cube oriented ones. In materials with 70% reduction, growth and disappearance of fine recrystallized grains in the vicinity of grain boundary were observed with formation of preferred orientation.

11:30 AM

(ICOTOM-S10-023-2008) Effects of Elastic Modulus on Deformation and Recrystallization of High Purity Nb

D. C. Baars*, H. Jiang, T. R. Bieler, A. Zamiri, C. Compton, F. Pourboghrat, Michigan State University, USA; K. Hartwig, Texas A&M University, USA

Deformation and recrystallization textures of pure niobium and other BCC metals differs markedly, in that both deformation and recrystallization textures tend to be weaker in pure Nb than in steels or other BCC metals. A major difference between Nb and other BCC metals is that the elastic anisotropy is the opposite of Fe; $A \sim 0.5$ for Nb, $A \sim 2$ for Fe, and the other BCC metals are in between. Several experimental approaches used for characterizing deformation and recrystallization textures in Nb are summarized, including rolling of a

tapered slab of a starting material with a moderate rotated cube texture, deformation and recrystallization studies of a commercially produced Nb sheet with unusual sheet anisotropy and texture gradients, equal channel angle extrusion experiments, and uniaxial tensile deformation followed by rapid heating of single crystals. These observations are compared with literature results from other BCC metals, and analyzed using several recrystallization theories, including oriented nucleation or growth, strain induced grain boundary migration, and maximum elastic strain energy release. In steels, significant deformation textures develop on the alpha fiber while they do not in Nb. In Nb, deformation leads to formation of strong peaks on the gamma fiber rather than a smooth range of orientations. These differences in deformation texture clearly lead to differences in the recrystallization response. In steels, dislocation pileups develop in directions that are elastically the stiffest $\langle 111 \rangle$ direction, while $\langle 111 \rangle$ is the most compliant direction in Nb. The influence of these differences on boundary migration during primary recrystallization is examined to help explain the observed differences.

11:45 AM

(ICOTOM-S10-024-2008) Nucleation and Growth of New Grains in Deformed Quartz Single Crystals

L. Lagoeiro*, P. Barbosa, Federal University of Ouro Preto, Brazil

Intracrystalline microcracks developed in quartz single crystals deformed at temperatures around 300°C. We investigate how these microcracks initiated and how their structures evolved with ongoing deformation. Microstructural analysis and crystallographic orientation measurements were done using an optical microscope equipped with a Universal Stage. Two distinct microstructural and textural domains were separated: single crystals and new grains. In the single crystal domains elongate subgrains are decorated by trails of fluid inclusions. The c-axes of single crystals concentrate around the X-direction of the pole figure. Single crystals are crosscut by microcracks of variable width. These microcracks are filled with a polycrystalline aggregate of quartz crystals of nearly equant shape. The new grains in microcracks have straight boundaries and wide size distributions. The transition between single crystals and the equant quartz grains observed along the microcrack walls is abrupt. Crystallographic orientations of the poly crystals contrast with those of single crystal. The c-axes of new grains are oriented in a range of 20-70° to the X-direction. Within the host grain, microstructures are indicative of deformation by glide-controlled lattice rotation and microfracturing. New grains formed within the microcracks have strong crystallographic preferred orientation that differs from those of single crystals. The misorientation angle between single crystal and new grains can be higher than 50°. Based on the microstructures and the CPO pattern contrast between host and new grains we conclude that the new grains developed by preferred growth from small nuclei which were mechanically formed and rotated within the microcracks. New grains are optically strain-free and have straight boundaries suggesting growth by static recrystallization as result of annealing in the ductile field subsequent to deformation in the brittle field. The deviation of c-axis orientation of the new grains from the host grains as well as the sudden transition between those microstructural domains are used as arguments for mechanical rotation and formation of nuclei which subsequent coarsening by annealing.

12:00 PM

(ICOTOM-S10-025-2008) Effect of Solute Atoms on the Recrystallization Texture of Mg Alloys: In-Situ Annealing Experiments

R. Shahbazian Yassar*, Michigan Technological University, USA; S. Agnew, University of Virginia, USA; P. Kalu, National High Magnetic Laboratory, USA

At room temperatures, the ductility of Mg alloys is limited ascribed to their hexagonal close-packed (HCP) crystal structure and the shortage of independent slip systems. Several researchers have reported the dramatic improvement of Mg ductility using rare-earth solute atoms. The present research work aims to understand the effect of the rare-earth solute atoms on recrystallization texture of Mg alloys by means

Abstracts

of the in-situ heating experiments in scanning electron microscopy along with electron backscatter diffraction technique. Several specimens with different concentration of solute atoms were subjected to deformation and the subsequent recrystallization behavior was tracked in the microscope. A study of both boundary motion and texture development as a function of plastic strains and solute atoms concentration is presented.

Monday, June 2 and Tuesday, June 3, 2008

Poster Session

Room: Rangos 2 & 3

(ICOTOM-P-001-2008) Texture Evolution in Dissimilar Al/Fe Welds: Influence of the Pin Position

I. Drouelle, A. Etter, T. Baudin, R. Penelle*, Université d'Orsay - Paris Sud, France

As automotive industry, aeronautic industry need to lighten the structure of their car or plane, welded spots have been realized on a stacking of two sheets (Aluminum alloy-steel) by the Friction Stir Welding (FSW) process. By FSW, different configurations of welding can be done : alloys can be superposed, or placed side to side. In this work, alloys were side to side. Different process parameters have been tested (as dwell-time, pressure...) and the influence of the position of the spot will only be described in the present paper. A study of the microstructures and the crystallographic textures associated to mechanical tests (shear and tensile tests) allowed us to determine the best set of welding parameters. In this study, samples were characterised by numerous experimental technics as optical microscopy (MO), scanning electronic microscopy (SEM/EDX), microhardness and at least X-ray diffraction. It has been found that a very high quantity of intermetallic compounds (especially AlFe, Al₅Fe₂ and Al₂Fe were formed (so controlling the formation of those precipitates in order to have a welding with good mechanical properties is very important). In some cases, cracks were mainly observed in the welding on the intermetallic areas (so the chemical composition plays an important role) Moreover, the recrystallized area around the welding has been characterized by Electron BackScattered Diffraction. A mechanism of continuous dynamic recrystallization has been identified since misorientation of sub-boundary increases close to the welding. At least, texture characterisation should be correlated to the recrystallized area.

(ICOTOM-P-002-2008) Anisotropic Texture Evolution in Ti and Ni-based Alloys After Friction Stir Processing

O. M. Barabash, R. I. Barabash*, G. E. Ice, Z. Feng, S. David, Oak Ridge National Laboratory, USA

Plastic deformation and structural changes of a Ti and Ni-based superalloy surface after Friction Stir Processing (FSP) were analyzed by means of SEM, EBSD and advanced 3D polychromatic X-ray micro diffraction at the APS synchrotron. Spatially resolved 3D Laue diffraction allowed observing the changes in dislocation arrangement with depth in different regions of the FSP alloys. Formation of two specific zones was established: friction stir zone, and thermomechanically and heat affected zones. It was shown that FSP generates a large number of geometrically necessary dislocations. Anisotropy of the all stir processing zones is demonstrated. Bimodal distribution of grain size is observed in the stir zone.

(ICOTOM-P-003-2008) Effect of Microstructure on Mechanical Properties of Friction-welded Joints between Aluminum Alloys (6061, 5052) and 304 Stainless Steel

S. K. Sahoo, IIT Bombay, India; N. T. Kumbhar, Bhabha Atomic Research Centre, India; I. Samajdar*, IIT Bombay, India; A. Laik, G. K. Dey, K. Bhanumurthy, J. Krishnan, D. J. Derose, R. L. Suthar, Bhabha Atomic Research Centre, India

Commercial Aluminum alloys 5052 and 6061 were welded to AISI 304 stainless steel using a continuous drive welding technique. The

welded microstructures consisted of a reaction layer, between aluminum and stainless steel – approximately of 2 μm thickness under condition of relatively long friction time and low upset pressure, and plastically deformed regions. The former consisted of FeAl intermetallics, while the latter had shown clear signatures of grain refinement and of in-grain misorientation development. In order to study the effect of interlayer on the joining efficiency, Cu interlayer was diffusion bonded to stainless steel and subsequently friction welded to Al alloys. The interlayer affected the nature of the interface – noticeable absence of intermetallic precipitates. The Cu interlayer also reduced the severity of the plastic deformation in the respective alloys.

(ICOTOM-P-004-2008) Grain Boundary Characteristics of the PED Nano-twin Copper Films

D. R. Waryoba*, FAMU-FSU College of Engineering, USA; B. Cui, National High Magnetic Field Laboratory, USA; P. N. Kalu, FAMU-FSU College of Engineering, USA

Nano-twin copper films have been sensitized by the pulsed electrodeposition (PED) technique using cold-rolled 304 stainless steel (304SS) and MP35N alloy as substrates. The PDE was carried out in an electrolyte of CuSO₄ solution with cathodic square wave pulses generated by turning on and off the current periodically. The resulting crystallographic textures of the films showed dependence on both the peak current density (PCD) and the substrate used. While for $\text{PCD} \leq 0.75 \text{ A/sq cm}$, the MP35N substrate developed a quasi-epitaxial {110} texture in the Cu film, the 304 SS substrate resulted in a {111} texture at a moderately higher PCD. This paper addresses the effects of these processing conditions on the grain boundary structure of the films. Electron backscatter diffraction (EBSD) technique in the Zeiss XB1540 field emission gun scanning electron microscope (FEGSEM) was used in this study.

(ICOTOM-P-005-2008) X-Ray Microdiffraction Study of Grain-by-Grain Epitaxy of YBCO on Polycrystalline Ni

E. Specht*, A. Goyal, Oak Ridge National Laboratory, USA; W. Liu, Argonne National Laboratory, USA

Consistent epitaxy is critical to the application of coated-conductor films to high-temperature superconductors; by studying epitaxy on each grain of the polycrystalline substrate, we determine which grains provide the proper conditions for favorable epitaxy. White-beam x-ray microdiffraction is used to analyze substrate and film orientations for a high-critical current superconducting YBCO film grown on a Ni-alloy substrate. A novel image-analysis technique is introduced in which a Hough transform is used to recognize arcs in Laue microdiffraction patterns which correspond to low-index zone axes. The YBCO is systematically misoriented with respect to the Ni, with its [001] axis rotated toward the surface normal. Crystal mosaic is measured over a range of length scales. In the $0.5 \mu\text{m}^2$ area of a single diffraction pattern, YBCO mosaic is $\sim 0.7^\circ$ on Ni grains with low tilt, increasing for substrate grains with higher tilts. YBCO mosaic measured over the entire area of a Ni grain is $\sim 2.5^\circ$, varying inversely with substrate grain size. YBCO mosaic for the entire film is $\sim 4^\circ$. Careful tailoring the substrate microstructure is required for consistent epitaxy. Work sponsored by the Office of Electricity Delivery and Energy Reliability, Superconductivity Program for Electric Power Systems and the Division of Materials Sciences and Engineering, Office of Basic Energy Sciences, United States Department of Energy.

(ICOTOM-P-006-2008) Epitaxial Substrates of Ni-based Ternary Alloys with Cr and W

I. Gervasyeva*, D. Rodionov, J. Khlebnikova, Russian Academy of Sciences, Russian Federation

Obtaining high levels of critical current in tape high-temperature superconductors made by RABiTS(TM) process requires development of sharp biaxial texture in superconducting film YBaCuO. This is achieved by its epitaxial deposition via buffer layers onto thin metal strip of nickel or its alloys. Metal tape should possess sharp cube texture and, in addition, should be strong enough to enable manufactur-

ing of long tapes; it is also desirable to be non-ferromagnetic at the superconductor operating temperature (77 K). Texture, structure, physical and mechanical properties in thin tapes – substrates from some Ni-based ternary alloys have been studied depending on the content of alloying elements (W - 1.8; 2.6; 3.6 at.%; Cr - 8.6; 7.8; 7.2 at.%). An increase of tungsten concentration in nickel binary alloy results in intensive strengthening of tapes, addition of chromium decreases Curie temperature. Formation of cube texture in rolled (98-99%) tapes of binary nickel-based alloys is possible if deformation texture of the tapes has sum of components $S\{123\}<634>$ and $C\{112\}<111>$ volume fractions higher than double volume fraction of component B $\{110\}<112>$. Lattice parameter of the alloy in this case should not be above 3.55 Å. It was revealed in this work, that in all alloys investigated Curie temperature is lower 77K. The alloy with 3.6%W Ni89.2W3.6Cr7.2 has deformation texture component composition closer for “brass type” and the lattice parameter approximates to the upper limit 3.55 Å. Cube texture scattering in this alloy is much more then in the alloys with lower concentration of tungsten. Ni89.6W1.8Cr8.6 and Ni89.6W2.6Cr7.8 alloys have “copper type” deformation texture and sharp recrystallization cube texture. Strength value in these alloys exceeds those of pure nickel by several times. So, the last two ternary alloys Ni-W-Cr have a good chemical composition for producing non-magnetic, strengthening tapes for HTS.

(ICOTOM-P-007-2008) Texturing in Functional Thin Film Ceramic Battery Cathode Materials

J. Whitacre*, Carnegie Mellon University, USA

Thin film Li-ion battery cathode materials have been produced for over a decade and are important both for application in thin film solid-state batteries, and also as a platform for basic studies on interfacial and bulk functionality for novel Li battery cathode materials. As in metallic films, a preferred out-of-plane crystallographic orientation typically evolves during the deposition process (and sometimes is modified during post-deposition processing). The anisotropic nature of Li diffusion and migration through these solids make the type and degree of texturing of utmost importance. This talk will cover observed texturing phenomena in both the layered/rhombohedral LiMO₂ system (where M is some combination of Co, Ni, and Mn) as well as the olivine LiMPO₄ system (where M is Fe, Mn, or Co). The importance of deposition parameters and post-deposition treatments will be discussed and the relationship between electrochemical performance and degree and type of texture will be shown.

(ICOTOM-P-008-2008) Improvements in EBSD Data Analysis as Applied to Tantalum

D. Field*, Washington State University, USA; L. Maiocco, K. R. Ackley, Cabot, USA

The sputtering performance of tantalum targets is highly dependent on the crystallographic texture of the bombarded surface. The sputtering rates vary significantly as a function of crystallographic orientation. As a result, texture analysis of tantalum has been a focus of much research, and numerous methods for analyzing and representing texture data have been investigated. In this paper, an improved method of quantifying and comparing EBSD data will be presented with enhanced data filtering and noise reduction. Performance of the new algorithm will be demonstrated on a range of microstructure exhibiting varying degrees of inhomogeneity.

(ICOTOM-P-009-2008) Microstructures and Microtextures of Au Flip Chip Bonds during Microelectronics Packaging

P. Yang*, C. Li, University of Science & Technology Beijing, China; D. Liu, M. Hung, M. Li, ASM Assembly Automation Ltd., China; W. Mao, University of Science & Technology Beijing, China

Au flip chip bonding play important roll in the quality control of the production of microelectronic devices. The microelectronics packaging industry interests mainly in the relationship between processing parameters (such as ultrasonic power, loading force, ultrasonic loading time and bonding temperature) and shear strength which reflects

the bondability at interfaces. However, the shear strength did not increase always proportionally with the processing parameters and the deformation in bonds is quite inhomogeneous. Therefore, it is necessary to establish the relationship among the processing parameters, shear strength and the related microstructures/microtextures. This paper presents results of orientation mapping which reveal the microstructures and microtextures in Au flip chip bonds and addresses the relationship between microstructure/microtextures and shear strength.

(ICOTOM-P-010-2008) Microstructure and Texture of Nb/SmCo₅ Bilayers

W. Skrotzki, R. Schaarschuch*, Technische Universität Dresden, Germany; S. Haindl, Leibniz-Institut für Festkörper- und Werkstofforschung, Germany; M. Reibold, Technische Universität Dresden, Germany; V. Neu, B. Holtzapfel, Leibniz-Institut für Festkörper- und Werkstofforschung, Germany; C. Oertel, Technische Universität Dresden, Germany; L. Schultz, Leibniz-Institut für Festkörper- und Werkstofforschung, Germany

Since the possibility of “magnetic pinning” of vortices was reported many attempts were made to join the obvious antagonistic couple in the form of multilayers with a certain superconductor/ferromagnet sequence. Magnetic pinning describes the interaction between vortices of a superconductor with domain walls of a ferromagnet situated directly above or below the superconductor. So-called hybrid structures based on superconducting Nb and high coercive ferromagnetic SmCo₅ films grown on MgO(100) substrates were fabricated by pulsed laser deposition under UHV conditions. Thin film architectures of SmCo₅ on Nb and the reversed system both, with and without Cr-spacer layer between superconductor and ferromagnet, were examined. The microstructures and textures/epitaxial relationships of the grown films were characterized by TEM and X-ray diffraction, respectively. As a result, for the layer system Nb/SmCo₅ the epitaxial relationships

$MgO(001)[100]//Cr(001)[110]//Nb(001)[110]//Cr(001)[110]//SmCo_5(11-20)[0001]//Cr(001)[110]$ were found. With decreasing thickness of the Cr-spacer layer the SmCo₅ texture becomes random. In contrast, for the system SmCo₅/Nb with decreasing thickness of the Cr-spacer layer the Nb texture changes from the component given above to a $\langle 110 \rangle$ fibre. The findings are discussed with regard to lattice matching.

(ICOTOM-P-011-2008) On the Role of Nucleation during Microtexture Evolution in CVD Deposition of Diamond Thin Films

T. Liu*, S. Zaeferrer, D. Raabe, Max-Planck-Institut fuer Eisenforschung, Germany

This paper presents the evolution of microstructure and microtexture in the nucleation zone of diamond thin films deposited with variations in substrate, methane concentration, and film thickness. The films have been investigated using high-resolution electron backscattering diffraction (HR-EBSD) and transmission electron microscopy (TEM). The microstructures, microtextures, and grain boundary character distributions were characterized. Based on the texture observation, the grain orientation principally exhibited the low-index fiber textures.

(ICOTOM-P-012-2008) Influence of the As-Cast Microstructure on the Evolution of the Hot Rolling Textures of Ferritic Stainless Steels with Different Compositions

P. Nnamchi*, D. Ponge, D. Raabe, Max-Planck-Institut für Eisenforschung, Germany; A. Barani, G. Bruckner, J. Krautschik, ThyssenKrupp Nirosta GmbH, Germany

The influence of the initial texture and microstructure on the subsequent hot rolling texture of continuously cast ferritic stainless steels with different compositions was studied using deformation dilatometry, optical microscopy and EBSD analysis. The initial as-cast slab microstructures in the steels contains layers both of columnar and equiaxed grains. By an addition of Nb and Ti the appearance of columnar grains can be suppressed arising from the variations in

Abstracts

composition. The starting texture, microstructure and composition in ferritic stainless steels play a very important role in the subsequent texture evolution. However, the microstructure and texture of the slab has received relatively little attention. The aim of this study is to discuss the influence of the as-cast microstructures on the evolution of the hot rolling texture in different types of ferritic stainless steels.

(ICOTOM-P-013-2008) Texture of Warm Rolled and Accumulative Roll Bonding (ARB) Processed Ferrite

A. Akbarzadeh*, Sharif Univ. of Technology, Iran; A. Kolahi, Sharif University of Technology, Iran

An IF steel was severely deformed using Accumulative Roll Bonding (ARB) process and warm rolling. The maximum equivalent strains for ARB and warm rolling were 4.8 and 4.0, respectively. The micro-texture was studied using scanning electron microscopy equipped with Electron Back Scattered Diffraction (EBSD). The through thickness texture gradient in the ARB samples is different from the warm rolled samples. The shear textures were limited to the surface region prior to the 6th cycle of ARB and quarter thickness and mid-thickness layers show very strong and relatively strong rolling fibre textures, respectively. At the 6th cycle, there was, however, a relatively strong shear texture across the thickness, except at mid-thickness and the shear texture from surface toward the center becomes weaker. Lack of shear texture at the mid-thickness layers related to destructive effect of plane strain deformation on shear orientations at this region. This combination of shear texture and rolling texture across the thickness results in a weak overall texture. The warm rolled samples display sharp rolling textures through the thickness with increasing the sharpness toward the center. EBSD study on samples following the annealing at 750 °C verified texture gradient through thickness of ARB processed and warm rolled samples. The annealing process could not change the texture gradient and in the ARB samples shear orientations at surface and quarter thickness layers can be identified even after annealing.

(ICOTOM-P-014-2008) Microstructure and Texture of Two Ferritic Stainless Steels

A. L. Pinto*, Instituto Militar de Engenharia, Brazil; C. S. da Costa Viana, A. L. Costa, Universidade Federal Fluminense, Brazil

The present work is an investigation on the microstructure, texture and microtexture of two ferritic stainless steels, AISI 430A and AISI 430E, subject to thermomechanical treatments aiming at a better understanding of the formation of their recrystallisation texture. The materials were supplied as 4mm thick hot rolled sheets, being 80% cold rolled and annealed in a salt bath, for 30 seconds, at various temperatures. Samples were analysed by quantitative metallography, texture measurement by X-ray diffraction and microtexture by EBSD and OIM techniques. The results showed that the texture observed in both steels were similar as far as the hot and cold rolling conditions were concerned. However, the hot rolling texture of the 430A steel displayed a mild $\{110\}\langle 1\ -1\ 0\rangle$ component not observed in the 430E steel in the same condition. In none of these textures was the Goss component observed, contrary to observations in the literature. The analysis of the orientation maps, inverse pole figures and ODF plots showed that the main components present in the treated materials were $\{111\}\langle 1\ 0\ -1\rangle$, $\{001\}\langle 100\rangle$ and $\{001\}\langle 110\rangle$. It was also observed that the $\{111\}\langle uvw\rangle$ grains recrystallise first and in the fashion of elongated colonies while grains whose orientations fall near to $\{001\}\langle uvw\rangle$ tend to remain unrecrystallised (recovered). A technique was developed for separating the ODF of the recrystallised grains from the general orientation distribution, in the partially recrystallised materials. This technique, based on fitting gaussian functions onto selected QI (quality index) points, was considered both a useful and reliable first approach method to the analysis of this kind of microstructure.

(ICOTOM-P-015-2008) Effect of Tin on the Texture of Non-oriented Electrical Steels

C. Hou*, T. Lee, C. Liao, National Yunlin University of Science and Technology, Taiwan

The effect of tin, range from 0.029- 0.21wt% on the inclusion size in hot bands, grain size and texture of four nonoriented electrical steels after final annealing has been investigated. The steel ingots were reheated to 1200°C and finished rolled at 950°C. Then hot bands were annealed at 750°C for two hours and cold rolled to 0.5mm. After cold rolled sheets annealing at 750-950°C for one minute, both X-ray diffractometer with texture attachment and EBSD were conducted to measure specimen texture. It were found that 5-10 μm coarse MnS+AlN inclusions existed in the hot bands containing 0.029wt% tin. However, 1-2μm fine MnS+AlN inclusions existed in the hot bands containing 0.21wt% tin. After final annealing, grain size decreased with increasing tin content and became level off while tin reached 0.10wt%. At the same cold rolled annealing temperature, the intensity of (110)[001] texture increased with increasing tin content. In the same steel, the intensity of (110)[001] texture increased with increasing annealing texture and reached a maximum value and then fell down. The temperature to obtain maximum intensity of (110)[001] texture strongly correlated to tin content. EBSD showed that the number and volume fraction of (110)[001] grain per mm² increased with increasing tin content. It is postulated that tin promote the number of (110)[001] nuclei during final annealing.

(ICOTOM-P-016-2008) Combination of two X-ray Diffraction Settings for Determining the Texture of Small Sheared Samples

D. Barbier*, B. Bolle, J. Fundenberger, C. Laruelle, A. Tidu, LETAM, France

Texture measurement limitations occur when small size samples (ie with a small gauge area) are investigated by classical XRay diffraction. As the irradiated surface increases with the tilt angle (χ), it becomes larger than the gauge area. The analyzed pole figures are then reduced to low values of the tilt angle χ and do not allow a accurate texture determination on the whole Euler space. In the case of small sheared samples, used to test high strength alloys, the gauge area is generally less than 3mm width which limits the pole figure measurement to $\chi = 50^\circ$ for a XRay beam section of 0.8 mm. Therefore, to study the texture evolutions of small samples submitted to shear tests, the use of adapted XRay techniques is necessary. To enlarge the measurement range of pole figures and perform measurements on small samples, we have used two complementary methods. The first one is the Bragg-Brentano geometry which is used for small tilt angles. In the second one, used for larger tilt angles, the section of the incident XRay beam remains lower than the sample surface thanks to a specific diffraction setting developed for thin film measurement. The diffraction experiment is conducted so that the incidence angle between the incident beam and the sample surface is kept constant. Consequently, the irradiated area is constant during the measurement. The choice of the convenient incidence angle, which permits to extend the pole figure measurements for high tilt angles is then an important parameter. This method requires to drive three angles of the goniometer (θ_{inc} , χ , ϕ) and to perform two treatments of the diffracted intensities: 1) the intensities are corrected considering the evolution of the diffracting volumes 2) the intensities at the nodes of a convenient regular grid are calculated by interpolation. The pole figures are reconstructed from the intensities obtained by these different measurements and by adjusting the intensity levels in the overlapping measurement zones. In this contribution, we present in details these combined techniques applied to the texture measurement of a high strength FeMnC austenitic TWIP steel during simple and reverse shear testing.

(ICOTOM-P-017-2008) Analysis of the Formation and Growth of Recrystallizing Grains in IF Steels by In-Situ EBSD

H. Nakamichi*, Steel Research Lab., JFE Steel, Japan; J. F. Humphreys, University of Manchester, United Kingdom

The texture evolution of IF steels during recrystallization is very important for the control of drawability, and many experiments have

been carried out to evaluate the nucleation and growth of recrystallized grains in order to understand the mechanisms of recrystallization. We have performed *in-situ* SEM-EBSD microstructural analysis on IF steels to directly observe and quantify the recrystallization processes. Samples deformed to strains of 0.75 and 1.6 were heated in an FEG-SEM chamber up to 800°C, and sequential recrystallization phenomena such as the formation and growth of new grains were recorded through rapid EBSD mapping. Analysis of the data enabled the orientation relationships between each deformed grain and the new recrystallized grains in the same area to be determined. The growth kinetics of particular texture components and the final recrystallization textures were also investigated. In the highly deformed material, it is found that $\{111\}\langle 123 \rangle$ grains are preferentially formed from deformed γ -fibre. It is also found that in the initial stages of recrystallization of the highly deformed sample there is a preferred rotation angle of $\sim 30^\circ$ between the deformed and recrystallizing grains. Although the statistics are rather poor, a slight tendency for $\langle 111 \rangle$ rotation axes was also detected. During the later stage of recrystallization, the growing grain encounters other deformed grains, and if they have higher misorientation ($>40^\circ$) then it is found that the growth rate is much lower. This suggests that recrystallizing grains of $\sim 30^\circ$ misorientation to a deformed grain are the first formed and exhibit preferential growth. However, from the present observation, there is no strong evidence of a $27^\circ/\langle 110 \rangle$ relationship between deformed and recrystallized grains, as has been previously suggested. In the lower deformed sample it was found that the rotation angle and axis between deformed and recrystallized material tended to be random, the formed peaking at $\sim 50^\circ$. Although these observations were made only on the surfaces, comparison with bulk experiments gives confidence that the recrystallization phenomena of the present experiment are valid.

(ICOTOM-P-018-2008) Primary and Secondary Recrystallization texture in Fe-3%Si Grain-Oriented Silicon Steels Containing Antimony

H. Joo*, J. Park, K. Han, J. Kim, Technical Research Laboratories, POSCO, South Korea

Sb like Sn is well known as a segregating element. It was reported that addition of Sb and Sn inhibits grain growth and changes texture during primary as well as secondary recrystallization. Sb segregation to grain boundary prevents the nucleation of recrystallization near the original grain boundaries and decreases the (111) texture component. In this study, primary and secondary recrystallization texture in 3% Si grain-oriented silicon steel containing Sb was investigated. In our experiments, Eta Fiber component (Rolling Direction// $\langle 100 \rangle$) in the specimens bearing Sb is strongly developed during primary recrystallization. Especially, $\{012\}\langle 100 \rangle$ and $\{013\}\langle 100 \rangle$ components are very strong. The orientations of secondary recrystallized grain bearing Sb are also measured. In order to study the orientation of individual grain in large sized polygranular materials, we developed the automatic orientation measurement system based on x-ray Laue method. Accuracy of orientation measurement which is tested using Si single crystal with (100) orientation is less than 0.5° . In order to estimate the deviation angle from Goss orientation, we calculated the misorientation angles such as α , β , and γ . α and β is angles between rolling direction and the projected direction of [001] on sample surface and on the plane perpendicular to transverse direction in the sample coordinate, respectively. γ is angle between normal direction and the projected direction of [110] on the plane perpendicular to rolling direction. The average α , β , and γ angles of Sb-free specimen and Sb-bearing specimen are measured. It was reported that beta angle is closely connected with domain width. As long as the β angle does not exceed about 2° , the decrease in magnetostatic energy occurs through a width reduction of the 180° domains without creating such harmful structures as spike domains. However, too large β angles cause the onset of harmful secondary structures. Therefore, the measurements of α , β , and γ angles are very important to control magnetic properties.

(ICOTOM-P-019-2008) Texture, Microstructure and Drawability of Frictionally Rolled AA 3003 Al Alloy Sheets

I. Kim*, S. Akramov, N. Park, J. Kim, Kum Oh National Institute of Technology, South Korea

The preferred crystallographic orientations (texture) of the metals are related to the physical, mechanical properties, and drawability of sheet metal forming. In this study, texture evolution and plastic strain ratio are investigated after frictionally rolled and subsequent heat treated AA 3003 Al alloy sheets. The specimens after frictionally rolling showed a very fine grain size and the specimens after frictionally rolling and subsequent heat-treatment were increased the ND // $\langle 111 \rangle$ texture component. One of the most important properties in sheet metals is drawability. The r-value or plastic strain ratio has been used as a parameter that expresses the drawability of sheet metals. The change of the plastic strain ratios after frictionally rolling and subsequent heat-treatment conditions have been investigated and it were found that they were about two times higher than those of the original Al sheets. These could be attributed to the formation of ND // $\langle 111 \rangle$ texture components texture components through asymmetry rolling in AA 3003 Al sheets.

(ICOTOM-P-020-2008) TEM study of the inhibition layer of Commercial Hot-Dip Galvanized Steels

J. Elia*, LETAM, France

Hot-dip galvanized steels are largely used in automotive industry. The control of microstructure of the coating is mandatory to improve the mechanical performance to enhance formability, adhesion and damage resistance. In continuous galvanization process, small amounts of aluminum are added to galvanization alloys, the fast reactivity of aluminum with steel produces a thin Fe-Al layer which inhibits the formation of the brittle Fe-Zn intermetallics. Extensive research has been made to understand the formation process of the inhibition layer that governs the nucleation and the growth of the coating. The extreme thinness of this layer, around 50 to 150 nm makes the buried layer characterization delicate on plane view because the samples are difficult to prepare for TEM studies. In this paper, the inhibition layer was analyzed after the Zinc coating and the steel substrate have been stripped away by electrochemical etching. TEM imaging, selected area electron diffraction and EDX analysis have been made on the samples of GI galvanized steel at 0.35%Al in the bath. The double layer model proposed by Baril et l'Espérance have been confirmed with big Fe-Al grains spread on a continuous Fe-Al nanograins layer at Fe interface, and a Fe-Zn layer surrounding the Fe-Al grains on the Zn interface has also been identified.

(ICOTOM-P-021-2008) Texture Formation and Nucleation Observation during Recrystallization in Nonoriented Electrical Steels

J. Park*, K. Han, J. Kim, Technical Research Lab. POSCO, South Korea; J. A. Szpunar, McGill University, Canada

Nonoriented electrical steels have been widely used as core materials in motors and generators. The magnetic properties of these steels are influenced by the grain size and crystallographic texture of final products. Although nonoriented electrical steels have been one of the steel products that can benefit most from texture optimization for improvement of magnetic properties, the focus of processing technology has largely been on the control of grain size. Therefore, there is much more possibilities to improve the magnetic properties of nonoriented steels through texture control. Recrystallization texture has long been a subject of research, but the detailed phenomena occurring during the evolution of recrystallization texture is still disputed. This dispute is associated with the complexity of microstructural inhomogeneity that exists in the deformed state. Additionally, the formation of recrystallization texture in nonoriented electrical steels has not been extensively studied compared with other kinds of steels. In the present study, systematic investigations on the formation of recrystallization texture are carried out for nonoriented electrical steels with 2% Si.

Abstracts

Microstructure transformation obtained from EBSD measurements on partially recrystallized specimens is also analyzed. Most nuclei have a high misorientation relationship with the surrounding deformed matrix: 25~55 degree. Main texture components of nuclei or recrystallized grains during the progress of recrystallization are Goss and $\{111\}\langle 112 \rangle$. Deformed ND fibre grains generally disappear at the early stage of recrystallization whereas deformed RD fibre grains are mostly consumed at the late stage of recrystallization. This difference is attributed to the difference in stored energy with the orientation of deformed grains. The formation of the substructures is closely related to the orientation of deformed grains. The local misorientation between adjacent points in the deformed $\{001\}\langle 110 \rangle$ grain is very low, whereas the misorientation in the deformed $\{111\}\langle 110 \rangle$ grain is high. This high misorientation can be expected to be the preferential site for nucleation during recrystallization.

(ICOTOM-P-022-2008) Including Elastica Anisotropy of Welds in Finite Element Predictions of Residual Stresses

K. Decroos*, C. Ohms, JRC Petten, Netherlands; M. Seefeldt, F. Verhaeghe, mtm leuven, Belgium

The effect of including welding texture in a finite element model of an austenitic weld is investigated. Due to a preferential $[100]$ growth in the solidification direction the weld material is not elastic isotropic but transversal isotropic with the solidification direction as the fiber axis. Results show a significant difference of the predicted residual stress in the weld when considering this effect compared with a traditional model where elastic isotropic materials are used.

(ICOTOM-P-023-2008) OBSERVATION OF SOLID-STATE WETTING MORPHOLOGY IN ABNORMALLY GROWING GRAIN OF Fe-3%Si STEEL

K. Ko*, Seoul National University, South Korea; J. Park, J. Kim, POSCO, South Korea; N. Hwang, Seoul National University, South Korea

Abnormal grain growth (AGG) which is also called secondary recrystallization takes place in many metallic systems especially after recrystallization of deformed polycrystals. A famous example is the evolution of the strong Goss texture after secondary recrystallization in Fe-3%Si steel. Extensive efforts have been made to identify the growth advantage of Goss grains due to its scientific and technological interests. However, the Goss secondary recrystallization or AGG still remains as a puzzling phenomenon since its first report by Goss in 1935. In this study, we suggest a new approach to the growth advantage of AGG by solid-state wetting, where a grain wets or penetrates the grain boundary or the triple junction of neighboring grains just as the liquid phase wets along the grain boundary or the triple junction. Once the solid-state wetting occurs, the triple junction, which tends to be a rate-determining step in grain growth, migrates much faster than the grain boundaries in contact and therefore, the triple junction constraint in grain growth disappears. According to the solid-state wetting mechanism, the sub-grain boundaries which have very low energy can play a critical role in inducing AGG, because they provide grains with the exclusive growth advantage by increasing the wetting probability. The experimentally-observed abnormally growing grain by solid-state wetting has the microstructural feature of AGG such as the formation of numerous island and peninsular grains. The misorientation angles between island or peninsular grains and the abnormally-growing Goss grains were mostly low angles less than 15° with some high angle boundary of coincidence site lattice relationship, which indicates that they have the low grain boundary energy. 3-sided or 4-sided grains with negative curvatures, which are formed near the growth front of abnormally growing grains, are the two-dimensional section vertical to the triple junction wetting in three-dimensional polycrystalline structure. Very low angle sub-grain boundary inside abnormally growing grain were observed using kernel average misorientation mapping by EBSD.

(ICOTOM-P-024-2008) Microstructural Characterization of Dual Phase Steels by means of Electron Microscopy

L. Barbe*, P. Pouteau, Centre for Research in Metallurgy (CRM), Belgium; K. Verbeken, Ghent University, Belgium

Dual phase (DP) steels have a low yield strength due to the soft ferrite matrix and a high tensile strength due to the hard dispersed martensite second phase islands. This makes them excellent steels for use in light weight automobile structural parts. However, a profound understanding of microstructure-properties relationships of advanced high strength steels is of crucial importance to the rational development of these steels. This demands the ability to perform advanced quantification of the complex multi phase microstructure, addressing the full range of microstructural properties that are relevant to the macroscopic mechanical behaviour. The ferrite-martensite microstructure will be studied by means of Light Optical Microscopy, Scanning Electron Microscopy and Electron BackScattering Diffraction technique. The martensite fraction in ferrite-martensite DP steels will be measured both on a FEG-SEM and a LaB6-SEM. The influence of the microscope resolution on the determination of the martensite fraction by means of the Image Quality (IQ) value will be investigated. Possible texture effects on the mechanical properties will also be taken into account. Several microstructural parameters influencing the mechanical properties of the material, e.g. grain size, island size, martensite dispersion, banding... will be determined.

(ICOTOM-P-025-2008) Characterization of Mosaicity in a Mechanically Cycled Cu-13.1% Al-4.0% Ni Single Crystal Shape Memory Alloy

G. K. Kannarpady, University of Arkansas at Little Rock, USA; S. C. Vogel, Los Alamos National Laboratory, USA; A. Bhattacharyya*, University of Arkansas at Little Rock, USA

We have studied the pseudoelastic to transformation in CuAlNi shape memory alloy single crystal at 200 deg C and have found that while the maximum overall strain on the wire had been maintained at 7%, the amount of martensite at the wire mid-section (estimated from neutron diffractograms) at the end of a loading cycle decreased to 40% at the end of 1000 cycles. Other studies (optical micrography at room temperature and non-contact video extensometry of deforming samples at high temperature) prompt the hypothesis that the high temperature austenitic phase, with its $[001]$ direction originally along the wire axis of the virgin sample, may have developed mosaicity that results in a unique self-accomodated martensitic arrangement at room temperature and the low martensite conversion at high temperature at the end of 1000 cycles. This paper reports on the characterization of the mosaicity in a Cu-13.1Al-4.0Ni (wt.%) shape memory alloy that is single crystalline in the high temperature austenitic phase. The specific material used underwent cyclic pseudoelastic deformation over 1000 cycles at 200 deg C. This characterization was done under zero stress and over the temperature range, 25 deg C to 200 deg C in HIPPO at Los Alamos Neutron Science Center, Los Alamos National Laboratory, New Mexico. Cu-13.1%Al-4%Ni (wt.%) single crystal wires grown in the $[001]$ austenite basis using the method of edge-defined-film fed growth, and with nominal dimensions of 2.0 mm (diameter) and 100 mm (length) were used. The neutron diffraction data will be used to study the temperature dependent evolution of the volume fraction of different martensitic variants, as well as correlate the martensitic variant formation to the underlying texture of the austenitic phase through the kinematics of the phase transformation.

(ICOTOM-P-026-2008) X-ray Diffraction Studies on Texture Development in Aluminium Processed by Equal Angle Channel Pressing

J. te Nijenhuis*, PANalytical B.V., Netherlands; I. Cernatescu, PANalytical Inc., USA

Metal and alloys with ultrafine grains are known to have special properties, compared to more coarsely grained materials. For instance,

from the Hall-Petch relation it is known that the yield stress of metals increases with decreasing grain size. These special properties makes it attractive to fabricate metals with small grain sizes. Equal channel angular pressing (ECAP) has emerged as effective process for fabrication, because it does not change the cross-section of the sample material during the multiple passes of the process. However, the ECAP process has not only an influence on the grain size, but also on the crystallographic orientation of the crystallites, constituting the material. In order to understand the nature of the fine-grained materials, one also should study the orientation distribution and the development of the texture as a function of the various passes and different routes in the ECAP process. In the present work we have studied the development of textures in aluminium process along three different routes in the ECAP process: route A, route Bc and route C. Textures have been determined using X-ray diffraction. Due to the limited size of the samples investigated, the measurements have been performed in the parallel beam geometry with a reduced irradiated area. A description of the development related to the slip processes in the materials is given.

(ICOTOM-P-027-2008) Correlation Between Austenitic and Martensitic Textures on Cu-Al-Ni-Ti Shape Memory Alloys

C. Sobrero, A. Roatta, J. Malarria, R. E. Bolmaro*, Instituto de Fisica Rosario, Argentina

Cu-13%Al-5.5%Ni-1%Ti (Wt%) shape memory alloys were measured at room and above A_f temperatures to search for texture correlations between different phases. Textures were measured by X-ray diffraction techniques. High temperature textures were measured by a specially designed device allowing textures to be measured until 200 °C. Room temperature textures were obtained in a material produced by hot square extrusion and further annealing thermal treatment. They belong to the martensitic β' 1 monoclinic phase. At high temperature the phases are the austenitic FCC β 1, with a next-nearest neighbor order, and a low volume fraction of the X phase as precipitates. The correlation between textures is investigated by quantitative texture analysis and computer simulations. Preferential variant selection is evaluated for a few cycles to quantitatively assess shape memory effect.

(ICOTOM-P-028-2008) 3D-Orientation Microscopy in Electrodeposited CoNi

A. B. Fanta*, S. Zaefferer, D. Raabe, Max Planck Institute for Iron research, Germany

Electrodeposited nanocrystalline materials have been in continuous research in recent years. This interest is based on the general knowledge that this process allows the formation of high density films with nanocrystalline grain size, narrow grain size distribution and high fraction of large angle grain boundaries. The microstructure and texture of electrodeposited materials, however, depends strongly on the deposition conditions, as for example bath composition. While the mechanical properties of electrodeposited metals has received constant attention, only a restrict amount of research has been concentrated in their microstructure characteristics. We have conducted a detailed characterization of electrodeposited CoNi produced in a Watts electrolyte with different levels of additive by electron backscatter diffraction (EBSD). The microstructure, texture and grain boundary character of the samples depend strongly on the film thickness. The two dimensional orientation microscopy has indicated that the development of columnar grains extending in film growth direction is related to the formation of low energy triple junctions, and to the density of lattice defects in the grains, which is also related to the grain orientation. The fully automated 3D-EBSD study has allowed us to verify this suggestion and to determine the boundary planes of these triples. At low additive levels the formation of triple junctions consisting of two low energy twin boundaries together with a tilt boundary and with a common $\langle 11-20 \rangle$ rotation axis favours the formation of elongated grains parallel to film growth direction. These three grains growth together and are continuously deflected by lattice

defects from the macroscopic growth direction. This continuous deviation slowly hinders further crystal growth. When the density of defects is high the crystal rotates quickly from the preferential growth direction and is overgrown by other crystals. Transmission electron microscope was applied to investigate the defects character. For this propose a sample was prepared with the FIB from the last slice of the 3D-EBSD investigation and the microstructure features that could not be resolved with the EBSD technique were studied.

(ICOTOM-P-029-2008) 3D Microstructures and Textures of a Plane Strain Compressed $\{110\}\langle 112 \rangle$ Al-0.3%Mn Single Crystal

H. Paul*, Institute of Metallurgy and Materials Science PAS, Poland; J. Driver, C. Maurice, Ecole des Mines, France

A crystal subdivision pattern of microbands has been extensively reported but mostly by studies on only one section, using either TEM or SEM-EBSD. To better correlate substructure with slip patterns we have carried out a systematic study of the 3D deformation microstructure in a deformed stable single crystal (i.e. over the 3 perpendicular surfaces). The microstructure and microtexture evolutions during plane strain deformation of high purity single crystals of Al-0.3%Mn alloy with initial brass $\{110\}\langle 112 \rangle$ orientation were characterised by in situ microtexture by TEM and high resolution FEG-SEM/EBSD after strains of 0.15 and 0.56. These two different techniques enable one to examine the macroscopically stable crystal subdivision deformation pattern at different microscopic scales, on the 3 orthogonal sections, i.e. perpendicular to the $\langle 110 \rangle$, $\langle 112 \rangle$ and $\langle 111 \rangle$ crystallographic directions. Particular attention is paid to a comparison of the microband orientations with the expected slip traces of the 2 active slip systems on all 3 surfaces. It appears that there is a good correlation for the TEM microstructure and orientation analyses compared with the orientation distribution from FEG-SEM/EBSD.

(ICOTOM-P-030-2008) Grain Boundary Orientations in a Fe-Mn-Cu Polycrystalline Alloy

M. Takashima*, JFE Steel Corporation, Japan; P. Wynblatt, Carnegie Mellon University, USA

Grain boundaries of a Fe-30mass%Mn-10mass%Cu (face centered cubic structure) polycrystalline alloy have been investigated as a function of the five macroscopic degrees of freedom of grain boundary orientation, using the serial sectioning method, SEM and EBSD. Certain grain boundary orientations appear at over 10 times the frequencies expected in a randomly oriented polycrystal. These include: (111)(111) 60 degree boundaries, which correspond to $\Sigma 3$ twin grain boundaries having (111) grain boundary planes, (110)(110) 0 degree boundaries, which are small-angle grain boundaries having (110) grain boundary planes, (111)(111) 0 degree boundaries, which are small-angle grain boundaries having (111) grain boundary planes, and (100)(100) 0 degree boundaries, which are small-angle grain boundaries having (100) grain boundary planes. The simple dislocation structures and lower energies of small-angle grain boundaries with low-index grain boundary planes may increase their populations during grain growth.

(ICOTOM-P-031-2008) Reconstruction of Three-Dimensional Microstructure of a Ni-based Superalloy and Its Grain Boundary Distribution

S. Lee*, G. S. Rohrer, A. D. Rollett, Carnegie Mellon University, USA; M. Uchic, AFRL/MLLMD, USA

We propose a new method for reconstructing a three-dimensional microstructure using focused ion beam and orientation imaging microscopy (FIB-OIM). The FIB-OIM opens a tremendous possibility for the study of three-dimensional microstructures of materials because it can automatically give a series of parallel sections with both topological information and orientation information at the sub-micrometer scale. The proposed reconstruction procedure goes as follows. The set of (2D) orientation maps are aligned based on the assumptions that the layers are parallel to one another with no rotations involved and that good alignment can be obtained when the

Abstracts

adjacent layers are positioned to give the minimum value of the average disorientation between them. The resulting alignment is used to stack the sections using a voxel-based regular grid. With appropriate clean-up of non-indexed points, individual grains are identified with a burn algorithm. After obtaining such a voxelated three-dimensional microstructure, a surface mesh is created over the grain boundaries using a generalized multi-spin marching cubes algorithm. The resultant surface mesh is then relaxed using various smoothing algorithms and used for direct measurement of the 5-parameter analysis of grain boundary character distribution (GBCD). A quantitative analysis of the Ni-based superalloy microstructure is described including the grain shape, the grain size distribution and the 5-parameter grain boundary character distribution. One may notice that the 5-parameter GBCD can be also measured using a stereological approach derived from the two-dimensional electron back-scattered diffraction maps. The results from both methods on the same series of the orientation maps are compared to each other in order to verify the effectiveness of both methods.

(ICOTOM-P-032-2008) Influence of Tape Casting Parameters on Texture Development in Alumina Ceramics

M. Snel*, J. van Hoolst, A. de Wilde, F. Snijkers, J. Luyten, Flemish Institute for Technological Research, Belgium

One of the methods to create texture in ceramics is by templated grain growth (TGG). Generally, in TGG processing a small number, usually highly anisotropic, seeding particles are mixed with a fine powder. These seeding particles will consume the fine powder, yielding a highly oriented ceramic piece. To obtain a highly textured ceramic material, it is crucial that the seeding particles are aligned in the green product. We choose to align the seeding particle, in our work alumina platelets, by using the tape casting process. In this process the shear stress will align the seeding particles in the casting direction. The influence of five parameters of the tape casting process on the final texture were studied; 1) the amount of seeding particles, 2) the carrier tape speed, 3) the gap height, 4) the solid loading and 5) the deairing time. This paper will present results on the pole figures and Lotgering factors of the resulting pieces as function of the different parameters. Preliminary results on the influence of the heat treatment on the formation of the texture will be presented as well.

(ICOTOM-P-033-2008) Influence of the Method of Ion Exchange and Copper Loading on the Physico-chemical of Cu-exchanged Pillared Clay Catalysts

R. Ben Achma*, A. Gorbil, Faculte des sciences de Tunis, Tunisia; F. Medina, A. Dafinov, University Rovira i Virgili, Spain

A novel method of preparing copper-exchanged aluminum-pillared montmorillonite has been developed. Catalysts containing different ratio of Cu/clay were prepared by exchange of the Al-pillared clay with copper nitrate. The resultant materials were then calcined at 300°C and characterised by X-ray diffraction, nitrogen sorption, chemical analysis, temperature programmed reduction (TPR), and UV-visible diffuse reflectance spectroscopy, Transmission electronic and Scanning electronic microscopy (TEM; SEM). The properties of copper-based catalysts have been studied in the wet hydrogen peroxide photocatalytic oxidation WHPCO of tyrosol. The obtained results show a good conversion rate of the tyrosol, with the tested catalysts, after 2 hours. This conversion is accompanied by an important abatement of TOC. The H₂O₂ concentrations in the solutions are superior to 3.10⁻²M, even after 24 hours of reaction. The reproducibility tests show that the activity of these catalysts persists after 3 cycles. Taking into account the good results of the tyrosol oxidation obtained in the static regime we study the same reaction in a continuous one. The feed solution was a mixture of pollutant (500ppm) and H₂O₂ (10/1) flowing at rate of 30 mL.hour⁻¹ in the reactor containing 1g of catalyst. The reaction was realized at 55°C under atmospheric pressure. The products were analyzed by HPLC coupled with DAD and using C18 column. The results obtained show that the catalytic activity decreases and reaches a stationary state after 4 hours.

(ICOTOM-P-034-2008) Microstructural Studies of Solid Oxide Fuel Cell Cathodes by Orientation Imaging Microscopy

R. Petrova*, L. Helmick, P. A. Salvador, S. Seetharaman, G. Rohrer, Carnegie Mellon University, USA; R. Gemmen, K. Gerdes, U.S. Department of Energy, USA

Solid Oxide Fuel Cell (SOFC) cathode performance and stability are associated with the surface and interfacial properties of a complex three phase region composed of ionic conducting material, electronic conducting material, and gas conducting pores. The crystallographic microstructure of these cathode materials can impact the overall degradation and can evolve over time under high temperature and electrochemical loads. We hypothesize that degradation is associated with changes in the bounding interfaces due to a number of features including grain orientations, grain misorientation across interfaces and grain boundary plane orientation. Orientation Imaging Microscopy (OIM) has been used to characterize the evolution of the three-phase structure composed of strontium-doped lanthanum manganese oxide (LSM), yttria-stabilized zirconia (YSZ), and pores. Microstructural analysis has been performed with respect to various annealing and operational temperatures and operational loads. Our goals are to statistically characterize the grain boundaries in the complex three phase cathode and to ultimately understand the driving forces for crystallographic evolution over different operation conditions. We present data on the misorientation angle distribution, the grain boundary normal distributions, and the phase boundary normal distributions (in addition to traditional metrics such as grain size). These will be discussed with respect to their observed steady state values and the implications they have for SOFC microstructural evolution.

(ICOTOM-P-035-2008) Fabrication of TiO_{2-x} by SPS and Improvement of the Thermoelectric Properties

Y. Lu*, M. Hirohashi, H. Yoshida, Chiba University, Japan

Non-stoichiometric titanium dioxide TiO_{2-x}, prepared by SPS was reduced by the reduction treatment using carbon powder for improving thermoelectric properties. The carrier density and x of TiO_{2-x} were calculated by using thermogravimetry (TG). Thermoelectric properties of TiO_{2-x} to 823 K were measured and discussed. The results show that layer of TiO on the surface and TiO_{2-x} inside samples were formed after the reduction treatment. The x of TiO_{2-x} and carrier density increased with holding time of the reduction treatment. Therefore, electrical resistivity of TiO_{2-x} was reduced, thus thermoelectric properties were largely improved by the reduction treatment. The maximum value of power factor reached about 3×10⁻⁴ W m⁻¹ K⁻² at 823 K. Also, the TiO layer became thick with holding time of the reduction treatment, but was finite in the improvement of thermoelectric properties.

(ICOTOM-P-036-2008) Influence of Cold-Rolling in IF-Steel on Texture near Grain Boundaries

A. Wauthier*, CNRS, France; H. Regle, Arcelor Mittal R&D, France

In deformed steels, nucleation generally occurs near grain boundaries. Thus the texture of the nuclei, which reflects the final texture, finds its origin in the scatter of orientations of the deformed matrix. It is then important to finely characterize and to understand how is generated the scatter of orientations during deformation, particularly near the grain boundaries, as they are enhanced sites for nucleation. A texture study has thus been led in order to understand the influence of region near grain boundary compared to the interior of the grains. The results are given for different thickness reductions, from 15% to 90%. The distance around the grain boundary that is the most relevant to study the change in texture is discussed with calculations of texture but also local misorientation. A distinction between grains that belong to alpha or gamma fibers is also realized. It is found that slight differences exist in term of principal components between the texture at grain boundaries or in grain interior. In all cases, the texture near grain boundaries is weaker than in the grain interior.

(ICOTOM-P-037-2008) Crystallographic Investigation of Nitrided c-sapphire Substrate by Grazing Incidence X-ray Diffraction and Transmission Electron Microscopy

H. Lee*, J. Ha, Tohoku University, Japan; S. Hong, Chungnam National University, South Korea; S. Lee, H. Lee, S. Lee, T. Minegishi, T. Hanada, M. Cho, T. Yao, Tohoku University, Japan; O. Sakata, H. Tajiri, Japan Synchrotron Radiation Research Institute (JASRI), Japan; J. Lee, J. Lee, Korea Advanced Institute of Science and Technology, Japan

Sapphire, a single crystal of aluminum oxide, has become an important substrate for the growth of III-nitride semiconductors in spite of the large lattice mismatch and the large difference of thermal expansion coefficient. In order to improve crystalline properties of gallium nitride (GaN) films in growing the GaN on sapphire, in general, the nitridation treatment and the low temperature deposition of GaN were sequentially performed on the sapphire substrate before the main growth of high temperature GaN. In fact, the sapphire nitridation is the critical step for the defect reduction, high electron mobility and yellow luminescence reduction in the subsequently deposited films. In order to understand the nitridation effect, first of all, it is highly needed to find out the overall chemical compounds formed on the nitrided sapphire surface and each crystalline orientation relationship. A grazing incidence X-ray diffraction with a synchrotron radiation and cross-sectional high-resolution transmission electron microscopy were performed on the sapphire surface nitrided at 1080 degree Celcius for 30min. The thickness of the nitrided layer was about 2 nm. It was found out that the wurtzite, zinc-blend, and 30° rotated zinc-blend aluminum nitrides were formed on the sapphire surface. Considering the atomic configurations, the 30° rotated zb-AlN shall form the in-coherent interface and has higher activation energy of formation, while the non-rotated zb-AlN shall form the coherent interface. Therefore, the non-rotated zb-AlN shall be formed preferably compared to the 30° rotated zb-AlN.

(ICOTOM-P-038-2008) Impurity Segregation Energy in fcc Al Determined from First Principles

M. Gao*, A. Rollett, Carnegie Mellon University, USA

It is known that grain boundary energy determines grain boundary character distribution, but what is less known is how grain boundary segregation anisotropy will impact grain boundary energy quantitatively. This becomes the objective of the current study, which attempts to determine the segregation energy of selected impurity elements (Mg, Ca and Cu) in fcc Al for a flat tilt grain boundary with tilting angle of 0, 32, 35, 37 38 and 40 degrees respectively using first principles density functional theory. The segregation energy determined from first principles calculations are compared with those determined from embedded atom method. Intergranular embrittlement due to substitutional impurity segregation at grain boundaries will also be discussed in light of present study for Al alloys.

(ICOTOM-P-039-2008) Quartzite Textures in the Córdoba Sierra (Argentina). The Guamanes Region

R. D. Martino, F.C.E.F y N. Universidad Nacional de Córdoba., Argentina; A. L. Fourty, R. E. Bolmaro*, Instituto de Física Rosario, Argentina; H. Brokmeier, GKSS-Research Centre, Germany

The deformation fringe of Guamanes (DFG) is a shearing zone on Sierras de Córdoba (Argentina) extending approximately 45 kilómetros parallel to the 64°50'00" meridian. Its width varies in between 1 and 4 kilometers and can be divided in the north and south parts. The south part has been already quite well studied with a complete description of its milonitic rocks and the cinematic. Filonites in the north and milonites with filonites and non deformed rocks in the south apparently separate two well defined domains of deformation. Two different deformation events, one ductile followed by a fragile stage, have been identified. We will present textures of some granitic pegmatites that are layered by quartz veins codeformed during the same events. The data will be analyzed by regular texture analysis and viscoplastic self consistent simulations. The cinematic is inferred from

the simulations contributing to the description of the tectonics of the region.

(ICOTOM-P-040-2008) EBSD Study of Delamination Fracture in Al-Li Alloys

W. Tayon*, Old Dominion University and the Applied Research Center, USA; R. Crooks, National Institute of Aerospace, USA; M. Domack, J. Wagner, NASA Langley Research Center, USA; A. Elmustafa, Old Dominion University and the Applied Research Center, USA

Al-Li alloys offer attractive combinations of high strength and low density for aerospace structural applications. However, a tendency for delamination fracture has limited their use. Identification of the metallurgical mechanisms controlling delamination may suggest processing modifications to minimize the occurrence of this mode of fracture. In the current study of AA2090-T8 plate, OIM analyses along with nano-indentation in regions exhibiting delamination fracture were used to compare microtextural and mechanical properties in the surrounding grains. A correlation was found between delamination fracture locations and near-Σ3 CSL boundaries. Delamination frequently occurred between sample-symmetry-related variants of the same texture component. A tendency for concentration of localized deformation along one side of the fractured boundary was also observed through kernel average misorientation (KAM). Insignificant variations in the nano-mechanical elastic properties derived from indentation data were detected between grains surrounding delaminations, generally falling within 3 to 5% for all grains tested. No distinct correlation between nano-mechanical properties and delamination fracture was observed, which implies that the increase in plastic deformation is not due to localized softening. Taylor factor maps, using a stress tensor which accounted for normal and shear stresses at the interface, revealed large differences between the delaminating grains. Through-thickness EBSD mapping away from the cracks showed that large Taylor Factor differences corresponded to the location of delaminations. This suggests a lack of slip accommodation across the interface, resulting in an excess of deformation damage on the (crystallographically) "softer" side; which is consistent with the increased KAM. The associated stress concentrations at the interface facilitate delamination fracture. Further research is being conducted to corroborate these findings.

(ICOTOM-P-041-2008) 5-Parameter Interfacial Boundary Character Distribution of Cu-Nb Composites

S. Lee*, C. Lim, Carnegie Mellon University, USA; A. Misra, Los Alamos National Laboratory, USA; A. D. Rollett, Carnegie Mellon University, USA

The orientation relationship for the interface in Cu-Nb composites is examined using a novel approach from the orientation data obtained from electron backscattering diffraction (EBSD) technique. Given an orientation map, the two-dimensional interfacial boundaries between Cu and Nb are reconstructed using the marching square algorithm. The resultant Cu-Nb interfacial boundaries are then relaxed using various smoothing algorithms. For each relaxed interfacial boundary segment, the method keeps track of the orientations of neighboring Cu and Nb regions. By assuming that the interface is perpendicular to the cross-section plane, the full 5-parameter interfacial boundary character distribution is obtained, based on two-dimensional electron diffraction maps. A detailed explanation on the experimental and numerical procedures will be given for two different Cu-Nb composites. One is Cu-Nb multilayer structure prepared using sputter deposition while the other is a roll-bonded Cu-Nb laminate. For both composites, a quantitative analysis of the 5-parameter interfacial boundary character distribution is given. Interfacial normals can also be approximated by connecting the centers of the mass of the Cu and Nb regions enclosed by the circle drawn with the interfacial pixel as its center. The resulting 5-parameter interfacial boundary analysis shows qualitatively similar characteristics to the result from the interfacial boundary reconstruction using the marching square algorithm.

Abstracts

(ICOTOM-P-042-2008) Crystallographic Features during Martensitic Transformation in Ni-Mn-Ga Ferromagnetic Shape Memory Alloys

D. Cong, Northeastern University, China; Y. Zhang*, C. Esling, University of Metz, France; Y. Wang, X. Zhao, L. Zuo, Northeastern University, China

In the present paper, the martensitic transformation crystallography in Ni-Mn-Ga alloys has been investigated. Two Ni₅₃Mn₂₅Ga₂₂ (at. %) alloys were prepared by repeated melting of the constituent elements in an arc furnace. Subsequently, one alloy (denoted as Alloy I) was first annealed at 1073K for 4h, and then cooled to 473K (above martensitic transformation temperature) at ~4K/min and held for 30min, followed by cooling to room temperature at ~10K/min. The other alloy (denoted as Alloy II) was annealed at 1173K for 4h followed by furnace cooling. The orientation information of the martensitic variants was obtained by electron backscattered diffraction (EBSD) measurements. The twinning relationship between martensitic variants was determined by misorientation calculation and the orientation relationship between austenite and martensite was determined from the information of the orientation of the martensitic variants [1, 2]. It is found that there are only two kinds of differently orientated martensitic lamellae with a misorientation angle of ~83° distributed alternatively in each initial austenite grain in Alloy I. There is a compound twinning orientation relationship between the two lamellae with the twinning elements $K1=\{112\}$, $K2=\{11-2\}$, $\eta1 =\langle 11-1 \rangle$, $\eta2 =\langle 111 \rangle$, $P=\{1-10\}$ and $s =0.379$. The prevalent orientation relationship between austenite and martensite is Kurdjumov-Sachs (K-S) relationship with $(111)A//\langle 101 \rangle M$, $[1-10]A//\langle 11-1 \rangle M$. In Alloy II, nanoscale twins inside the martensitic lamellae were observed and the orientation relationships both between the nanotwins within one lamella and between the nanotwins in two neighboring lamellae were determined by means of misorientation calculation. The influence of different heat treatments on the formation and crystallographic features of martensitic lamellae and nanotwins was discussed. 1. M. Humbert, F. Wagner, H. Moustahfid, and C. Esling, *J. Appl. Cryst.* 28, 571 (1995). 2. M. Humbert, S. R. Dey, E. Bouzy, A. Hazotte, *Mater. Sci. Forum* 495-497, 1219 (2005).

(ICOTOM-P-043-2008) Effect of High Magnetic Field During Annealing on Texture of Silicon Steel

H. Garmestani*, C. M. Bacaltchuka, Georgia Institute of Technology, USA

Cold rolled silicon steel samples were annealed at 800°C for annealing times varying from 10 to 30 minutes in an inert atmosphere, and in the presence of a 17 Tesla magnetic field oriented parallel to the plane of the sheet. In order to evaluate the effect of the magnetic field, cold rolled samples were annealed at the same conditions as for the magnetic annealing but without the application of the magnetic field. The texture development was analyzed by means of Pole Figure and Orientation Distribution Function using X-Ray diffraction. Magnetic annealing was found to be more effective in enhancing the Goss component in the primary recrystallized microstructure. This finding suggests that silicon steel can be affected by an external magnetic field even when the material is found at its paramagnetic state.

(ICOTOM-P-044-2008) Recrystallization Texture Development in Non-oriented Silicon Steel under Magnetic Annealing

W. Pei, Y. Sha*, S. Zhou, L. Zuo, Key Lab for Anisotropy and Texture of Materials, China

High magnetic field was applied during annealing of the asymmetrically and symmetrically cold rolled non-oriented silicon steel. It was found that either magnetic annealing or asymmetric rolling increased recrystallization *ita* ($\langle 001 \rangle // RD$) and $\{100\}$ fibers while decreased gamma fiber ($\langle 111 \rangle // ND$). The favorable *ita* and $\{100\}$ fibers could be further enhanced by combing magnetic annealing with asymmetric rolling, to the extent dependent on speed ratios. The effect mechanism of magnetic annealing was proposed in terms of the orientation-dependent magnetic driving force for grain boundary migration.

(ICOTOM-P-045-2008) Effects of Magnetic Field Direction on Texture Evolution in a Cold-rolled Interstitial-free Steel Sheet During High Magnetic Field Annealing

Y. Wu, X. Zhao*, S. C. He, L. Zuo, Northeastern University, China

Effects of magnetic field direction on texture evolution in cold-rolled IF steel sheet during high magnetic field annealing were investigated by means of X-ray diffraction ODF analysis. Samples of cold-rolled (75%) IF steel sheet were annealed at 750°C for 30min with and without a 12-tesla magnetic field respectively. During the magnetic annealing, they were respectively placed at the center of the applied field, being oriented differently with respect to the magnetic field direction. The transverse direction of all specimens was kept perpendicular to the magnetic field, while the rolling direction was tilted different angles (initial angle =0°, step=15°, final angle=90°) to the magnetic field direction. For comparison, the non-field annealing was carried out in the same furnace under the same heat treatment conditions. The results show that altering the specimen orientation to the magnetic field direction during annealing does not change the mechanism of formation and development of recrystallization texture in cold-rolled IF steel sheet in the present case, and the annealed specimens have the same final annealing textures. The average intensity of γ -fiber textures of field-annealed specimens is higher than that of the non-field annealed specimen, especially at the rotation angle of 45°, the result is more remarkable. The intensity of $\{111\}$ texture components present a similar periodic variation with respect to the specimen orientation to the magnetic field. With the increasing of rotation angle, they were first weakened and then strengthened, and their intensity reached the maximum value at the rotation angle of 45°, then they were weakened with further increasing of rotation angle. And the reason may attribute to the differently magnetically induced effect in different angles. The results of this study demonstrate that the texture in ferromagnetic IF steel sheet can be effectively changed when annealing in a high magnetic field by altering the sample orientation angles to the magnetic field direction. This may provide a new method to control the development of crystallographic texture in magnetically anisotropy materials.

(ICOTOM-P-046-2008) Lattice Reconstruction - A Crystallographic Model for Grain Reorientation in Basal Texture of HCP Magnesium

B. Li*, E. Ma, K. Ramesh, Johns Hopkins University, USA

A new, crystallographic model was proposed to explain the formation of basal texture in HCP Mg during plastic deformation. In this model, original lattices can be reoriented by 90 degrees by reconstructing new basal planes from the existing lattice points, such that the new basal planes are parallel to the loading axis. The new basal planes are reconstructed from the lattice points on the $\{10-10\}$ prismatic planes by involving a simple shear along the dominant twinning system in HCP Mg, i.e. $\{10-12\} \langle 10-1-1 \rangle$, such that correct stacking sequence is obtained. Molecular dynamics simulations were performed to investigate the mechanism of lattice reorientation of a single crystal during tensile deformation.

(ICOTOM-P-047-2008) Effects of Alloying Elements on the Texture of Extruded Magnesium Alloys

J. Choi*, J. Hwang, K. Shin, Seoul National University, South Korea

Magnesium alloys are attractive for automobile components because of their low density and high strength/weight ratio. The mechanical properties of magnesium can be improved by the addition of appropriate alloying elements such as Al, Zn, Sn, etc. Since AZ31 is a representative wrought magnesium alloy, research on the deformation behavior and texture of AZ31 has been pursued actively in recent years. Nevertheless, the effects of alloying elements on the texture of magnesium alloys have not yet been studied systematically. In the present study, the changes in the texture of extruded Mg-Zn-Al alloys with different compositions were examined. Plate extrusions of Mg-Zn-Al alloys were fabricated with varying contents of Zn and Al from 1wt. %

to 3wt.%. In order to examine the texture of the extrusions, $\{10-10\}$, $\{0002\}$, $\{10-11\}$, $\{10-12\}$, $\{11-20\}$ pole figures were measured with an x-ray diffractometer. It was found that basal planes of the extruded Mg-Zn-Al alloys tilted more towards the extrusion direction with increasing Zn and Al contents. Tensile tests were conducted to examine the effect of the texture on the mechanical properties of the extrusions at room temperature. The tensile strength and elongation of the extrusions were found to be affected by the texture. Simulations based on the visco-plastic self-consistent (VPSC) model were also conducted to determine the deformation mechanisms during tensile deformation. The results of VPSC simulations showed that the basal $\langle a \rangle$ slip and prismatic $\langle a \rangle$ slip were the main deformation mechanisms during tensile deformation of Mg-Zn-Al alloys at room temperature.

(ICOTOM-P-048-2008) Analysis of the Formation of gamma-Massive Microstructures in a TiAl-based Alloy

A. Sankaran, E. Bouzy, M. Humbert*, A. Hazotte, UPVM, France

By quenching, we have promoted massive $\alpha \rightarrow \gamma$ transformation in samples of a Ti-45Al-7Nb-0.2C (at.%) intermetallic alloy. The morphology of the γ -massive colonies located at grain boundaries and their orientation relations with respect to the parent α grains were characterized using SEM and EBSD/SEM techniques. The results obtained confirmed some observations already reported for massive transformation of other metallic systems: γ nuclei germinate in one α grain (the host grain) at the boundary of two adjacent α grains, - the γ nucleus in the host α grain is in a strict crystallographic orientation relation (Blackburn Orientation Relation) with the adjacent grain (the parent grain). Moreover, we observed that the γ -massive colonies develop in the host grain by a specific mechanism. From their crystallographic investigation performed by EBSD, we have deduced that: i) a less strict plane matching is sometimes observed between the γ nucleus and the host α grain (it is statistically related to the very specific α texture of the sample), ii) the growth of γ massive colonies operates by the development of successive sub-domains; the first sub-domains are in twin orientation with respect to the nuclei, whereas the following sub-domains are in twin orientation with respect to the previous ones, iii) there is a clear evidence for γ -variant selection during either nucleation and growth. These observations allow to infer the mechanisms involved in both the nucleation and growth stage and, consequently, to understand the texture and microstructure evolution occurring during this phase transformation.

(ICOTOM-P-049-2008) Microstructure and Texture Evolution in Grain-refined $\alpha_2 + \gamma$ Titanium Aluminides

S. Roy*, Indian Institute of Science, India; S. d. Waziers, Institut National Polytechnique de Toulouse, France; S. Suwas, Indian Institute of Science, India

Owing to their high strength-to-weight ratio, excellent mechanical properties and corrosion resistance, titanium (Ti) and its alloys, especially $(\alpha + \beta)$ alloys like Ti-6Al-4V and intermetallics like $(\alpha_2 + \gamma)$ Titanium Aluminides, are the backbone materials for aerospace, energy, and chemical industries. To increase the specific thrust of industries further, lightweight material such as Titanium Aluminide intermetallics based alloys has been developed over the years. These materials remain ordered up to melting point ($\sim 1440^\circ\text{C}$) and consist of γ -TiAl (ordered face centred tetragonal L10 structure) and α_2 Ti₃Al (ordered hexagonal DO19-structure). The primary problem for any titanium metallurgist is the large grain size (often in the millimeter range) that evolves during the solidification of the as-cast titanium ingot. Extensive hot working in the β -phase field followed by recrystallization is an effective industrial practice for reducing the grain size of the wrought product. This process, popularly known as 'ingot breakdown' increases the production cost of the finished titanium products and restricts its extensive use to some extent. Any development in terms of grain refinement in as-cast titanium and its alloys will certainly popularize its massive use. In the present study, the influence of addition of

grain refiners like elemental boron and niobium for γ -TiAl alloys on the microstructure and texture evolution have been discussed vis-à-vis the original alloys without any addition by normal microscopy and EBSD technique. The primary effect of the grain refiners seems to be the microstructural refinement by almost an order of magnitude. The texture developed in these alloys is markedly different from that of the alloys without grain-refiners. Also, the boride precipitates seem to influence the texture during solid state phase transformations.

(ICOTOM-P-050-2008) Bulk Texture Changes in Rolled Zr-1%Nb Alloy under Electron Irradiation

Y. Perlovich, M. Grekhov*, M. Isaenkova, O. Krymskaya, Moscow Engineering Physics Institute, Russian Federation; V. Lazorenko, V. Tovtin, Institute of Metallurgy RAS, Russian Federation

In the course of experiments, modeling conditions of neutron irradiation, a number of effects, accompanying electron irradiation of textured metal materials, were revealed by use of X-ray methods as applied to Zr-1%Nb alloy, cold-rolled up to different deformation degrees (0, 25, 75%). The electron beam with energy of 20 MeV by density ~ 1012 particles/cm² traversed sheets 1,7 – 0,5 mm thick from Zr-based alloy without noticeable weakening. Heating of irradiated samples was practically absent. A total dose attained $\sim 3 \times 10^{17}$ particles/cm². The following new phenomena were discovered: (1) texture changes in samples under irradiation become stronger with increase of their deformation degree; (2) in the case of sufficiently high deformation degree both texture and substructure changes at the back side of irradiated samples are more significant than those at the front side; (3) electron irradiation removes the initial layer-by-layer non-uniformity of the rolling texture, so that the texture of the sheet's back side approaches that of the front side. The proposed mechanism of bulk texture changes includes production of interstitial atoms and vacancies by percussion of high-energy electrons with Zr atoms in points of crystalline lattice, immediate preferential migration of interstitial atoms to dislocations and their resulting climb, accompanied by lattice rotation and formation of dislocation walls. The observed effects increase with deformation degree, since the higher is the dislocation density, the more numerous are sinks for interstitial atoms and the less stable is the initial substructure of samples. Therefore, substructure rearrangement within the irradiated matrix is the most intensive in the case of cold rolling by 75%. Intensification of texture and structure changes by passing from the front side to the back one of the irradiated sample testifies about development of cascade branches by going of the initial electron beam through material.

(ICOTOM-P-051-2008) Recrystallization Kinetics in Deformed Pure Copper

B. Zakaria*, B. Ghania, Biskra University, Algeria; G. Thierry, T. Isabelle, Rennes University, France

The recrystallization kinetics in pure copper deformed by cold rolling is mainly investigated by differential scanning calorimetry (DSC-111) during anisothermal treatment (from 298 to 723 K). DSC curves show exothermic peaks corresponding to the stored energy released during recrystallization process. The variation of the heating rate and application of different methods allowed us to calculate two kinetic parameters of recrystallization: i) the activation energy of the process was calculated using three different methods. ii) the Avrami exponent was estimated using the Matusita method. On the other hand, the microstructural evolution during different steps of recrystallization and grain growth were investigated by optical microscopy, scanning electron microscopy and electron back scattered diffraction.

(ICOTOM-P-052-2008) Through-Process Texture Modeling of AA6016 from Hot Rolling to Final Annealing

C. Bollmann*, G. Gottstein, RWTH Aachen University, Germany

The automotive industry requires aluminum sheet with excellent formability and high in-service strength. In addition, a good sur-

Abstracts

face appearance after forming is needed for automotive skin applications. The outstanding alloys to match these requirements are the heat-treatable 6xxx alloys. In order to improve these properties, the texture and microstructure evolution throughout the aluminum process chain has to be optimized. In the present study the texture and microstructure evolution of AA6016 were measured during cold rolling, intermediate annealing, and a final solution treatment for various compositions and processing conditions. A through-process texture modeling concept was applied to analyze the texture controlling processes deformation and recrystallization with respect to their underlying mechanisms. The texture changes during deformation were modeled with the grain cluster model GIA. For simulating the texture evolution during recrystallization both processes nucleation and nucleus growth were considered. The spectrum of potential recrystallization nuclei with respect to different nucleation mechanisms was described by the ReNuc model, which is a GIA derivative. The cellular operator model for recrystallization CORE was used for simulating the recrystallization texture evolution during intermediate and final annealing. The results obtained from through-process texture modeling will be compared to experimental results of texture and microstructure for several compositions and processing conditions. The texture evolution will be discussed with regard to the center plane ($s = 0$) and the near surface ($s = 0.8$) layer to address especially the recrystallization behaviour under different loading conditions and hence, to reveal the essential physical mechanisms for recrystallization in AA6016.

(ICOTOM-P-053-2008) Statistical Analysis on the Orientation Relationship between Recrystallized Grains and Deformed Grains in the IF Steel

D. Kim*, Korea Institute of Science and Technology, South Korea; K. Oh, H. Lee, Seoul National University, South Korea

Recrystallization behavior and texture development of 0.002wt% C, 0.07wt% Ti, Ti added IF steel was investigated by statistical analysis with EBSD. 80% cold rolled IF steel specimens were annealed in the salt bath with various time at 650C, and recrystallized grains and deformed grains were differentiated by the combination of intra grain misorientation and inter grain misorientation. Misorientation angle between recrystallized grains and surrounding deformed grains were calculated and statistically analyzed. This statistical analysis reveals that nucleation of recrystallized grains with $\{111\}$ //ND orientation in $\{111\}$ deformed grains are main mechanism which determine final texture of Ti stabilized IF steel.

(ICOTOM-P-054-2008) Investigation on Microstructure Evolution of Gold Bonding Wires during Annealing Using EBSD and MC Modeling

J. Cho*, Korea Institute of Materials Science, South Korea; S. Choi, Suncheon National University, South Korea; K. Oh, Seoul National University, South Korea

Fine bonding wires of pure Au or Cu, are used for interconnection in semiconductor packaging. As packaging technology continues to advance, improved properties in bonding wire are needed. A better understanding of annealing processes in order to obtain optimum bonding wire will be helpful to optimize the microstructure. Axisymmetrically-drawn bonding wires of face centered cubic (FCC) metals have typical textures consisting of two types of fibers with $\langle 111 \rangle$ and $\langle 100 \rangle$. Those drawn fibers changed into new microstructure and textures during annealing process. The bonding wires experience three stages of microstructural changes during annealing. The first stage is subgrain growth to keep elongated grain shapes and to be varied in aspect ratio. The second stage is recrystallization, during which equiaxed grains appear. The third stage is grain growth. The $\langle 111 \rangle$ and $\langle 100 \rangle$ grains compete with each other at each step. In particular, increase in aspect ratio during subgrain growth reflects the difference between mobilities of twist and tilt boundaries among the same kind of fibers. The overall features of

microstructure and texture evolutions at each annealing stage were investigated using a two-dimensional (2D) Monte Carlo (MC). In order to consider anisotropic properties of grain boundary energy and grain boundary mobility, functions of boundary misorientation were introduced. Orientation-dependent stored energy was evaluated by reconstructing of data measured using electron back-scattered diffraction (EBSD) analysis. Subgrain method based on subgrain structure was used for quantitative analysis of the stored energy. Anisotropic grain boundary mobility was assumed for twist and tilt boundaries to reflect the aspect ratio change during extended recovery.

(ICOTOM-P-055-2008) Effect of Mg Concentration on the Texture Formation in Al-Mg Solid Solution Alloys during High Temperature Compression Deformation

K. Okayasu*, H. Takekoshi, M. Sakakibara, H. Fukutomi, Yokohama National University, Japan

The authors have been investigated the behavior of uniaxial compression deformation and texture formation in Al-3mass%Mg solid solution at high temperatures. Texture measurement revealed that the main component of the fiber texture changes from $\{011\}$ (compression plane) to $\{011\}+\{001\}$ and to $\{001\}$ with an increase in strain when the viscous motion of dislocation dominates the deformation. In this study, the texture formation in Al-5mass%Mg alloy and Al-10mass%Mg alloy under high temperature compression deformation was investigated experimentally, in order to elucidate the effect of solute atmosphere of dislocation on grain boundary migration. Uniaxial compression tests were conducted at 673K and 723K in air. The range of strain rates was between 0.0001/s and 0.001/s. Texture measurements were conducted on the mid-plane section of the specimen by the Schulz reflection method using Cu $K\alpha$ radiation. Orientation distribution function was calculated by the Dahms-Bunge method. Textures are examined on the basis of pole figures and inverse pole figures. EBSD measurements were conducted to evaluate the spatial distribution of the texture component. The measurements are performed 4 micrometers interval. The major results are summarized as follows. 1) No big differences are seen among the levels of flow stresses of Al-3mass%Mg, Al-5mass%Mg and Al-10mass%Mg. 2) Fiber textures are formed independently of deformation conditions. 3) Accumulation of pole density at $\{001\}$ is enhanced by an increase in solute content. It was concluded that the formation of $\{001\}$ fiber texture can be attributed to the preferential grain boundary migration effective for the growth of $\{001\}$ grains.

(ICOTOM-P-056-2008) Comparison of the Texture Development During Static Recrystallization and Dynamic Recrystallization of Dilute Binary Mg-Y Alloys

R. Cottam*, J. Robson, G. Lorimer, University of Manchester, United Kingdom; B. Davis, Magnesium Elektron, United Kingdom

Recrystallization can occur both dynamically (during hot working) and statically (during annealing). Both types of recrystallization can occur in magnesium alloys and the mechanisms are influenced by both processing conditions and alloy composition. Dilute yttrium alloys were chosen because of the influence yttrium has on the deformation and potentially the recrystallization of magnesium alloys. A 0.23wt%Y binary magnesium alloy was initially extruded at 390°C and then subjected to plane strain compression at 300°C to produce dynamic recrystallization. A 0.5wt%Y alloy was hot rolled under conditions that led to full dynamic recrystallization and then cold rolled and annealed to produce static recrystallization. Electron backscattered diffraction (EBSD) was used to determine both the macro and microtexture which provided evidence for the mechanism of recrystallization which was then related to the final texture development. It was found that during dynamic recrystallization under these conditions the mechanism of recrystallization was strain induced

boundary migration (SIBM) where the rotation of the recrystallizing grains was found to be due to slip on the basal slip systems. While for static recrystallization {10-11} - {10-12} double twinning was found to act as a nucleation site for recrystallization and hence the texture component due to double twinning was found to dominate in the recrystallized structure.

(ICOTOM-P-057-2008) Texture Evolution in O and β (B2) Phases of Ti-22Al-25Nb Alloy during Deformation in Two-phase Region and its Effect on O+B2- \rightarrow β - \rightarrow O+B2 Transformation Texture

S. R. Dey*, Technische Universität, Germany; S. Suwas, Indian Institute of Science, India; J. Fundenberger, Université Paul Verlaine - Metz, France; R. K. Ray, Tata Steel, India

The higher amount addition of Nb in Ti3Al base (hexagonal) intermetallic alloy develops O (ordered orthorhombic) phase with the stabilization of β (bcc) phase. O phase is known to increase strength and ductility of Ti3Al base intermetallic alloy. Different thermo-mechanical processing generates variety of microstructures with various properties. In spite of the fact that texture plays an important role in determining the mechanical behaviour of Ti-Al-Nb base alloys containing β + (α and/or O) phases, there still lacks a thorough study of texture evolution during thermo-mechanical processing as carried out to achieve the desired microstructure and properties. In the present work, two-phase alloy, namely Ti-22Al-25Nb (at%), processing-texture evolution has been studied. The alloy consists of O and B2 (ordered cubic) phases at room temperature. Heating above β -transus temperature produces single-phase β , which on rapid cooling can be retained at room temperature in its ordered form B2, while slow cooling results in (O+B2). Hot rolling at 900°C when the alloy exists in two-phase (O+B2) region was carried out. Hot rolling texture of O and B2 phases were measured through electron backscatter diffraction. The so-obtained specimens were further heat treated at 1100°C (single β phase region) for solutionising. Texture evolution during O+B2 \rightarrow β \rightarrow B2 / O+B2 transformation has been studied. The study, therefore, addresses two important aspects of texture evolution in this alloy, namely the evolution of deformation texture in O and B2 phases, and the transformation texture in O-phase. The complete recrystallization of the hot rolled specimens during solutionising showed complete microstructure-texture changes in the transformed B2 and O phases.

(ICOTOM-P-058-2008) Textural Inhomogeneity Effect during the Monte Carlo Simulation of the Abnormal Goss Grain Growth in Fe-3%Si Steel Grade HIB

T. Baudin, D. Ceccaldi, R. Penelle*, University of Paris Sud, France

Various mechanisms have been proposed to explain the development of the {110}<001> texture during secondary recrystallization of Fe-3%Si sheets but the preferential growth of Goss grains is not still well understood. They can be divided into two types [1]. The first one assumes that CSL grain boundaries (GB) are at the origin of the preferential growth of Goss grains and the second one that the high mobility is a feature of the so called "high energy" (HE) GB (misorientation angle of 20 to 45°). From these considerations, it clearly appears that the orientation distribution around Goss grains is an important parameter. Then, it becomes necessary to test the influence of textural inhomogeneities (no random distribution of orientations in the microstructure, cluster of grains) observed in the Fe-3%Si sheet [2] on the abnormal Goss grain kinetics. For that, a Monte Carlo simulation is used from two sets of data measured by EBSD. The Helming method [3] is applied to improve the definition of the orientation classes used in the simulation. Then, these orientation classes are used to describe the distribution of GB energy on experimental microstructures introduced as input data in the simulation. The results obtained from the two different maps are compared and allow to enlighten several differences: So, the Goss grain growth kinetics are different and then the final microstructures after complete secondary recrystallization are also different (grain number and grain size). Moreover, the growth kinetics of other components can also present

very important variations inducing different mechanisms (normal growth or no of the {111}<112> component, ...). [1] A. Morawiec, Scripta mater., 43 (2000) 275-278. [2] T. Baudin, J. Jura, J. Pospiech and R. Penelle, ICOTOM 11, Xi'an, China, September 16-20 (1996), International Academic Publishers, Vol. 2, 1319-1324 (1996). [3] K. Helming, Habilitationsschrift, Clausthal, Germany (1995)

(ICOTOM-P-059-2008) Study on Evolution of Partial Texture from Different Size Grains during Grain Growth in IF Steels

W. Tong*, Northeastern University, China; F. Wagner, Metz University, France; W. Chen, L. Zuo, J. He, Northeastern University, China

Interstitial Free (IF) steel sheets, known for their excellent formability properties, have aroused attention in production and research of metallurgical industry since 1980's. In early studies, much research was focused on mean grain size calculation, full texture measurement, and microstructure observations. There is few experimental results deal with the investigation on relation between grain size and texture, and evolution of texture from different size grains during grain growth. It is no doubt that such investigation is very important for both practical and theoretical interests. Recently, EBSD is a well developed and widely used tool for the texture measurement, and it supports partial texture analysis and grain size distribution calculation for considered grains assemble in measured data. Many EBSD investigations of metal material have been carried out. In the present work, we selected an IF steel sample which was cold rolled to a reduction of 80% and subsequently submitted to annealing treatment at 650°C, 710°C and 770°C for various durations, respectively. The grain size and evolution of partial texture from small, medium and big grains were investigated during grain growth. It was found that the growth rate and partial texture characteristic is temperature dependent, both styles were absolutely distinct at different annealing temperature. But it was clear that at same annealing temperature, partial texture for various annealing time was similar, though its intensity increase with an increment of duration. And the relation between partial texture from different size grains and their mean grain size can be expressed by an empirical formula from experimental data.

(ICOTOM-P-060-2008) Textures and Multistructure of Single to Multi-Layered Modern Brachiopod Shells

E. Griesshaber*, A. Götz, W. W. Schmahl, Ludwig-Maximilians Universität München, Germany; C. Lüter, Humboldt Universität, Germany; R. D. Neuser, Ruhr-Universität Bochum, Germany

Magnesian calcites of biogenic origin are hierarchically structured, multifunctional materials. We have investigated the texture and shell microstructure together of the modern calcitic brachiopods of the genera *Kakanuiella chathamensis*, *Liothyrella uva* and *Liothyrella neozelanica* with SEM and EBSD as well as nano- and microhardness measurements. One of the most distinctive feature of the studied genera is the number of layers that compose the brachiopod shell. *Kakanuiella chathamensis* is built entirely of nano- to microcrystalline primary layer calcite. *Liothyrella uva* contains of a nanocrystalline outer primary and an inner fibrous secondary layer. *Liothyrella neozelanica* is composed of three layers, a nanocrystalline outer primary, a columnar secondary and an innermost fibrous tertiary shell layer. Even though *Kakanuiella chathamensis* is composed of primary layer material we observe some textural features and a pattern in the distribution of hardness within the shell. The texture of *Liothyrella uva* and that of *Liothyrella neozelanica* is significantly sharper than that of *Kakanuiella chathamensis*. The hardness distribution in *Liothyrella neozelanica* and *Liothyrella uva* is such that the outermost part of the shell is hard while the innermost part of it is soft: The secondary layer of *Liothyrella neozelanica* consists of calcite crystals that form long prisms which are perpendicular to the shell and parallel to the c-axis of calcite. Our observations on the interface between the prismatic secondary and the fibrous tertiary layer of *Liothyrella neozelanica* suggest a mechanism by which the unusual texture of the fibrous layer may arise.

Abstracts

(ICOTOM-P-061-2008) Texture and Ultrastructure of Brachiopod Shells: A Mechanically Optimized Material with Hierarchical Architecture

W. W. Schmahl, Ludwig-Maximilians-Universität München, Germany; K. Kelm, Rheinische Friedrich-Wilhelms Universität Bonn, Germany; E. Griesshaber*, Ludwig-Maximilians-Universität München, Germany; S. Enders, Max-Planck-Institut für Metallforschung, Germany

Brachiopod shells consist of low-Mg calcite and belong to one of the most intriguing species for studies of marine paleoenvironments and variations in oceanographic conditions. We have investigated the texture and ultrastructure together with nano- and microhardness properties of modern brachiopod shells with SEM-EBSD, TEM and nanoindentation and Vickers microhardness analyses. The shells are structured into several layers. Next to the outermost organic lining, the shells consist of a thin, outer, hard, primary layer composed of randomly oriented nanocrystalline calcite, which is followed inward by a much softer shell segment built of long calcite fibres, stacked parallelly into blocks. While the crystallographic c-axes of the fibres are perpendicular to the shell vault, the morphological fibre axes run parallel to the shell vault with changing directions between different blocks or layers. The hardness distribution pattern within the shells is non-uniform and varies on scales as small as a few tens of microns. The maximum hardness in nanohardness indents has been observed in the youngest part of the primary layer and in transverse cross sections through fibres of the secondary layer, while the lowest hardness in nanoindents within the shells has been measured in the longitudinally cut fibres of the secondary layer, predominantly those next to the soft tissue. Our results confirm that optimal mechanical performance and fracture toughness of the shell is given by structural features such as a distinct variation in crystal size and morphology, a varying degree of crystal orientation and the distribution of intracrystalline and intercrystalline organic matter.

(ICOTOM-P-062-2008) Defect Structures in Block Copolymer/Nanoparticle Blends

H. Ryu*, M. R. Bockstaller, Carnegie Mellon University, USA

The implications of nanoparticle additives and chain architectures on the grain boundary structure in block copolymer/nanoparticle blends are studied. Di- and tri-block copolymers composed of polystyrene (PS) and polyisoprene (PI) were blended with PS-coated gold nanoparticles. Polymer-coated nanoparticle additives are shown to stabilize the formation of high-energy grain boundaries such as omega or T-junction grain boundaries through relieving the stress of high-energy regions by the selective swelling of those regions. As a consequence, the addition of particle fillers is found to significantly increase the number of energetically unfavorable grain boundary structures as compared to neat block copolymer systems. Also, it is shown that the chain architecture of block copolymers affects the distribution of nanoparticle additives, and accordingly has an impact on the grain boundary structures. The direct visualization and quantitative analysis of grain boundary structures in block copolymer/nanoparticle blends give a way of understanding the microstructure of block copolymers.

(ICOTOM-P-063-2008) Microtexture and Microstructure Evolution in High Purity and Particle Containing Aluminum Alloys Processed by Accumulative Roll Bonding

A. Akbarzadeh*, H. Pirgazi, Sharif Univ. of Technology, Iran; R. Petrov, Sharif University of Technology, Iran; L. Kestens, Ghent University, Belgium

The role of second phase particles as well as the evolution of microstructure and texture of high purity (AA1100) and particle containing aluminum alloy (AA3003) sheets was studied during accumulative roll bonding (ARB) process. Electron Back-Scattered Diffraction (EBSD) technique and transmission electron microscopy (TEM) were utilized to investigate the development of the texture and deformation microstructures. Texture analysis revealed a cross-

sectional gradient with Copper and Dillamore components in the mid-layers and strong shear components in the subsurface regions. With increasing the strain over the ARB cycles, the overall texture intensity increases and a strong texture develops which leads to unrefined bands in AA1100 alloy. At high levels of strain, transition of the microstructure to a submicron level occurs. It was also found that large lattice rotation around the second phase particles in AA3003 alloy increases the local misorientation and produces new high angle grain boundaries. The presence of these particles also prevents development of a strong texture and improves the grain refinement during the process which in turn results in a homogeneous microstructure of ultra-fine grains in AA3003 alloy.

(ICOTOM-P-064-2008) Effect of Dislocation Stress on the Surface Corrosion Behavior on (111) and (112) Plan of Aluminum Single Crystal

D. Pei, W. Mao*, University of Science and Technology Beijing, China

There will be certain stress field around a dislocation, while it outcrops on the crystal surface. The stress will promote the nucleation and growth of surface pits in corrosion environment. The corrosion experiment of aluminum single crystal showed that the number of pits was larger on (111) than that on (112) surface plane, however the average size of the pits was smaller on (111) than that on (112). The tension stress fields of straight screw dislocations and straight edge dislocations on (111) and (112) surface planes of the aluminum single crystal were calculated, while the stress components referring the normal direction of crystal surface became zero. The calculation indicated much higher level of surface tension stress around edge dislocations than that around screw dislocations. It is believed therefore, that corrosion pits should appear preferentially around outcrops of edge dislocations. The distribution of edge dislocation outcrops and the corresponding characteristics of their stress fields on (111) and (112) plane are calculated under the assumption of homogeneous dislocation distribution, after which the reason of the different pitting nucleation on (111) plane and (112) plane is discussed according to the different variety of edge dislocations on the two surface planes.

(ICOTOM-P-065-2008) Formation of Al₃Ti/AlB₂ in an Al-Ti/Al-B Master Alloy

D. G. Mallapur*, S. A. Kori, Basaveshwar Engineering College, India

Grain refinement is one of the ways to control the microstructure of the castings. Small additions of Al-Ti/Al-B master alloys to an Al and its alloys results in refinement of α -Al dendrites. A fine equiaxed structure leads to several benefits such as improved mechanical properties, improved feeding during solidification, reduced and more evenly distributed porosity, better dispersion of second phase. In the early stages of development in this field, Ti and B were introduced into the melt as reducible halide salts such as K₂TiF₆ and KBF₄. However, this practice was later abandoned due to the difficulties in controlling the Ti and B content. Ti and B additions to Al its alloys in the form of master alloys like Al-Ti/Al-B were found to be more effective. Moreover, these master alloys offer better cleanliness and improved product quality. The addition of grain refiner to Al-Si alloys significantly refines the coarse columnar aluminium grains into fine equiaxed grains. Hence an attempt has been made to prepare indigenous Al-Ti/Al-B master alloys using halide salts in the laboratory. In the present study, the Al-5Ti and Al-3B master alloys have been prepared by the reaction of K₂TiF₆ and KBF₄ halide salts with liquid molten Al. The process parameters such as reaction temperature, reaction time and compositions were studied to optimize the manufacturing parameter. The prepared master alloys have been characterized by chemical analysis, particle size analysis, XRD and SEM/EDX microanalysis. The present results suggest that reaction time of 60min. and reaction temperature of 800 OC is essential to obtain Al₃Ti/AlB₂ intermetallic particles in an Al-Ti/Al-B master alloy respectively. Results also suggest that addition of 0.2wt% Al-5Ti and or Al-3B master alloys containing Al₃Ti/AlB₂ particles to Al and its alloys refines

coarse structure to fine equiaxed structure and in turn improves the mechanical properties and are confirmed by Computerized Universal Testing Machine (CUTM).

(ICOTOM-P-067-2008) Influence of Shear Bands on Microtexture Evolution in Polycrystalline Copper

H. Paul*, Institute of Metallurgy and Materials Science PAS, Poland; J. Driver, Ecole des Mines, France

There has been much discussion about the role of shear bands in deformation texture development. The main difficulty is to correctly describe the formation of certain deformation texture components, eg. $\{110\}\langle uvw \rangle$ in fcc metals, using classical deformation models. Related question is the mechanism the slip propagation across the grain boundaries in polycrystalline metals without changes in shear direction. In this work, the microstructure and (micro)texture development in pure copper is investigated in order to characterize influence of the crystal lattice re-orientation within particular grains on slip propagation and the formation of macroscopically visible clusters of shear bands. Polycrystalline copper (99.98%) with an initial grain size of 80 μm was deformed in plane strain compression up to a thickness reduction of 50%. At this deformation level the formation of clearly defined macroscopic shear bands (MSB) is observed. The deformation induced dislocation structures and local changes in crystallographic orientations were investigated by TEM and SEM, including high resolution EBSD. The orientation maps show that well defined crystal lattice re-orientations occur in particular grains situated within the area of the broad MSB, even these grains possess quite different crystallographic orientations. In all analyzed grains (within MSB) one observes a strong tendency to strain induced re-orientation. Their crystal lattice rotate towards such that one of the $\{111\}$ slip planes becomes nearly parallel to the direction of maximum shear. A natural consequence of this rotation is the formation of the specific microtexture of MSB which facilitate slip propagation across grain boundaries along the shear direction without any visible variation in slip direction. It is concluded that shear banding occurs across grain boundaries by continuity of slip direction even slip plane do not coincide exactly in the adjacent grains.

(ICOTOM-P-069-2008) Grain Coarsening Kinetic in ECAPed Al Containing 0.1%Sc

A. Bommareddy, M. Z. Quadir*, N. Burhan, O. Al-Buhamad, M. Ferry, The University of New South Wales, Australia

Super saturated solid solution of 0.1% Sc in Al was severely deformed by passing eight times through an equal channel angular machine aligned 90° between the entry and exit channels. This produced an extremely refined nano structured deformation microstructural distribution, can be resolved by transmission electron microscopy. A controlled pre-age heat treatment at 250C spheroidized the substructures into equiaxed (~1.00 μm), and remained stable until long heating period (30hrs). The subsequent grain growth kinetics was measured after heating at 300, 350, 400 and 450C for different time length. The grain size measurement was done by electron backscatter diffraction (EBSD) and transmission electron microscopy (TEM) depending on resolution requirement. A kinetic mechanism is proposed by correlating the size of the growth fronts of identically oriented clusters and early stage grown grains, backed by kinetic data and Al-Sc precipitate density.

(ICOTOM-P-070-2008) Study of the Evolution of Texture and Microstructure during Different Modes of Rolling and Annealing of Two-phase ($\alpha+\beta$) Brass

R. Garg, N. Gurao*, S. Suwas, S. Ranganathan, Indian Institute of Science, India

In two-phase copper alloy (Cu-40Zn alloy) the evolution of texture and microstructure was studied with the change of initial texture and deformation path (mode of rolling). Hot rolled bar of Cu-40Zn alloy (as-received material) and solution treated material (after solution treated condition) were subjected to unidirectional and cross rolling

(multi-step cross-rolling) at room temperature with strain per pass (true strain) being constant for each step. Strains corresponding to rolling reduction of 50% and 80% were given to as-received and solution treated material through each of the different mode of rolling. A piece was cut from each of the as-rolled materials and was subjected to annealing at 560°C for one hour for recrystallization. The bulk and micro textures were determined by measuring the pole figures and calculating orientation distribution function ODF for both the α (fcc) and the β (ordered cubic) phases. The initial texture had a pronounced effect on texture development of α phase for solution treated alloy during deformation. This material exhibited very strong $P(B_{ND}) \{011\}\langle 111 \rangle$ orientation for unidirectional as well as for multi-step cross rolling. The volume fraction of cube oriented grains was very low for all recrystallized samples. The texture of β phase for unidirectionally rolled solution treated alloy got sharpened on annealing. However, strength of texture decreased with increasing deformation. Grain boundary (and CSL boundary) analyses were carried out with EBSD data. These analyses indicated that all the recrystallized samples had a high number of $\Sigma 3$ boundaries. The proportion of $\Sigma 3$ boundaries was higher in multi-step cross-rolled annealed material. The deformed material had higher number fraction of low angle boundary than any other special boundary. Solution treated material had an average grain size of α phase smaller than the as-received material.

(ICOTOM-P-071-2008) Processing-Texture-Property Relationship in ECAE Processed Two Phase ($\alpha+\beta$) Brass

A. Bhowmik, S. Biswas, S. Singh, N. Gurao*, S. Suwas, Indian Institute of Science, Bangalore, India

Equal channel angular extrusion is one of the well know severe plastic deformation (SPD) process to generate ultra-fine grains in bulk materials. Owing to the large degree of deformation which the material experiences, the process is also associated with evolution of characteristic shear texture. However, till now most of the studies carried out so far have been aimed at studying single phase materials. For the possible enhancement of super-plastic properties of two phase materials such as ($\alpha+\beta$) brass, such a study is very relevant. The present work gives a thorough investigation of evolution of microstructure and texture during ECAE for both α and β (B2) phases separately. Mechanical properties corresponding to different texture and microstructure combinations have been reported.

(ICOTOM-P-072-2008) Microstructure Sensitive Design of a Polycrystalline alpha-Ti Compliant Beam

T. Fast*, S. R. Kalidindi, Drexel University, USA

Designers have had access, for some time, to powerful computational tools to optimize the performance of an engineering component by modifying its geometry. However, these methods often do not exploit the much richer space of the feasible material property combinations in a given material system through modification of the material's microstructure. Microstructure sensitive design (MSD) offers a mathematical framework for exploring the optimization of the performance of a component while considering material microstructure as a continuous design variable. MSD employs spectral methods to define the relevant space of feasible microstructures for a given application, and appropriate homogenization theories for the microstructure-property linkages. In this paper, the versatility of the MSD approach is demonstrated by applying it to the design of a compliant beam made from polycrystalline α -Ti. In this case study, the beam deflection is maximized without initiating plastic yielding. The design is first optimized assuming a statistically homogeneous microstructure (i.e. uniform texture in the sample), and then through-thickness texture gradients were incorporated to further enhance the performance of the beam. Significant improvements in performance have been noted in these design case studies, when compared to the design assuming isotropic material properties (i.e. a random texture).

Abstracts

(ICOTOM-P-073-2008) Modeling Cube Texture Effects on Formability of FCC Sheet Metal

J. W. Signorelli*, M. A. Bertinetti, P. A. Turner, R. E. Bolmaro, IFIR - CON-ICET, Argentina

Cube texture component is inevitably present in FCC sheet metal. Such preferred orientation leads to anisotropic properties which affect the sheet formability. In this research, the effect of the cube texture on forming-limit strains is studied using a rate-dependent viscoplastic law in conjunction with the Marciniak-Kuczynski approach. The forming limit diagram and yield locus are determined for several spreading of grain orientations around the ideal $\{100\} \langle 001 \rangle$ component. The spreading respect to the ideal orientation is taken assuming a uniform distribution with a standard deviation or cut-off angle from 0 to 15 degree. The trend of the predicted limit strains shows that the main differences in the forming limit strains have a correlation with the sharpness of the yield locus near equi-biaxial stretching path, and also with the texture evolution and subsequent selected slip systems predicted by each model.

(ICOTOM-P-074-2008) Electroless Nickel Plating on Magnesium Alloys used in Space Applications

N. Dhawan*, Punjab Engineering College, India

Magnesium (Mg) and its alloys are being used as structural components in industry because of their high strength-to-weight ratio and relatively high stiffness. A shortcoming of Mg based alloys is their high electrochemical activity and poor corrosion resistance. Therefore, coatings or surface treatment are needed for protection purpose. Electroless nickel-plating on magnesium alloys is one of proper protection method because the deposited nickel is very resistant to corrosion and abrasion. This paper reports work on Electroless plating of Ni on Mg alloys. Mg alloys were used as the substrates to investigate the deposition rate, nucleation process, and microstructure of the Electroless Ni coatings. It was found that deposition processes are strongly affected by the alloy substrates. Ni plating on AZ31 alloy has higher deposition rates and lower surface roughness than that of other substrates. SEM investigations showed that nodular morphology of Ni coatings formed on the substrates. Application of electrochemical plating on Mg and its alloys requires surface pretreatment to ensure adhesion and integrity of the coatings. These steps include cleaning, etching and fluoride activation. Deposition was initiated on the phase and grain boundaries due to the inter-grain galvanic coupling. Future work is on the lines how to improve corrosion resistance of Magnesium alloys by conversion treatment.

(ICOTOM-P-076-2008) Simulation of Microstructure Evolution of Polycrystalline Ice: Model Set-up

A. Grier*, CNRS-Université Paul-Sabatier, France; R. Lebensohn, Los Alamos National Laboratory, USA; M. Jessell, CNRS-Université Paul-Sabatier, France; L. Evans, University of Melbourne, Australia

We present a new numerical scheme to simulate deformation and recrystallisation of 2-D polycrystalline materials. The scheme is based on the coupling of a full-field crystal plasticity code (Lebensohn, 2001) and the Elle modelling platform (www.materialsknowledge.org/elle). Since both codes use periodic boundary conditions and a regular distribution of discrete nodes, a direct one-to-one mapping between both data structures is possible. The crystal plasticity code computes the micromechanical response of a polycrystalline medium deforming by dislocation glide using the Fast Fourier Transform (FFT) algorithm. Based on the evolution of the local misorientation field predicted with the FFT-based model, we have implemented the calculation of the corresponding geometrically-necessary dislocation density field, which in turn is used to predict recrystallization in the aggregate, using the Elle platform. Elle is an open-source code for the simulation of microstructural evolution of rocks during deformation and metamorphism. The modular architecture of the code allows us to efficiently simulate

multiple and competitive processes. A front-tracking approach, in which the Gibbs free energy is minimized, is used to simulate grain growth. Grain boundary curvatures and dislocation densities are used as driving forces for grain boundary migration. When the stored energy exceeds a threshold value, new free-dislocation grains are nucleated. An oriented nucleation model is assumed and nucleation is only permitted at boundaries of old grains. The first predictions of dynamic recrystallisation of polycrystalline columnar ice are presented. These results show that the new numerical scheme can simulate the influence of spatial variation of subgrain scale heterogeneities on the recrystallisation of polycrystals. Further validation of the FFT-Elle predictions will include comparison with cryo-EBSD annealing experiments of experimentally pre-deformed samples of synthetic columnar ice. Lebensohn, R. A. (2001) *Acta Materialia* 49, 2723-2737. This presentation is supported by the European Science Foundation (ESF) under the EUROCORES Programme EuroMinSci of the European Commission, DG Research, FP6 (198)

(ICOTOM-P-077-2008) Grain Interaction and Related Elastic Fields at Triple Junction in Low Deformed IF Steel: Micromechanical Model and Reconstruction from EBSD Orientation Data

A. Zisman*, V. Rybin, CRISm "Prometey", Russian Federation; M. Seefeldt, S. Van Boxel, P. Van Houtte, Kathoic University of Leuven, Belgium

Incompatible plastic strains of grains, forming a triple junction in a low deformed IF steel, have been reconstructed from their interfacial disorientations with a simple micromechanical model that suggests the minimum level of internal stresses. Then, based on these strains, respective defects induced on the grain boundaries are quantified and related long-range fields of elastic rotation and stress are calculated. The calculated rotation field, accommodating the strain induced part of interfacial disorientations, proves to fit satisfactorily EBSD orientation data and evidences for a disclination of about 3 degrees on the junction line and planar stress sources on the involved boundaries. The corresponding stress field locates probable areas of plastic accommodation, which are also in good correspondence with appropriate features of the EBSD data.

(ICOTOM-P-078-2008) Two-Phase Microstructure Generation in 3D based on 2D Sections of a Nickel Alloy

C. Roberts*, Carnegie Mellon University, USA; L. Semiatin, Air Force Research Laboratories, USA; A. Rollett, Carnegie Mellon University, USA

A series of new and existing techniques have been developed to generate a three-dimensional microstructure based on geometric and texture characteristics of the primary phase and secondary phase (i.e. carbides) of a nickel alloy, Waspaloy. Each technique is addressed to describe its advantages and proposed modifications to improve the representations of specific features. A Potts-based Monte Carlo grain growth model and Ellipsoid Packing/Cellular Automaton approach were compared to determine which method could construct a grain structure with size and shape distributions that match the experimental distributions. Using the experimental grain orientation distribution (ODF) and misorientation distribution (MDF) as input, an orientation assignment algorithm generated the digital texture distributions. The low volume fraction (~0.2%) secondary phase particles were inserted onto grain boundaries and grain interiors using an injection technique. The MC grain growth model produced grains with equiaxed morphologies and a lognormal grain size distribution while the orientation assignment algorithm produced orientation and misorientation distributions nearly identical to the nickel alloy. Particle placement on grain boundaries was consistent with the experimental particle-associated misorientation distribution (PMDf); that is, the PMDF suggests a non-random correlation with grain boundary type (disorientation angle) and was reproduced in the simulation microstructure. The agreement between the digital and experimental features indicates the techniques

can be applied to generate a statistically representative two-phase microstructure.

(ICOTOM-P-079-2008) Study on Cold Drawing Texture of High-Strength Low-Expansion Fe-Ni Alloy

L. Chen*, University of Science and Technology Beijing, China; J. Zhang, Central Iron & Steel Research Institute, China; L. Zhang, University of Science and Technology Beijing, China

Cold drawing textures for different reductions in area of high-strength and low-expansion Fe-Ni alloy used as heat resisting electric transmission core wire were investigated using X-ray and electron back scattered diffraction (EBSD) technique. It was found that the $\langle 111 \rangle$ and $\langle 100 \rangle$ fibre textures are the main texture components and grains on the sides are more fine and uniform than those in the center of Fe-Ni alloy undergoing cold drawing. The experimental results showed that the volume fraction of $\langle 111 \rangle$ fibre texture determined by quantitative regression calculation of Gaussian distribution function reached more than 60% and the strong $\langle 111 \rangle$ fibre texture favors the torsional property of Fe-Ni alloy. The final stable orientations were determined based on the rotation rates of lattice referring to the sample coordinate system and relative orientation density change.

(ICOTOM-P-080-2008) Model of Plastic Spin Taking in Account Grain Interaction during Rolling

R. E. Bolmaro*, A. L. Fourty, J. W. Signorelli, Instituto de Física Rosario, Argentina

The fragmentation of grains after large and severe deformation processes is an experimental fact that still lacks an easy, computationally economical and fast simulation model. During the last years some attempts to introduce microstructural features have been successful in reproducing a few experimental results. However the price in computer time is high and localization, as seen by experiments as geometrically necessary and incidental dislocation boundaries, is still elusive. On the current paper we perfect a previous co-spin model allowing the whole velocity gradient of spin sharing grains to be compatible with the average deformation field. The model is implemented in a Taylor type deformation model allowing neighbor grains to share deformation rates and spins by simultaneous averaging in coincidence with macroscopic values. Misorientation distributions are compared with literature data. The results show the characteristic lognormal distribution with a close match with the experiments until a von Mises strain of 2.0. They are discussed in terms of the microstructural influence on texture development rate and components.

(ICOTOM-P-081-2008) Numerical Simulation of Mechanical Behavior and Failure Process for Heterogeneous Brittle Materials in Uniaxial Tension by use of Fast Lagrangian Analysis of Continua

W. Xue-bin*, Department of Mechanics and Engineering Sciences, Liaoning Technical University, China

In the paper, the macroscopic stress-strain curve and the propagation process of tensile cracks for concrete specimen in uniaxial plane strain tension are investigated numerically. The concrete specimen is composed of the aggregates of arbitrary shape that is obtained by digital image process, the thinner interface layer surrounding the aggregates and the matrix. The strength of the interface layer and the matrix is different for different elements and a Weibull distribution law is taken into account. The aggregate is always elastic, while the matrix and the interface exhibit elastic-brittle behavior. The numerical results show that the propagation direction of cracks is approximately parallel to the applied tensile stress. A crack can be decomposed into two cracks in the propagation process when the tip of the crack meet with the elastic aggregate. The phenomenon is called crack bifurcation. When the peak stress of stress-strain curve is reached, some cracks have appeared. When longer cracks intersect the specimen, the load-carrying capacity of the specimen has nearly decreased to zero. The paper also presents the effects of aggregate size and constitutive parameters on the stress-strain curve and the fracture process of concrete specimen.

(ICOTOM-P-082-2008) Simulating Recrystallization Texture Evolution in FCC and BCC Polycrystals

B. Radhakrishnan*, G. Sarma, Oak Ridge National Lab, USA

The paper discusses a new model for nucleation of recrystallization based on orientation dependent recovery of subgrains. The rate of recovery is assumed to depend on the amount of non-coplanar slip activity at a given microstructural site, calculated using a crystal plasticity based finite element approach with grain level discretization. The recrystallization of the deformation substructure is simulated using a Monte Carlo approach that implements the above nucleation theory. The simulations are able to consistently capture the evolution of recrystallization texture in both FCC and BCC polycrystals subjected to plane-strain compression, wire drawing or shear deformation. Research sponsored in part by the U.S. Department of Energy Office of Electricity Delivery and Energy Reliability, and performed at the Oak Ridge National Laboratory (ORNL), managed by UT-Battelle, LLC for the U. S. Department of Energy under Contract No. DE-AC05-00OR22725.

(ICOTOM-P-083-2008) Quantitative Texture Analysis Using Area Detector

N. Yang*, Bruker AXS Inc., USA; K. Helming, Bruker AXS GmbH, Germany; U. Preckwinkel, K. Smith, B. He, Bruker AXS Inc., USA

In recent years, two-dimensional (2D) area detectors have been extensively used for X-ray diffraction applications. The trend in using 2D detectors for x-ray diffraction is increasing for its much faster speed and considerably more information obtained compared with the point detector or position-sensitive detector. A new approach using 2D detector for quantitative texture analysis has been developed recently. The new approach and the software package (MULTEX AREA) allows us to calculate the orientation density functions (ODF) of multi-phase texture samples from diffraction pole figures measured with 2D detector. The textures of up to three crystalline phase fractions can be determined simultaneously provided there is a sufficient number of pole figure data. The new approach decomposes the texture into multiple components and each component is represented as the orientation, the volume fraction and the standard deviation. In this presentation, selective application of texture analysis using Bruker D8 Diffractometer with GADDS and MULTEX AREA 2.0 software are demonstrated. The Euler angles, the volumetric fraction and the standard deviation from the ideal model of each component are calculated.

(ICOTOM-P-084-2008) Mechanism of Cube Grain Nucleation during Re-crystallization of Deformed Commercial Purity Aluminium

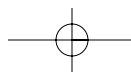
K. Kashyap*, C. S. Ramesh, PES Institute of Technology, India

Cube structure is a sharp recrystallization texture component in fcc metals like aluminium, copper, etc. It is described by an ideal orientation i.e. $(100) \langle 100 \rangle$. The subject of cube texture nucleation i.e. cube grain nucleation, from the deformed state of aluminium and copper is of scientific curiosity with concurrent technological implications. There are essentially two models currently in dispute over the mechanism of cube grain nucleation i.e. the differential stored energy model founded on the hypothesis proposed by Ridha and Hutchinson and the micro-growth selection model of Duggan et al. In this paper, calculations are made on the proposal of Ridha and Hutchinson model and the results are obtained in favor of differential stored energy model. It is also shown that there is no need for micro-growth model.

(ICOTOM-P-085-2008) Effect of Thermomechanical Treatment on the Grain Boundary Character Distribution in a 9Cr-1Mo Ferritic Steel

T. Karthikeyan*, Indira Gandhi Centre for Atomic Research, India; S. Mishra, IIT Bombay, India; S. Saroja, M. Vijayalakshmi, Indira Gandhi Centre for Atomic Research, India; I. Samajdar, IIT Bombay, India

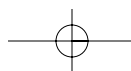
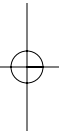
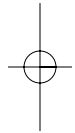
The increase in DBTT due to grain boundary embrittlement is a major obstacle in the development of ferritic steels for fast reactor



Abstracts

nuclear core applications. In order to minimize the fraction of high energy boundaries, which act as preferential sites for segregation of impurities and precipitation of brittle phases causing embrittlement, grain boundary engineering methods were employed. This was brought about by subjecting the (Nb, V) modified 9Cr-1Mo ferritic steel to a variety of thermomechanical treatments (TMT), such as hot/cold/cryo forging/rolling followed by different heat treatments

(recrystallisation/re-austenitisation, normalization/tempering). The TMT's resulted in different fractions of coincident site lattice boundaries, which are low energy boundaries, resistant to grain boundary segregation and precipitation of brittle phases. The 'Effective Grain Boundary Energy' was evaluated for the different treatments, based on which the optimum TMT to be adopted for this steel is identified. Details would be presented at the conference.



Author Index

A

| | |
|-------------------|---------------------|
| Ackley, K.R. | .93 |
| Adachi, Y. | .57 |
| Adams, B. | .59 |
| Adams, B.L. | .31, 40, 46, 60 |
| Adams, B.L.* | .59 |
| Agnew, S. | .91 |
| Agnew, S.R. | .34, 42, 47, 71, 79 |
| Ahmadi, S. | .46, 59 |
| Ahmadi, S.* | .60 |
| Ahzi, H. | .39 |
| Ahzi, S. | .39, 47, 61 |
| Akbarzadeh, A.* | .94, 104 |
| Akimune, Y.* | .43 |
| Akramov, S. | .78, 95 |
| Alankar, A.* | .85 |
| Alapati, G. | .39 |
| Al-Buhamad, O. | .78, 105 |
| Al-Buhamad, O.* | .80 |
| Al-Fadhlah, K.J.* | .61 |
| Ali, A. | .35 |
| Allain, S. | .68 |
| Allen, V. | .34 |
| Almer, J. | .39 |
| Al-Sawalmih, A. | .37 |
| Al-Sawalmih, A.* | .38 |
| Anne-laure, E. | .68 |
| Arai, S. | .66 |
| Aydelotte, B. | .59 |
| Azzi, M.* | .58, 65 |

B

| | |
|---------------------|--------------|
| Baars, D. | .77 |
| Baars, D.C.* | .91 |
| Bacaltchuka, C.M. | .100 |
| Bacroix, B. | .68 |
| Bailey, R.S. | .31 |
| Balachandran, S.* | .77 |
| Banarjee, S. | .37 |
| Banerjee, S. | .34 |
| Barabash, O.M. | .92 |
| Barabash, R.I.* | .29, 92 |
| Barani, A. | .93 |
| Barbé, L.* | .68 |
| Barbe, L.* | .96 |
| Barber, R.E. | .77 |
| Barbier, D.* | .68, 94 |
| Barbosa, P. | .91 |
| Barlat, F. | .61 |
| Barlat, F.* | .86 |
| Barmak, K. | .46 |
| Barmak, K.* | .63 |
| Barnett, M.R.* | .33 |
| Bassman, L. | .78 |
| Bate, P. | .77 |
| Baudin, T. | .65, 92, 103 |
| Beaudoin, A.J. | .61 |
| Beausir, B.* | .48 |
| Beer, A.G. | .33 |
| Bell, N. | .42, 43 |
| Belouettar, S. | .61 |
| Ben Achma, R.* | .98 |
| Bennett, T.* | .74 |
| Bernacki, M. | .81, 82 |
| Berry, D.C. | .63 |
| Bertinetti, M.A. | .106 |
| Bhanumurthy, K. | .85, 92 |
| Bhattacharjee, D. | .87 |
| Bhattacharjee, P.P. | .90 |

| | |
|--------------------|------------------|
| Bhattacharyya, A.* | .96 |
| Bhowmik, A. | .105 |
| Bi, H. | .89 |
| Bieler, T. | .77 |
| Bieler, T.R. | .91 |
| Bieler, T.R.* | .85 |
| Bingert, J.* | .58 |
| Bingert, J.F. | .83 |
| Biswas, S. | .105 |
| Bocher, P. | .57 |
| Bockstaller, M.R. | .104 |
| Boehlert, C.J.* | .58 |
| Böhm, A. | .42 |
| Bolle, B. | .68, 94 |
| Bollmann, C.* | .101 |
| Bolmaro, R.E. | .106 |
| Bolmaro, R.E.* | .89, 97, 99, 107 |
| Bommareddy, A. | .105 |
| Böttcher, A. | .66 |
| Bouzy, E. | .101 |
| Bouzy, E.* | .35 |
| Bowman, K.J.* | .44 |
| Boyce, D. | .60 |
| Boyce, D.E. | .81 |
| Bozzolo, N. | .91 |
| Bozzolo, N.* | .34 |
| Bracke, L. | .67 |
| Brahme, A.* | .69 |
| Bray, G.H. | .86 |
| Brekelmans, M. | .77 |
| Brenner, R. | .81 |
| Brochet, S. | .90 |
| Brokmeier, H. | .40, 42, 89, 99 |
| Brown, D.W. | .70, 71 |
| Brown, D.W.* | .34 |
| Bruckner, G. | .93 |
| Budai, J.D.* | .29 |
| Buffiere, J.* | .78 |
| Burhan, N. | .105 |
| Butterfield, M. | .72 |

C

| | |
|---------------------|--------------|
| Calcagnotto, M.* | .67 |
| Camata, R.P.* | .38 |
| Campissi, P.R. | .54 |
| Carpenter, J.O. | .88 |
| Carsten, L. | .37 |
| Carter, C. | .44 |
| Castelnau, O. | .68, 81 |
| Castro, C. | .44 |
| Ceccaldi, D. | .103 |
| Cernatescu, I. | .96 |
| Cernik, M.* | .69 |
| Chakraborty, A.* | .87 |
| Chan, L.H.* | .46 |
| Chang, L. | .49 |
| Chang, S.K.* | .65 |
| Chastel, Y. | .82 |
| Chattopadhyay, P.P. | .70 |
| Chauveau, T. | .68 |
| Chen, L.* | .89, 107 |
| Chen, W. | .58, 103 |
| Cheng, L. | .80 |
| Cheong, S. | .46 |
| Cho, J.* | .49, 84, 102 |
| Cho, M. | .99 |
| Choi, J.* | .100 |
| Choi, S. | .102 |
| Choi, S.* | .47 |
| Chu, A.O. | .39 |

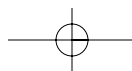
| | |
|---------------------|----------|
| Chuang, P. | .83 |
| Chulist, R. | .42 |
| Chun-Chih, L.* | .66 |
| Chun-Kan, H. | .66 |
| Clausen, B. | .47 |
| Clausen, B.* | .71 |
| Coghe, F.* | .57 |
| Colligan, K.J. | .83 |
| Comer, M.L.* | .83 |
| Compton, C. | .91 |
| Cong, D. | .100 |
| Coolley, J. | .80 |
| Costa, A.L. | .94 |
| Cottam, R.* | .36, 102 |
| Counts, A. | .50 |
| Coupez, T. | .81, 82 |
| Crimp, M.A. | .85 |
| Crooks, R. | .99 |
| Cruz-Gandarilla, F. | .65 |
| Cui, B. | .55, 92 |
| Cusack, M. | .39 |

D

| | |
|----------------------|-----------------|
| da Costa Viana, C.S. | .54, 94 |
| da Fonseca, J.Q. | .71 |
| da Fonseca, J.Q.* | .34 |
| Dafinov, A. | .98 |
| Dahlman, P. | .69 |
| Dalbeck, P. | .39 |
| Das, D. | .70 |
| Das, S.K. | .86 |
| Dashwood, R.J. | .71 |
| David, S. | .92 |
| Davis, B. | .36, 102 |
| Dawson, P.* | .81 |
| Dawson, P.R. | .60 |
| Daymond, M.R.* | .36 |
| De Graef, M. | .41, 83 |
| De Keyser, K. | .55 |
| De Keyser, K.* | .63 |
| de Wilde, A. | .98 |
| Decroos, K.* | .96 |
| Delannay, L. | .51, 81 |
| Delannay, L.* | .82 |
| Derose, D.J. | .92 |
| Detavernier, C. | .63 |
| Detavernier, C.* | .55 |
| Dey, G.K. | .34, 37, 85, 92 |
| Dey, S.R.* | .40, 103 |
| Dhawan, N.* | .106 |
| DiAntonio, C. | .42 |
| DiAntonio, C.* | .43 |
| Diener, M. | .78 |
| Digonnet, H. | .82 |
| Dillamore, I.* | .28 |
| Dillon, S.J. | .45 |
| Dillon, S.J.* | .30 |
| Dmitrieva, O.* | .30 |
| Domack, M. | .99 |
| Dosovitskii, G. | .64 |
| Driver, J. | .28, 97, 105 |
| Driver, J.H. | .52 |
| Drouelle, I. | .92 |
| Duchêne, L.* | .77 |
| Dye, D. | .71 |

E

| | |
|---------------|---------|
| Eberl, F. | .52 |
| Eisenlohr, P. | .67, 85 |



Author Index

Eisenlohr, P.*81
 El-Dasher, B.*72
 Elia, J.*95
 Elmustafa, A.99
 Elwazri, A.36
 Emelianenko, M.46
 Enders, S.39, 104
 Engleberg, D.45
 Engler, O.52
 Engler, O.*41
 Enomoto, M.57
 Esling, C.32, 100
 Esling, C.*32
 Es-Said, O.S.39
 Etter, A.92
 Evans, L.106

F

Fabritius, H.37, 38
 Faghihi, S.58
 Fang, W.87
 Fang, Z.Z.55
 Fanta, A.B.*69, 97
 Farrer, J.K.44
 Fast, T.*105
 Feng, H.67
 Feng, Z.92
 Ferrante, M.89
 Ferrie, E.78
 Ferry, M.30, 78, 80, 105
 Fesenko, V.28
 Field, D.72
 Field, D.*93
 Field, D.P.85
 Field, D.P.*84
 Flater, P.J.77
 Flemming, S.40
 Fonda, R.W.40, 85
 Fonda, R.W.*83
 Fourty, A.L.89, 99, 107
 Freeze, S.72
 Friak, M.50
 Friak, M.52
 Friedel, F.56
 Fromm, B.S.60
 Fromm, B.S.*46
 Frommert, M.*66
 Frommeyer, G.67
 Frost, H.J.62
 Fu, Z.87
 Fukutomi, H.102
 Fukutomi, H.*76
 Fullwood, D.31, 50, 61, 82
 Fullwood, D.*59
 Fullwood, D.T.40, 51
 Fundenberger, J.48, 94, 103
 Fundenberger, J.J.35
 Furrer, D.46

G

Gabryel, C.80
 Gan, W.89
 Gao, M.*99
 Garbe, U.42
 Garbe, U.*40
 Garcia, R.*43, 78
 Garg, R.105
 Garmestani, H.32
 Garmestani, H.*39, 100
 Gaudet, S.55
 Geers, M.77
 Geltmacher, A.B.51
 Gemmen, R.98
 Gerdes, K.98

Gerspach, F.*91
 Gervasyeva, I.*64, 92
 Gesing, M.52
 Gey, N.57, 68
 Ghana, B.101
 Gholinia, A.*41
 Ghosh, C.54
 Ghosh, P.54
 Gibala, R.*87
 Glavicic, M.58
 Glavicic, M.G.35
 Glez, J.90
 Gobernado Hernandez, P.29
 Godet, S.36
 Godet, S.*68
 Golovaty, D.46
 Gorbel, A.98
 Gottstein, G.47, 71, 73, 101
 Götz, A.37, 103
 Gourgues, A.53
 Goyal, A.92
 Goyal, A.*63
 Grekhov, M.*101
 Griera, A.*106
 Griesshaber, E.39
 Griesshaber, E.*37, 103, 104
 Griffin, R.B.77
 Groeber, M.41
 Gruber, J.56
 Gueguen, O.*61
 Gulsoy, E.B.41
 Gupta, V.K.*79
 Gurao, N.89
 Gurao, N.*105
 Gurao, N.P.35
 Gurao, N.P.*72
 Gururajan, M.56

H

Ha, J.99
 Habraken, A.77
 Haefner, D.39
 Haindl, S.93
 Haldar, A.*53, 54, 70
 Han, H.29, 90
 Han, K.95
 Hanada, T.99
 Hänninen, H.84
 Hansen, N.79
 Hantcherli, L.A.*67
 Harmer, M.P.45
 Hartley, C.S.*60
 Hartwig, K.91
 Hartwig, K.T.77
 Hasani, A.48
 Hatano, M.64
 Hawreliak, J.72
 Hazotte, A.35, 101
 He, B.107
 He, J.103
 He, S.C.100
 He, Y.*45
 Hefferan, C.M.41
 Heisel, M.C.42
 Helm, D.48
 Helmick, L.98
 Helming, K.107
 Her, E.29
 Hernandez-Silva, O.*75
 Herrera, C.*64
 Hirohashi, M.98
 Hiwarkar, V.D.34
 Hiwarkar, V.D.*37
 Hochrainer, T.61
 Hochrainer, T.*48

Hofmann, H.67
 Hofmann, M. I.*40
 Holt, R.A.36
 Holtzapfel, B.93
 Homma, H.66
 Honda, K.56
 Hong, S.99
 Hongyun, B.64
 Hori, M.75
 Hoseini, M.*77
 Hosford, W.F.77
 Hou, C.*88, 94
 House, J.W.*77
 Hrabcakova, L.*88
 Hsu, E.48
 Hu, X.87
 Hu, X.*86
 Hualong, L.77
 Huang, M.75
 Huang, X.79
 Huh, M.*52
 Humbert, M.57, 68
 Humbert, M.*101
 Humphreys, J.77
 Humphreys, J.F.94
 Hung, M.93
 Hünsche, I.76
 Hutchinson, B.*87
 Hwang, J.100
 Hwang, N.96

I

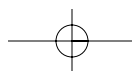
Ice, G.29
 Ice, G.E.29, 92
 Illson, D.61
 Imai, N.86
 Inagaki, H.73
 Inagaki, H.*53
 Inal, K.*52
 Inoue, H.*75
 Ioana, A.*87
 Isabelle, T.101
 Isaenkova, M.28, 101
 Isaenkova, M.*58
 Ito, K.*73
 Izadbakhsh, A.52

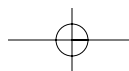
J

Jackson, M.71
 Jacques, P.36
 Jacques, P.J.68
 Jain, M.86
 Janssens, K.29
 Jeoung, H.78
 Jepson, P.*31
 Jessell, M.106
 Jiang, H.91
 Jiang, L.36
 Jiang, L.*33, 50
 Jiang, X.86
 Jonas, J.36
 Jonas, J.J.33, 45
 Jones, J.L.*43
 Jones, R.45
 Joo, H.*95
 Jordan-Sweet, J.55, 63

K

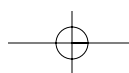
Kacher, J.31
 Kacher, J.P.*40
 Kalidindi, S.59, 82
 Kalidindi, S.*50
 Kalidindi, S.R.51, 60, 61, 105

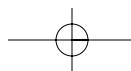




Author Index

- Kalu, P.91
 Kalu, P.N.55, 92
 Kamikawa, N.*79
 Kang, H.52
 Kang, J.29, 57
 Kang, S.49
 Kanjarla, A.K.82
 Kanjarla, A.K.*51
 Kannarpady, G.K.96
 Kapoor, R.72
 Karthikeyan, T.*107
 Kashihara, K.*73
 Kashyap, K.*107
 Kassner, M.50
 Kato, H.49, 91
 Kaul, A.64
 Kelm, K.39, 104
 Keshavarz, Z.33
 Kestens, L.29, 55, 57, 67, 74, 79, 87, 104
 Kestens, L.A.74
 Kestens, L.A.*53
 Khatirkar, R.*55
 Khatonabadi, M.39
 Khlbnikova, J.64, 92
 Kiely, C.J.45
 Kim, D.29, 47
 Kim, D.*102
 Kim, H.47, 49, 62
 Kim, I.*42, 78, 95
 Kim, J.57, 95, 96
 Kim, S.29, 90
 Kimura, K.*64
 Kimura, T.*45
 Kinderlehrer, D.*46
 King, A.*62
 Klein, H.37, 38, 74
 Knabl, W.76
 Knezevic, M.60
 Knezevic, M.*61
 Knippling, K.*85
 Knutson Wedel, M.69
 Ko, K.*96
 Kobayashi, S.75
 Kobayashi, S.*80
 Koh, H.49
 Kokawa, H.83
 Kolahi, A.94
 Komatsubara, T.75
 Konijnenberg, P.41
 Kori, S.A.104
 Kozaczek, K.*62
 Krautschik, J.93
 Krishnan, J.92
 Krupitzer, R.P.87
 Krymskaya, O.101
 Kulovits, A.*62, 79
 Kumar, V.*55
 Kumbhar, N.T.85, 92
 Kunze, K.78
 Kusters, S.*59
- L**
- Lagoeiro, L.*44, 91
 Lahn, L.66
 Laik, A.92
 Landheer, H.*57
 Landi, G.50
 Landi, G.*51
 Landon, C.D.40
 Landon, C.D.*31
 Larson, B.29
 Laruelle, C.94
 Laughlin, D.E.*63
 Lauridsen, E.M.40
 Lavoie, C.55, 63
- Lazorenko, V.101
 Lebensohn, R.47, 60, 106
 Lebensohn, R.*51, 81
 Lebensohn, R.A.61
 Leber, H.J.78
 Lecomte, J.40
 LeDonne, J.*46
 Lee, C.83
 Lee, D.*90
 Lee, D.N.65
 Lee, H.29, 99, 102
 Lee, H.*99
 Lee, J.99
 Lee, M.*37, 39
 Lee, S.99
 Lee, S.*41, 97, 99
 Lee, S.I.65
 Lee, T.94
 Leffers, T.*52, 60
 León García, O.*79
 Leonard, J.P.62
 León-García, O.29
 Lesko, A.69, 88
 Lewis, A.55
 Lewis, A.C.*51
 Li, B.*38, 100
 Li, C.38, 93
 Li, D.S.39
 Li, H.*48
 Li, J.86
 Li, J.*86
 Li, L.87
 Li, M.93
 Li, S.*49
 Li, T.86
 Liang, Z.64, 79
 Liao, C.94
 Lienert, U.41
 Lienert, U.*39
 Lim, C.99
 Lim, C.*89
 Liqing, C.64
 Lischewski, I.*71
 Littlewood, D.85
 Liu, C.88
 Liu, D.93
 Liu, D.*76
 Liu, T.*30, 62, 93
 Liu, W.29, 92
 Liu, X.49
 Liu, Y.89
 Liu, Y.*86
 Logé, R.81
 Logé, R.E.*82
 Loic, M.68
 Long, Z.86
 Lopez, M.F.58
 Lorenzana, H.72
 Lorich, A.76
 Lorimer, G.36, 102
 Lu, Y.*98
 Lubin, S.*53
 Ludwig, W.40, 78
 Lüter, C.103
 Luyten, J.98
- M**
- Ma, D.35, 50
 Ma, D.*52
 Ma, E.100
 Ma, X.33
 MacSleyne, J.*83
 Maiocco, L.93
 Majumdar, B.S.*70, 76
 Makradi, A.61
- Malaria, J.97
 Mallapur, D.G.*104
 Man, C.*75
 Mandal, S.56
 Mani Krishna, K.V.37
 Maniatty, A.*85
 Mao, S.X.79
 Mao, W.62, 93
 Mao, W.*31, 67, 104
 Marchi, A.N.90
 Marrow, J.45
 Martin, <.*36
 Martino, R.D.99
 Mason, J.*60
 Mastorakos, I.85
 Masui, H.*41, 72
 Matrisciano, L.39
 Matsuo, K.43
 Maudlin, P.J.58
 Maurice, C.97
 McKenna, I.56
 McNaney, J.72
 Medina, F.98
 Mel'nikov, K.E.58
 Melchior, M.A.82
 Mendoza-Leon, H.65
 Meratian, M.77
 Merkel, S.*69
 Merriman, C.C.*72
 Mguil, S.*47, 61
 Milathianaki, D.72
 Miller, H.M.*46
 Miller, J.84
 Miller, M.P.81
 Miller, M.P.*31
 Minamiguchi, S.49
 Minegishi, T.99
 Miracle, D.58
 Miracle, D.B.35
 Miroux, A.74
 Mishra, R.K.52, 86
 Mishra, S.74, 107
 Mishra, S.K.*88
 Misra, A.99
 Mithieux, J.90
 Mohles, V.47, 73
 Molodov, D.A.*32
 Mononen, J.84
 Morawiec, A.*40
 Morita, K.91
 Morris, P.R.*59
 Motohashi, T.45
 Mu, S.*47
- N**
- Nakamichi, H.*94
 Namba, E.*66
 Narasimhan, K.37, 88
 Neale, K.W.48
 Necker, C.T.*90
 Neil, C.*47
 Nelson, T.W.84
 Neu, V.93
 Neugebauer, J.50, 52
 Neuser, R.37
 Neuser, R.D.103
 Niewczas, M.61
 Niezgoda, S.50, 59
 Niezgoda, S.R.*82
 Nikolov, S.61
 Ningileri, S.86
 Nishiyama, N.70
 Nnamchi, P.*93
 Norton, D.29
 Noureddine, M.*68





Author Index

Nowell, M.*88
 Nowell, M.M.55
 Nuhfer, T.79
 Nyborg, L.69
 Nylander, C.59

O

O'Brien, J.M.77
 Oertel, C.42, 93
 Oertel, C.*76
 Offerman, E.57
 Oh, K.102
 Oh, K.*29
 Ohms, C.96
 Okada, A.43
 Okayasu, K.76
 Okayasu, K.*102
 Oliveira, T.R.65
 Ooishi, R.43
 Ookubo, Y.91
 Owen, A.W.37

P

Palle, S.56
 Pan, Z.29
 Pant, P.34, 88
 Papillon, F.*45
 Paris, O.38
 Park, B.42
 Park, J.31, 95, 96
 Park, J.*95
 Park, N.95
 Park, Y.*57
 Paul, H.*97, 105
 Pei, D.104
 Pei, W.66, 100
 Penelle, R.*65, 66, 92, 103
 Penning, J.67
 Pérez-Huerta, A.39
 Pérez-Prado, M.50
 Perlovich, Y.58, 101
 Perlovich, Y.*28
 Pesci, R.40
 Petrov, M.50
 Petrov, R.53, 55, 74, 79, 104
 Petrov, R.H.74
 Petrov, R.H.*29
 Petrova, R.*98
 Pinto, A.L.*54, 94
 Piot, D.28
 Piot, D.J.*52
 Pirgazi, H.104
 Ponge, D.64, 67, 93
 Ponte Castaneda, P.51
 Pötschke, M.42
 Poulon, A.*90
 Pourboghrat, F.91
 Pouteau, P.96
 Prakash, A.48
 Prakash, A.*61
 Preckwinkel, U.107
 Predmersky, M.69
 Preuss, M.34, 71
 Proudhon, H.78
 Pyle, D.85

Q

Qidwai, M.A.51
 Qiwu, J.79
 Qadir, M.Z.80
 Qadir, M.Z.*78, 105
 Quey, R.52
 Quey, R.*28

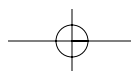
R

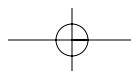
Raabe, D.30, 38, 52, 56, 62, 64, 66, 67, 68, 69, 73,
 85, 93, 97
 Raabe, D.*28, 35, 37, 38, 50, 67
 Rabet, L.57
 Radhakrishnan, B.*107
 Raghunathan, S.L.*71
 Rainforth, M.75
 Ramesh, C.S.107
 Ramesh, K.100
 Ramesh, M.*78
 Randau, C.40
 Randle, V.*45
 Ranganathan, S.105
 Rao, K.S.*45
 Raue, L.37, 38
 Raveendra, S.*74
 Ray, R.K.46, 54, 87, 103
 Ray, R.K.*54, 90
 Réglé, H.53
 Regle, H.68, 98
 Reibold, M.93
 Reiche, H.70
 Resk, H.82
 Resk, H.*81
 Reynolds, A.P.83
 Reynolds, A.P.*84
 Richard, P.68
 Riedel, H.48, 61
 Riesterer, J.L.*44
 Ro, Y.79
 Roatta, A.89, 97
 Robert, W.52
 Roberts, C.*106
 Robson, J.36, 102
 Rodionov, D.64, 92
 Rodrigo, S.P.65
 Rodriguez, M.42, 43
 Rohrer, G.45, 46, 98
 Rohrer, G.S.30, 41, 46, 97
 Rohrer, G.S.*44
 Rollett, A.29, 46, 79, 89, 99, 106
 Rollett, A.D.41, 45, 46, 56, 74, 81, 97, 99
 Romano, P.*56
 Romero, J.*71
 Roters, F.28, 50, 52, 67, 81, 85
 Rouag, N.66
 Rowenhorst, D.40
 Rowenhorst, D.*55
 Roy, S.*35, 101
 Ruano, O.50
 Rugg, D.*46
 Rybin, V.106
 Rytberg, K.*69
 Ryu, H.*104
 S
 Sachdev, A.86
 Sachs, C.37
 Saha, R.*54
 Sahoo, S.37
 Sahoo, S.K.85, 92
 Sahoo, S.K.*34
 Saimoto, S.*80
 Sakai, T.*49
 Sakakibara, M.76, 102
 Sakata, O.99
 Sakka, Y.33
 Salem, A.A.60
 Salem, A.A.*35
 Salvador, P.A.98
 Samajdar, I.34, 37, 55, 74, 88, 107
 Samajdar, I.*85, 92
 Sander, B.35
 Sandim, H.R.*65
 Sankaran, A.35, 101

Sarma, D.29
 Sarma, G.107
 Saroja, S.107
 Sato, Y.S.*83
 Saukkonen, T.*84
 Savolainen, K.84
 Schaarschuch, R.*93
 Schäfer, C.*73
 Schestakow, I.36
 Schmahl, W.37
 Schmahl, W.*39
 Schmahl, W.W.103, 104
 Schuh, C.A.60
 Schultz, L.93
 Schuren, J.C.31
 Seefeldt, M.59, 82, 96, 106
 Seefeldt, M.*68
 Seetharaman, S.98
 Seetharaman, V.76
 Sekkak, C.66
 Semiatin, L.60, 106
 Semiatin, S.L.35
 Seo, J.57
 Serebryany, V.*34, 58
 Sha, Y.*66, 100
 Shahbazian Yassar, R.*91
 Sheikh-Ali, A.D.*32
 Shenoy, G.29
 Shi, M.*49
 Shin, K.100
 Shoji, T.45
 Sidor, J.*74
 Siegel, S.38
 Signorelli, J.W.82, 107
 Signorelli, J.W.*106
 Simmons, J.P.41, 83
 Singh, S.105
 Siniawski, M.T.39
 Sintay, S.46
 Sintay, S.D.*79
 Sisneros, T.A.70
 Skrotzki, W.76, 93
 Skrotzki, W.*42
 Smith, K.107
 Smith, M.G.90
 Snel, M.*98
 Snijkers, F.98
 Sobrero, C.97
 Sordi, V.L.89
 Sotoudeh, K.*77
 Spanos, G.55
 Specht, E.*92
 Spolenak, R.78
 Srinivasan, R.35
 Srivastav, D.34, 37
 Steigauf, T.38
 Sugimoto, A.83
 Sun, C.66
 Suter, R.M.*41
 Suthar, R.L.92
 Suwas, S.35, 48, 72, 89, 101, 103, 105
 Suwas, S.*35
 Suzuki, T.S.*33
 Swift, D.72
 Szpunar, J.48, 58, 65, 77
 Szpunar, J.A.95

T

Ta'asan, S.46
 Tabrizian, M.58
 Tajiri, H.99
 Takahashi, A.64
 Takashima, M.*97
 Takasugi, T.75
 Takayama, Y.49





Author Index

- Takayama, Y.*91
 Takekoshi, H.102
 Takeuchi, T.57
 Tamirisakandala, S.35, 58
 Tang, W.83
 Tanimoto, Y.*33
 Tayon, W.*99
 te Nijenhuis, J.*96
 Tewari, R.34, 85
 Thierry, B.68
 Thierry, G.101
 Thomas, I.69
 Thomsson, C.V.*62
 Tidu, A.94
 Timofeev, V.34
 Tischler, J.29
 Tiwari, R.37
 Tome, C.47
 Tomé, C.60
 Tome, C.N.51, 71
 Tomida, T.*86
 Tommaseo, C.E.*74
 Tong, W.*103
 Torney, C.37
 Toth, L.S.48
 Toth, L.S.*48
 Tovtin, V.101
 Tsurekawa, S.32, 80
 Tsuzuki, K.45
 Turner, P.A.106
 Turner, T.J.60
- U**
- Uchic, M.41, 97
 Uchikoshi, T.33
 Umetsu, T.49
 Ushioda, K.*56
 Uta, E.*57
 Utsunomiya, H.49
 Uyar, F.56
- V**
- V.L., N.89
 Vadlamani, S.S.*56, 89
 Van Bael, A.50
 Van Bael, A.*51
 Van Boxel, S.82, 106
 Van Boxel, S.*82
 van Hoolst, J.98
 Van Houtte, P.51, 57, 59, 68, 82, 106
 Van Houtte, P.*50
 Van Meirhaeghe, R.63
 Verbeken, K.67, 68, 96
 Verbeken, K.*67
 Verhaeghe, F.96
 Verlinden, B.68, 82
 Vijayalakshmi, M.107
 Vogel, S.36, 76
 Vogel, S.C.34, 96
 Vogel, S.C.*70
 Vogt, J.90
 Volz, H.M.70
 Voorhees, P.*56
- W**
- Wagner, F.34, 91, 103
 Wagner, J.99
 Wakita, M.86
 Wang, B.63
 Wang, C.63
 Wang, S.*74
 Wang, Y.70, 87, 100
 Wang, Y.*49
- Waryoba, D.R.*55, 92
 Watanabe, H.49
 Watanabe, T.80
 Watanabe, T.*32
 Watson, T.76
 Wauthier, A.*68, 98
 Waziers, S.d.101
 Weidong, L.64
 Weiland, H.46, 74, 79
 Wen, X.86
 Wendt, U.89
 Wenk, H.*70
 Wert, J.A.83
 Whitacre, J.*93
 Wiezorek, J.M.62, 79
 Wilkinson, D.S.86
 Wilson, S.*56
 Winning, M.69
 Winning, M.*73
 Winter, M.43
 Winter, M.*42
 Winther, G.79
 Winther, G.*28
 Wollmershauser, J.A.*42
 Wright, S.I.42, 55, 88
 Wright, S.I.*88
 Wu, G.*31
 Wu, P.86
 Wu, Q.*87
 Wu, Y.100
 Wynblatt, P.45, 97
 Wynne, B.P.75
- X**
- Xiang, Z.79
 Xie, Q.*47
 Xu, L.67
 Xu, M.87
 Xu, W.*30
 Xu, Y.80
 Xue-bin, W.*107
 Xusheng, Y.*79
- Y**
- Yamada, W.56
 Yandong, L.79
 Yandong, L.*64
 Yang, E.63
 Yang, N.*107
 Yang, P.42, 43, 47, 67
 Yang, P.*33, 93
 Yao, T.99
 Ye, B.70, 76
 Yerra, S.51
 Yerra, S.K.50
 Yi, S.36, 38
 Yongming, J.64
 Yoshida, H.98
 Yoshida, M.86
 Youssef, H.47
 Yu, H.89
 Yuan, H.63
- Z**
- Zaafarani, N.28
 Zaefferer, S.28, 30, 31, 42, 56, 62, 66, 69, 93, 97
 Zaefferer, S.*30, 36
 Zakaria, B.*101
 Zaliznyak, Y.34
 Zambaldi, C.*42
 Zamiri, A.91
 Zeng, Q.86
 Zhai, T.86
- Zhang, J.70, 107
 Zhang, L.80, 107
 Zhang, Y.32
 Zhang, Y.*80, 100
 Zhao, H.87
 Zhao, X.32, 49, 100
 Zhao, X.*100
 Zhao, Y.70
 Zheng, T.75
 Zhou, S.100
 Zimovcak, P.88
 Zisman, A.*82, 106
 Zobrist, C.66
 Zong, R.62
 Zuo, L.32, 66, 100, 103

